canada/yukon economic development agreement



INDIAN AND NORTHERN AFFAIRS CANADA
NORTHERN AFFAIRS: YUKON REGION

Open File 1994-1 (T)

# AN EVALUATATION OF GROUND PENETRATING RADAR AS A TOOL IN PLACER EXPLORATION

By

M. A. Power - Amerok Geophysics

Canada

Yukon
Government

**This report is available from:**
**Exploration and Geological Services Division,**
**200 Range Road, Whitehorse, Yukon Y1A 3V1**

## ABSTRACT

A test of ground penetrating radar (GPR) was conducted on 10 placer deposits throughout the Yukon in March 1993. At each site, profile surveys were conducted near known depths to bedrock (drill holes, shafts or excavations), overburden GPR velocities were measured with common mid-point (CMP) velocity surveys and overburden resistivity was measured with horizontal loop electromagnetic (HLEM) resistivity soundings. Survey sites were located in frozen deposits in unglaciated terrain, in thawed deposits in glaciated terrain and in frozen deposits in glaciated terrain.

In frozen unglaciated deposits in the Klondike and Moosehorn areas, GPR penetration varied from 10 to 28 m and averaged 19 m. Signal attenuation in thawed black muck and scattering within boulder layers limited penetration at two sites to about 10 m. The weathering of phyllitic and schistose rocks to clay enhances bedrock reflections; weak bedrock reflections were recorded due to a lack of dielectric contrast in deposits underlain by resistant bedrock. GPR performance is enhanced by surveying during winter or late spring when the zone of seasonal thawing is thoroughly frozen. Under optimum conditions, strong continuous bedrock reflections were recorded over distances of several hundred metres and accurate bedrock mapping was possible with a minimum of confirmatory drill holes.

In thawed placer deposits in glaciated terrain at Mayo, Stewart River and Livingstone Creek, GPR penetration varied from 10 to 28 m and averaged 17 m. Liquid water content varies considerably in these deposits depending upon the sediment grain size. The boundaries between layers with contrasting liquid water content are good GPR reflectors; consequently many reflections and in some cases multiples are generated in these placer deposits. This signal cluttering tends to obscure bedrock reflections. In addition, signal attenuation within clay beds and scattering in boulder layers limited penetration at two sites to approximately 10 m. Filtering and predictive gain algorithms can screen out many of the overburden reflections and the bedrock reflection can often be identified and followed with confidence despite these problems. A higher density of confirmatory drill holes or bedrock depth controls is required in these deposits than in Klondike type placer deposits. GPR performance over these deposits is not significantly enhanced by surveying when the ground is frozen. In areas with high water tables, multiples are generated at the base of seasonal frost and GPR surveys are best conducted when the ground is thawed.

GPR penetration in frozen placer deposits in glaciated terrain in the Mt. Nansen and Burwash areas varied from 10 to 24 m and averaged 16 m. As in Klondike area placer deposits, clay alteration of the bedrock surface is necessary to generate strong reflections. Poor dielectric contrast between fresh, unweathered bedrock and overburden obscured bedrock reflections at one site.

Tests of the accuracy of GPR depth determinations were made at all sites and a trial production survey was conducted at Discovery Creek in the Mt. Nansen area to determine the coverage possible during a full scale survey. In most cases, GPR indicated depths to bedrock calculated using the normal moveout velocity of the bedrock reflector agreed with the depth controls to within $\pm$ 10%. The test production survey determined that approximately 1.5 to 2.0 line-km per day can be surveyed at a 2 m station spacing under optimum winter conditions. The results of the trial production survey were used to create a map of the bedrock surface. Mining during the summer of 1994 confirmed the accuracy and utility of the GPR survey in mapping bedrock.

## Table of Contents

## List of Figures

**Acknowledgements**

This project was commissioned and funded by the Canada/Yukon Geoscience Office as part of the Canada/Yukon Mineral Development Agreement. Lori Walton and John Kowalchuk of the MDA office supervised the work and provided efficient help throughout the project. Larry Lebedoff designed and constructed the GPR sled and instrument containers and, together with Graham Davidson, P. Geol. assisted the author in the field. The author benefitted from reviews of the final report by Les Davis, P. Eng. of Canpolar Ltd. and Graham Davidson, P. Geol.. The author extends special thanks to the miners who participated in the program:

| | |
|---|---|
| Harlan Svean<br>Sikanni Oilfield Construction Ltd. | Soya Creek |
| Al Falle | Frying Pan Creek |
| Ron Asuchak & Mike Brown | Livingstone Creek |
| Bud Kenzie | Klondike River |
| Jerry Klein<br>Teck Mining Corporation | Gold Run Creek |
| Eugene Bekar | Stewart River |
| Hans Barchen<br>Bardusan Placers Ltd. | Lightning Creek |
| Frank Taylor<br>Duncan Creek Golddusters Ltd. | Duncan Creek |
| Norm Ross<br>Ross Mining Services Ltd. | Dominion Creek |
| Bill Trerice | Discovery Creek |

and to all miners who took the time to apply for test surveys.

# 1. INTRODUCTION

Placer mining exploration in the simplest sense is the search for gold-bearing gravel which can be worked at a profit. Historically, this has been a difficult and expensive undertaking requiring extensive excavation and testing. In a time when labour was inexpensive, shaft sinking and drifting were common methods of testing deposits; these have largely been supplanted by mechanical excavation and drilling. The cost of exploration has been further increased by the expense, delay and uncertainty involved in obtaining permits to move heavy equipment onto remote properties. Without exploration however, the placer industry cannot continue to operate on a sustained basis.

Along with grade, most placer miners are critically concerned with the depth of overburden and the bedrock topography. There are three reasons for this. First, alluvial placers are generally found on bedrock with the richest portions lying in bedrock depressions. Secondly, stripping ratios are a critical factor determining whether a given placer deposit can be mined at a profit. Finally, most deposits must be drained before mining and this requires a knowledge of the bedrock topography. Unfortunately, obtaining reliable information on the depth to bedrock is an expensive undertaking. Drilling, shafting and excavation provide only very local information on the depth of overburden and shape of the bedrock surface. Seismic methods have been used in some cases to determine the depth to bedrock and, when combined with topographic surveys, the topography of bedrock. Unfortunately, the cost of seismic surveys is high relative to the information they provide. Modern technology has yet to provide placer miners with a reliable and inexpensive means of determining the depth to bedock.

Ground penetrating radar (GPR) was developed in the 1970's for shallow investigations of soil and bedrock in geotechnical applications. Original models provided very high resolution of overburden and bedrock layers to shallow depths. Early models were tested on placer deposits in the Klondike but failed to pick up the gravel/bedrock contact because of their limited penetration (Annan and Davis 1977a). Since these tests, the technology has been improved by lowering the operating frequency and incorporating digital data acquisition and processing into the designs. These improvements have increased the depth of penetration to the point where GPR has potential to be a useful tool in placer exploration.

This report describes the results of a test of GPR as a tool in placer exploration contracted by the Canada/Yukon Mineral Development Agreement. GPR surveys were run on ten placer properties throughout the Yukon to determine how accurately currently available instruments can measure the depth to bedrock. At each site, three surveys were conducted:

a. Common mid-point (CMP) velocity surveys - to determine the radar wave velocity.

b. GPR profile surveys - to map the bedrock surface and other layers within the overburden.

c. Horizontal loop electromagnetic (HLEM) resistivity soundings - to determine the electrical resistivity of the overburden material in the placer deposit and the likely GPR attenuation.

d. Topographic surveys - to correct the GPR profiles for surface topography and determine the true bedrock topography.

In addition, a full scale survey was conducted over a small grid at one property to determine the expected production rate under normal operating conditions.

## 2. PLACER DEPOSIT GEOLOGY

Geological studies of Yukon placer deposits began before the 1898 Klondike Gold Rush (Dawson 1889) and have been a component of government sponsored geological research since then. The general character of Yukon placer deposits is described by Debicki (1983) and Morison (1985); Boyle (1990) provides a comprehensive summary of general placer deposit geology.

Boyle (1990) cites four requisites for the development of extensive placer deposits:

1. The presence of abundant gold occurrences in quartz veins or disseminated in country rock.

2. A fairly long period of deep chemical and mechanical weathering in which gold is released from bedrock sources.

3. Concentration of gold by the action of water and gravity.

4. Absence of extensive glaciation.

The Yukon is generously endowed with placer deposits because of three unique geological factors. Gold occurrences and elevated levels of background gold are common in bedrock throughout many areas of the Yukon. Secondly, portions of the central Yukon escaped Pleistocene glaciation and consequently late Tertiary placer deposits are preserved on the uplifted Klondike Plateau. Finally, the rugged topography locally mitigated the erosion and dilution of placer deposits during glaciation. As a result, economic placer deposits are preserved in glacial and proglacial settings.

A general classification combining systems suggested by Morison (1985) and Debicki (1983) includes:

**a. Pliocene - Recent eluvial deposits**: Small high grade placer deposits in eluvium or colluvium near bedrock sources. (eg. Moosehorn area placer deposits)

**b. Pliocene alluvial deposits**: Well sorted, buried alluvium deposited in braided stream environments on elevated benches consisting of organic clay (black muck) overlying gravel on weathered bedrock. Deposits are commonly frozen. (eg. White Channel Gravels, Klondike district)

**c. Pleistocene buried preglacial or nonglacial deposits**: Moderately sorted, locally derived alluvium preserved in valley fill and alluvial terraces, commonly preserved beneath lacustrine deposits. They usually consists of crudely stratified gravel covered by thick clay, sand and till. Deposits are often thawed. (eg. Clear Creek and Livingstone Creek placer deposits)

**d. Pleistocene interglacial alluvial deposits:** Valley fill and alluvial terraces commonly preserved beneath lacustrine deposits. Source material could be preglacial placers. Deposits consist of gravel either on bedrock or within a sequence of sand and silt capped by till. They are commonly thawed. (eg. deposits on Spruce and Pine Creeks, Atlin area)

**e. Pleistocene glacial deposits:** Placers concentrated from proglacial and ice contact deposits. These generally consist of gravel beds within a package of sand, silt and clay, locally capped by till or colluvium. Deposits are commonly thawed but may be capped by permafrost. (eg. Duncan Creek and Clear Creek placer deposits)

**f. Recent placer deposits:** Post-glacial placers resulting from uplift and erosion of older placers. These usually consist of a gravel bed overlying bedrock with a thin cover of overbank deposits or colluvium. (eg. placers within present drainage basins of lower Clear, Bonanza and Hunker Creek)

Geophysical signatures are determined by the composition and physical state of a placer deposit and not by its age or mechanism of formation. Variation in clay content is an important factor governing GPR performance and, in general, placer deposits in glaciated terrain have a higher proportion of clay than otherwise comparible deposits in unglaciated terrain. The presence or absence of frozen ground is also important as this influences the attenuation of radar waves and the strength of reflections. Finally, the character of bedrock is important in determining the relative strength of the reflections arising at the bedrock surface. In glaciated regions, bedrock is relatively fresh and dry while bedrock in unglactiated terrain is commonly altered to clay-rich water saturated saprolite.

A classification scheme appropriate to this investigation includes the following categories:

**a. Frozen placers in unglaciated terrain**: These deposits commonly consist of well sorted gravel beneath a variable thickness of black much and lying on top of weathered bedrock. Aside from several feet of seasonal thawing, the deposits are thoroughly frozen. These deposits are common throughout the Klondike district and include the Gold Run, Klondike River, Soya Creek and Dominion Creek sites studied in this report.

**b. Frozen placers in glaciated terrain:** These deposits commonly consist of moderate to well sorted gravel overlain by sand, silt, clay and till or colluvium. Underlying bedrock is relatively fresh although it may be heavily jointed of fractured. Aside from several feet of seasonal thawing, these deposits are frozen. Deposits in this category are found in the Carmacks, Mayo and Burwash areas and include the Discovery Creek and Frying Pan Creek sites discussed in this report.

**c. Thawed placers in glaciated terrain:** These deposits have the same composition as frozen placers in glaciated terrain but are thawed and have a generally high water table. Deposits in this category are found in the Mayo, Livingstone and Atlin B.C. districts and include the Livingstone Creek, Duncan Creek, Lightning Creek and Stewart River sites discussed in this report.

GPR performance in each of these settings in discussed in section 6.

## 3. PLACER EXPLORATION

Probable deposit size and available capital generally determine the approach taken in placer exploration. Deposits on many creeks are small and do not justify significant exploration expenditures. Larger bench and alluvial deposits with sizeable reserves can support significant exploration. Mining beneath deep overburden also requires significant exploration because the consequences of a miscalculation are much more expensive and the room for error is reduced. Finally, most placer miners are independent operators with limited access to outside capital. Consequently, only those operating with large cash flows can undertake extensive exploration programs.

Recommended placer exploration methods closely resemble those employed in hard rock exploration (Hester 1970, Vallee 1992, Debicki 1983). Target areas are identified from air photographs, historical research and basic prospecting. Once an occurrence of placer gold has been located, systematic testing is undertaken by extensive drilling, shafting and excavation, followed by sampling. Geophysical surveys may be used to extend drill hole indications of bedrock topography. If sufficient yardage is proved up, a bulk test is conducted to confirm recoveries and a mine plan is drawn up before mining commences. Unfortunately, these recommended approaches requires a large capital outlay and the return on this investment is unacceptable if the resulting orebody is small..

An alternative approach is often used in cases where capital is limited and targets are small. Scarce capital is spent on heavy equipment and recovery systems which can be used on a number of deposits rather than committed to exploring a single deposit. A minimum of drill holes or shafts are sunk prior to a bulk test, which serves to establish both grade and recovery. If the test is successful, mining commences forthwith and continues until the local reserves are exhausted. The operator must then decide to either recommence exploration or abandon the property. The essence of this approach is to minimize the uncertainty inherent in working unexplored ground by minimizing the capital investment in any particular deposit. This method is particularly well suited to erratic alluvial placer deposits on small creeks where probable reserves do not justify the cost of a systematic exploration program. A miner has to be mobile, adaptable, frugal and lucky to continue mining in this fashion over the long haul since he or she will not enjoy the certainty involved in mining a thoroughly explored deposit. It is the author's experience that most Yukon placer miners employ this method of exploration and mine development.

Regardless of the approach taken, reliable grade and recovery determinations are critical in an exploration program. These are complicated by the relatively coarse nature of placer gold and the variable grade of placer deposits (Vallee et al. 1992, Stokes 1990). In general, the larger the mean gold size, the larger the sample required for statistical relevance. Consequently, most placer deposits are initially explored by excavation, shafting or drifting rather than by drilling since the latter produces a smaller, less reliable sample. Drilling has been used successfully in situations where mean gold size is relatively small and where ground conditions permit adequate recovery. Miners often place considerably more confidence in the results of a bulk testing program than in the results of drill hole sampling.

Most placer miners are very concerned with the depth to bedrock and the topography of the bedrock surface. In some cases, depressions in bedrock containing paystreaks are the primary target and the adjacent gravels are of little concern. In other situations where the miner intends to mine full width, bedrock topography is less important than the thickness of overburden. Drill holes, shafts and excavations provide conclusive point depth information but are of little use in defining bedrock topography unless there is a large number of them available and they are distributed in a systematic fashion. In ground deeper than about 15 m, the cost of extensive drilling, shafting or excavation is prohibitive. In these situations, miners have occasionally resorted to geophysical methods to determine bedrock topography.

Gravity, electrical resistivity, seismic and GPR surveys have been recommended to determine depth to bedrock (Debicki 1983). In practice only seismic surveys have been used to any extent. Two types of seismic survey are employed. Refraction surveys are generally used to depths of about 30 m while reflection surveys have been used in deeper ground. Velocity inversions can develop where frozen ground overlies thawed ground; this invalidates the results of refraction surveys, producing depth estimates which are generally too large. High velocity permafrost creates problems in running reflection surveys (Pullen and Hunter 1983). Under ideal circumstances, the error in seismic survey depth determinations is $\pm$ 5%; in practice errors are often greater. As a result, seismic surveys require testing with drill holes or shafts. In addition to the uncertainties, seismic survey costs are high. The net result is that these methods are generally applied only in deposits covered by thick overburden.

GPR was first tested for placer exploration in the Yukon by the Geological Survey of Canada in 1976 (Annan and Davis 1977). A two mile traverse using first generation equipment was unsuccessful in mapping bedrock on Hunker Creek. The first commercial GPR placer survey was conducted on Australia and Wounded Moose Creeks (Power and McIntyre 1990). Bedrock was intermittently detected in frozen shallow ground and the information used in a subsequent drill program. To date however, GPR surveys are rarely used in placer exploration programs in the Yukon.

# 4. GPR THEORY

GPR is an electromagnetic (EM) geophysical technique developed during the 1970's for shallow subsurface investigations. An understanding of the basic physics of radar wave propagation and the principles behind instrument design is necessary to assess whether the technique will work in a given situation. A non-technical outline of the key aspects of GPR operating theory can be found at the end of this section. The summary of EM theory and radar design which follows is drawn from Reitz et al. (1980), Ward and Hohmann (1987), Davis and Annan (1987), Annan and Cosway (1991) and Annan and Davis (1976, 1977). The section on electrical properties of sediments and bedrock is drawn from McNeill (1980). Amery (1993) provides a comprehensive summary of seismic velocity determination methods which are also used in GPR surveys.

## 4.1 Radar wave propagation

GPR operates on the same principle as reflection seismic, sonar or conventional radar instrumentation. Pulsed EM energy is focussed into the earth where it reflects off subsurface targets and a portion of the initial energy returns to the surface. The strength of the returning echo and its travel time are governed by EM theory and the theory of geometric optics.

EM wave propagation is governed by Maxwell's Equations:

$$\nabla \times H = J + \frac{\partial D}{\partial t} \qquad (4.1)$$

$$\nabla \times E = -\frac{\partial B}{\partial t} \qquad (4.2)$$

$$\nabla \cdot D = \rho \qquad (4.3)$$

$$\nabla \cdot B = 0 \qquad (4.4)$$

where **E** is the electric field, **H** is the external magnetic field, **B** is the magnetic induction, **D** is the displacement current, **J** is the current density, t is time and $\rho$ is the electrical charge. Respectively, these are the vector forms of Ampere's, Faraday's and Gauss' Law and the statement that there are no isolated magnetic poles. Taking the curl of (4.2) and applying an elementary identity yields the Helmholtz equation for EM wave propagation in a source-free region:

$$\nabla^2 E - \mu\sigma \frac{\partial E}{\partial t} - \mu\epsilon \frac{\partial^2 E}{\partial t^2} = 0 \qquad (4.5)$$

Solutions to this equation describe the behaviour of radar waves in the earth. At GPR frequencies of 1 - 1,000 MHz, earth materials are generally nonmagnetic, weakly conductive and subject to electrical polarization. Consequently, only electrical permittivity and conductivity are important properties controlling GPR wave behaviour.

The simplest solution to (4.5) which demonstrates the importance of these properties without loss of generality is that of a plane wave. Solutions to this problem are in the form:

$$E(r,t) = Ee^{-i(\omega t - \kappa \cdot r)} \qquad (4.6)$$

where $\omega=2\pi f$, f is frequency, **r** is the direction of propagation and $i= -1^{-0.5}$. Substituting this solution into (4.6), noting that $\mu=\mu_o$ in nonmagnetic media and using the simplified derivatives of (4.6) with respect to t and r yields:

$$-\kappa^2 E - i\omega\sigma E + \omega^2 \mu_o \epsilon E = 0 \qquad (4.7)$$

or

$$\kappa^2 = \omega^2 \mu_o \epsilon + i\omega\mu_o\sigma = \frac{\omega^2}{c^2}\left[K + \frac{\sigma}{\omega\epsilon_o}\right] \qquad (4.8)$$

which can be rewritten as

$$\kappa = \omega\frac{\sqrt{K^*}}{c} \qquad (4.9)$$

where c is the velocity of light *in vaccuo*, $\kappa$ is the wave number and K* is defined as the complex dielectric permittivity. Complex dielectric permittivity governs both the wave phase velocity and attenuation.

Dielectric permittivity is the ease with which a material may be polarized in an electric field. When placed in an electric field, the abundant charges in a polar material will realign themselves to oppose the external field and thus reduce the internal field. In an external field of a given strength, polar materials will undergo much more charge realignment than nonpolar materials and thus the polar materials have a higher permittivity. If the electrical field is changed, the charges in a polar material must realign themselves and in the process will resist the change in the external field during realignment. As a result, polar substances have a higher electrical impedance than nonpolar substances. This phenomenon is log-linear at low frequencies but changes abruptly when the applied frequency exceed the harmonic frequency of the dipolar molecules. At this frequency - the relaxation frequency - the attenuation increases dramatically creating a phenomenon termed dielectric loss.

Wave velocity can be extracted from (4.6) by noting that the second term in the exponent must be dimensionless and $\kappa$ therefore must have the dimension of 1/r. This can only occur if the phase velocity is:

$$v = \frac{c}{\sqrt{K^*}} \qquad (4.10)$$

At low frequencies in relatively poor conductors, $K^* \sim K$ (real dielectric constant). It is immediately apparent from (4.10) that the EM wave will travel at a slower speed through media with a higher dielectric permittivity. In addition, the wave packet will shorten in this slower media. Because of the short distances measured relative to the wave velocity, it is common practice to quantify GPR velocities in metres per nanosecond (m/ns).

Attenuation of EM waves is a complex function of both conductivity and dielectric permittivity. At radar frequencies and in earth materials with moderate conductivity and dielectric permittivity, attenuation may be expressed in simple terms. Defining a complex refractive index $n^*=(K^*)^{0.5}$ and then decomposing it into real ($\alpha$) and imaginary ($\beta$) components, yields:

$$\alpha = \sqrt{\frac{1}{2}\sqrt{1+\frac{\sigma^2}{\epsilon^2\omega^2}}-1} \qquad (4.11)$$

$$\beta = \sqrt{\frac{1}{2}\sqrt{1+\frac{\sigma^2}{\epsilon^2\omega^2}}+1} \qquad (4.12)$$

Then, (4.6) may be rewritten as:

$$E(r,t) = E_o \cdot e^{-\frac{\omega\beta r}{c}} \cdot e^{-i\omega\left(t-\frac{\alpha r}{c}\right)} \qquad (4.13)$$

The first exponential term describes the attenuation of the EM wave with distance. It is readily apparent that attenuation will increase with frequency and with electrical conductivity. The inner term in (4.12) is frequently rewritten as the loss tangent:

$$\tan\delta = \frac{\sigma}{\epsilon\omega} \qquad (4.14)$$

Davis and Annan (1987) derive an expression for attenuation ($\alpha_m$) in dB/m:

$$\alpha_m = \frac{1.69\times10^3\sigma^*}{\sqrt{K}} \qquad (4.15)$$

which is useful in estimations of GPR penetration. In this case, $\sigma^*$ is the complex conductivity incorporating both DC conductivity and dielectric losses.

**4.2 Radar wave reflection**

Radar wave reflection occurs at the boundary between materials with different conductivity and dielectric permittivity. Most earth materials are relatively nonconductive; consequently, reflections arise primarily at the boundaries between materials with contrasting dielectric permittivity.

Most radar surveys are reflection surveys conducted with the transmitting and receiving antennas separated by only a small distance. Consequently, reflections received at surface are generated by incoming waves at normal incidence to the target. Under these conditions, the Fresnel reflection coefficient (R) reduces to:

$$R=\frac{\sqrt{K_1}-\sqrt{K_2}}{\sqrt{K_1}+\sqrt{K_2}} \qquad (4.16)$$

where $K_1$ and $K_2$ are the dielectric permittivities of the upper and lower medium respectively. It is apparent from (4.16) the the strength of the reflection increases with the contrast in permittivity. Since GPR signal velocity is proportional to $K^{0.5}$, the strength of the reflection is also proportional to the difference in radar wave velocity on either side of the boundary.

The texture and shape of the target will also influence the strength of the returning reflected radiation. Texture is determined by the size of irregularities compared to the wavelength of the GPR signal. For the purposes of this discussion, smooth reflectors are those with relief less than approximately $\lambda/4$ where $\lambda$ is the radar wavelength in the medium (eg. less than 0.5 to 1.0 m at 50 MHz). The power reflected back to surface is determined by $g\phi$ - the product of the target back-scatter gain and the target cross-sectional area. Not suprisingly, the strongest returns are from a smooth planar reflector (eg. ice lenses, fresh:

$$g\phi=\pi L^2R^2 \qquad (4.17)$$

where L is the distance from the transmitter to the target. Most geological surfaces are rough however. In this case, provided the irregularities are in the order of a quarter wavelength,

$$g\phi=\frac{\pi\lambda LR^2}{2} \qquad (4.18)$$

Very small targets reflect the least energy. As an example, a spherical target of radius a with $a<<\lambda$ has a target back-scatter gain/cross-sectional area product of

$$g\phi=65\pi^5a^6\lambda^4 \qquad (4.19)$$

In this last case, Rayleigh scattering rather than reflection governs the strength of the return.

### 4.3 Resolution versus range

A trade-off exists between range and resolution in radar imaging. As noted above (4.13), the attenuation of the EM wave increases exponentially with frequency. In other words, the higher the operating frequency, the less the penetration depth. In seismic applications, the resolution is generally defined as one half the signal wavelength. To improve the resolution, it is necessary to increase the operating frequency. Consequently, resolution can be increased only at the expense of range and vice versa. A partial solution to this dilemma is to increase the transmitter power and improve the receiver sensitivity.

### 4.4 Electrical properties of placer deposit materials

The above discussion has demonstrated that electrical conductivity and permittivity are the two key physical properties controlling radar wave propagation in the earth. Conductivity is the most important factor governing attenuation and dielectric permittivity is the most important factor governing wave velocity. Since reflections arise at velocity contrasts, two geological materials must have contrasting dielectric permittivities if their mutual boundary is to imaged with a radar wave. In order to assess whether GPR can detect a given horizon in a placer deposit, it is necessary to quantify the electrical properties of the materials to some extent.

Most earth materials are electrical insulators and conduction at low frequencies occurs via ion exchange and transport in electrolytes. In the presence of an electrical field, ions will migrate from surfaces where charge exchange occurs, through an electrolyte and undergo a reverse charge exchange at another surface. McNeill (1980) states the conductivity depends primarily upon:

**a. Porosity**. The amount of void space in a material governs the amount of electrolyte that it may hold and hence the capacity of the material to transport current. The higher the capacity, the greater the potential conductivity.

**b. Permeability.** If the electrolyte cannot move through the material because void spaces are not connected, electrical current will be impeded. Saturated permeable materials are therefore usually conductive.

**c. Ion concentration.** The charge carriers in an electrolyte are dissolved cations and anions. Increasing the concentration of mobile ions such as $H^+$, $OH^-$, $Cl^-$ and $K^+$ increases the charge carrying capacity of a material and improves the conductivity.

**d. Saturation.** The water saturation naturally determines the bulk quantity of electrolyte available for ion transport and, hence, the conductivity. Dry materials are generally insulators and wet materials are generally weak to good conductors depending on the above factors.

**e. Temperature and phase of the electrolyte.** This factor frequently influences surficial conductivity in the North. If the electrolyte is frozen, it will naturally not conduct electricity. Freezing of an electrolyte is not complete at 0° C and free water persists at temperatures well below this. Consequently, while there is a change in conductivity at the freezing point, the contrast is not as dramatic as might otherwise be expected. (Scott et. al. 1979)

It is the combination of these factors which determines the bulk electrical conductivity of a given material. At higher frequencies, dielectric losses will be also be significant; these are primarily a function of water content.

In general, unconsolidated sediments found in placer deposits can grouped into clays, silts, sands, gravels and till. Clays commonly display high electrical conductivity. This is attributed to their structure which incorporates a high concentration of bound water and electrolytes. An abundance of weakly held charge carriers in turn permits high electrical conductance. The composition of the parent bedrock appears to influence the conductivity of clay (Keller 1987) with clays derived from mafic rocks being more conductive than clays derived from felsic rocks. Silts display a conductivity range slightly lower than clays. Saturated sands and gravel are still less conductive, largely due to the absence of electrolytes. Glacial till displays a range of conductivities largely determined by the concentration and source of the clay in the till. Bedrock is naturally less conductive than most sediments with its conductivity largely determined by the extent of chemical weathering and the fracture density.

The effect of freezing on electrical conductivity and especially on liquid water content is important. The concentration of liquid water in a material below the freezing point is largely determined by the concentration of dissolved salts and the extent to which the water is bound within mineral structures. Clays show a marked ability to retain liquid water and high conductivity at temperatures below freezing (McNeill 1980). When juxtaposed against frozen gravel or bedrock, relatively conductive water bearing clay layers can both attenuate signals within the beds and create strong reflections at their boundaries.

Dielectric permittivity in earth materials is mostly controlled by water content. At GPR frequencies, the dielectric permittivity of liquid water is 80 while that of virtually all other earth materials ranges from 2 to 4 (Keller 1987). As a result, the volume concentration of liquid water largely determines the bulk dielectric constant and reflections occur at the boundary between layers with contrasting water content.

There are a number of boundaries which can be detected in a GPR survey on the basis of a contrast in dielectic permittivity. The water table often produces the strongest reflections in a radargram and the base or top of a frozen layer can also yield a strong reflection if the transition from frozen to thawed material is quite sharp and if the thawed sediments are water saturated. The large difference in dielectric permittivity between water saturated sediments and relatively "dry" bedrock in a thawed placer deposit allows the detection of the bedrock/gravel interface. To a lesser extent, the boundary between frozen gravel with no liquid water and frozen clay-altered bedrock with some bound liquid water allows the detection of the top of bedrock in frozen placer deposits. Lastly,

layers of differing composition within the overburden will produce individual reflections which tend to clutter the radargrams - particularly in thawed ground where variations in liquid water content are more pronounced.

## 4.5 GPR instrumentation

GPR instrumentation is based on conventional radar designs developed in the 1940's with several specific modifications necessary to achieve penetration and resolution in soils and rock. All radars consist of a transmitter and matched antenna through which energy is radiated, a receiving antenna and signal processing circuitry to amplify, filter and display the returning echoes and timing circuitry to synchronize the time bases of the two units and so permit accurate determination of the travel times. Geophysical instrumentation has undergone a significant transformation from analog to digital signal processing and from transistor-based to microprocessor-based circuitry over the past twenty years; GPR instrumentation has followed this path. The first commercial ground radar systems were developed by Geophysical Survey Systems Inc. of Concord N.H. in the early 1970's. They incorporated analog signal processing, continuous profiling, limited (analog) filtering and offered only paper printouts. The latest generation of instruments are fully digital, are microprocessor based with full digital data storage capabilities, offer sophisticated filtering and real-time data processing and are lighter and consume less power than the original models. The most significant improvements however has been in the range of frequencies offered and in the penetration depth.

The penetration depth of a GPR system is governed by the radar range equation:

$$Q=-10\log\left[\frac{\epsilon_{TX}\epsilon_{RX}G_{TX}G_{RX}c^2 g\sigma e^{-4\alpha_m r}}{64\pi^3 f^2 r^4}\right] \qquad (4.20)$$

where:

Q - system performance factor

$\varepsilon_{TX}$ - transmitter antenna efficiency

$e_{RX}$ - receiver antenna efficiency

$G_{TX}$ - transmitter antenna gain

$G_{RX}$ - receiver antenna gain

f - frequency

r - radar range

(Annan and Davis 1977b)

Q is explicitly defined as:

$$Q=-10\log\left[\frac{P_{MIN}}{P_S}\right] \qquad (4.21)$$

where $P_{MIN}$ is the minimum detectible power at the receiver and $P_S$ is the power applied to the transmitting antenna. GPR system performance factor improvements over the past two decades have dramatically improved the penetration depth without sacrificing too much resolution. Average Q has increased from 100 dB in early models to 150 dB in more recently developed systems.

Q determines whether a given reflection can produce a detectible GPR signal. In practice, weak detectible signals are often obscurred by noise and the true penetration depth is less than that indicated by the radar range equation. Consequently, noise suppression and signal enhancement features have been incorporated into recent GPR design. These include signal stacking, filtering and variable gain. Signal stacking is the summation of measurements taken at a fixed location. Since the signal is coherent from trace to trace while the noise is random, the signal-to-noise ratio will be improved. Common filtering capabilities include high-pass, low-pass and notch filters. In most situations, the frequency spectrum of the noise and signal do not differ significantly and consequently filtering is of limited utility. In addition, low pass filtering degrades resolution. Two types of varying gain are useful in GPR surveys; automatic gain control (AGC) and predictive gain. AGC algorithms vary the gain along the trace according to the local amplitude. High amplitude early arrivals are amplified less than later, weaker arrivals. The result is a trace with roughly equal amplitudes over most of the time range. Predictive gain incorporates a known or inferred geological model of subsurface attenuation into the gain control. Short time - near surface arrivals can be suppressed to enhance later and deeper reflections. The incorporation of an *a priori* model of ground attenuation can be dangerous in situations where the thickness and attenuation constants of layers are not well known or where they vary along a survey profile. In these situations, it is possible to suppress true reflections and enhance noise if the true geology departs significantly from the model geology.

Antenna design is an important factor governing the penetration and field utility of a GPR system. There is a trade-off between penetration and portability; the lower the frequency, the larger the antenna required to allow efficient propagation. Any antenna design must focus the radiated energy into the earth and minimize any lateral signal leakage. Early designs were essentially rough adaptations of above-ground radar antennas to subsurface applications. The radiation pattern from any antenna near the air/ground interface is distorted and most recent designs exploit this behaviour by using the ground to focus the transmitted radiation. Davis and Annan (1987) discuss this effect in the design of the Pulse EKKO IV system. This system incorporates flat dipole antennas which are easier to transport than bulkier conventional antennas.

## 4.6 Reflection surveys

Most GPR surveys are reflection profiles designed to determine two dimensional structure. Transmitting and receiving antennas are moved in tandem at a constant separation and constant station interval along a survey line (Figure 4.1). To avoid aliasing the response, the station spacing should be kept to within one quarter the wavelength of the transmitted signal in the material (Nyquist Frequency):

$$x_n = \frac{c}{4f\sqrt{K}} \qquad (4.22)$$

If the reflector is steeply dipping or irregular, it may be necessary to tighten the station even further to ensure that the reflection is clearly visible in the radargram. Over flat-lying continuous reflectors, the station spacing can be increased without degrading the data.

Data is normally presented in a stacked profile format termed a radargram. A diagramatic example is shown in Figure 4.1. The horizontal axis is distance along the survey line and the vertical (increasing downward) axis is time in nanoseconds ( $1 \times 10^{-9}$ s). Profiles are commonly displayed in wiggle trace, variable area or variable density formats used in seismic sections. The first arrival on all reflection radargrams is a direct wave travelling through the air between the transmitting and receiving antennas. In surveys conducted on frozen ground, surface waves travelling along the top of ice or snow also develop (Annan et. al. 1976). Subsequent arrivals are reflections - primary, multiples and lateral reflections. Primary reflections are the signals of interest which arise from a single reflection at a boundary. Multiples occur when a returning wave is reflected back into the ground one or more times before arriving at the receiving antenna. They commonly display lower amplitudes than primary reflections and repeat at a constant interval down the radargram.

## 4.7 Velocity determination

Reliable GPR depth determinations require accurate velocity determinations. The most reliable means of determining GPR velocity is survey near at least two different depth controls and use the recorded arrival times and known depths to directly determine an *in-situ* velocity. In cases where such controls do not exist, indirect techniques must be applied to determine the velocity structure.

Figure 4.2(a) illustrates how this can be accomplished. Consider the case of transmitting antennas separated by a distance $x$ on top of a layer with velocity $v_1$ overlying a second layer with velocity $v_2$. The boundary between the layers is horizontal and $t_o$ is

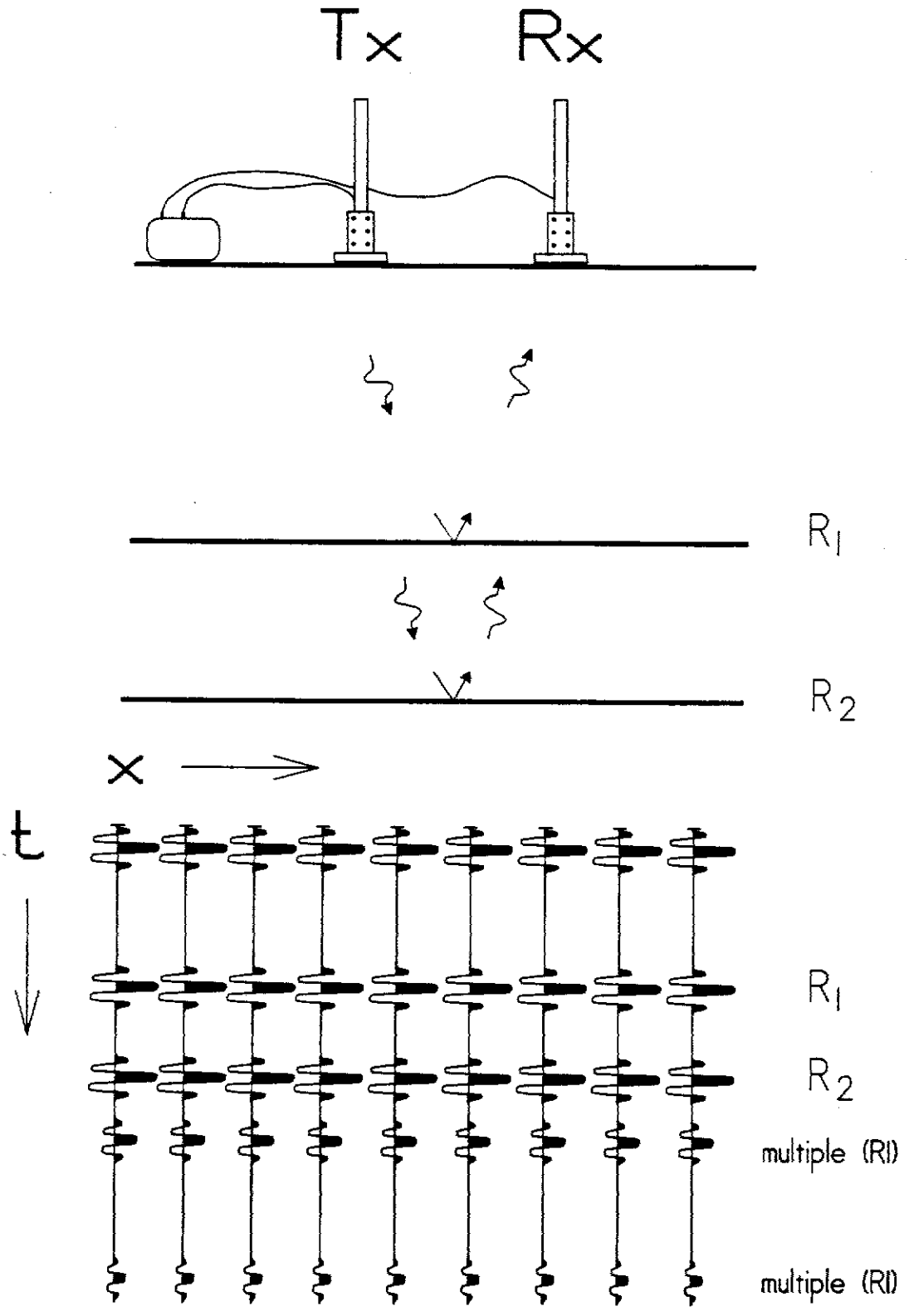


Figure 4.1. Basic GPR profile survey procedure. Transmitting (Tx) and receiving (Rx) antennas are spaced a fixed distance apart and moved in short steps along the survey line. Radargram beneath shows the reflections at each setup. The first arrival is a direct wave, R1 and R2 are reflections from the first and second reflectors and multiples of the first reflection arrive after R2.

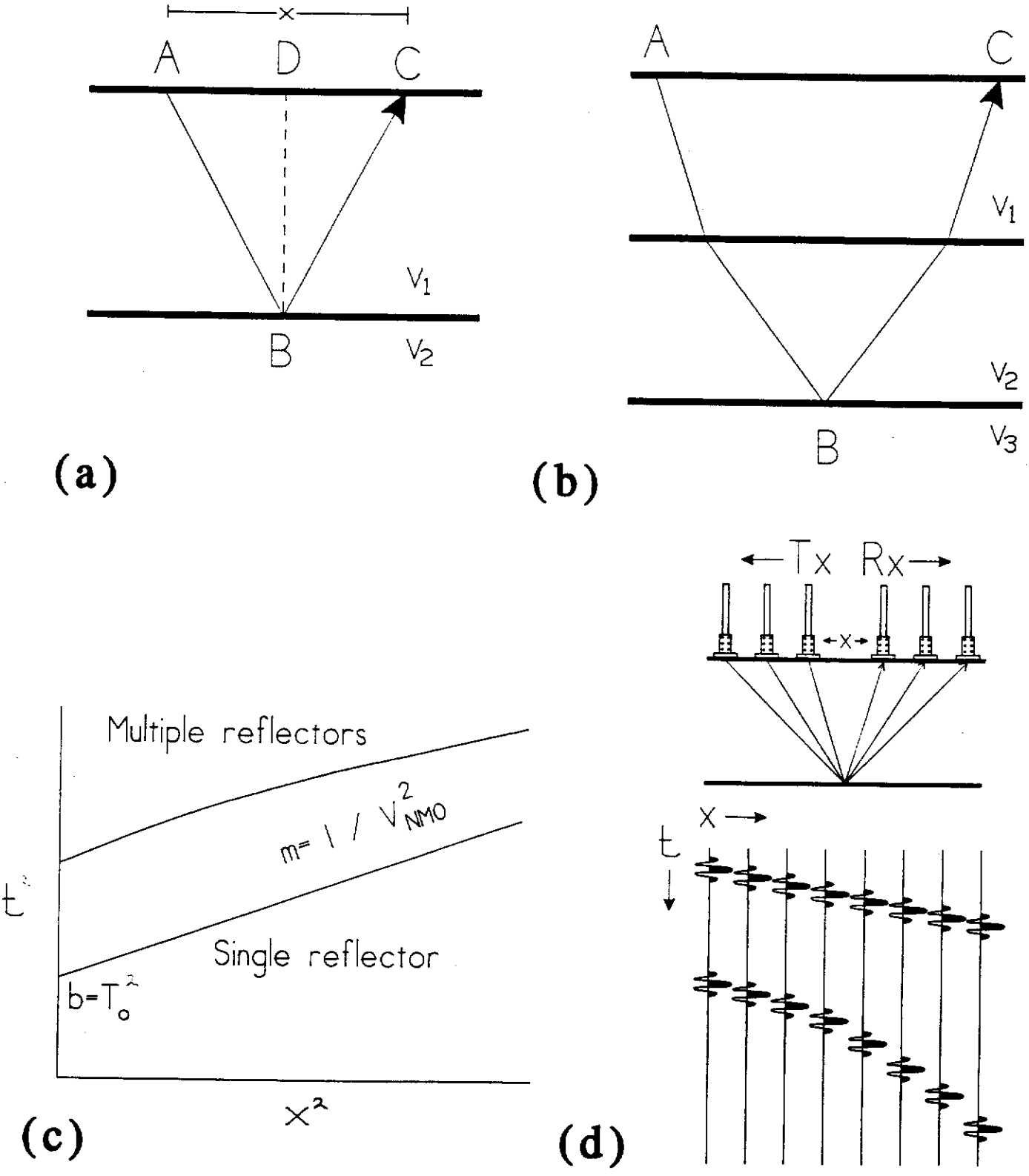


**Figure 4.2. GPR velocity surveys. (a) Geometry of reflected wave. (b) Refraction and reflection at two boundaries. (c) $X^2$ - $T^2$ plot for single and multiple reflections. (d) CMP velocity survey procedure.**

the travel time at vertical incidence. The distance the radar wave must travel is:

$$(v_1 t)^2 = x^2 + (v_1 t_o)^2 \qquad (4.23)$$

where **t** is the travel time, $t_o$ is the time required to travel the vertical distance DB. This may be rewritten as:

$$t^2 = \frac{x^2}{v_1^2} + t_o^2 \qquad (4.24)$$

This is the equation of a straight line in the form **y=mx+b** where the slope $\mathbf{m=1/v_1^2}$. This suggests that the *in-situ* velocity can be determined by a linear regression of the square of the arrival times versus antenna separation. It is important to note that such a regression is only valid for reflectors which are horizontal or, at worst, gently dipping. The situation is somewhat more complicated if there are two or more layers overlying the reflector of interest (Figure 4.2(b)). In this case, the radar waves are refracted at the first interface and a quadratic regression of $\mathbf{t^2}$ versus $\mathbf{x^2}$ is required to determine a root mean square velocity ($\mathbf{v_{rms}}$). At short antenna separations, the difference between the velocity derived from a linear regression and a quadratic regression is negligible. Figure 4.2 (c) illustrates this graphically.

Figure 4.2 (d) indicates how the velocity is determined in practice. Antennas are placed close together and a reading taken. The antenna separation is then increased by a contant increment and additional readings taken. Because the reflections all occur at the same point, this procedure is referred to as a common midpoint or CMP survey. The resulting radargram is also shown. The first arrival - the surface wave between the antennas - will form a line on the radargram with a slope equal to the inverse velocity of the radar wave in free space. Often a second linear arrival (direct ground wave) occurs immediately after the air wave. Subsequent arrivals will form parabolas on the radargram. Arrival times are read for each antenna separation and the data used in the linear regression described above to determine a velocity. Care must be taken to ensure that refracted arrivals are not mistaken for reflections in this analysis; this is achieved by using data collected at separations less than 2.5 times the apparent reflector depth. In seismic work, the parabolic pattern is termed normal moveout; hence the resulting velocity is a normal moveout velocity or $\mathbf{v_{NMO}}$. If the reflector is relatively flat at the CMP survey site, the velocity structure is uniform throughout the survey area and the antenna separation is short relative to the depth of penetration, $\mathbf{v_{NMO}}$ can be used to convert travel times into accurate depths to reflectors.

Annan et al. (1976) describe GPR velocity surveys conducted in permafrost terrain near Tuktoyaktuk, N.W.T. They found that the initial arrivals often consisted of both an air wave and ground wave. To invert their data, they used a model consisting of a horizontal layer over a half space with their target reflector forming the half-space boundary. This practical procedure is usually all that is necessary in ordinary survey work where determining the depth to the target reflector is all that is required.

More sophisticated analysis is justified in cases where the survey must determine the detailed velocity structure of several layers. If several horizontal layers are present and if detectible reflections develop at the layer boundaries, it is possible to determine the velocity of the layers. At short antenna separations, the velocity for an interval **n** bounded by reflections at the top and bottom of the layer can be derived from the CMP survey using the Dix Interval Equation:

$$v_n^2 = \frac{v_{NMO_n}^2 t_{o_n} - v_{NMO_{n-1}}^2 t_{o_{n-1}}}{t_{o_n} - t_{o_n} - 1} \qquad (4.25)$$

In seismic velocity surveys it has been determined that the average velocity found using this analysis is slightly faster than the corresponding velocity from a down-hole velocity survey. This has been attributed to seismic velocity anisotropy (Amery 1993) and the same phenomenon could occur in radar velocity surveys.

## 4.8 Summary

In general terms, GPR operating theory may be summarized as follows:

a. GPR is an echo ranging technique in which a high frequency electromagnetic wave is focussed into the ground, reflects off different layers and returns to the earth's surface where it is detected by a receiving antenna. The deeper the layer boundary, the greater the time between the transmission and reception of the wave.

b. To determine the depth to a boundary, it is necessary to know the velocity of the material through which the radar wave travels. In general, radar waves travel quickly through dry material and slowly through water saturated material. The radar wave velocity can be determined by

i) surveying near depth controls such as shafts, drill holes or excavations

ii) by conducting a common mid-point survey in an area where the layers are relatively flat or

iii) by using an inferred velocity based on local geology.

c. Reflections occur at the boundary between materials with different velocities. In practice, this means the boundary between layers with different concentrations of liquid water. In placer deposits, the boundaries at which reflections can occur include the base or top of frost, the water table, the contact between sand, gravel and clay and at the top of bedrock. The strongest bedrock reflections will occur in deposits where this is water saturated gravel overlying fresh, dry bedrock. Reflections in frozen placer deposits can be more subtle because there is less contrast in water saturation. In frozen

deposits, clay can retain liquid water below freezing and reflections commonly occur at the top of clay layers and the top of bedrock where saprolitic clay may have developed during weathering.

d. Radar waves are absorbed by materials which can conduct electricity. In placer settings, clay or salt water saturated layers will limit penetration. Radar wave penetration is greatest in dry materials such as frozen ground.

e. There is a trade-off between resolution and penetration. A radar survey can be designed to provide a very detailed picture of a shallow reflector or a more general and less precise image of a deeper reflector. It cannot provide great resolution at great depth and the absolute error in depth determinations will increase with depth.

f. To provide an accurate picture of a subsurface reflector, measurements must be taken at short interval - generally 2 m or less.

g. The results of a radar survey are displayed in a series of profiles which illustrate the pattern of the returning echoes. Some of these are echoes returning directly from layers within the earth, others may have reflected off targets off to the side of the antennas and some may have reflected several times within the earth before returning to the surface (multiples). To determine the depth to bedrock from a radargram, the interpreter must know the overburden radar velocity and there must be a strong reflection from bedrock.

# 5. SURVEY AND DATA PROCESSING PROCEDURES

## 5.1 Survey site selection

In November 1992, newspaper advertisements were placed and a mailing was sent out to members of the Klondike Placer Miners Association soliciting test site submissions. A total of ten properties were selected on the basis of winter accessibility and availability of depth controls. All accessible properties submitted before the submission deadline were accepted and several additional properties were also surveyed. Test site locations are shown in Figure 5.1

## 5.2 Survey procedures

At each test site, the field crew ran GPR reflection and velocity surveys to test GPR performance and a horizontal loop electromagnetic (HLEM) parametric sounding to determine the electrical properties of the materials in the placer deposit. Topographic surveys were run to correct the GPR data and produce reflector elevation sections.

Technical descriptions of the instruments used in the survey are in Appendix B. GPR surveys were conducted with a Pulse EKKO IV GPR manufactured by Sensors and Software Inc. of Mississauga ON. This instrument is a digital multifrequency radar equipped with 100 MHz, 50 MHz, 25 MHz and 12.5 MHz antennas. Antennas are linked to a control console via fibre optic cables and the instrument is run by a 80X86 laptop computer. To permit the instrument to operate in cold conditions (-35°C to -10°C) and to withstand continual impact by brush, the control console and laptop computer were placed in a "hot box" mounted on a small toboggan, the fibre optic cables were sheathed in one inch O.D. heater hose and the antennas were mounted on wooden skis. The HLEM parametric sounding were conducted with a Maxmin I-10 manufactured by Apex Parametrics of Uxbridge ON. This instrument can accommodate coil spacings of 12.5 to 400 m and has a frequency spectrum ranging from 110 Hz to 56.320 KHz. Commonly used in mineral exploration, the Maxmin required no modifications to meet the field conditions encountered at the test sites.

The reflection survey parameters were:

a. 25 MHz antennas with a 4 m antenna separation and 2 m station spacing

b. 50 MHz antennas with a 2 m antenna separation and 2 m station spacing.

To optimize penetration, the 4 m - 25 MHz antennas were used wherever possible and the 2 m - 50 MHz antennas were used only in shallow ground less than 10 m or where line conditions prevented using the larger antennas. The antennas were mounted on wooden skis and separated by a distance equal to their length. The hot box was normally mounted on a snowmobile and the antenna array towed behind it. One person can perform the survey but much better progress is made with one person running the snow machine and checking the chainage while a second operates the GPR. Existing cut lines, roads or

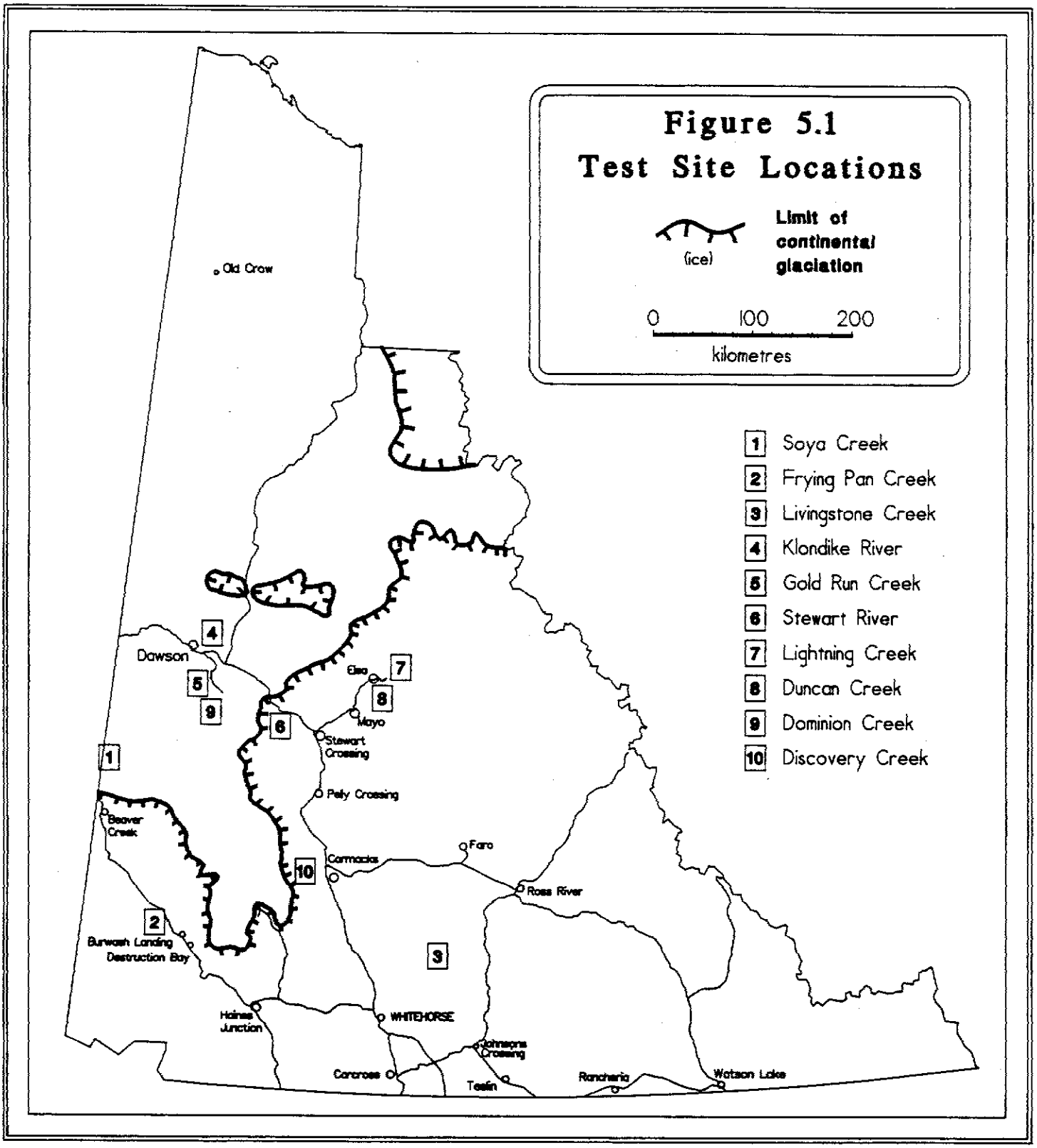
Figure 5.1
Test Site Locations
(ice)
Limit of continental glaciation
0 100 200
kilometres
1 Soya Creek
2 Frying Pan Creek
3 Livingstone Creek
4 Klondike River
5 Gold Run Creek
6 Stewart River
7 Lightning Creek
8 Duncan Creek
9 Dominion Creek
10 Discovery Creek
Old Crow
Dawson
Elsa
Mayo
Stewart Crossing
Pelly Crossing
Beaver Creek
Carmacks
Faro
Ross River
Burwash Landing
Destruction Bay
Haines Junction
WHITEHORSE
Johnsons Crossing
Carcross
Teslin
Rancheria
Watson Lake

ploughed CAT trails were used as survey lines. At each test site, the reflection surveys were conducted over known bedrock depth controls (shafts, drill holes or excavations) to test the accuracy of the GPR depth and velocity determinations. In order to maintain horizontal control, stations were chained-in with a hip chain as the survey progressed. Breaks-in-slope were marked both on the radargram and on the ground. During a subsequent topographic survey, these points were surveyed-in and the radargram corrected for topography to show reflector elevations.

CMP surveys were conducted at sites along the refection profile lines where flat reflectors were detected and where there was enough room to manipulate the antennas. Antenna separation was varied from 2 m to as much as 38 m in 1or 2 m steps with readings taken at each separation.

Frequency domain EM soundings are an inexpensive means of determining the electrical resistivity of overburden and bedrock (Spies and Frischknecht 1991). The HLEM sounding was performed using coplanar level coils maintained at coil spacings of either 25 m or 50 m, depending upon the depth to bedrock. Measurements of the in-phase and quadrature component of the vertical magnetic field were made using frequencies of 110, 220, 440, 1760, 3520 and 7040 Hz and 14.1, 28.2 and 56.3 KHz. Sounding sites were positioned on the reflection profile lines near known depth controls where possible.

### 5.3 Data processing

Data processing consisted of the following procedures:

a. HLEM sounding inversion

b. CMP velocity analysis

c. Topographic correction of GPR data

d. Production of reflection depth sections

e. Synthetic radargram analysis.

These are discussed in turn.

The HLEM parametric sounding inversion was performed with the EMIX-MM software package produced by INTERPEX Ltd. of Boulder CO. This program incorporates digital (Ghosh) filters to calculate the EM response of a vertical magnetic dipole over a horizontally layered earth and ridge regression to minimize the discrepancy between the model response and the field data. In a placer setting, this earth model is an appropriate approximation of the electrical structure of the bedrock and overburden. Summary plots are included with the site visit descriptions in Appendix A and inversion output is in Appendix C.

The CMP velocity analysis consisted of measuring the arrival times of reflections

in the velocity profiles and conducting a linear regression of the squared arrival times versus the squared antenna separations. To avoid mixing reflections and refractions, the regression was run once with all data to gain an initial set of velocities, apparent depths were calculated and then the regression was rerun after deleting data from separations greater than 2.5 times the apparent depth. Velocity analysis was performed with software written by the author which produced $X^2$-$T^2$ plots showing the regression and the derived velocities. The normal moveout velocity ($v_{NMO}$) of the interval extending from surface to the top of bedrock was used as the overburden velocity in the subsequent reflection data processing.

Topographic elevations of control points along the survey lines were merged with the radar data to produce elevation sections. Finally, drill hole information was transferred to the elevation sections to check on the accuracy of the bedrock depth determinations. Reflection data was processed with one of two variable gain algorithms. Automatic gain control (AGC) was used as a standard method of display and where this proved inadequate, spherical and exponential loss corrected (SEC) gain was used. AGC uses the average amplitude of the signal within a short moving time window to set the gain. Weak later arrivals are amplified more than strong early arrivals to produce a radargram with equalized signal display amplitudes. In situations where the bedrock reflection was relatively flat and where multiples or unwanted overburden reflections were present, SEC gain was applied. This algorithm varies the gain using the GPR velocity and attenuation of the medium to suppress the early time arrivals and enhance later arrivals. By adjusting the gain parameters, the bedrock reflection can often be highlighted and discriminated from overburden reflections. All GPR data processing was performed with software developed by Sensors and Software Inc. of Mississauga, ON.

Synthetic radargrams were constructed to investigate the effect of various survey parameters on probable GPR performance in a given placer setting. Vertical profiles of ground conductivity derived from the HLEM soundings were merged with information on the local geology available from shaft or drill hole records to produce a layered model of the overburden stratigraphy. Each layer was assigned attenuation and dielectric constants and a synthetic radargram produced for comparison with the survey radargram. These radargrams provided useful insight into the ultimate GPR penetration depth in some placer deposits.

# 6. RESULTS

This section summarizes the results of the test surveys. Detailed descriptions of individual site visits and test surveys are contained in Appendix A. Vertical resistivity profiles from the HLEM sounding inversions are contained in Appendix C.

GPR performance depends entirely upon the physical properties of the placer deposit. Yukon placer deposits may be subdivided into three classes (Section 2) based on their physical properties:

a. **Klondike Type:** Frozen placer deposits in unglaciated terrain found throughout the Klondike, Sixty Mile and Ladue River basins.

b. **Mayo Type:** Thawed placer deposits in glacial sediments found south and east of the continental glacial limit.

c. **Nansen Type:** Frozen placer deposits in glacial sediments found south and east of the continental glacial limit.

## 6.1 Klondike Type deposits

The Soya Creek, Klondike River, Gold Run Creek and Dominion Creek sites contain placer deposits classified as Klondike Type. A typical Klondike Type placer deposit consists of a layer of black muck overlying gravel on top of weathered bedrock. The muck layer varies from 2 to 20 m and consists of black organic clay with a variable silt fraction with occasional lenses of ground ice. Gravels are well rounded, moderately sorted and vary in thickness from 0 to 20 m. Large boulders (>1 m) are reported on some creeks. Locally, gravels have undergone epithermal (argillic) alteration, reducing granitic clasts to clay. Bedrock weathering varies from 3 m to tens of metres and well developed saprolite horizons can occur in areas underlain by schistose or phyllitic rocks. Undisturbed sequences are frozen to bedrock although a seasonal thaw extending one or two metres will occur in some areas.

Table 6-1 summarizes apparent resistivity and GPR attenuation constants in the four Klondike Type deposits. Apparent resistivities are taken from the results of the HLEM soundings and include the resistivity of the overburden (muck + gravel) and of bedrock. Davis and Annan (1987) present an expression for attenuation (eq. 4.16) which, after substituting GPR velocity for dielectric constant becomes:

$$\alpha = 5.57 x 10^4 \frac{\sigma}{v} \qquad (6.1)$$

where $\sigma$ is the electrical conductivity in Siemens per m and $v$ is GPR velocity in metres per nanosecond. This expression was used to calculate the attenuation constants using the measured resistivities and GPR velocities. In the case of bedrock, an average velocity of 0.161 m/ns was assumed.. The lowest overburden apparent resistivities were recorded in

areas with thick black muck while low bedrock resistivities appear to be associated with saprolite development in schists or phyllite.

**Table 6-1. Summary of electrical properties - Klondike Type placer deposits.**

| Site | $\rho_{overburden}$ ( Ω-m ) | $\alpha_{overburden}$ ( dB/m ) | $\rho_{bedrock}$ ( Ω-m ) | $\alpha_{bedrock}$ ( dB/m ) |
|---|---|---|---|---|
| Soya Creek | 770 | 4.43 | 509K | 0.001 |
| Klondike River | 466 | 8.42 | 466 | 7.42 |
| Gold Run Creek | 3431 | 1.31 | 113 | 30.6 |
| Dominion Creek | 2237 | 1.71 | 9574 | 0.361 |

Measured GPR velocities at the four Klondike Type placer deposits are summarized in Table 6.2. The best estimate of overburden velocity is the normal moveout velocity of the bedrock reflector. This quantity approximates the RMS velocity of overburden and minimizes discrepancies between drill hole and GPR indicated bedrock depths. The range of apparent velocities of individual layers (Dix velocities) is also shown. Dix velocities of black muck are significantly lower than those of gravel and variations in the thickness of muck can produce static shifts in the bedrock reflection. The sole bedrock Dix velocity may be overstated because of dip effects.

**Table 6-2. Summary of GPR velocities - Klondike Type placer deposits.**

| Site | Overburden $V_{NMO}$ (m/ns) | Overburden $V_{DIX}$ (range - m/ns) | Bedrock $V_{DIX}$ (m/ns) |
|---|---|---|---|
| Soya Creek | 0.163 | 0.147 | n/a |
| Klondike River | 0.139 | 0.071 - 0.154 | n/a |
| Gold Run Creek | 0.124 | 0.124 | n/a |
| Dominion Creek | 0.146 | 0.121 - 0.175 | 0.179(?) |

The relatively high overburden resistivity and absence of large velocity contrasts within overburden permit good resolution of bedrock in Klondike Type placer deposits. Figure 6.1 is an example of a GPR survey conducted under optimum conditions on

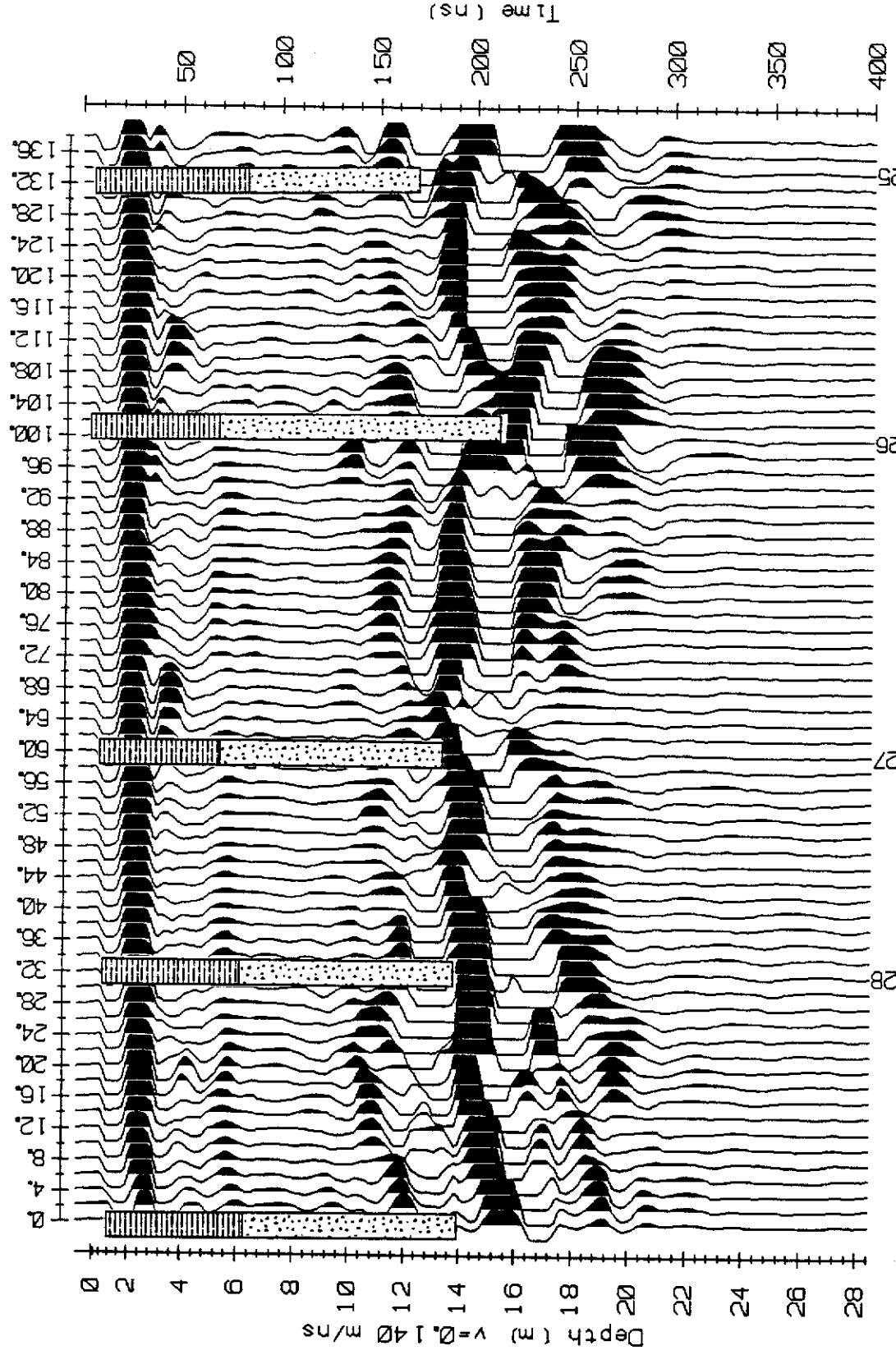


Figure 6.1. Profile radargram on line 1, Dominion Creek processed with SEC gain algorithm. Strong bedrock reflection occurs at 200 ns and is verified by auger drill hole data. Dashed upper portions of drill hole logs indicate muck and lower stippled portions indicate gravel. All holes bottom in bedrock.

Dominion Creek. A strong bedrock reflection is recorded, static shifts introduced by variations in muck thickness are minimal and there is close agreement between depth to bedrock calculated with $V_{NMO}$ and the drill hole indicated bedrock depth. In some situations, bedrock can be difficult to resolve because of:

a. Signal attenuation in black muck

b. Signal scattering in boulder layers

c. Poor dielectric contrast between overburden and bedrock

d. Poor returns from dipping bedrock

e. Cultural noise (buried metal)

In general, these problems limit rather than preclude the use of GPR in Klondike Type placer deposits.

An example of attenuation by black muck is shown in Figure 6.2 where a muck layer screens deeper reflections near the start of the profile. This problem is particularly serious if a survey is run over thawed muck where penetration may be as low as 3 or 4 m. Fortunately, ice lenses and wedges are common in muck layers and these provide "windows" through which deeper reflections may be detected.

Scattering of radiation by boulder layers was encountered at a site on lower Dominion Creek (Figure 6.3). Bedrock is at approximately 23 m in this area and the deepest recorded reflection is clearly within overburden. The reflection is irregular and steeply dipping diffraction trails occur below it. Lag deposits also produce this pattern (Figure 6.4). Fortunately, in this case boulders or heaved blocks of bedrock define the reflector of interest.

Bedrock reflections in areas underlain by resistant rock tend to be weaker and discontinuous. Power and McIntyre (1990) noted the importance of clay weathering in GPR surveys during surveys on Wounded Moose and Australia Creeks in the south Klondike. GPR indicated depths to fresh bedrock were consistently short of the drill hole depths and this discrepancy did not vary with depth to bedrock as would be expected for a velocity mismatch. This "static shift" was attributed to intense clay weathering of bedrock. Below 0°C clay retains a significant proportion of liquid bound water in contrast to cleaner sediments which freeze completely (McNeill 1980). This creates a dielectric contrast at the top of bedrock which reflects GPR radiation. The dielectric contrast between frozen gravel and fresh bedrock is smaller, producing a weaker bedrock reflection. Figure 6.5 is an excerpt from a survey in an area underlain by blocky quartzite. The bedrock reflection is difficult to pick from amongst the overburden reflections and multiples and is particularly weak where the reflector dips. It is very difficult to reliably pick bedrock in these cases without drill hole information or "walking off" bedrock outcrops.

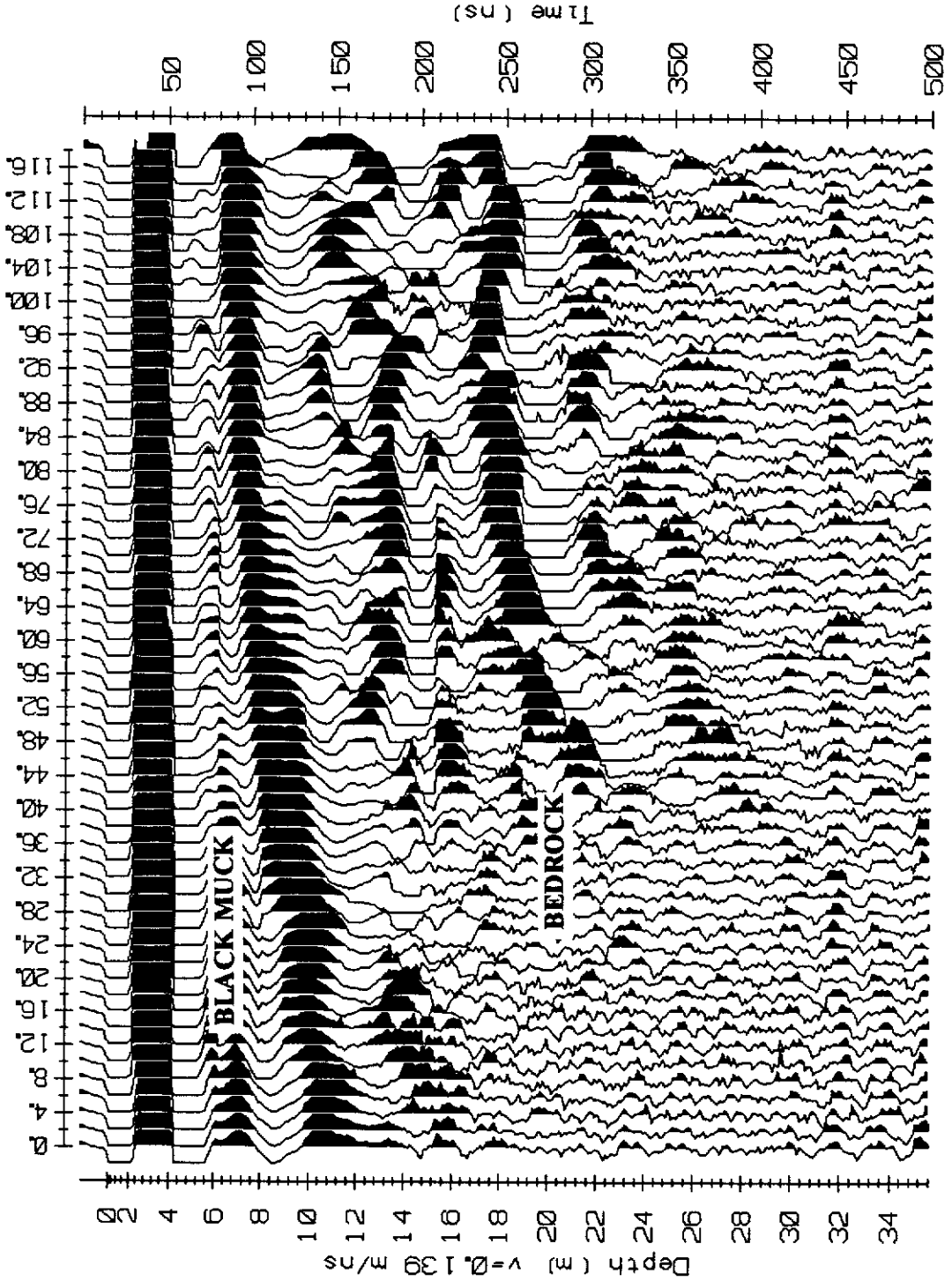


Figure 6.2. Profile radargram from Klondike River test site. A layer of black muck, thinning to the right, screens bedrock reflections near the start of the profile.

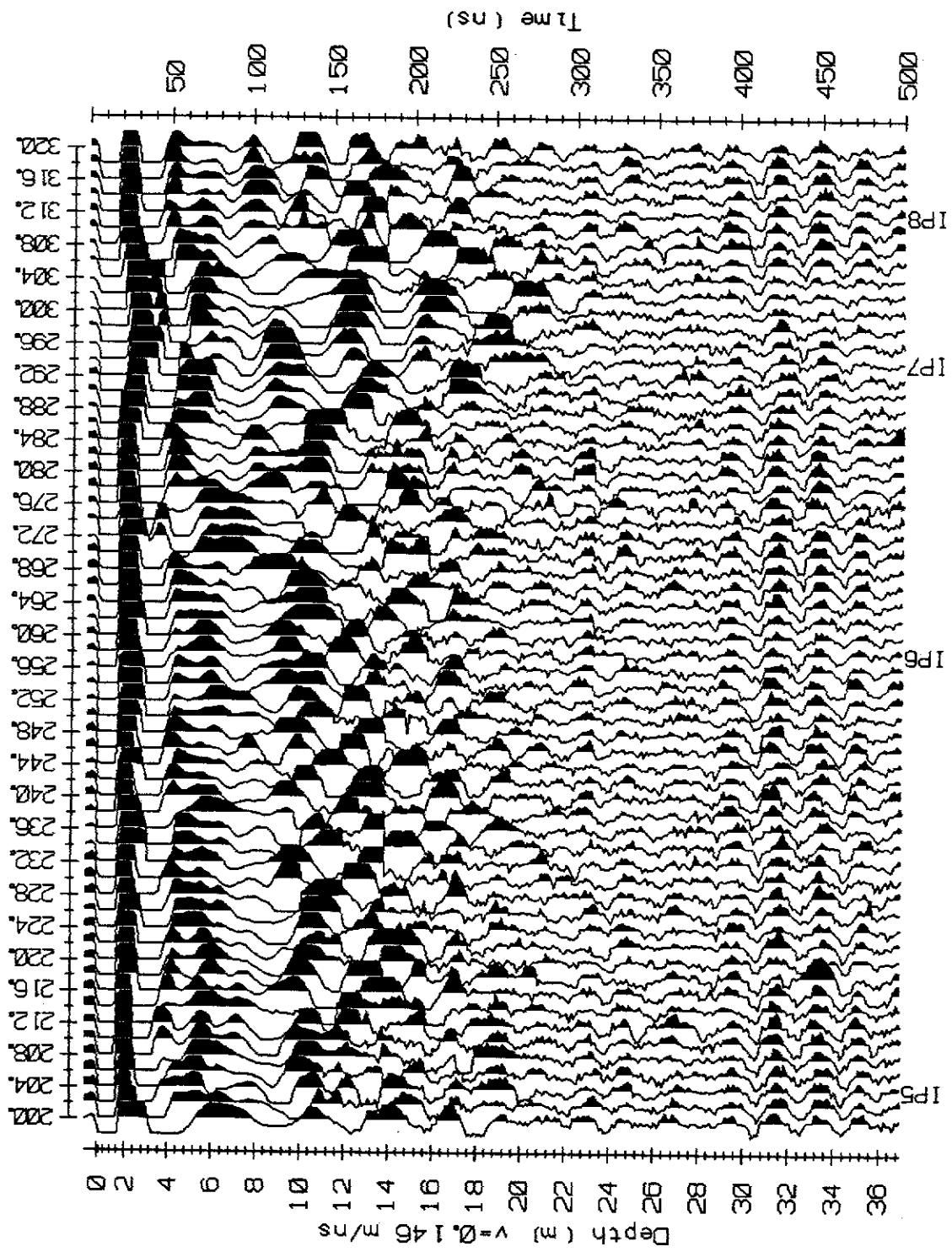


Figure 6.3. Profile radargram from lower Dominion Creek. A layer of boulders at a depth of 10 m scatters the radar signal, screening deeper reflections and producing steeply dipping diffraction trails.

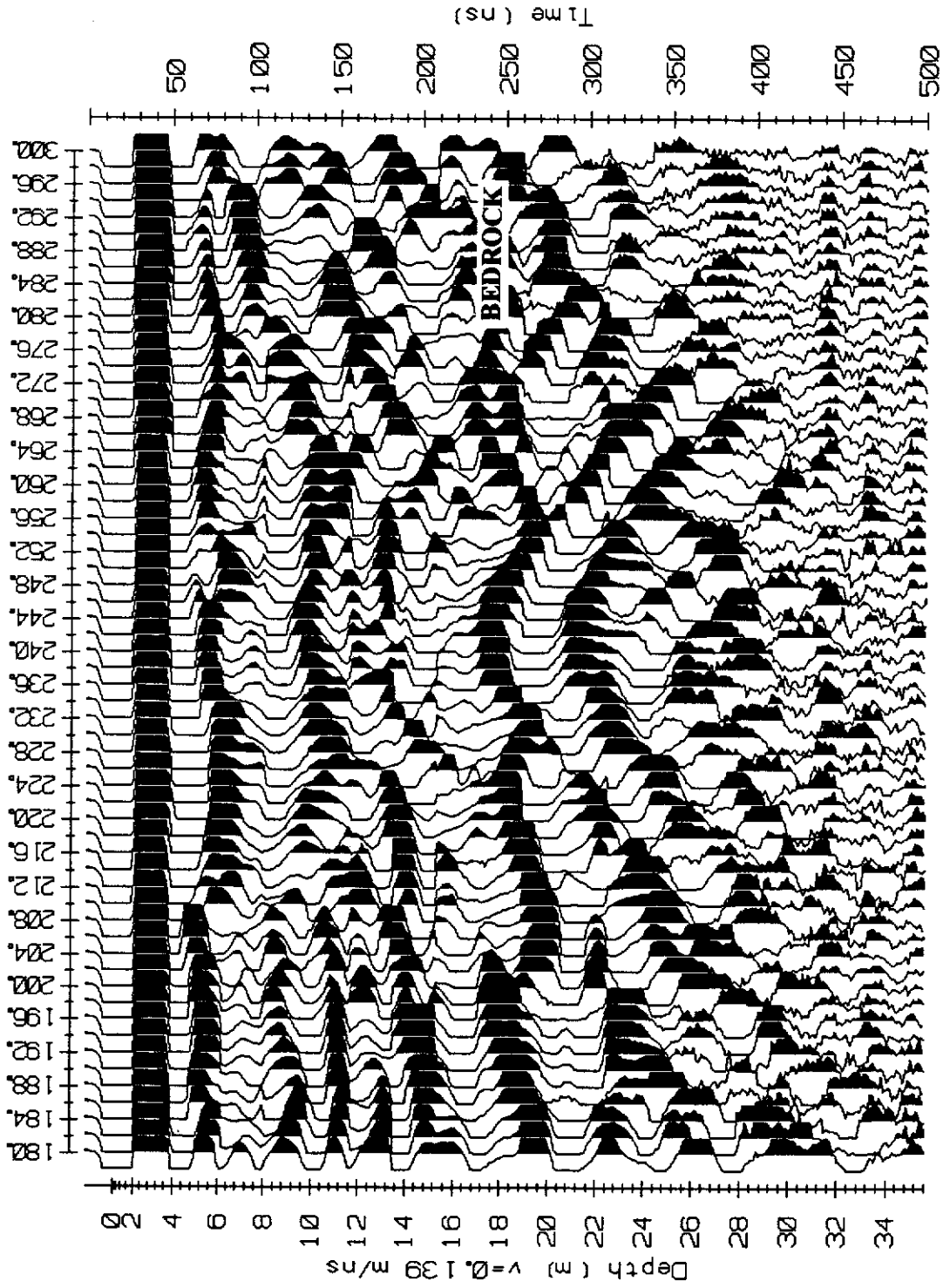


Figure 6.4. Profile radargram from Klondike River test site. Irregular bedrock surface or boulder lag deposit on bedrock produces diffractions.

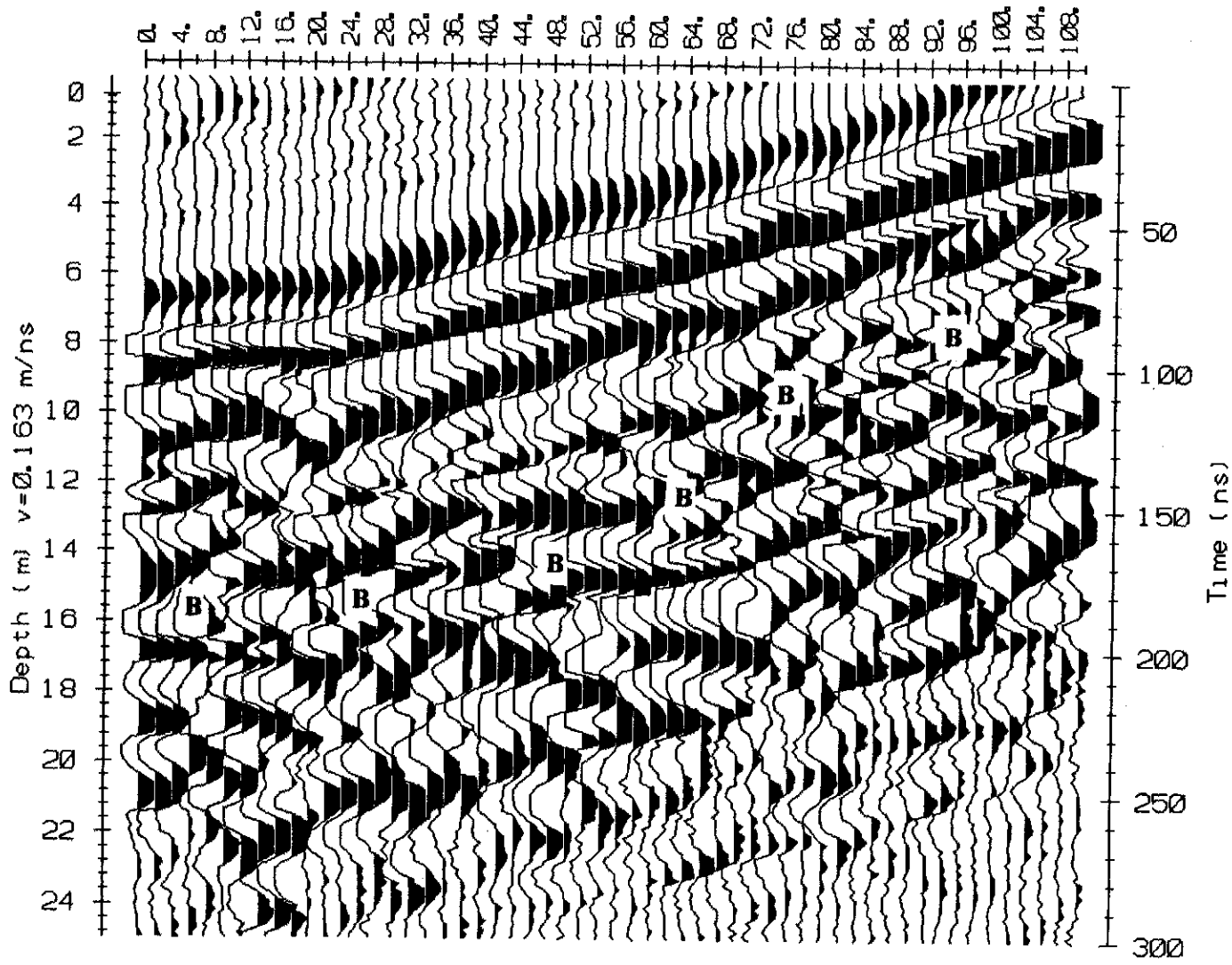


Figure 6.5. Profile radargram from Soya Creek test site. Bedrock depths from nearby drill fence are projected into section (B). Bedrock reflection is discontinuous and difficult to resolve in places as a consequece of dip and poor velocity contrast.

Metallic debris is common on creeks in the Klondike area and occasionally is a problem in GPR surveys. Figure 6.6 is an excerpt from a survey of dredge tailings on Gold Run Creek. Reflections from metallic debris contaminate the radargram and obscure deeper reflections. Cultural noise is rarely a major problem and is occasionally useful in locating heavy equipment parts.

Table 6-3 summarizes observed penetration at the four Klondike Type placer deposit test sites. The depth of penetration is quite evident in the radargrams; it is the depth at which the relatively low frequency signal is obscurred by higher frequency noise or by horizontal multiples. Effective depths of penetration would be about 2 m less than the average penetration listed in the table.

**Table 6-3. Summary of GPR penetration at 25 MHz - Klondike Type placer deposits**

| Site | Maximum Penetration (m) | Minimum Penetration (m) | Average Penetration (m) |
|---|---|---|---|
| Soya Creek | 24 | 15 | 18 |
| Klondike River | 28 | 10 | 24 |
| Gold Run Creek | 28 | 10 | 18 |
| Dominion Creek | 26 | 10 | 17 |
| **Range / average** | **28** | **10** | **19** |

GPR works quite well in Klondike Type placer deposits which are underlain by altered, moderate to flat dipping bedrock and relatively uniform muck. Fresh or dipping bedrock, layers of large boulders or thick muck can reduce the effectiveness of GPR by either screening the bedrock reflections or reducing their amplitude to the point where it becomes difficult to pick bedrock reflections without depth controls.

## 6.2 Mayo Type placer deposits

The Livingstone Creek, Stewart River, Lightning Creek and Duncan Creek test sites are classified as Mayo Type placer deposits. These are thawed placer deposits in glaciated terrain. A typical Mayo Type placer deposit consists of poorly sorted gravel overlying bedrock and covered by silt, clay, sand and/or till. Bedrock is usually weathered in preserved preglacial deposits while fresh bedrock often underlies interglacial deposits. The proportion of clay and silt within overburden is a function of proximity to the ice limit; proximal ice marginal sediments are usually coarse while distal proglacial sediments

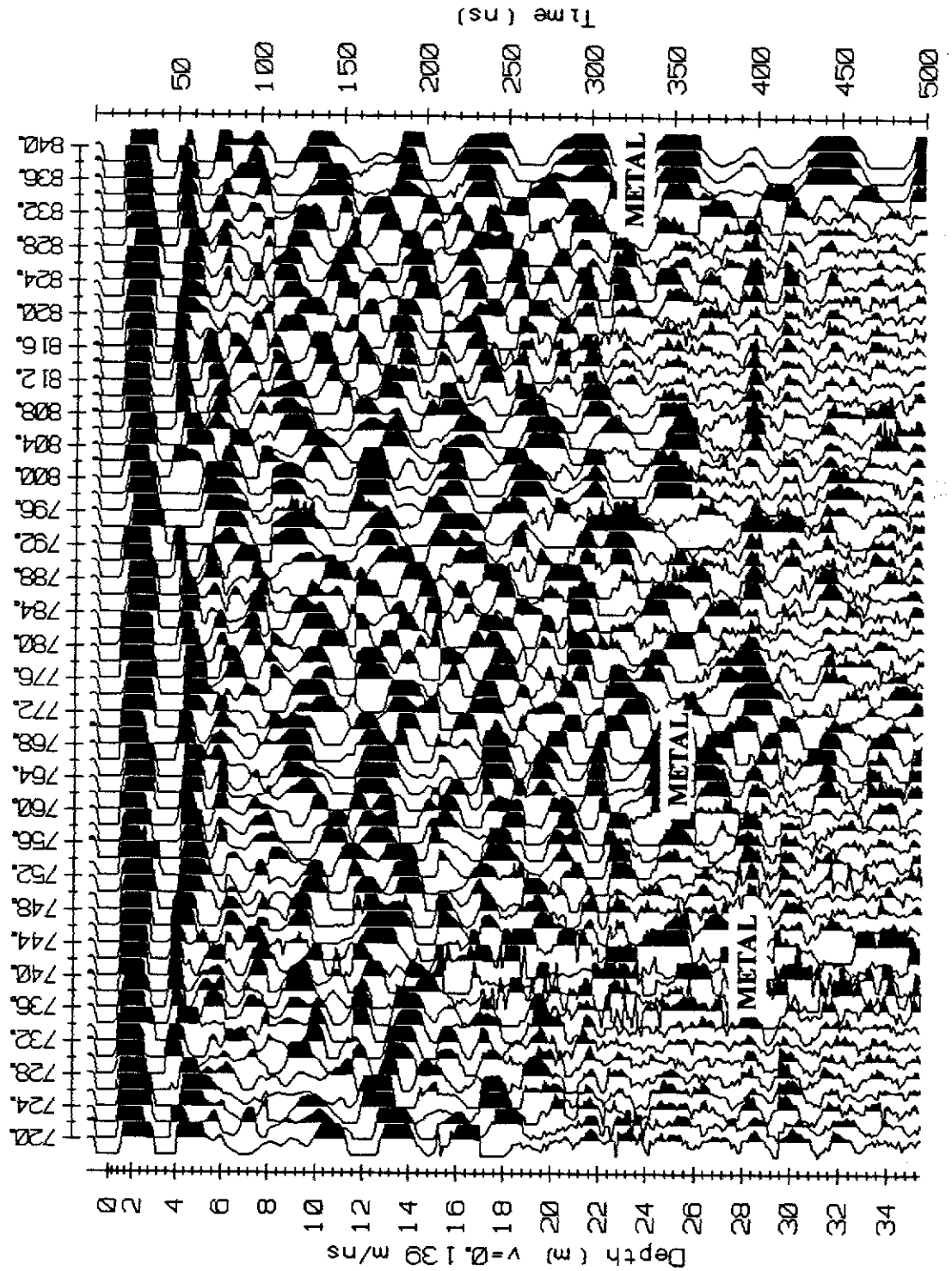


Figure 6.6. Profile radargram from a survey of dredge tailings on lower Gold Run Creek showing noise introduced by nearby metal.

contain a higher proportion of fines and may contain lacustrine clay beds. It is possible to have a series of different sediment types overlying basal gravels in areas affected by complex glaciation patterns. Preglacial deposits are commonly preserved beneath thick proglacial sediments such as lacustrine clay or silt.

Electrical properties of Mayo Type placer deposits are summarized in Table 6-4. Apparent resistivities are lower and attenuation higher in Mayo Type deposits than in Klondike Type deposits as a consequence of their thawed state. The proportion of fine sediments is the most significant factor controlling electrical properties. The Livingstone Creek area is noted for thick clay and has a correspondingly low overburden resistivity while the Lightning Creek site is underlain by coarse resistive sediments.

**Table 6-4. Summary of electrical properties - Mayo Type placer deposits.**

| Site | $\rho_{overburden}$ ( Ω-m ) | $\alpha_{overburden}$ ( dB/m ) | $\rho_{bedrock}$ ( Ω-m ) | $\alpha_{bedrock}$ ( dB/m ) |
|---|---|---|---|---|
| Livingstone Creek | 548 / 115 | 14.7 / 78.1 | 776 | 4.80 |
| Stewart River | 255 | 16.1 | 8075 | 0.460 |
| Lightning Creek | 5460 | 1.15 | n/a | n/a |
| Duncan Creek | 290 | 15.0 | 1450 | 2.56 |

(assumed bedrock velocity - 0.15 m/ns)

**Table 6-5. Summary of GPR velocities - Mayo Type placer deposits.**

| Site | Overburden $V_{NMO}$ (m/ns) | Overburden $V_{DIX}$ (range - m/ns) | Bedrock $V_{DIX}$ (m/ns) |
|---|---|---|---|
| Livingstone Creek | 0.062 | 0.057 - 0.065 | n/a |
| Stewart River | 0.136 | 0.099 - 0.173 | n/a |
| Lightning Creek | 0.089 | 0.083 - 0.100 | n/a |
| Duncan Creek | 0.128 | 0.121 - 0.135 | n/a |

GPR velocities observed in Mayo Type placer deposits are summarized in Table 6-5. Velocities are slower and fall within a wider range reflecting the presence of liquid water in sediments of different porosity. Porosity and water saturation contrasts within overburden cause reflections at the boundaries between different sediment types and allow the internal structure of overburden to be resolved in fine detail. These reflections are

considered noise in placer exploration where the bedrock reflection is the primary target. In general, the overall GPR velocity of overburden is controlled by the level of the water table with deposits in water saturated environments (eg. Livingstone Creek) exhibiting slower velocities than partially drained deposits (eg. Duncan Creek).

In Mayo Type placer deposits consisting of coarse, relatively uniform sediments, impressive penetration can be achieved. Figure 6.7 is an excerpt from the survey on Lightning Creek where bedrock was successfully mapped at depths in excess of 20 m. More commonly, GPR performance is limited by:

a. Signal attenuation by clay-rich sediments

b. Signal scattering by coarse boulder layers

c. Signal cluttering by reflections within overburden

d. Multiples generated at the boundary between water saturated and dry sediments.

e. Poor or gradational bedrock/overburden velocity contrast

The effects of these limiting factors and measures to overcome them are best described with examples.

Preglacial placer deposits in the Livingstone Creek district are preserved beneath a blanket of up to 20 m of lacustrine clay and silt. An excerpt from the profile survey at the Livingstone Creek test site is shown in Figure 6.8. No continuous discordant reflection is apparent in the radargram and all reflections appear to be overburden contacts. The effective depth of penetration is approximately 12 m in this area and all reflections below this depth are screened by the clay layer and by attenuation within the overlying clay-rich till.

Figure 6.9 in an excerpt from the Duncan Creek profile illustrating scattering of GPR radiation by coarse boulders. Coherent reflections largely dissappear from the radargram in this section of the profile, steeply dipping diffraction arrivals appear and the depth of penetration is reduced by scattering within the upper till unit.

Signal cluttering by reflections within overburden is a serious problem in Mayo Type placer deposits. An example of this phenomenon is shown in Figure 6.10, an excerpt from the Stewart River test site survey. The overburden stratigraphy in this area consists of alluvial gravel and sand and overbank silt deposits. These horizons have contrasting porosities and degrees of water saturation, creating a complex series of reflections within overburden. Auger drill holes in this area were stopped by a layer of boulders at 5 to 7 m. Consequently, apart from outcrop about 200 m south of the test site

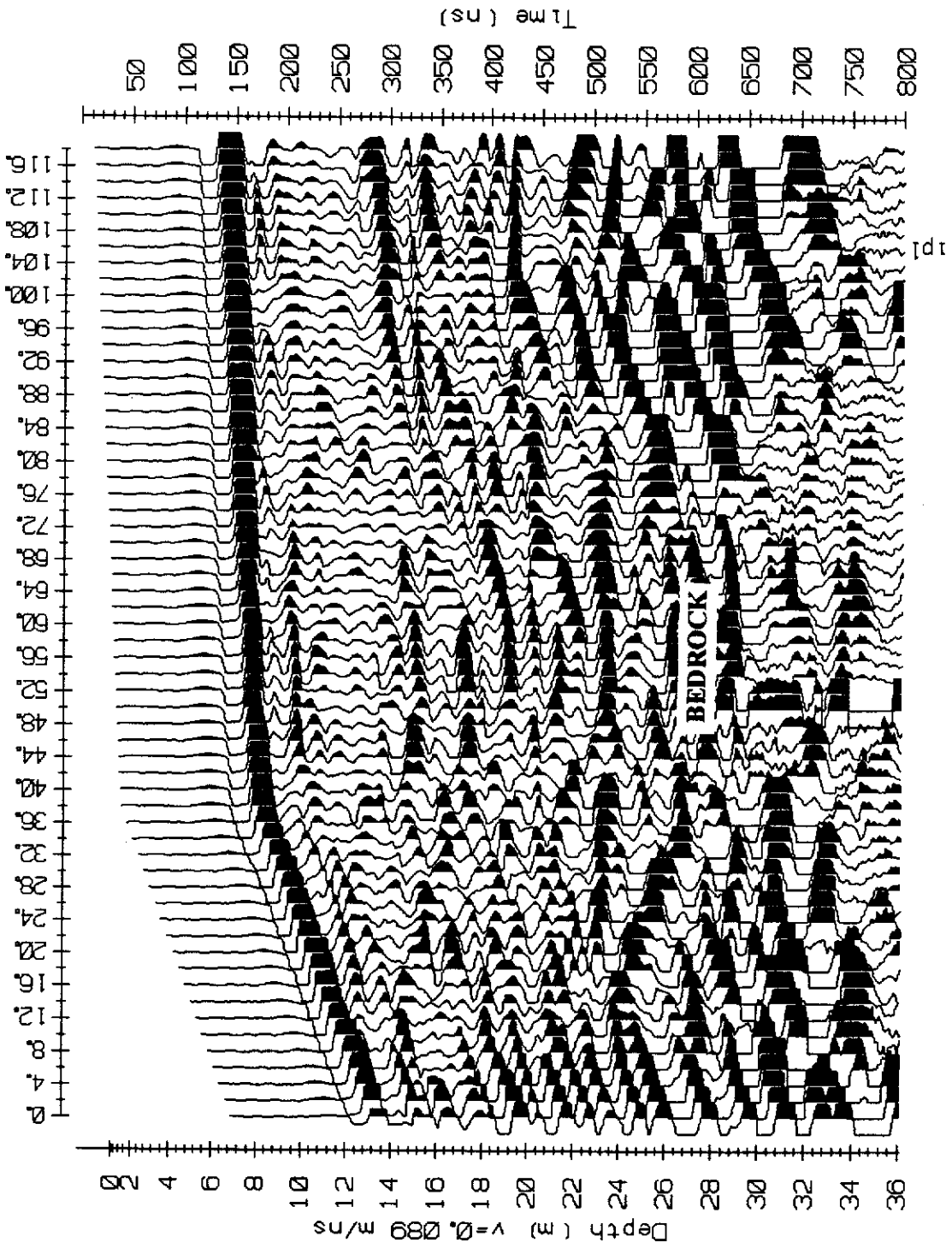


Figure 6.7. Profile radargram from Lightning Creek showing bedrock reflection beneath reflections generated within thawed overburden.

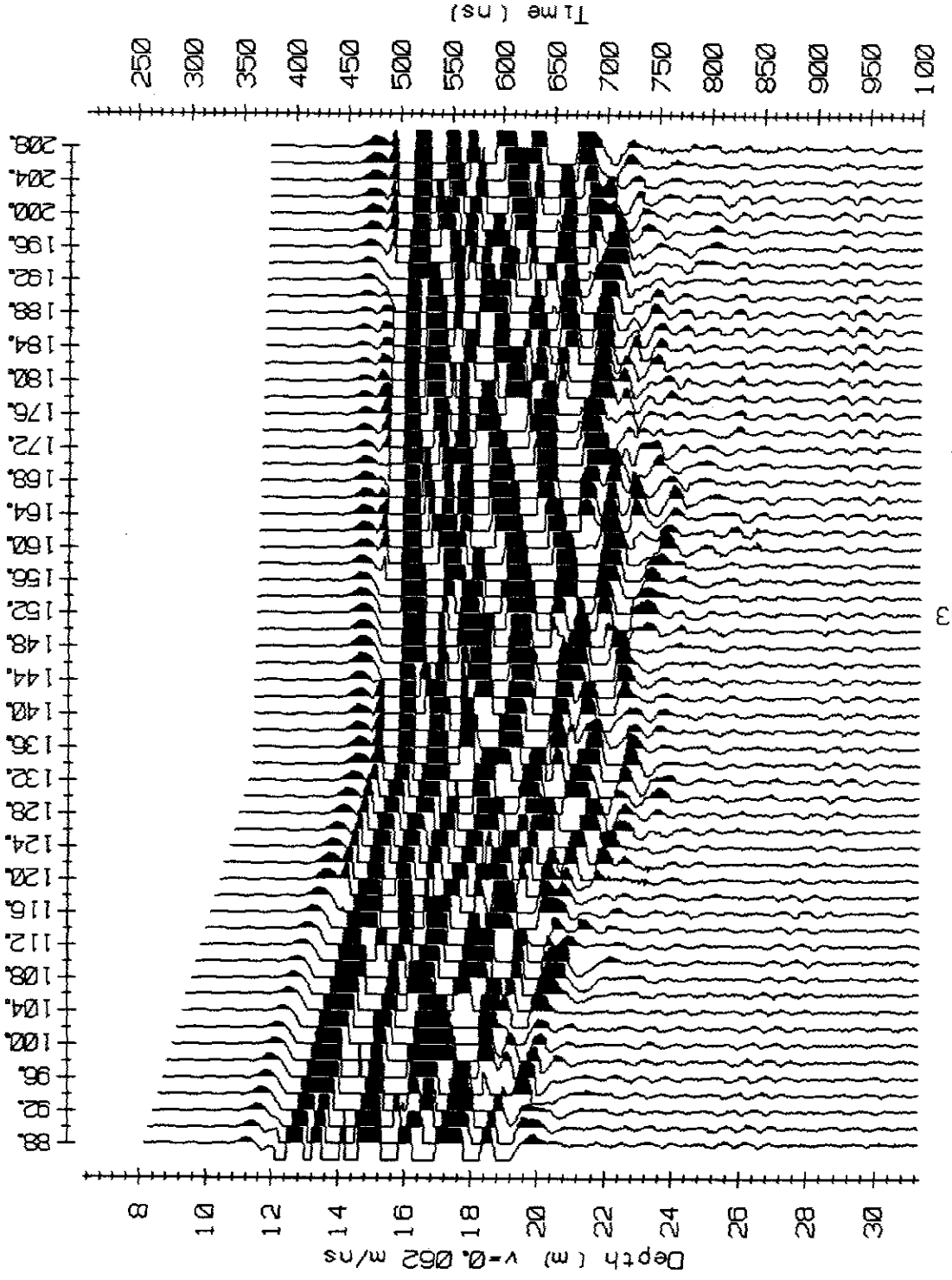


Figure 6.8 Profile radargram from Livingstone Creek test site. Conductive clay in thawed placer deposit screens reflections below 8 to 10 m.

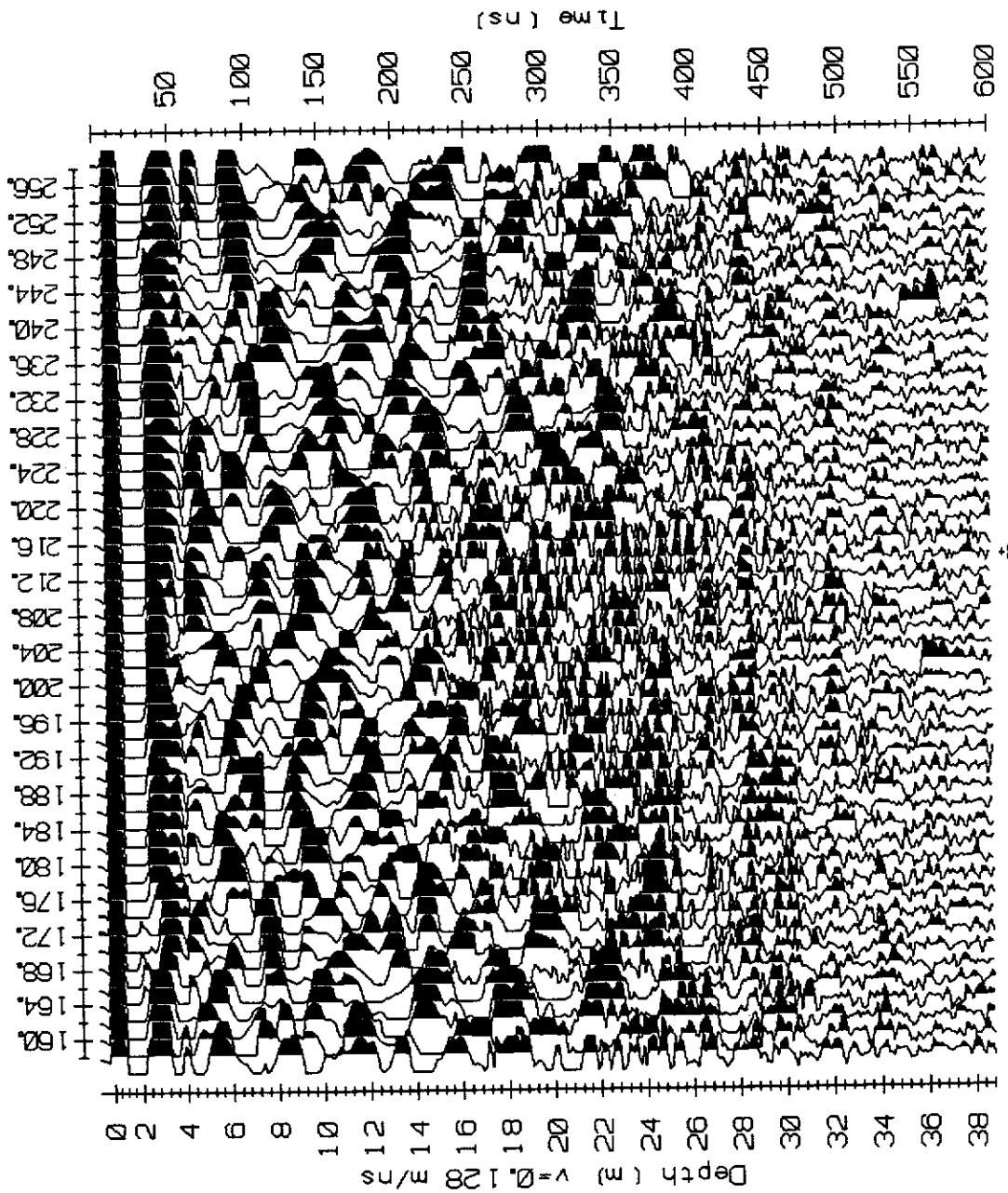


Figure 6.9. Profile radargram from Duncan Creek showing scattering of radar signal by boulders within an upper till layer.

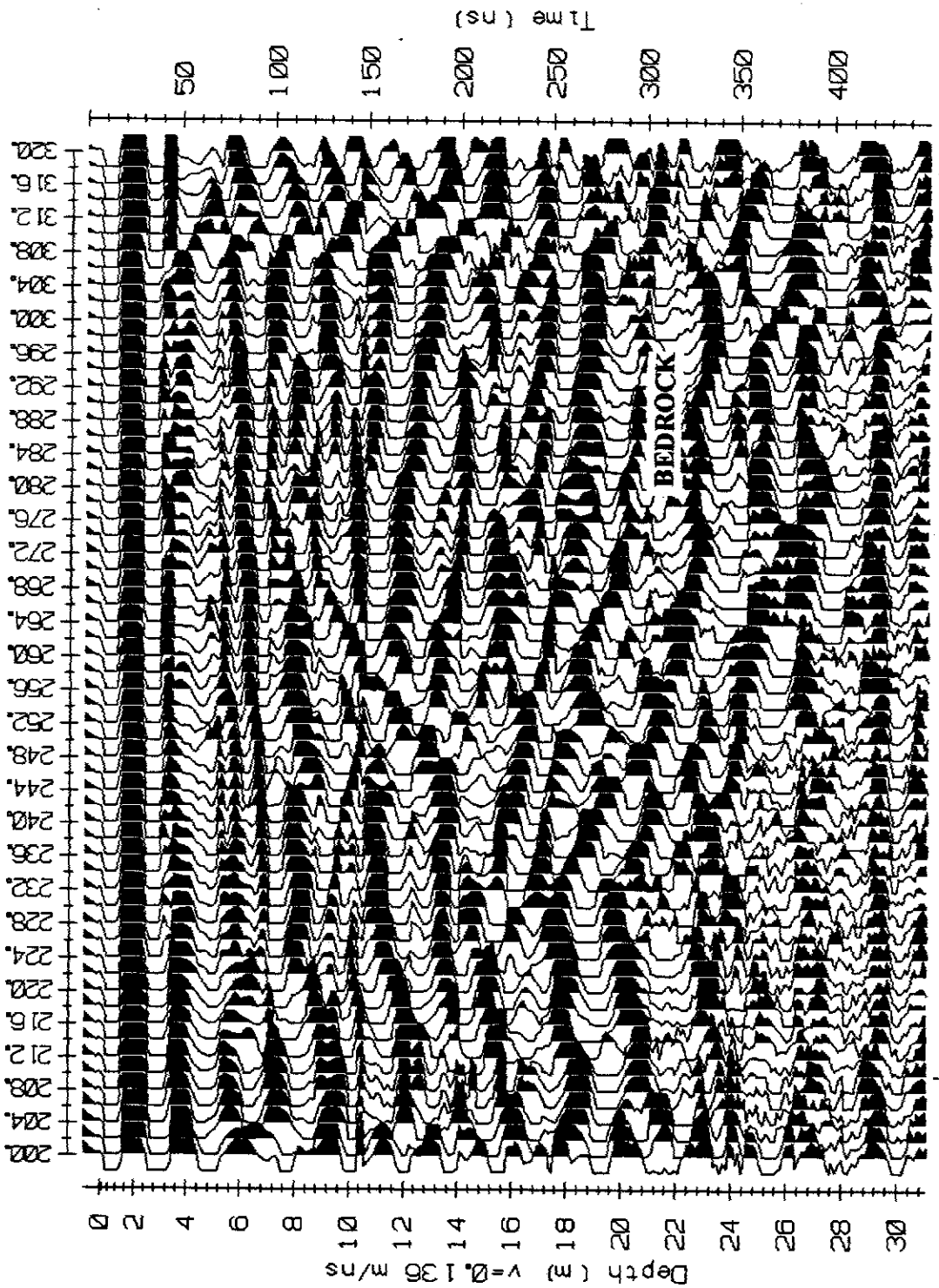


Figure 6.10. Profile radargram from Stewart River survey showing the effects of signal cluttering. Reflections generated within thawed overburden mask a bedrock reflection at 20 m. Section processed with AGC and gain limited to 3% of full range.

on the opposite side of the river, there is no hard information on the depth to bedrock. A continuous discordant reflection at 250 to 300 ns is probably bedrock based on the manner in which overlying reflectors are truncated by it. Filtering and variable gain algorithms can be used to suppress near surface reflections and enhance deeper bedrock reflections. Automatic gain control (AGC) tends to enhance all reflections equally and thus is not a useful tool in attacking signal cluttering. Variable gain algorithms which correct for spherical spreading and conduction losses in overburden are more useful provided the bedrock reflection is relatively strong and has little relief. To perform this correction, the overburden GPR velocity must be known and an estimate of attenuation made. Figure 6.11 shows the previous section processed with spherical spreading and exponential correction gain applied. Filtering can also be used if the bedrock reflection has low relief (trace to trace stacking) or if the frequency of the bedrock reflection is lower than the overburden reflections (low pass filtering).

When the ground surface is frozen, Mayo Type placers deposits with high water tables can generate strong multiples. Figure 6.12 is an excerpt from the Lightning Creek survey and shows the effect of multiples. A CMP velocity survey in the area found that multiples with a recurrence time of approximately 60 ns were being generated here between the water table and base of frost. These form bands of apparent reflections in the profile. True reflections from the base of frost and a lower gravel bed arrive at approximately 120 and 210 ns; the rest are predominantly reverberations in the top 6 m of the profile. This problem could be mitigated by conducting surveys only on thawed ground.

In Mayo Type placer deposits, bedrock reflections originate at the contact between water saturated sediments and dry bedrock. In contrast to Klondike Type placers, bedrock reflections are suppressed by alteration at the top of bedrock since this tends to produce a gradational change in water content. At the two Mayo Type sites where bedrock was successfully mapped by GPR, bedrock was resistant and strong reflections were observed.

**Table 6-6. Summary of GPR penetration at 25 MHz - Mayo Type placer deposits**

| Site | Maximum Penetration (m) | Minimum Penetration (m) | Average Penetration (m) |
|---|---|---|---|
| Livingstone Creek | 14 | 10 | 12 |
| Stewart River[1] | 24 | 15 | 18 |
| Lightning Creek | 28 | 15 | 20 |
| Duncan Creek | 26 | 14 | 19 |
| **Range /Average** | **28** | **10** | **17** |

1. Stewart River penetration data is at 50 MHz

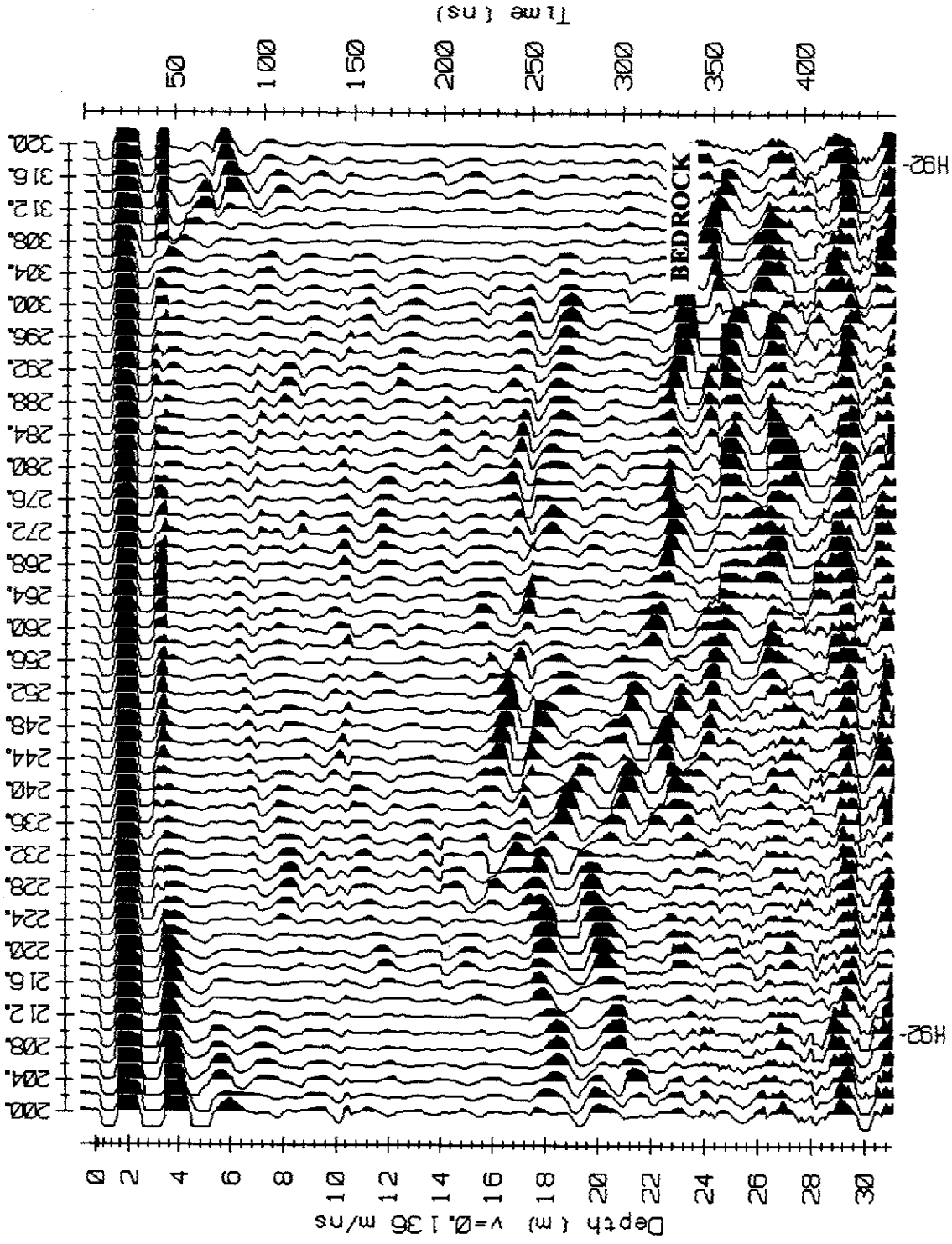


Figure 6.11. Profile radargram shown in Figure 6.10 reprocessed with spherical spreading and exponential attenuation correction gain algorithm. Surface reflections are suppressed to enhance the bedrock reflection.

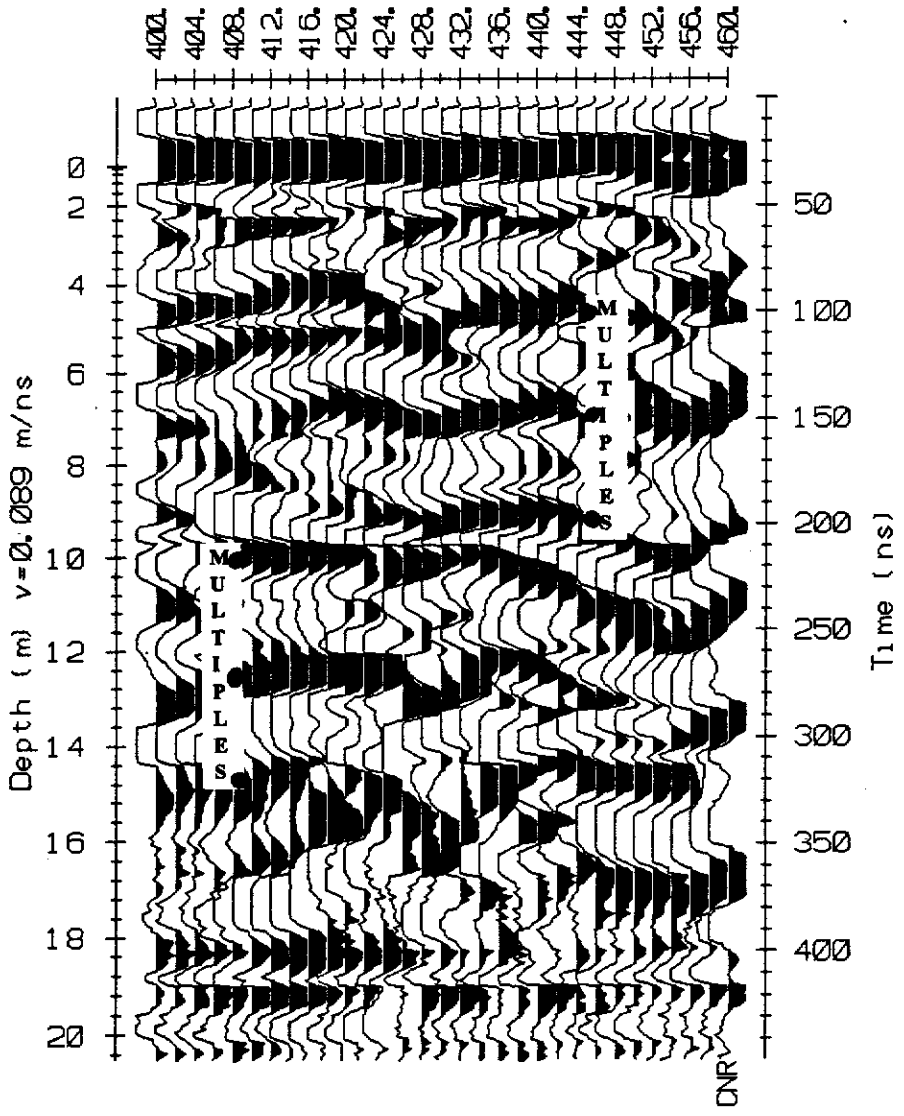


Figure 6.12. Multiples generated between the base of frost and the water table in a radargram taken on Lightning Creek. Other reflections interfere with the multiples, creating the impression that they are true reflections. CMP survey conducted on this section of the survey line determined that the arrivals have the same normal moveout velocity.

Table 6-6 summarizes observed penetration at the four Mayo Type placer deposit test sites. Depths of penetration are slightly less than those observed in Klondike Type placer deposits because of higher attenuation in thawed ground. Effective depths of penetration would be about 2 m less than the average penetration.

GPR works well in Mayo Type deposits which consist of coarse overburden underlain by moderately dipping resistant bedrock. Attenuation within clay and silt can seriously limit the depth of penetration and can be a problem in surveying these deposits. Signal cluttering by numerous overburden reflections and the generation of multiples between the base of frost and the water table degrade data quality and lower the effective depth of penetration. These problems can be mitigated by filtering and adjusting the gain during data processing, by lowering the operating frequency, by walking surveys off bedrock outcrops or by drilling or excavating depth controls.

## 6.3 Nansen Type placer deposits

Frozen placer deposits in glaciated terrain are termed Nansen Type placer deposits for the purposes of this study. Two test sites fall into this classification: Discovery Creek, near Mt. Nansen in the Carmacks area and Frying Pan Creek in the Burwash area. An average Nansen Type placer deposit consists of frozen poorly sorted gravel overlain by silt, clay, till or colluvium. Bedrock can be either fresh or deeply altered depending upon whether the deposit is preglacial or interglacial. Nansen deposits differ from Klondike Type deposits in that the overburden has a higher overall proportion of clay and generally little or no black muck.

Electrical properties and GPR velocities of Nansen Type placer deposits are summarized in Tables 6-7 and 6-8. Overburden apparent resistivities are suprisingly low given their frozen state. Frying Pan Creek has discontinuous permafrost and overburden may have been partially thawed beneath the HLEM survey site. Overburden at Discovery Creek was frozen to bedrock at the time of the survey. The low apparent resistivities are attributed to the high overburden clay content. GPR velocities are high reflecting the frozen state of overburden. High radar velocities permit acceptable penetration despite high attenuation in this environment. On average, attenuation constants are higher than those encountered in Klondike Type placer deposits.

**Table 6-7. Summary of electrical properties - Nansen Type placer deposits.**

| Site | $\rho_{overburden}$ ( Ω-m ) | $\alpha_{overburden}$ ( dB/m ) | $\rho_{bedrock}$ ( Ω-m ) | $\alpha_{bedrock}$ ( dB/m ) |
|---|---|---|---|---|
| Discovery Creek | 181 | 20.8 | 652 | 5.3 |
| Frying Pan Creek | 137 | 23.9 | 1002 | 3.7 |

(assumed bedrock velocity - 0.160 m/ns)

**Table 6-8. Summary of GPR velocities - Nansen Type placer deposits.**

| Site | Overburden $V_{NMO}$ (m/ns) | Overburden $V_{DIX}$ (range - m/ns) | Bedrock $V_{DIX}$ (m/ns) |
|---|---|---|---|
| Discovery Creek | 0.148 | 0.148 | n/a |
| Frying Pan Creek | 0.170 | 0.170 | n/a |

GPR performance in Nansen Type deposits is naturally similar to performance in Klondike Type deposits. Optimum resolution of bedrock requires a flat to moderately dipping, clay altered bedrock surface and relatively coarse overlying sediments. The absence of a muck layer creates relatively uniform overburden and reduces static shifts. Signal penetration is usually less than that encountered in Klondike Type placer deposits on account of the higher clay content. Figure 6.13 is an excerpt from the survey conducted on Frying Pan Creek. Fresh bedrock occurs at a shallow depth (4 to 7 m ) and the overburden appears to contain some liquid water. This creates a good velocity contrast and allows easy mapping of bedrock. Figure 6.14 is an example of a radargram taken under good conditions at Discovery Creek. It reveals shallow bedrock beneath till and colluvium on an elevated bench. Unfortunately radargrams of this quality are the exception, not the norm.

Most of the problems encountered in surveying Nansen Type placer deposits stem from a poor velocity contrast between bedrock and overburden. At Discovery Creek, bedrock is often physically weathered to a depth of several tens of metres. The bedrock contact is not sharp but instead is marked by a gradual increase in the size of rock fragments. This presents a difficult target, particularly if bedrock is overlain by coarse sediments. In addition, the bedrock surface is irregular with steep dips occurring near channel margins. As mentioned earlier, dipping reflectors can be difficult to detect and require a tighter station spacing. The effect of these factors on signal quality is shown in Figure 6.15. The bedrock reflection is not continuous and is difficult to pick with any confidence using a 2 m station interval. The top of gravel frequently produces a stronger reflection than bedrock and a bedrock depth control is necessary to ensure that the correct reflection is identified. Walking off bedrock is little help is this situation because the bedrock reflection often disappears near the banks of the creek. Consequently, a known bedrock reflection on the hill side cannot be followed into the creek bottom.

Most placer deposits in glaciated terrain are interglacial and deposited on fresh bedrock. Consequently, bedrock reflections in Nansen Type deposits will often be of poor quality. Frequent depth controls or implementation of tie-line techniques discussed in the next section may be required. Observed GPR penetration in Nansen Type deposits is summarized in Table 6-9.

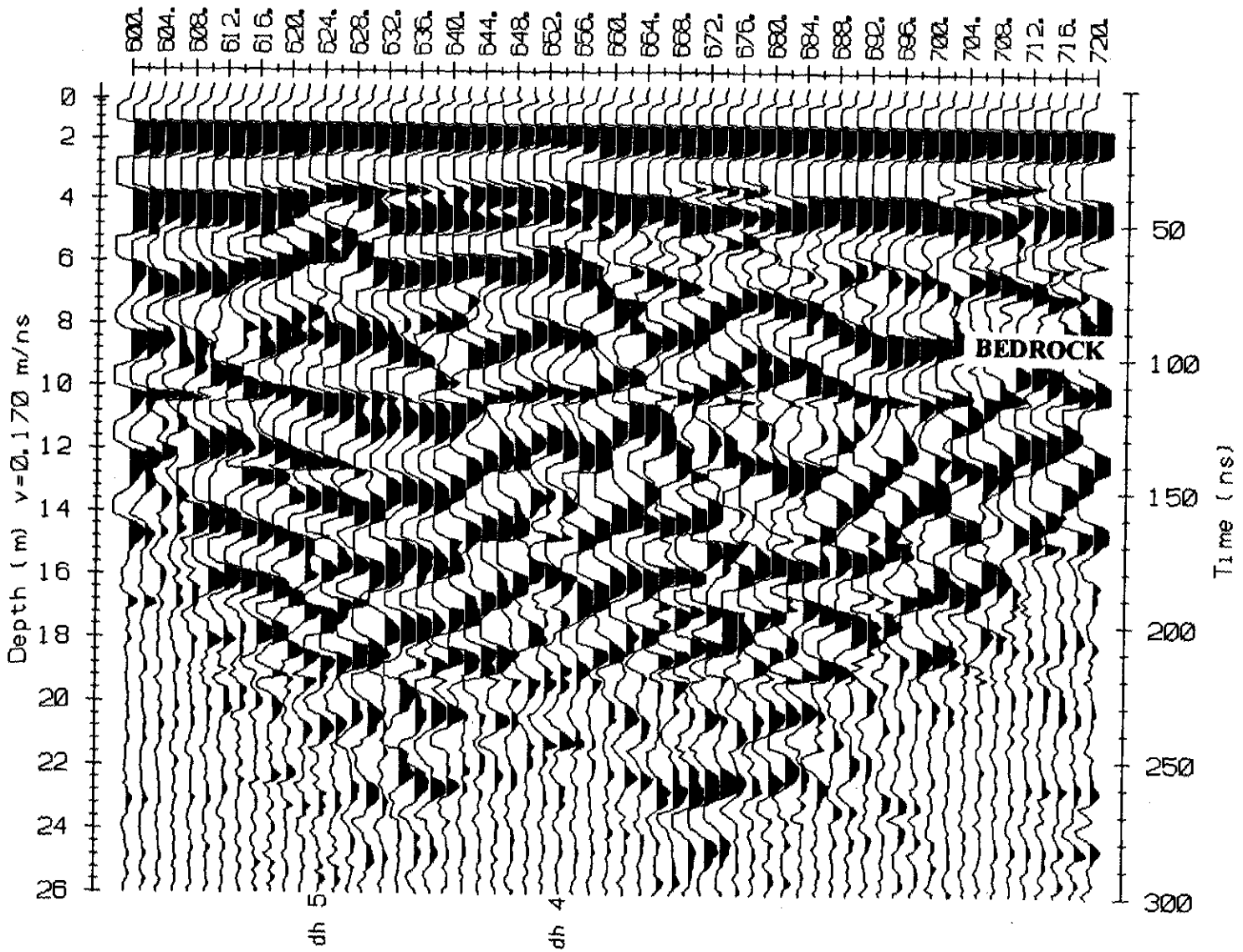


Figure 6.13. Profile radargram from Frying Pan Creek survey. Bedrock reflection is beneath a reflection from the base of overflow ice.

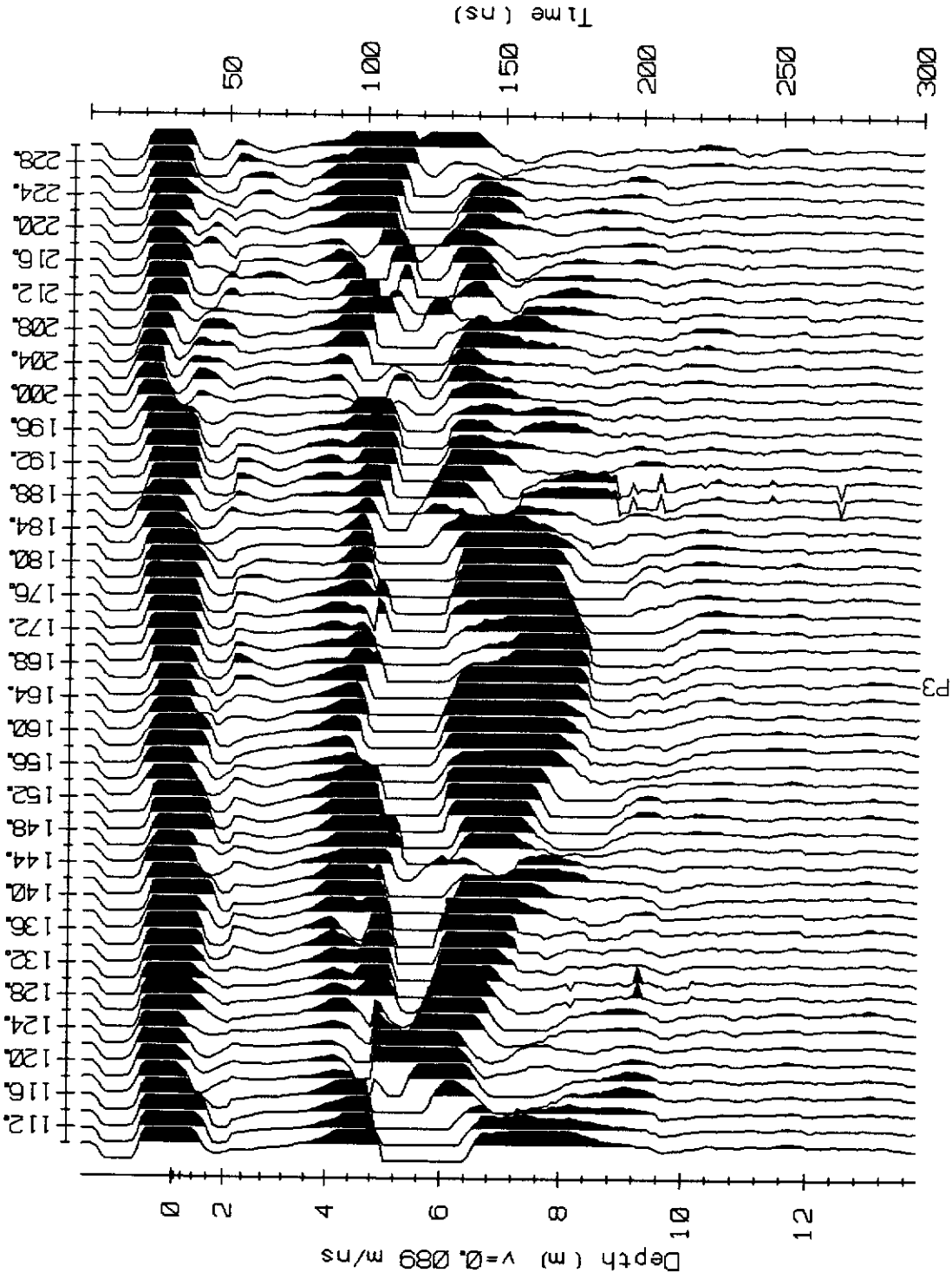


Figure 6.14 Profile radargram from Discovery Creek. Bedrock reflection occurs at 4 - 6 m beneath a thin layer of till and colluvium. Simple overburden stratigraphy, shallow depth and flat attitude of bedrock reflector result in a strong reflection.

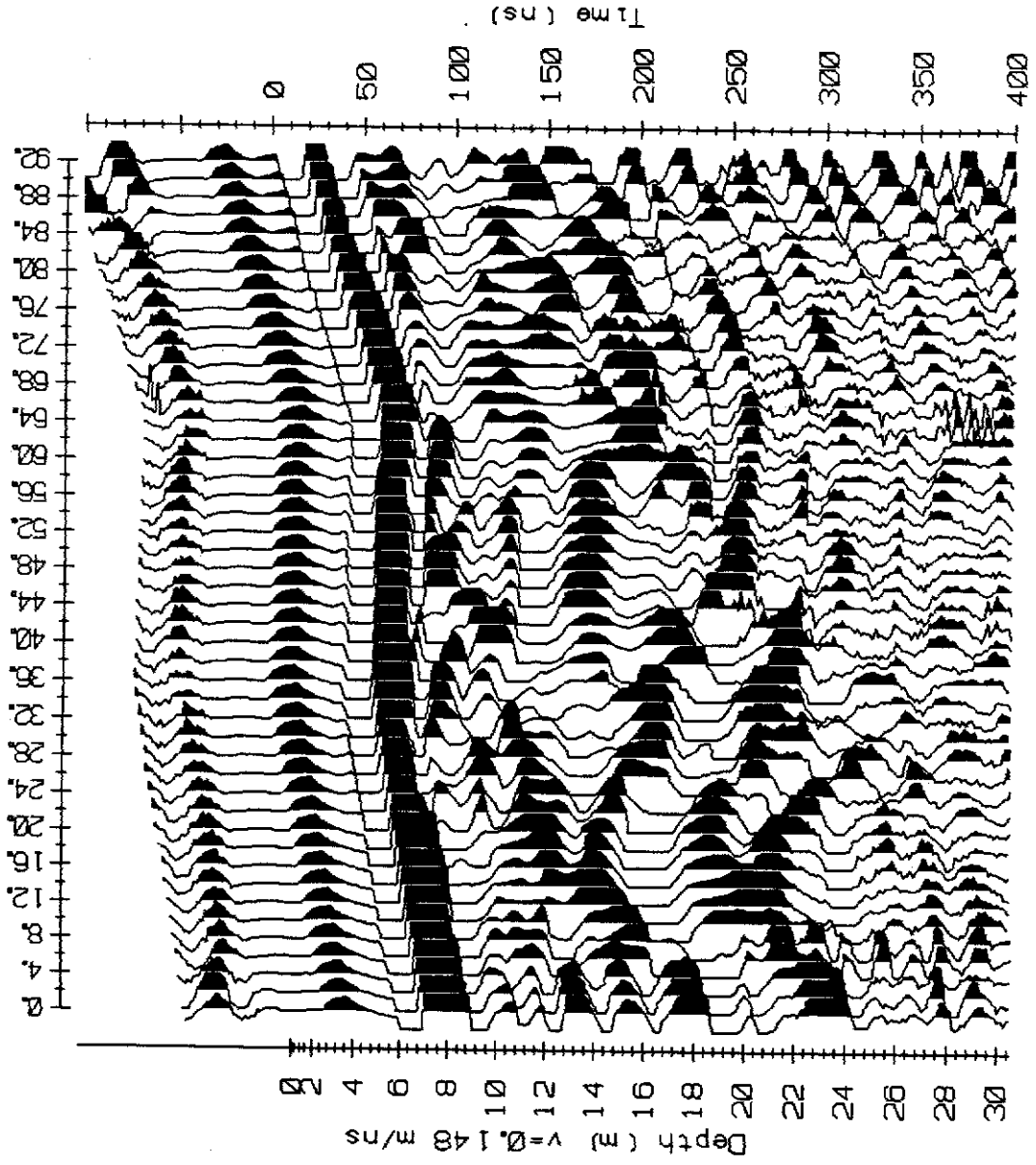


Figure 6.15 Profile radargram from Discovery Creek, Line 9. Weak reflections are recorded from a gradational dipping bedrock contact.

**Table 6-9. Summary of GPR penetration - Nansen Type placer deposits**

| Site | Maximum Penetration (m) | Minimum Penetration (m) | Average Penetration (m) |
|---|---|---|---|
| Discovery Creek | 18 | 10 | 14 |
| Frying Pan Creek | 24 | 14 | 18 |
| **Range /Average** | **24** | **10** | **16** |

## 6.4 Test production survey

A test survey was conducted over a grid of approximately 3 line-km at Discovery Creek to determine what production rates might be expected in a GPR survey of a placer deposit. A description of the test is contained on page A-79 and Figure 6.16 displays the test site and survey equipment. The property owner ploughed 4 m wide lines in a pattern which allowed the survey to proceed with a minimum of U-turns or doubling back. The GPR was mounted on a snow machine and run by a two man crew. Following the GPR survey, a topographic survey of the grid was conducted to allow determination of bedrock elevations. Topographic elevations and bedrock depths were merged to create a map of the bedrock surface. This is shown in an isometric block diagram (Figure 6.17). Bedrock elevations were interpolated between survey lines with a nearest neighbor search restrained to points on strike with the base line. The flat areas in the model are regions with no bedrock depth information. The general bedrock topography interpolated in the southeast portion of the block model was confirmed during subsequent mining. Of particular interest is the ridge labelled **A**; it was found to be a resistant auriferous quartz vein within a local fault zone.

Under optimum winter conditions, it appears that a placer GPR survey could cover an average of 1.5 to 2 line-km per day. This rate includes set-up, tear-down, topographic, GPR profile and velocity surveys. An additional 1 to 1.5 days of data processing is required for each survey day to process the topographic data, perform topographic corrections, pick and verify reflections and generate a map.

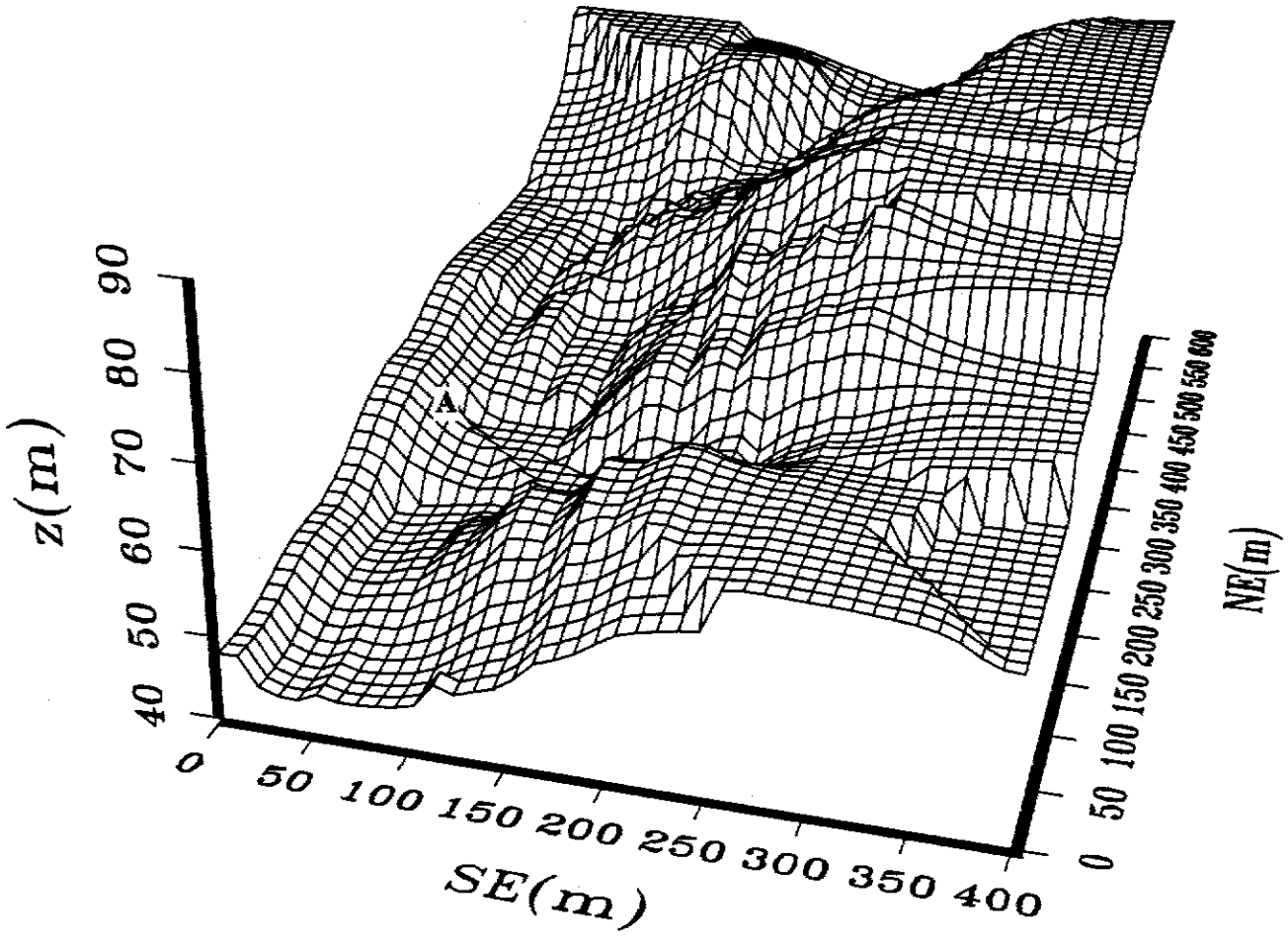


Figure 6.17. Isometric block diagram looking northwest of GPR indicated bedrock surface at Discovery Creek. Flat regions are areas with no bedrock depth information. A - indicates quartz vein forming bedrock ridge found during subsequent mining.

# 7. CONCLUSIONS AND RECOMMENDATIONS

## 7.1 Conclusions

The test program demonstrated that GPR can reliably map bedrock to maximum depths of 20 to 30 m. For most placer miners, this is the maximum depth to which open pit mining can be profitably conducted. GPR resolution and accuracy is quite sufficient for the purposes of placer exploration and GPR surveys can be conducted rapidly and cost-effectively over large grids.

GPR penetration and resolution can be degraded by several factors. Attenuation within thawed conductive clay is perhaps the most significant problem encountered in GPR surveys. In other situations, a poor dielectric contrast between bedrock and overburden or a rough bedrock surface can result in weak discontinuous bedrock reflections which cannot be easily identified or followed. This problem can be mitigated by tightening the station spacing when surveying a dipping or rough reflector and by using SEC type gain processing and low-pass filtering to enhance weak bedrock reflections. In difficult conditions, more frequent bedrock depth controls may be necessary.

GPR works very well in Klondike Type placer deposits with penetration ranging from 10 to 28 m and averaging 19 m in the test program. Attenuation within black muck and scattering of radar signals by boulders can be a problem in some situations. Using a lower operating frequency is the only practical method of overcoming these problems. Variations in the thickness of black muck can introduce static shifts into the deeper reflections and invalidate overburden velocity assumptions. In severe cases, static corrections may be necessary to resolve the bedrock reflection.

GPR works well in Mayo Type placer deposit with penetration ranging from 10 m to 28 m and averaging 17 m. Attenuation within conductive clay can seriously limit GPR penetration and scattering within boulder layers can be a local problem. Signal cluttering by numerous overburden reflections and occasionally by multiples generated between the water table and frost line is the most commonly encountered problem in surveying Mayo Type deposits. SEC gain can be used to enhance bedrock reflections when the bedrock surface is relatively flat; otherwise, frequent bedrock depth controls may be required.

GPR works well in Nansen Type deposits with penetration ranging from 10 m to 24 m and averaging 16 m. Poor dielectric contrasts between bedrock and overburden were the most serious problems encountered in the test surveys. This produces weak discontinuous reflections and frequent bedrock depth controls may be required in some cases to accurately map bedrock.

Overburden GPR velocity can be determined to acceptable accuracy by CMP surveys. GPR indicated depths to bedrock calculated using CMP overburden velocities agreed with drill hole or shaft indicated depths to within $\pm$ 10%. While a 2.0 m station separation increment worked satisfactorily, a closer spacing should be used if time permits. Dix interval velocities are not always reliable, particularly when resolving the velocity of thin near surface layers at low frequency.

As noted earlier, the cost of an exploration method is an extremely important factor governing its utility in the minds of placer miners. With limited capital and small reserves, most operators cannot afford to implement expensive new technology - regardless of how promising it may be. GPR is unlikely to be generally used in placer exploration until the survey cost is reduced.

## 7.2 Recommendations

The following recommendations for placer GPR surveys are based upon the test program experience:

1. Klondike and Nansen Type placer deposits should be surveyed when the ground is frozen and thawed muck or clay should be avoided if at all possible. Surveys of Mayo Type placer deposits are not affected by seasonal thawing.

2. A maximum profile station spacing of 2 m at 25 MHz is recommended and a shorter station spacing should be used where reflections apparently dip to ensure that reflections can be read across a radargram. CMP station separation increments should be no more than 2 m. The survey crew should pay particular attention to ensuring that velocity surveys are conducted where the reflectors are as flat as possible. In placer surveys this generally involves running the velocity survey parallel to the drainage.

3. For maximum survey efficiency and minimum surface wave noise, surveys should be run on ploughed lines whenever possible. A thoroughly packed trail can also be used in winter. If the surveys cannot be run using ski-mounted antennas, production rates will be much slower. The required width of a survey line depends upon the system operating frequency. To achieve maximum penetration, survey lines up to 4 m wide may be required to accommodate low frequency (25 MHz) antennas.

4. Depth controls are a necessity in running GPR placer surveys. It can be very difficult to identify the correct reflection in cluttered radargrams or in cases where the bedrock reflection is weak or discontinuous. Frequent depth controls will be required in Mayo Type deposits. Klondike and Nansen Type deposits with poor bedrock/gravel dielectric contrast may also require additional depth controls.

5. GPR surveys can be designed to minimize the requirement for depth controls by using available outcrop and favourable ground conditions to best advantage. A hypothetical example is presented in Figure 7.1 where a GPR survey is contemplated to map bedrock in a restricted area. Line spacings should not exceed one quarter the observed wavelength of the large meanders in the creek and should be "walked off" available rock outcrops where possible. This allows the interpreter to definitely identify the bedrock reflection at one end of the radargram and follow it along its length. In addition, the base line and perhaps one or more tie-lines running along-valley should be surveyed. Surveys along a valley will often detect strong, continuous reflections because of the flat bedrock dip. Along-valley profiles can be used to guide the interpreter to a correct pick in the across-valley profiles. If reflections can be tied together and then to known bedrock elevations, a reliable map of bedrock topography can be created.

**Figure 7.1 Suggestions for GPR survey grid layout.**

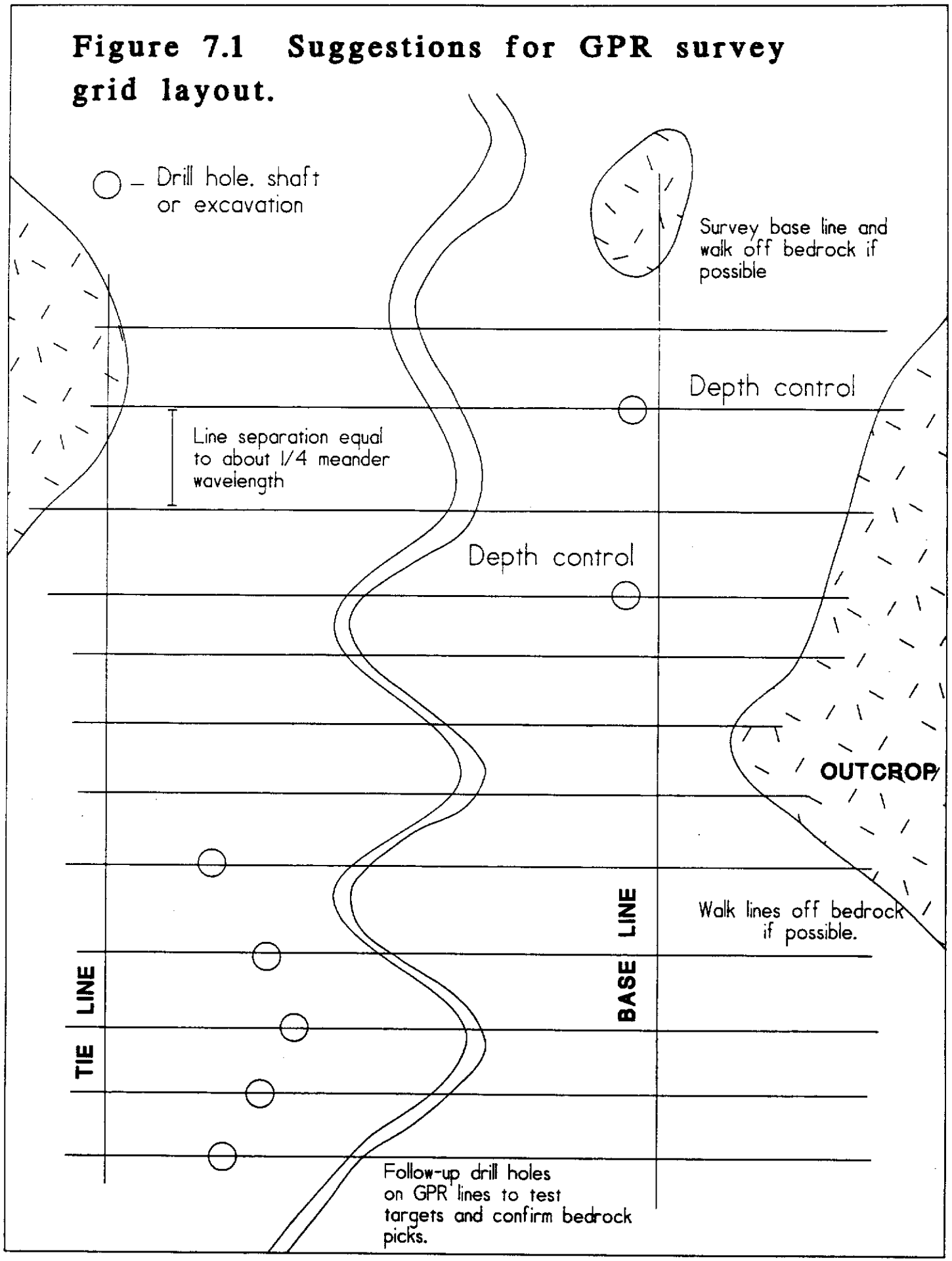

**References cited**

Amery, G.B. (1993) Basics of Seismic Velocities. The Leading Edge, Vol. 12, No. 11 pp1087-1093.

Annan, A.P., J.L. Davis and W.J. Scott (1976) Impulse radar wide angle reflection and refraction sounding in permafrost. in: Report of Activities, Part C; Geological Survey of Canada Paper 75-1C. pp 335-341.

Annan, A.P. and S.W. Cosway (1991) Ground Penetrating Radar Survey Design. Paper presented at 53rd Annual Meeting of the European Association of Exploration Geophysicists.

Annan, A.P. and J.L.Davis (1977a) Impulse radar and time domain reflectometry experiments in permafrost terrain during 1976. in: Report of Activities, Part B; Geological Survey of Canada Paper 77-1B.

Annan, A.P. and J.L. Davis (1977b) Radar Range Analysis for Geological Materials. in: Geological Survey of Canada Paper 77-1B.

Bostock (1963). Stewart Map area (105M) Geological Survey of Canada Map 1195.

Boyle, R.W. (1990) Gold: History and Genesis of Deposits. New York: Van Nostrand Reinhold Company.

Campbell, R.B. and C.J. Dodds (1979) S.W. Kluane Lake Map Area (115G & F(E 1/2)). Geological Survey of Canada Open File 829 (map).

Carlson, G.G. 1987. Geology of the Mount Nansen and Stoddart Creek Map Areas (115-I-6). Exploration and Geological Services Division, Indian and Northern Affairs Canada, Open File 1987-2.

Davis, J.L. and A.P. Annan (1987). Ground-penetrating Radar for High-Resolution Mapping of Soil and Rock Stratigraphy. Paper presented at Exploration '87.

Davis J.L., A.P. Annan and C. Vaughan (1987) Placer exploration using radar and seismic methods. Canadian Institute of Mining and Metallurgy Bulletin, Vol. 80, No. 898. pp 67-72.

Dawson, G.M. (1889) Report on an exploration in the Yukon District, N.W.T. and adjacent portions of British Columbia, 1887 Geological and Natural History Survey of Canada, Annual Report Volume III, Part 1, 1887-1888.

Debicki, R.L. (1983) Placer Deposits: Their Formation, Evaluation and Exploitation. in: Debicki, R.L. (ed.) Yukon Placer Mining Industry 1978-1982. Exploration and Geological Services, Indian and Northern Affairs Canada. pp18-35.

Debicki, R.L. (1984) Bedrock Geology and Mineralization of the Klondike Area (West), 115 O-14, 15 and 116 B-2,3. (1:50,000 scale map with marginal notes.) Exploration and Geological Services Division, Yukon, Indian and Northern Affairs Canada.

Hester, B.W. (1970) Geology and Evaluation of Placer Gold Deposits in the Klondike area, Yukon Territory. Institution of Mining and Metallurgy Transactions, Section B, pp 60-67.

Keller, G.V. (1987) Rock and Mineral Properties in: Nabighian, M.N. (ed.) Electromagnetic Methods in Applied Geophysics - Theory (Volume 1). Tulsa: Society of Exploration Geophysicists. pp 13-52.

Levson, V. (1992) The Sedimentology of Pleistocene Deposits Associated with Placer Gold Bearing Gravels in the Livingstone Creek Area, Yukon Territory, Canada. in: T.J. Bremner (ed.) Yukon Geology - Volume 3; Exploration and Geological Services Division - Yukon, Indian and Northern Affairs Canada.

Morison, S.R. (1985) Sedimentology of White Channel Placer Deposits, Klondike area, West Central Yukon. University of Alberta ( Unpublished M.Sc. Thesis).

McNeill, J.D. (1980) Electrical Conductivity of Soils and Rocks. Mississauga: Geonics Technical Note TN-5

Power, M.A. and R.L. McIntyre (1990) Mapping bedrock topography with ground penetrating radar. in: Twelfth Annual Alaskan Conference on Placer Mining (Proceedings) Fairbanks: 1990 Placer Mining Conference Committee.

Power, M.A. 1992. A seismic refraction survey of portions of lower Duncan Creek, Elsa area, Central Yukon. Unpublished assessment report.

Pullan, S.E. and J.A. Hunter (1983) Seismic Tests of Placer Deposits in Areas of Permafrost. in: Debicki, R.L. (ed.) Yukon Placer Mining Industry 1978-1982. Exploration and Geological Services, Indian and Northern Affairs Canada. pp 43-45.

Reitz, J.R., F.J. Milford, R.W. Christy (1979) Foundations of Electromagnetic Theory, Don Mills: Addison-Wesley.

Roots, C.F. and Murphy D.C. (1992). Geology of the Mayo Map Area (105M) Exploration and Geological Services, Indian and Northern Affairs Canada, Open File 2483. 1:250,000 map with marginal notes.

Scott, W.J., P.V. Sellmann and J.A. Hunter (1979). Geophysics in the study of permafrost. in: National Research Council (ed.) Proceedings of the Third International Conference on Permafrost. Ottawa: NRC

Spies B.R. and F.C. Frischknecht (1991). Electromagnetic Sounding. in: Nabighian, M.N. (ed.) Electromagnetic Methods in Applied Geophysics - Applications (Volume 2). Tulsa: Society of Exploration Geophysicists. pp 285-426.

Stokes, R. (1990) The Ten Commandments in Placer Exploration and Operation in: Twelfth Annual Alaskan Conference on Placer Mining (Proceedings) Fairbanks: 1990 Placer Mining Conference Committee.

Templeman-Kluit, D.J. (1974) Paper 73-41: Reconnaissance geology of Aishihik Lake, Snag and parts of Stewart River map areas, west central Yukon; Geological Survey of Canada (map 18-1973).

Templeman-Kluit, D.J. (1984) Open File 1101: Geology, Laberge (105E). Geological Survey of Canada.

Vallee, M., M. David, M. Dagbert, C. Desrochers (1992) Guide to the Evaluation of Gold Deposits. Montreal: CIM Special Volume 45.

Ward, S.H. and G.W. Hohmann (1987) Electromagnetic Theory for Geophysical Application in: Nabighian, M.N. (ed.) Electromagnetic Methods in Applied Geophysics - Theory (Volume 1). Tulsa: Society of Exploration Geophysicists. pp 131-312.

# Appendix A. Test Sites Results

## SITE 1 - SOYA CREEK

### A. Site location

The GPR survey was conducted on the lower end of Soya Creek on placer claims P3132 and P3170-3173 (Figure A-1-1). Access is via the Swamp Creek winter road.

### B. Local geology

No bedrock geology is mapped in the area (Templeman-Kluit 1974), but the property owner reported that Soya Creek is underlain by blocky quartzite. Overlying bedrock is a sequence of frozen gravel, silt and clay (black muck). The black muck has a much higher silt fraction than is normally encountered in other localities (eg. the Klondike), perhaps reflecting the source rock composition. Overburden is frozen to bedrock on the property.

### C. Survey specifications

Two short segments of GPR lines 1 and 2 were surveyed. GPR line 1 was profiled with both 25 MHz and 50 MHz antennas and GPR line 2 was profiled with only the 25 MHz antennas. Signals were stacked 64 times and recorded over a window of at least 800 ns. A CMP velocity survey and HLEM sounding was conducted on the north end of GPR line 1. The CMP survey was conducted with the 50 MHz antennas using separations of from 2 to 20 m in 1 m increments. The HLEM sounding was conducted with a 25 m coil spacing.

### D. Results

The CMP survey radargram is plotted in Figure A-1-2, the $X^2$-$T^2$ plot is shown in Figure A-1-3 and the results are tabulated in Table A-1-1. Four arrivals were detected; all are quite fast reflecting the frozen state of the placer deposit. The first pair of arrivals appear to be surface waves generated within disturbed ice and clay. The second arrival appears to be the base of the muck layer. The third arrival has an apparent depth close to that expected for bedrock in the area and the apparent velocity is approximately that expected from frozen gravel.

The results of the HLEM sounding are plotted in Figure A-1-4 and tabulated in Table A-1-2. Details of the inversion results are listed in Appendix C. The inversion is relatively poor with error in the in-phase data fit. The low quadrature and in-phase responses indicate that the ground is quite resistive. A model consisting of two layers and a half space produced the best inversion. The top layer appears to be a composite layer of air, disturbed silt and ground ice. The middle layer affords the best indication of the true resistivity of overburden. The half-space resistivity is quite high and correlates with frozen quartzite at the indicated

depth. This depth to the top of the half space is slightly greater than the depth to bedrock in this area (12 m), perhaps indicating the development of a weathered zone at the top of bedrock.

**Table A-1-1 Soya Creek CMP velocity survey results**

| Layer | $V_{NMO}$ (m/ns) | $V_{DIX}$ (m/ns) | Interval (m) | Remarks |
|---|---|---|---|---|
| 0 | 0.183 ± 0.002 | n/a | 0 | ice + entrained air |
| 0 | 0.114 ± 0.001 | n/a | 0 - 1 | ripped muck |
| 1 | 0.147 ± 0.002 | 0.147 | 1 - 5 | muck |
| 2 | 0.163 ± 0.005 | 0.178 | 5 - 12 | gravel |

**Table A-1-2. Soya Creek Resistivity Sounding Results**

| Layer | Resitivity (Ω-m) | Interval (m) | Remarks |
|---|---|---|---|
| 1 | 2703 | 0 - 5 | Snow/ice/silt |
| 2 | 770 | 5 - 16 | silt/gravel |
| 3 | 509K | 16 + | bedrock |

The survey on GPR line 2 was conducted quite close to a drill fence and the drill hole indicated depths to bedrock are plotted on the line 2 radargram in Figure A-1-5. The area had been stripped following drilling and none of the hole plugs were recovered. The first reflection appears to correlate with the base of muck and a weak bedrock reflection is recorded below it at approximately 100 ns. Because of the uncertainty in the drill hole locations, mismatch between drill hole and reflector depths does not necessarily indicate an incorrect GPR velocity. Since both bedrock and overburden is frozen and there is little weathering of bedrock, a very poor velocity contrast exists between bedrock and the sediments. Consequently, it is difficult to discriminate between reflectors within the sediments and the bedrock/gravel reflector. Reflections are particularly poor where the bedrock surface dips. It is very difficult to pick the bedrock reflector without knowing the depth to bedrock near at least one point on the survey line and having some knowledge of the stratigraphy.

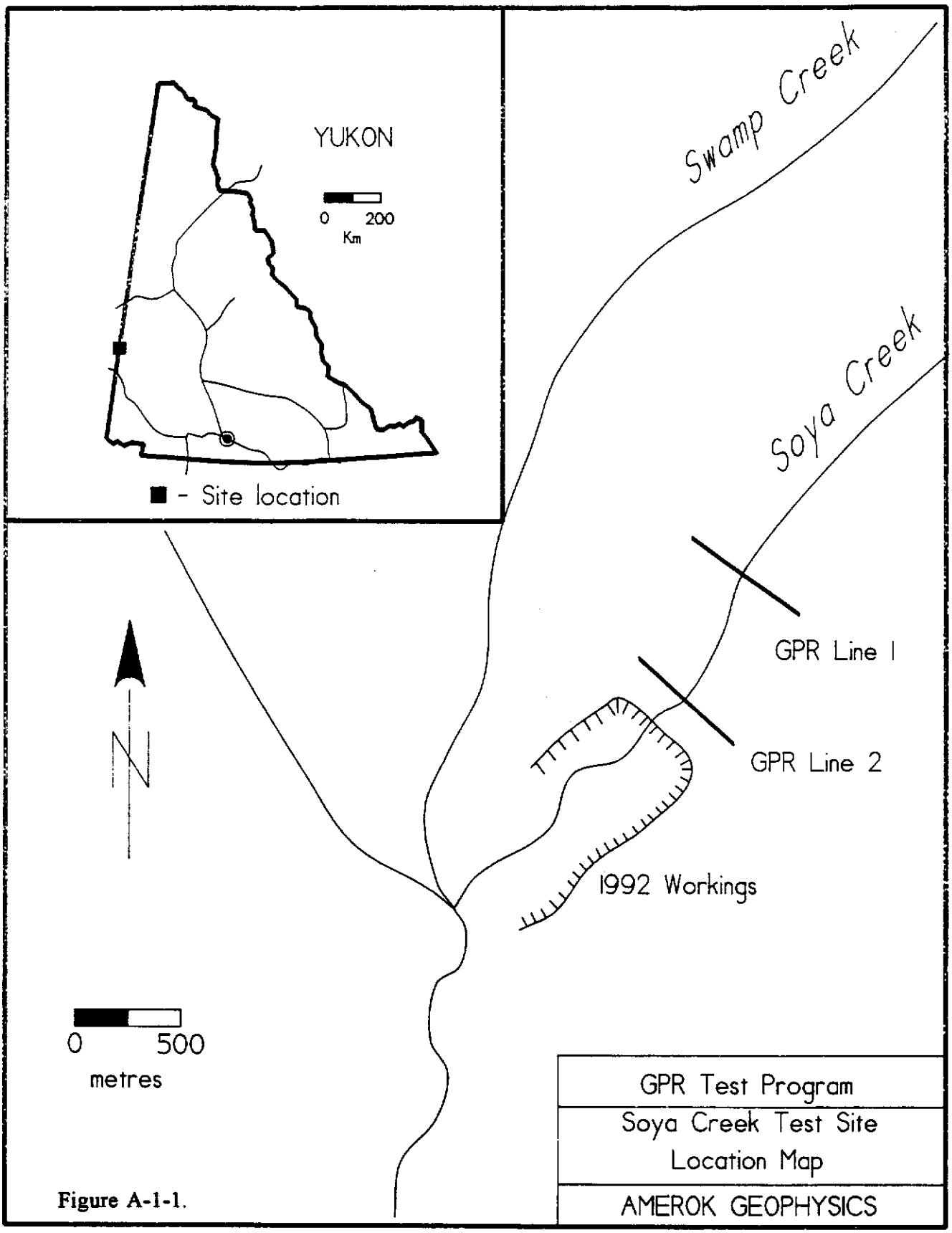
YUKON
0 200
Km
■ - Site location
Swamp Creek
Soya Creek
GPR Line 1
GPR Line 2
1992 Workings
N
0 500
metres
GPR Test Program
Soya Creek Test Site
Location Map
AMEROK GEOPHYSICS

**Figure A-1-1.**

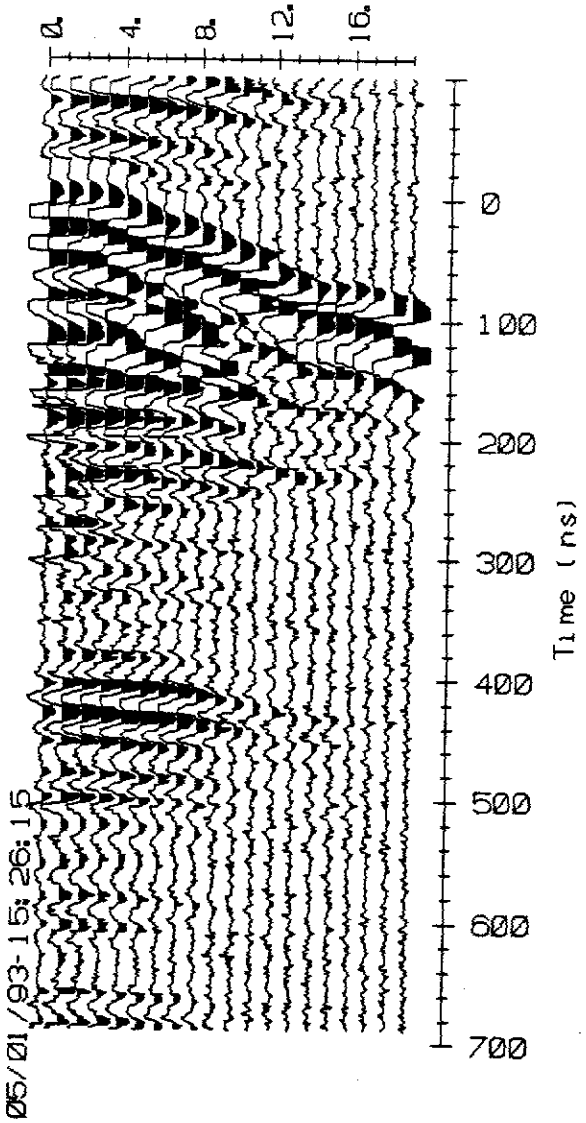


Figure A-1-2. Soya Creek 50 MHz CMP radargram. Measurement interval 1 m in separations from 2 to 20 m.

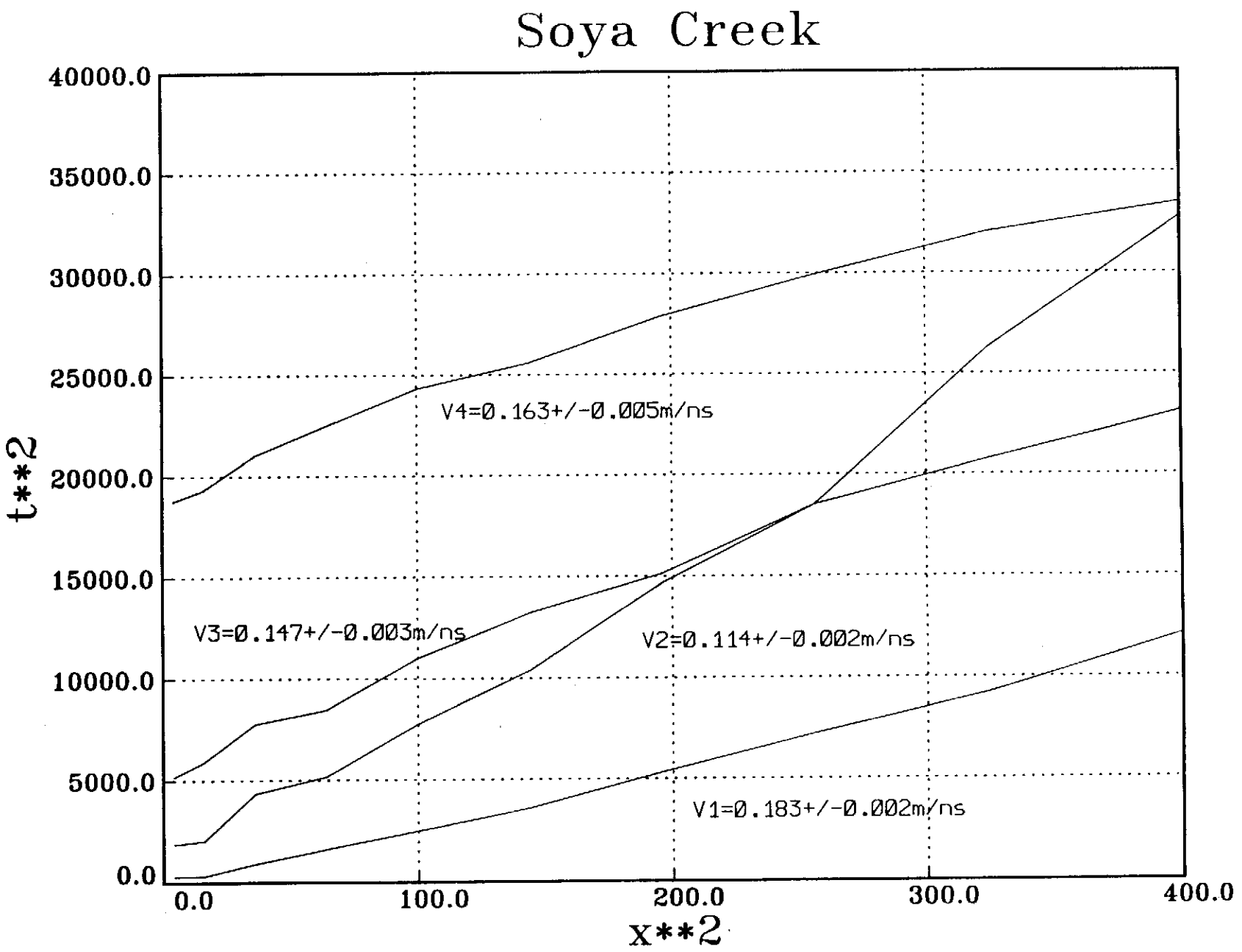


Figure A-1-3. Soya Creek $X^2$-$T^2$ diagram. Velocities derived from linear regression are plotted near curves.

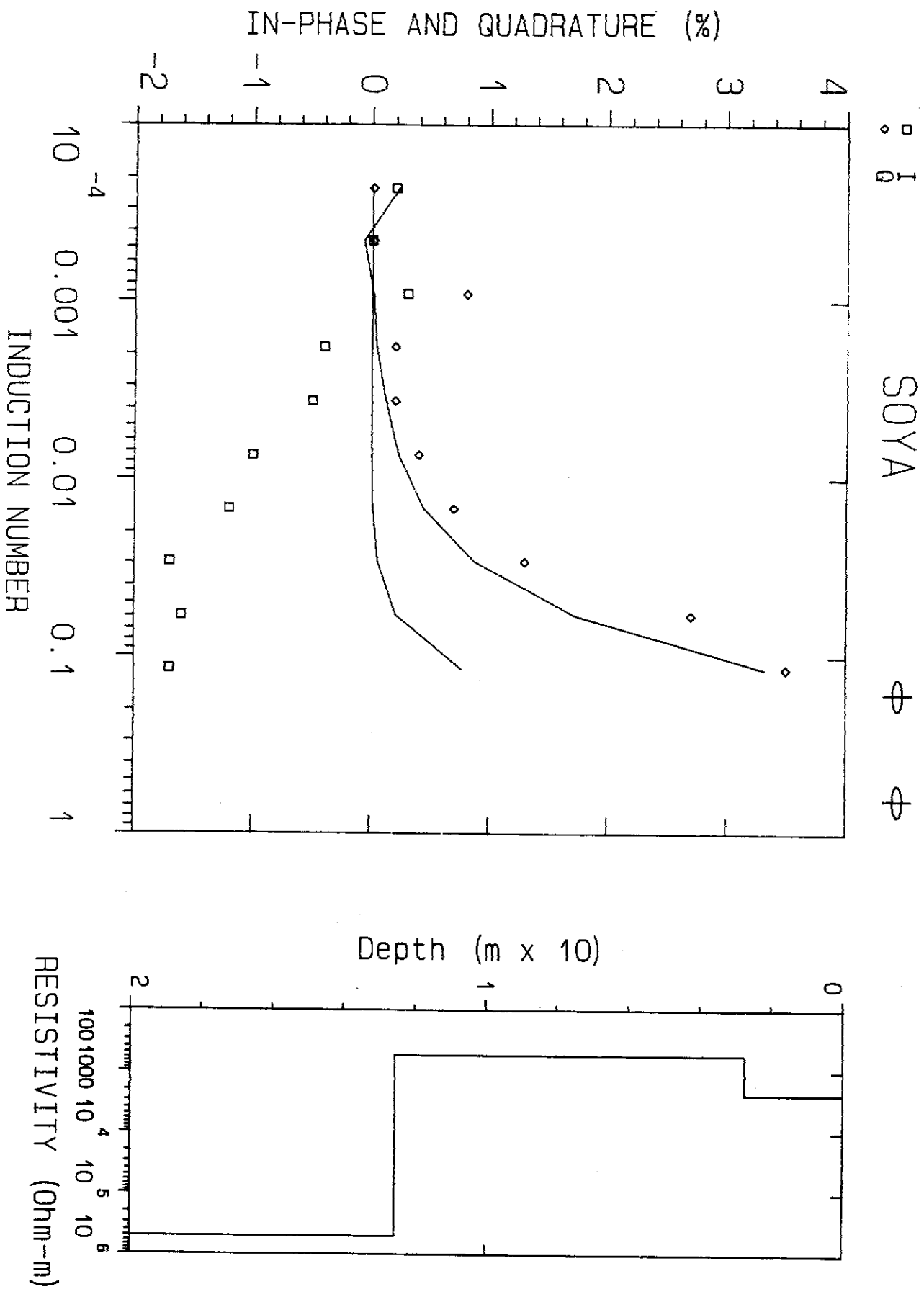


Figure A-1-4. Soya Creek HLEM sounding results. Synthetic and measured data is on the left. Square symbols indicate measured in-phase, diamonds indicate measured quadrature; curves display synthetic responses. Model is displayed on the right.

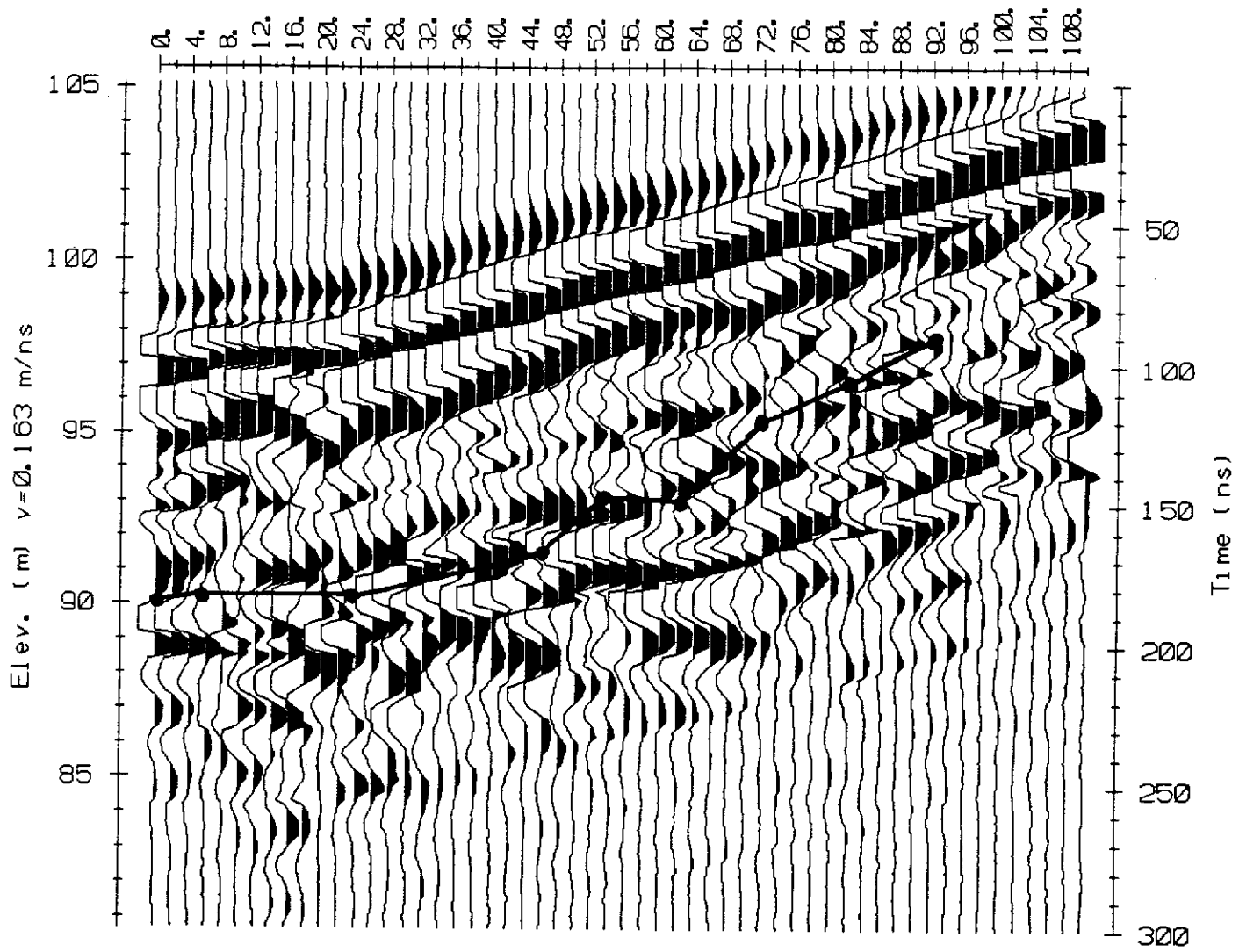


Figure A-1-5. Profile radargram on GPR line 2 at Soya Creek showing bedrock surface mapped in nearby drill fence (solid line).

## SITE 2 - FRYING PAN CREEK

### A. Site location

The GPR survey was conducted on the lower end of Frying Pan Creek on placer claims P23276, P23280, P23300-01 and P23356 (Figure A-2-1). Access is via the Duke River road from the Alaska Highway.

### B. Local geology

The area is underlain by metavolcanic rocks of the Station Creek Formation (Campbell and Dodds 1979). Auriferous gravel overlies bedrock and is in turn locally covered by colluvium. The gravel is composed of fresh clasts of local bedrock and is poorly sorted, reflecting the high gradient of the stream. The creek was covered by 1-2 m of overflow ice at the time of the survey and the owner stated that discontinuous permafrost is found along the creek. Where frozen, the sediments are easily ripped and thus probably contain significant liquid water.

### C. Survey specifications

The GPR profile survey was conducted along the centre of the creek over a distance of 900 m. The 50 MHz antennas were used with a 2.0 m separation and station spacing. The signal was recorded over a 600 ns window and stacked 32 times. A CMP velocity survey was conducted at station 880 on the survey line with the 50 MHz antennas using an antenna separation varying from 2 to 34 m in 2 m increments. An HLEM sounding was conducted at the start of the GPR profile line using a 25 m coil separation. A topographic survey of the profile line was conducted and used to correct the GPR profile to produce an elevation section. The arbitrary datum for this survey is the elevation of the Duke River at its confluence with Frying Pan Creek.

### D. Results

The CMP radargram is plotted in Figure A-2-2 and the $X^2$-$T^2$ plot is shown in Figure A-2-3; results are summarized in Table A-2-1. In retrospect, the CMP survey should have been conducted with a 1.0 or 0.5 m separation increment to better detect shallow reflections. In order to survey over the flattest section of bedrock available, the CMP survey was conducted in an alluvial fan at the confluence of Frying Pan Creek with the Duke River. Unfortunately, even here, the bedrock surface dips appreciably and this is evident in the attitude of the reflections in the CMP profile. As a result, no reliable estimate of the bedrock

velocity is possible. The velocities are very fast (>0.150 m/ns), reflecting the frozen state of the sediments and weathered bedrock. Normally, ice has a velocity in the range of 0.14 to 0.16 m/ns, depending upon liquid water content; the faster apparent velocity of the uppermost layer is probably due to air entrained in the overflow ice.

The results of the HLEM resistivity sounding are shown in Figure A-2-4 and listed in Table A-2-2; a detailed summary of the inversion including fitting error is contained in Appendix C. The inversion is relatively poor (RMS error - 0.921%) with significant mismatch between the measured and synthetic in-phase responses. This may have been caused by lateral variations in resistivity or sidewall effects. Nonetheless, the low quadrature and in-phase responses indicate that the environment is relatively resistive. The top layer is a composite resistivity of ice and air. The apparent resistivity of the middle layer is below the range expected for gravel. This suggests that either the interpretation assumptions are invalid or that conductive clay is present. The depth to the top of the third resistivity layer is lower than the depth to weathered bedrock and may indicate the top of fresh bedrock. A discontinuous reflection at an average depth of 10 m was apparent in the GPR profile in this area.

**Table A-2-1. Frying Pan Creek velocity survey results**

| Layer | $V_{NMO}$ (m/ns) | $V_{DIX}$ (m/ns) | Interval (m) | Remarks |
|---|---|---|---|---|
| 0 | 0.254 ± 0.008 | n/a | 0 | ice+entrained air |
| 1 | 0.170 ± 0.003 | 0.170 | 0 - 5 | ice / frozen gravel |

**Table A-2-2. Frying Pan Creek resistivity sounding results**

| Layer | Resistivity (Ω-m) | Interval (m) | Remarks |
|---|---|---|---|
| 1 | 7263 | 0 - 1.5 | ice |
| 2 | 137 | 1.5 - 9.5 | gravel / clay |
| 3 | 1002 | 9.5+ | bedrock |

An excerpt from the profile radargram is shown in Figure A-2-5 together with drill hole data. The surface wave is strong and uniform as expected in a survey conducted on ice. The variable thickness of the ice is obvious and two small lenses of liquid water appear to be present in the ice section. The ice/sediment contact also produces a strong reflection. The gravel/bedrock reflection is weaker and discontinuous; it is the first reflection below the ice/sediment reflection. The arrivals below the bedrock/gravel reflection include the top of weathered bedrock, sidewall reflections and steeply dipping diffractions.

The GPR survey was run along the centre line of the placer claims near a series of 13 auger drill holes. The antennas were towed as close to the drill hole locations as possible given the conditions. In general, only a rough correlation can be expected between the drill hole depths and the radargram results because of uncertainty in location of the drill holes, inability to profile directly over the drill holes and the presence of a variable thickness of overflow ice. Overall there was very close agreement between the drill hole depths and the depths to bedrock derived from the GPR survey. It would have been difficult to correctly select the bedrock reflection without data from at least one or two drill holes however.

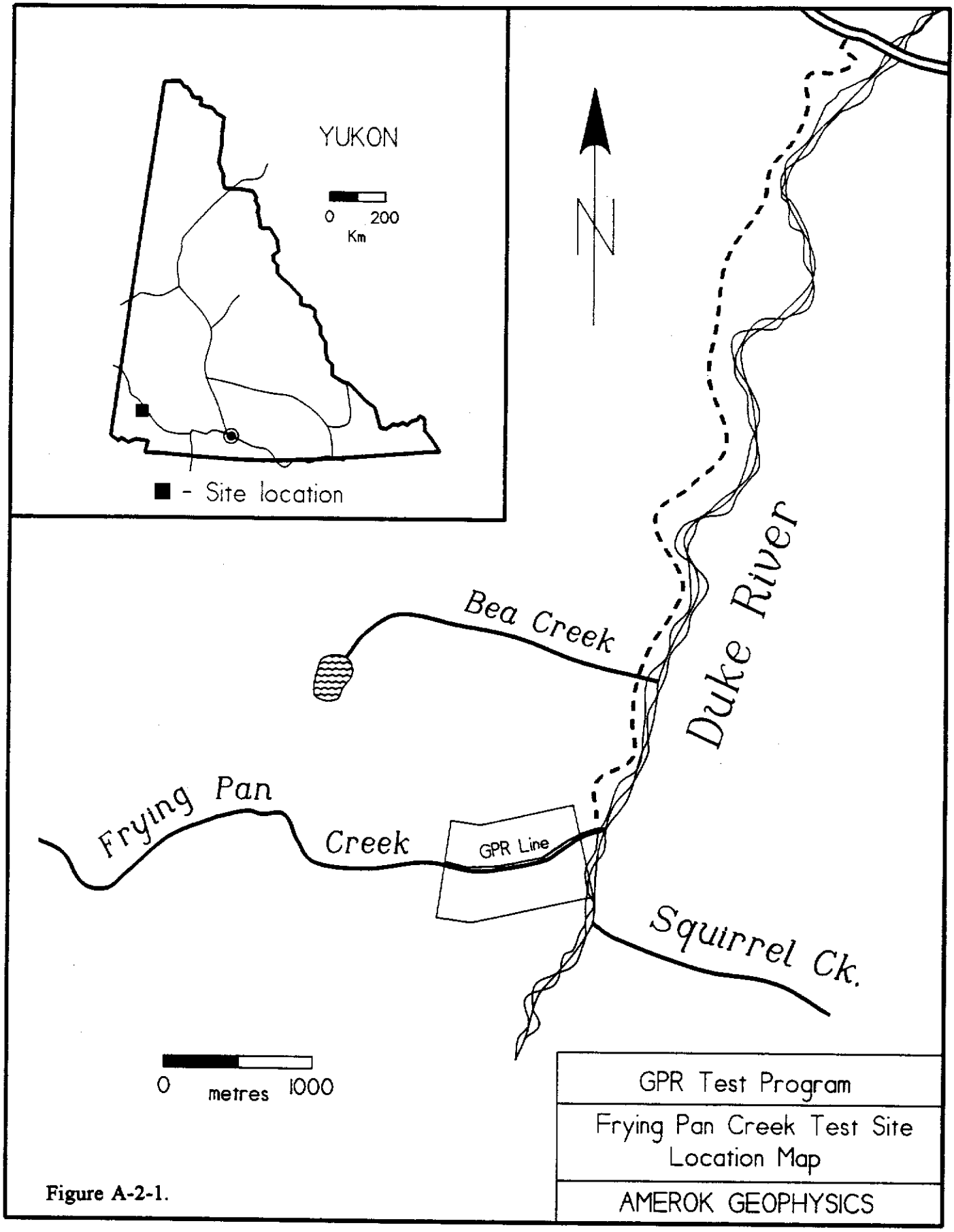
YUKON
0 200
Km
■ - Site location
N
Bea Creek
Duke River
Frying Pan
Creek
GPR Line
Squirrel Ck.
0 metres 1000
GPR Test Program
Frying Pan Creek Test Site
Location Map
AMEROK GEOPHYSICS

**Figure A-2-1.**

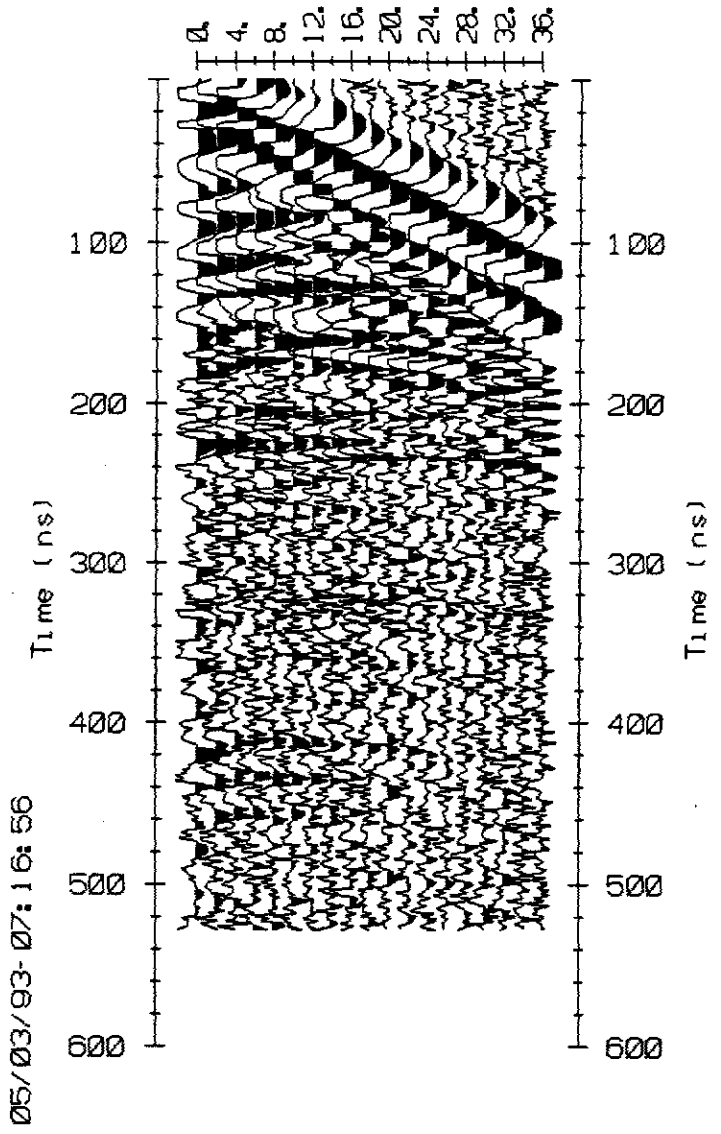


Figure A-2-2. Frying Pan Creek CMP radargram. Measurement interval 2 m in separations from 2 to 36 m.

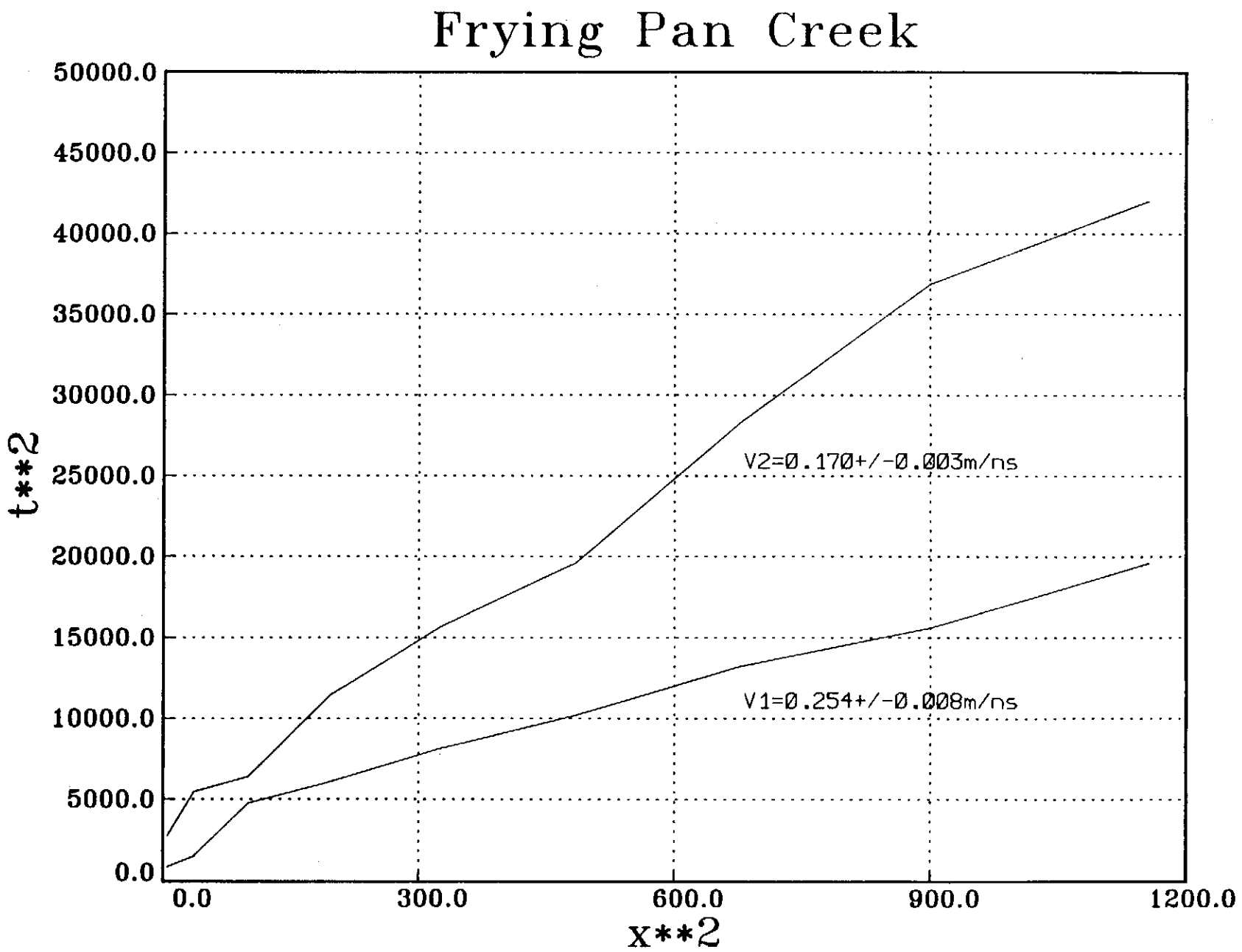


Figure A-2-3. Frying Pan Creek $X^2$-$T^2$ diagram. Velocities derived from linear regression are plotted near curves.

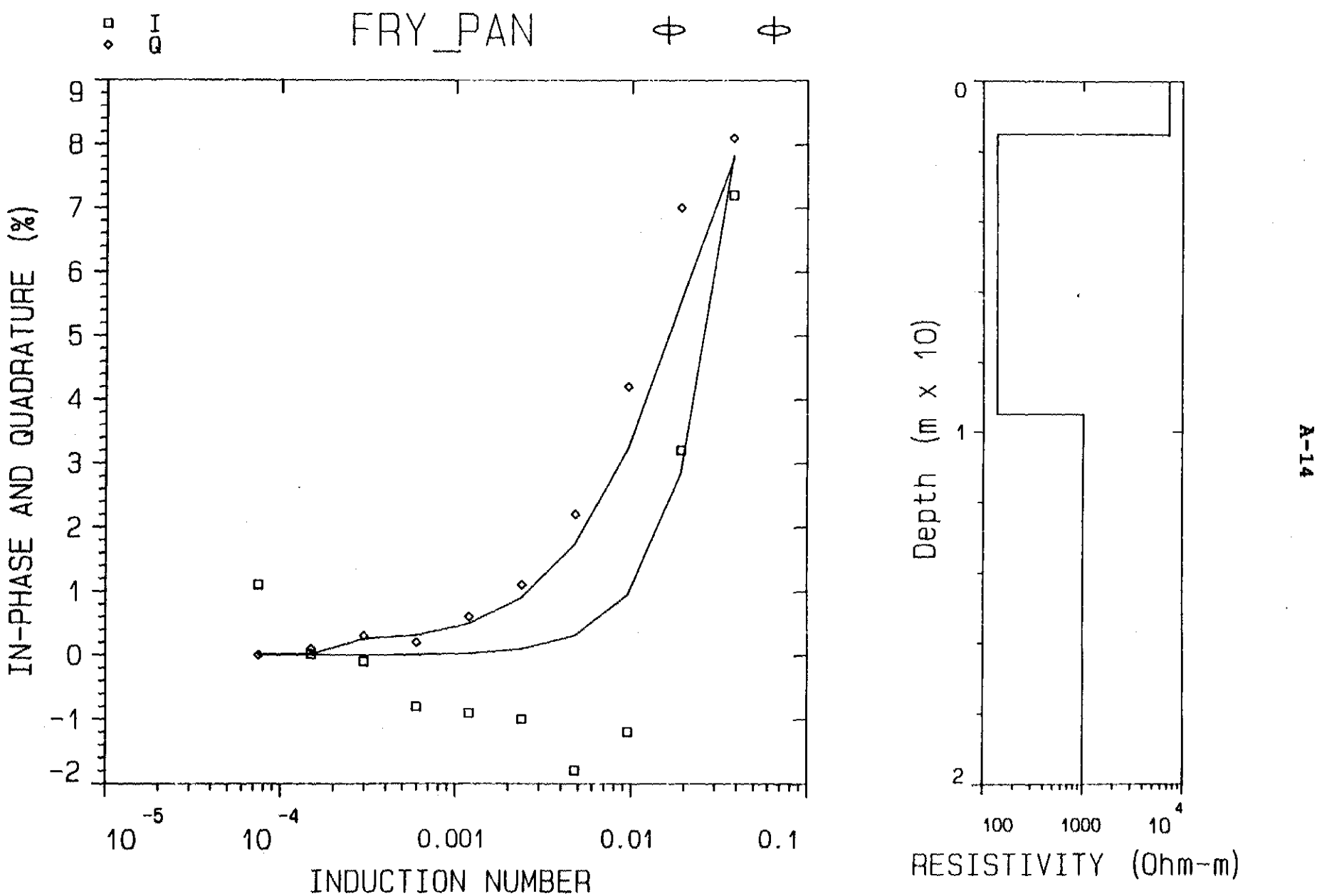


**Figure A-2-4.** Frying Pan Creek HLEM sounding results. Synthetic and measured data is on the left. Square symbols indicate measured in-phase, diamonds indicate measured quadrature; curves display synthetic responses. Model is displayed on the right.

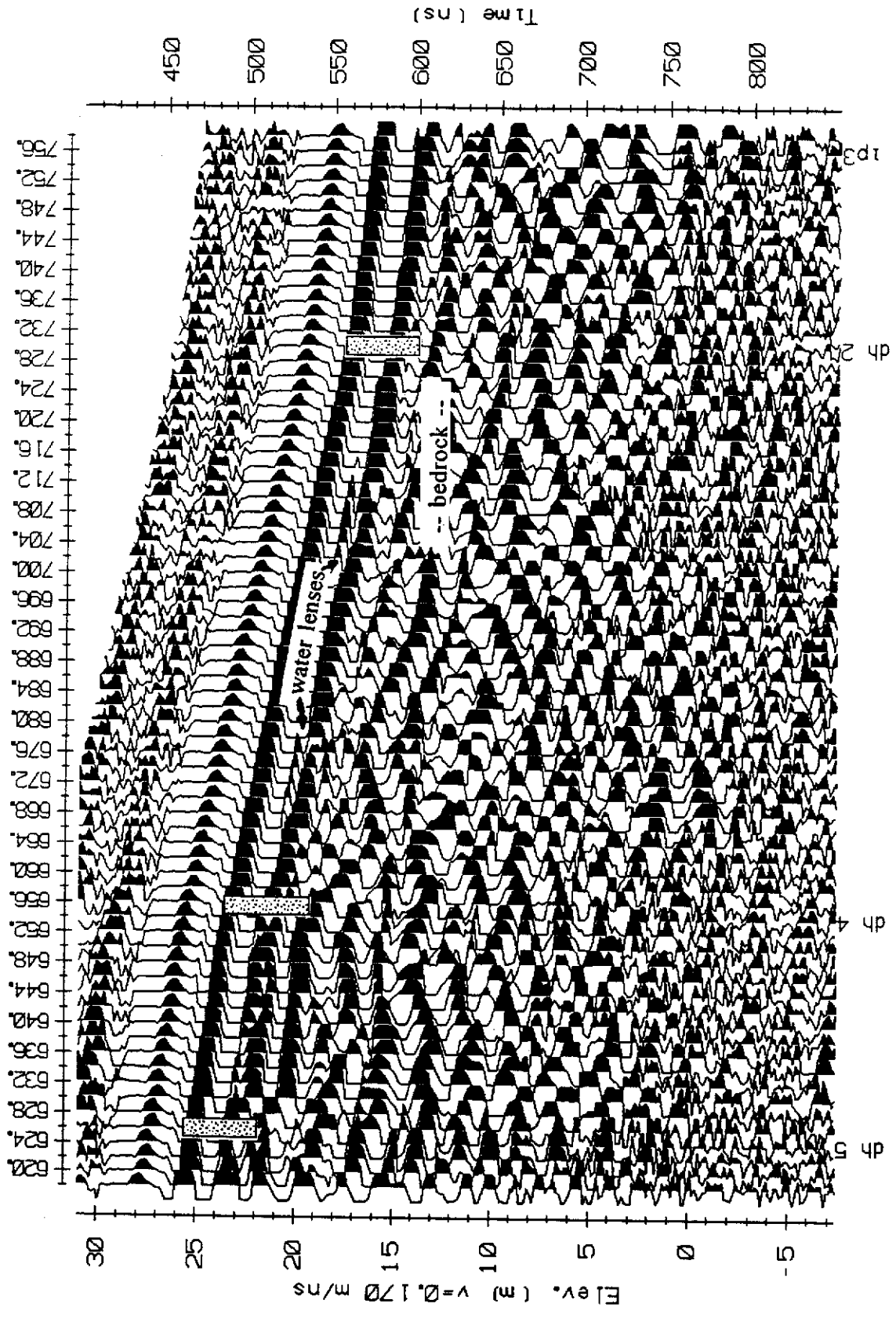


**Figure A-2-5. Profile radargram along centre line of Frying Pan Creek together with drill hole data. All holes bottom in bedrock.**

## SITE 3 - LIVINGSTONE CREEK

### A. Site location

The GPR survey was conducted on PL8861 on upper Livingstone Creek (Figure A-3-1). The property can be reached via the Livingstone Creek winter road and a CAT trail running up the south side of Lake Creek.

### B. Local geology

The survey site is underlain by metavolcanic and metamorphosed ultramafic rocks of the Anvil Allochthonous Assemblage (Templeman-Kluit, 1984). These consist of fine grained amphibolite, minor sheared and altered gabbro, serpentinized dunite, peridotite and pyroxenite. Bedrock is overlain by a thick sequence of basal gravel, lacustrine silt and clay, till and glaciofluvial gravels. Levson (1992) describes how the intermediate silt and clay beds protected auriferous basal gravels from glacial scouring in streams orthogonal to the ice flow. The upper till is clay-rich with only minor interbedded gravel. The sediments in the survey site area are thawed and the water table is quite high; seeps were observed on the survey line.

### C. Survey specifications

One line, transverse to the drainage, was surveyed at the Livingstone Creek site. The survey line was ploughed immediately prior to the survey, revealing very shallow frost beneath several feet of snow. The GPR survey was conducted with the 25 MHz antennas using a 2 m station interval and 4 m antenna spacing. The data was collected over a 1000 ns time window and signals were stacked 64 times at each station. A CMP velocity survey was conducted at station 280S on the survey line with 25 MHz antennas using antenna separations from 2 to 34 m in 2 m increments. The CMP data was collected with a 1000 ns time window and the individual readings were stacked 64 times. The EM sounding was conducted with a 50 m coil spacing at station 100S.

### D. Results

The CMP profile is plotted in Figure A-3-2 and Figure A-3-3 displays the $X^2$-$T^2$ plot; results of the velocity analysis are tabulated in Table A-3-1. A single surface wave was recorded with a velocity intermediate between that of ice and air. Two low velocity layers were detected. The upper layer is probably composed of till. The second layer may consist of clay and silt. Approximately 3 km downstream, Levson (*ibid.*) documented an exposure

consisting of 5 m of silt and clay beneath 12 m of till. In addition, the velocity of this layer is in the range expected for water saturated clay and silt (Annan and Davis 1987). The property owners attempted to excavate a test pit to check the results of the GPR survey but were thwarted at 6 m by excessive ground water flows.

The HLEM resistivity sounding results are shown in Figure A-3-4 and tabulated in Table A-3-2; details of the inversion are in Appendix C. Following unsuccessful attempts to obtain a solution with a two layer over half space model, an additional layer was added and a successful inversion achieved. The inversion is good; RMS error of 1.2% is small relative to the data amplitude (1-28%). Mismatch occurs in the low frequency in-phase readings but agreement is quite good in the quadrature component. The resistivity of the first layer is a composite of ice and free-space resistivity. The second layer resistivity is in the range expected for glacial till while the low resistivity of the third layer suggests that it may be clay (McNeill 1980). The resistivity of the half-space is in the range expected for local bedrock or gravel and thus affords little additional insight into the underlying stratigraphy.

**Table A-3-1. Livingstone Creek velocity survey results**

| Layer | $V_{NMO}$ (m/ns) | $V_{DIX}$ (m/ns) | Interval (m) | Remarks |
|---|---|---|---|---|
| 0 | 0.223 $\pm$ 0.007 | n/a | 0 | ice+entrained air |
| 1 | 0.057 $\pm$ 0.001 | 0.057 | 0 - 3.7 | till |
| 2 | 0.062 | 0.065 | 3.7 - 8.5 | clay? |

**Table A-3-2. Livingstone Creek resistivity sounding results**

| Layer | Resistivity ($\Omega$-m) | Interval (m) | Remarks |
|---|---|---|---|
| 1 | 5089 | 0 - 1 | air + surface ice |
| 2 | 548 | 1 - 15 | till |
| 3 | 115 | 15 - 33 | clay (?) |
| 4 | 776 | 33 + | gravel/bedrock (?) |

A portion of the profile radargram is shown in Figure A-3-5. It appears that the GPR survey did not detect the bedrock/gravel interface. No continuous reflector was detected at depth although an intermittent deep reflector (A in Figure A-3-5) which does not follow surface topography is present. This reflector occurs at the base of layer 2 in the CMP velocity model. The results of the resistivity sounding suggest that this reflector is probably too shallow to be bedrock. The irregular topography of the reflector is not strong evidence that it may be bedrock given that the top of the local lacustrine clay/silt layer is irregular due to ice scouring (Levson 1992).

The apparent resistivity of the third sounding layer is very low and likely to attenuate any GPR signal quite severely. It is interesting to determine to what depth a GPR survey *could* have detected bedrock in this area. A synthetic radargram derived from the following model:

| **Depth** | **Velocity** | **Attenuation** | **Material** |
|---|---|---|---|
| 0-8m | 0.07 m/ns | 0.615 dB/m | Till, gravel |
| 8-15m | 0.05 m/ns | 0.615 dB/m | Till, gravel |
| 15-18m | 0.07 m/ns | 2.914 dB/m | Clay, silt |
| 18 m + | 0.11 m/ns | 0.100 dB/m | Bedrock / gravel |

is shown in Figure Layer A-3-6. Velocities and attenuation are similar to those measured in the CMP and HLEM surveys. The reflection from the top of bedrock/gravel at 18 m is almost undetectable and most certainly would be in the presence of any noise. The synthetic radargram indicates that a GPR survey could not detect bedrock as shallow as 3 m below the top of the conductive layer; it effectively blocks any GPR signal.

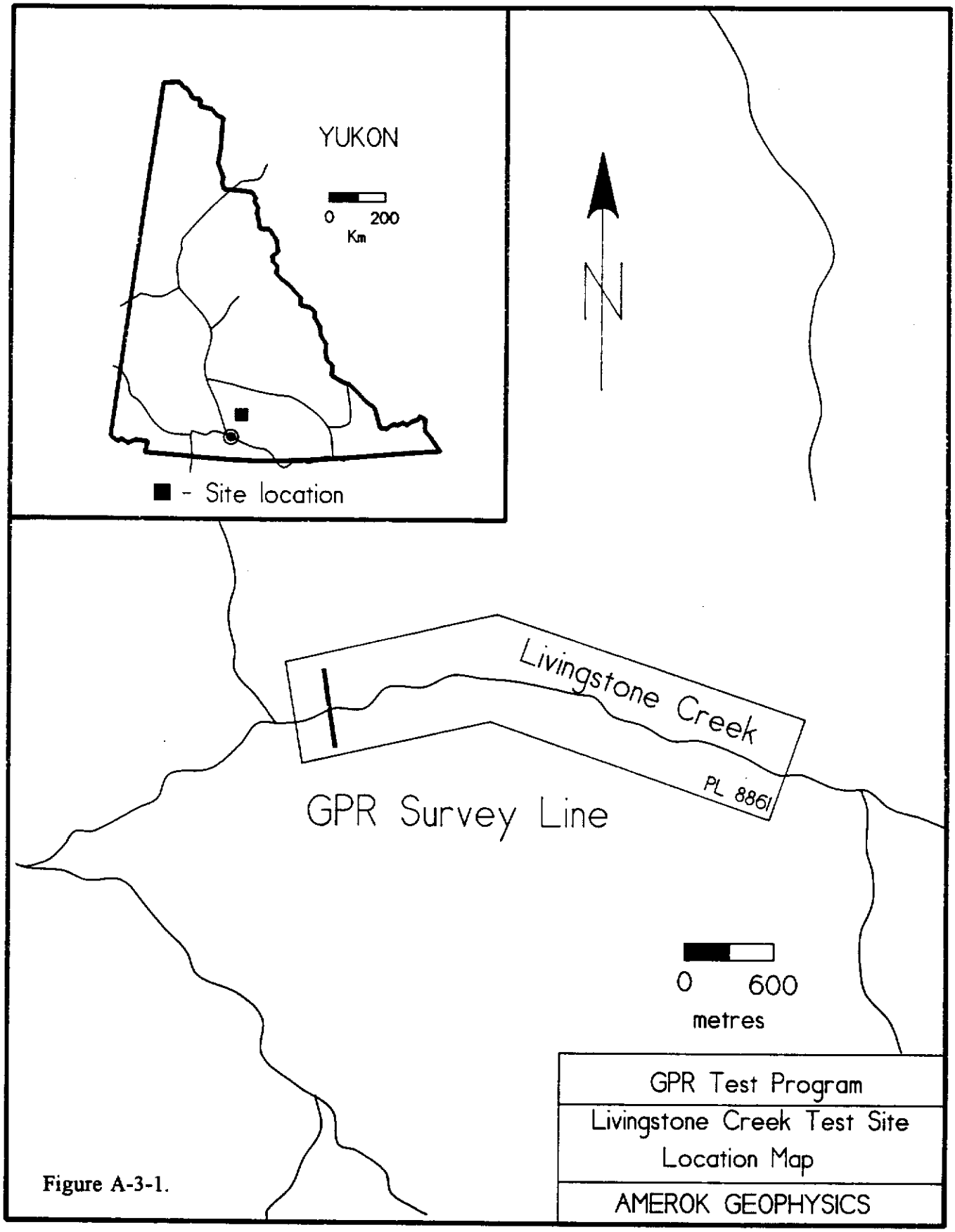
YUKON
0 200
Km
■ - Site location
N
Livingstone Creek
PL 8861
GPR Survey Line
0 600
metres
GPR Test Program
Livingstone Creek Test Site
Location Map
AMEROK GEOPHYSICS

Figure A-3-1.

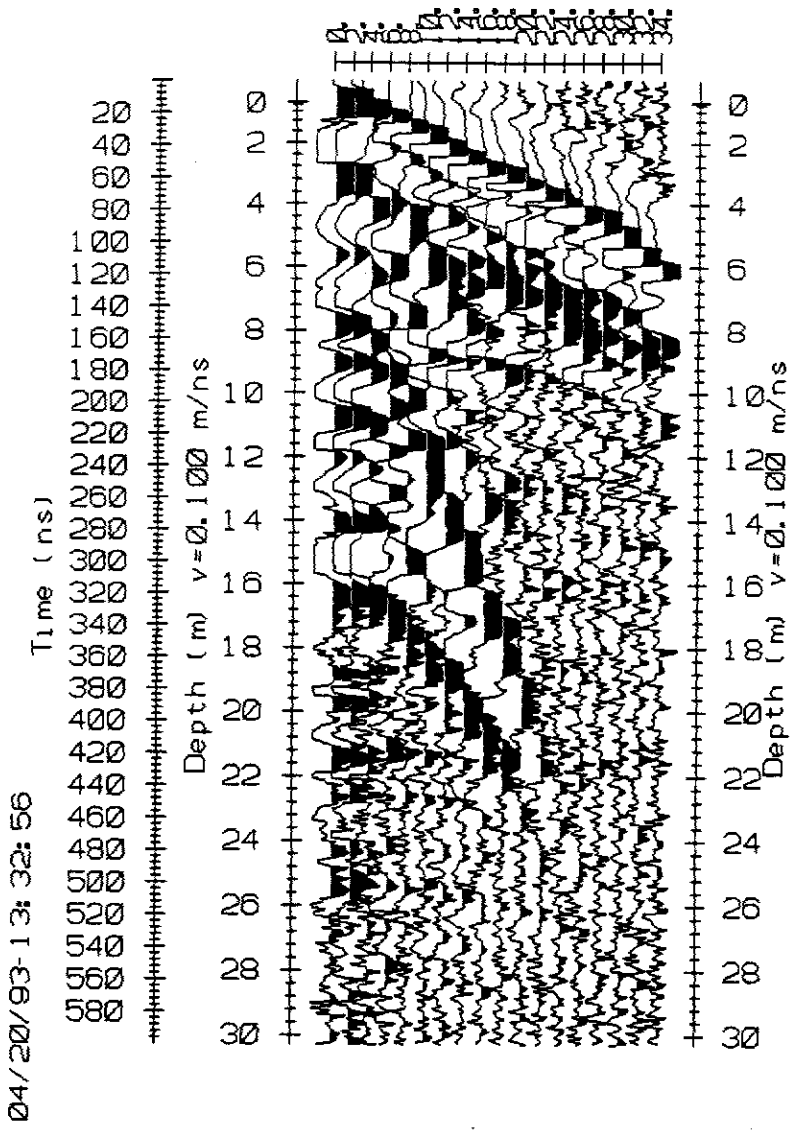


Figure A-3-2. Livingstone Creek 25 MHz CMP radargram. Measurement interval 2 m in separations from 2 to 34 m.

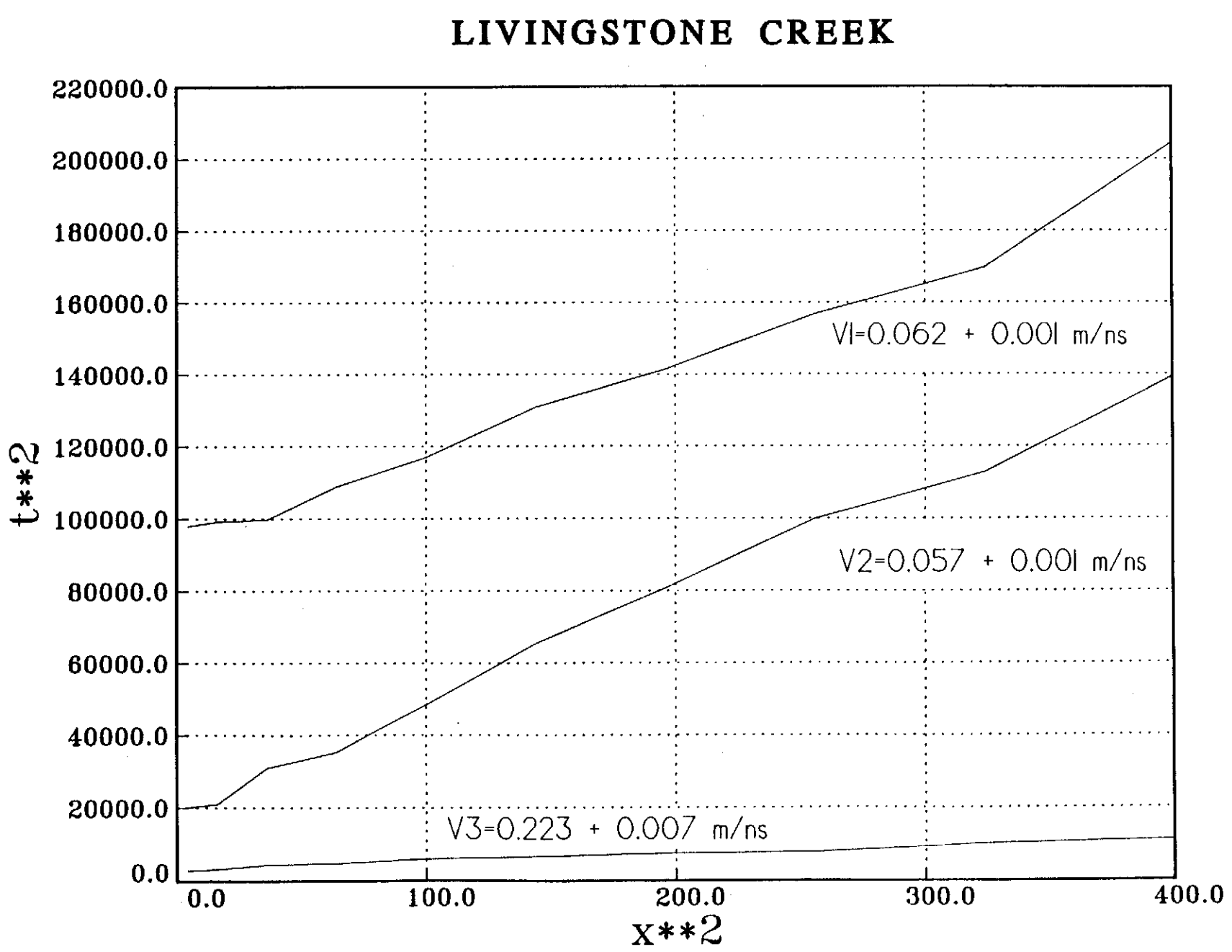


Figure A-3-3. Livingstone Creek $X^2$-$T^2$ diagram. Velocities derived from linear regression are plotted near curves.

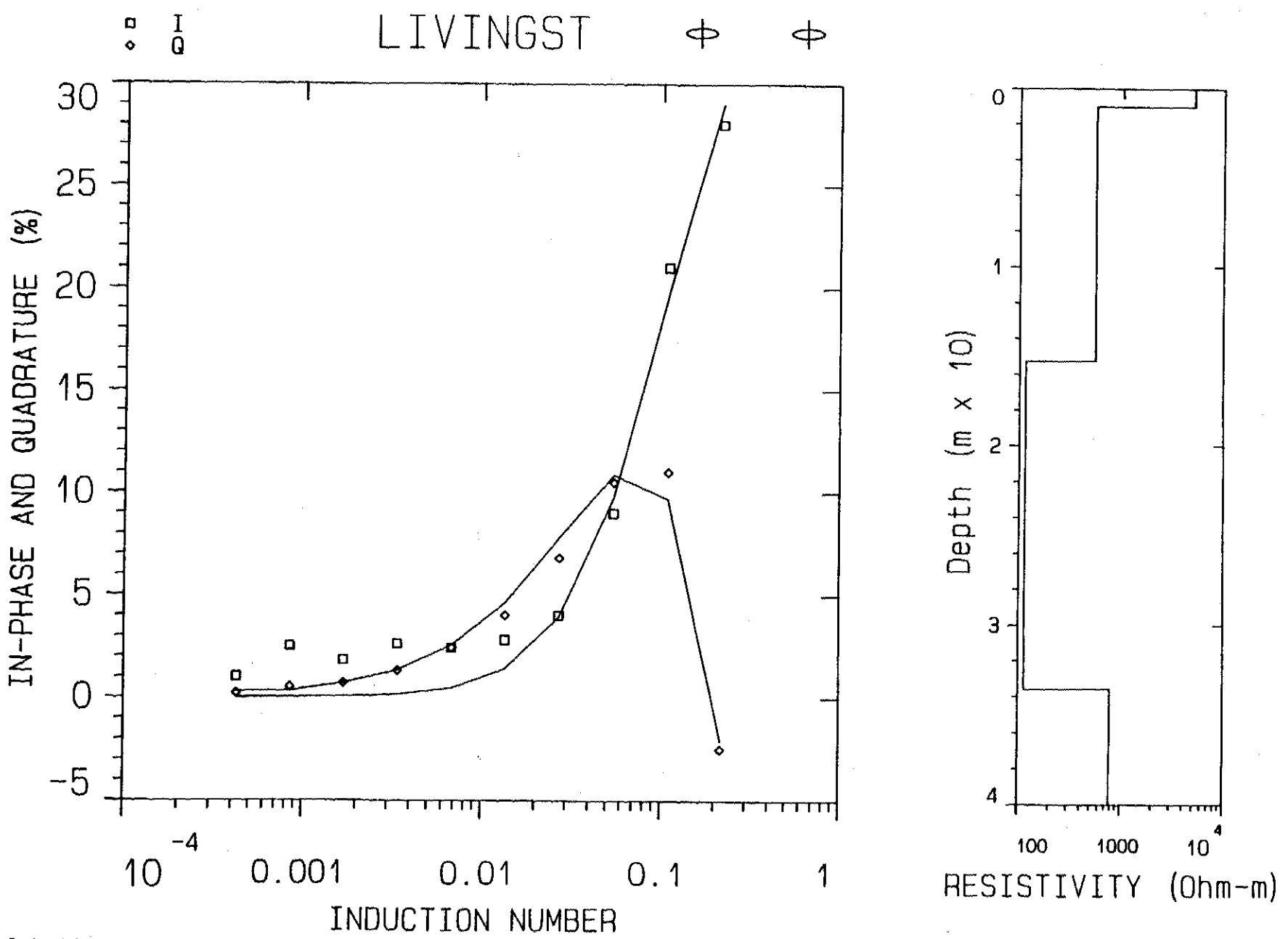


**Figure A-3-4.** Livingstone Creek HLEM sounding results. Synthetic and measured data is on the left. Square symbols indicate measured in-phase, diamonds indicate measured quadrature; curves display synthetic responses. Model is displayed on the right.

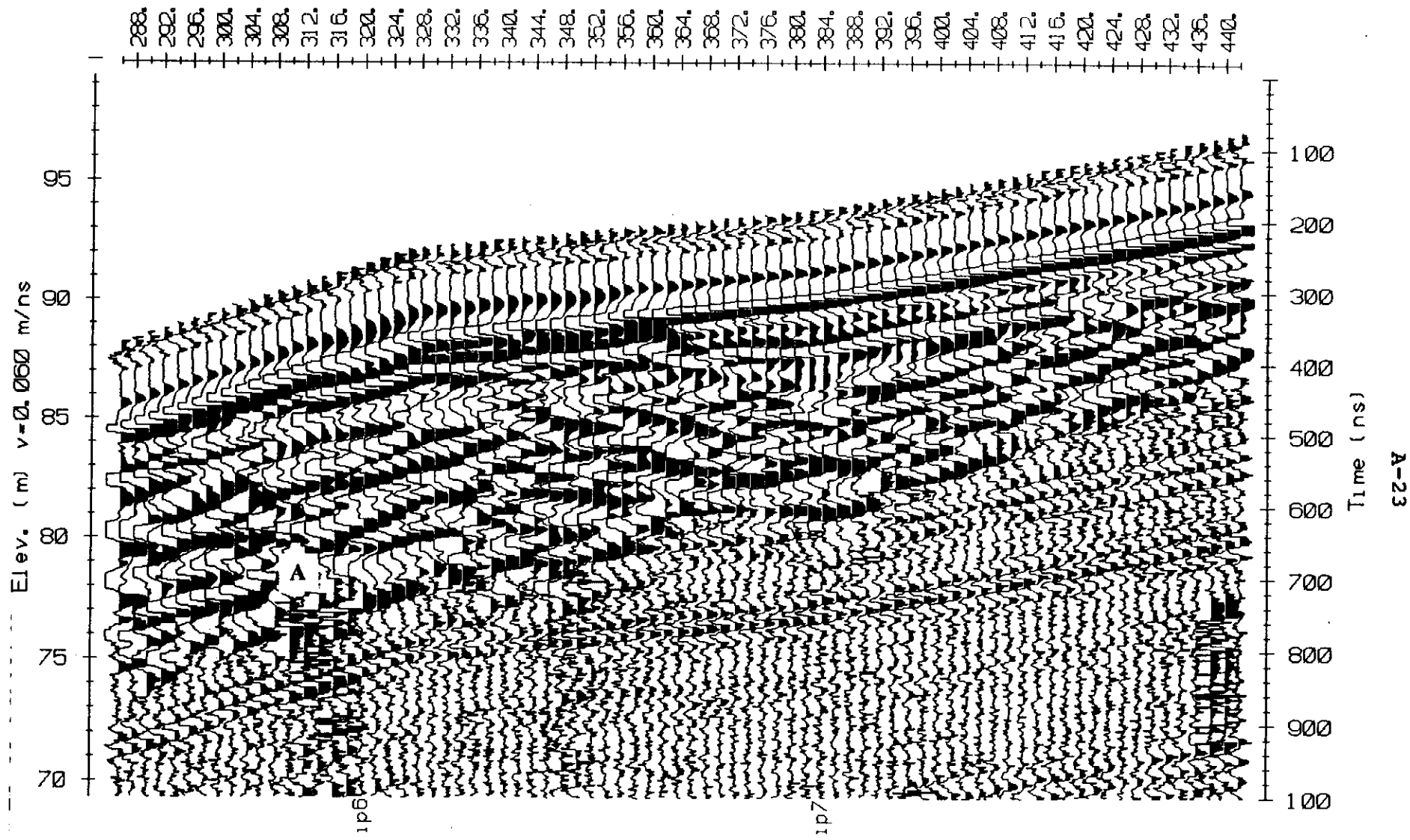


Figure A-3-5. Profile radargram along Livingstone Creek survey line. A indicates the base of the second velocity layer and the possible top of either gravel or clay.

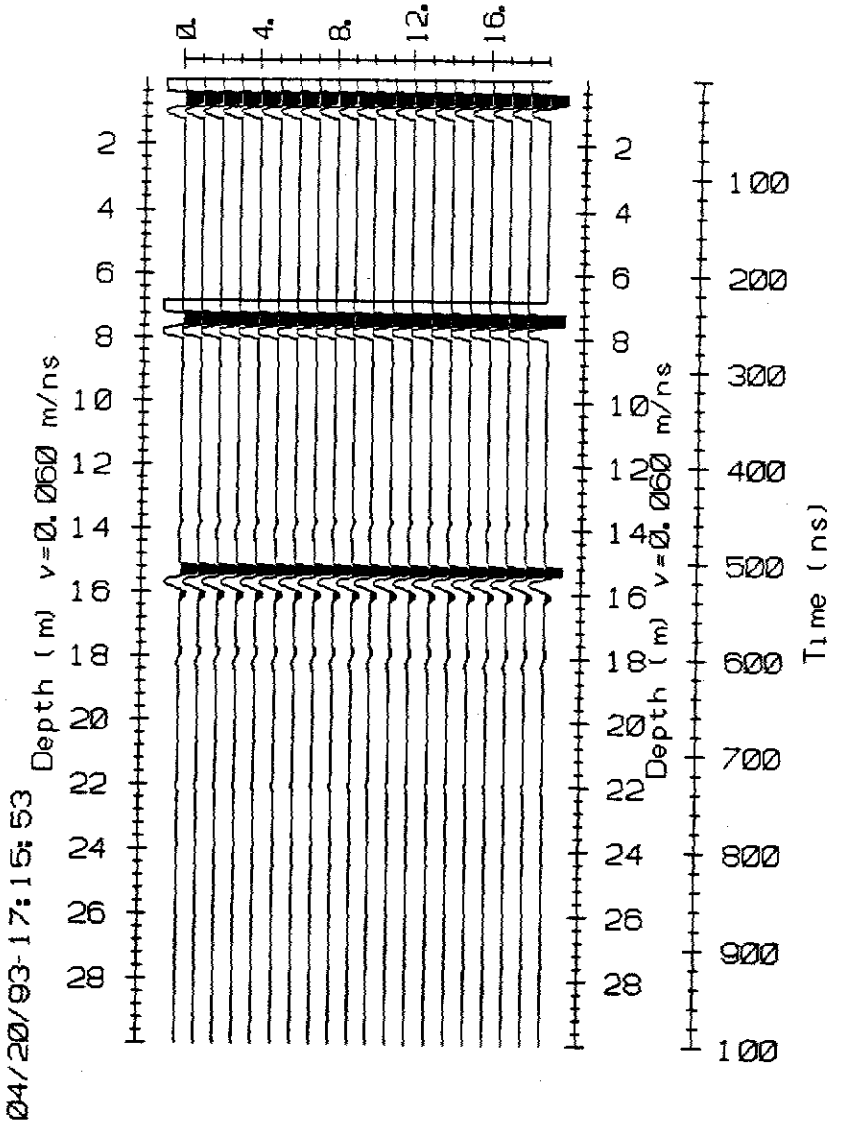


Figure A-3-6. Synthetic radargram based on the model described in the text. Top of clay layer is at 15 m; the reflection from underlying gravel/bedrock at 18 m is severely attenuated overlying clay.

## SITE 4 - KLONDIKE RIVER

### A. Site location

The survey site is located on placer claims P36591 - P36600 located on the second tier, left limit of the Klondike River. The survey site is adjacent to the Yukon Consolidated Gold Company (YCGC) dredge workings with the survey line starting at the junction of the Callison Landfill entrance and the Bear Creek Road and extending northeast to the Klondike Highway (Figure A-4-1).

### B. Local geology

The survey site is underlain by well foliated muscovite-feldspar-quartz schist (Debicki 1984). According to Tom Morgan, a shaft sinking contractor familiar with the area, bedrock is weathered and is overlain by layers of large boulders, silt and sand. Black muck and colluvium overlie gravel. Overburden is frozen in the bush adjacent to the road but appears to be thawed near the Callison Landfill and may be partially thawed beneath the roadbed.

### C. Survey specifications

A CMP velocity survey was conducted at station 200 using the 50 MHz antennas and a variable antenna separation from 2 to 38 m in 2 m increments. A HLEM sounding was conducted at station 0 with a coil spacing of 25m. GPR profiles were surveyed with the 50 MHz and 25 MHz antennas using 2 and 4 m antenna separations respectively and a 2 m station spacing. Measurements were made over an 800 ns window and stacked 64 times.

### D. Results

The CMP survey radargram is plotted in Figure A-4-2 and the $X^2$-$T^2$ plot is shown in Figure A-4-3; results are listed in Table A-4-1. Apparent reflections arriving at 160, 197 and 220 ns are considered suspect; they appear to originate from dipping or point targets and probably do not represent layer boundaries. An air wave arrives at 3 ns and events arriving at 53, 80 and 245 ns appear to be reflections. These correlate with continuous reflections in the profile radargram. The first reflection appears to be the base of seasonal frost while the second may be the base of muck. The third arrival correlates with the bedrock reflection.

The HLEM sounding inversion is shown in Figure A-4-4 and results are tabulated in Table A-4-2; details of the inversion are in Appendix C. The inversion is poor with an RMS error of 1.29% and measurement error of $\pm$ 0.5%. There is considerable mismatch between

the synthetic and measured in-phase responses. In general, high in-phase and quadrature measurements at a short coil spacing indicate that the ground is quite conductive at the sounding site. The half-space resistivity is low, particularly for frozen material and is probably due to conductive (thawed?) black muck.

**Table A-4-1. Klondike River velocity survey results**

| Layer | $V_{NMO}$ (m/ns) | $V_{DIX}$ (m/ns) | Interval (m) | Remarks |
|---|---|---|---|---|
| 0 | 0.354 ± 0.010 | n/a | 0 | air wave |
| 1 | 0.154 ± 0.002 | 0.154 | 0 - 4.1 | frozen roadbed/ muck |
| 2 | 0.132 ± 0.002 | 0.071 | 4.1 - 5.3 | muck (?) |
| 3 | 0.139 + 0.005 | 0.142 | 5.3 - 18.0 | gravel |

**Table A-4-2. Klondike River resistivity sounding results**

| Layer | Resistivity (Ω-m) | Interval (m) | Remarks |
|---|---|---|---|
| 1 | 320 | 0 - 0.4 | |
| 2 | 17 | 0.4 - 0.6 | |
| 3 | 466 | 0.6 + | |

Excerpts from the GPR profile radargrams are shown in Figures A-4-5 through A-4-7. In Figure A-4-5, a layer of black muck, thinning to the right, produces the first reflection below the direct wave arrival. The bedrock reflector is not apparent at the start of the profile but fades in at about station 40. The absence of a bedrock reflection at the start of the profile is probably caused by signal attenuation; YCGC drill sheets do not indicate that bedrock is significantly deeper in this area. Past station 40, a strong continuous reflection from the top of weathered bedrock was observed on the rest of the radargram. This reflector is irregular and where large blocks of bedrock are present, diffraction trails are recorded in the radargram (Figure A-4-6). As noted above, surveys were run with both the 25 MHz and 50 MHz antennas. Acceptable penetration was achieved with both frequencies over most of the survey line with the higher frequency providing greater detail in the radargrams. This is at the expense of clarity. Figures A-4-6 and A-4-7 are profiles over the same area with 25 and 50 MHz antennas respectively. The bedrock reflection is more apparent in the lower frequency profile.

YCGC drill holes near the end of the GPR line intersected bedrock at approximately 12 m while the GPR survey detected bedrock at 10 to 12 m in this area. In general, GPR appears to work quite well in this environment; bedrock reflections are strong and persistent and there is little signal cluttering from other layers at 25 MHz. It would have been possible to conduct an extensive GPR survey in this area with minimal drill hole or shafting control and still be quite confident that bedrock was accurately mapped. The exception to this optimistic observation occurs at the start of the survey line where deep reflections are screened by as little as 3 m of conductive black muck.

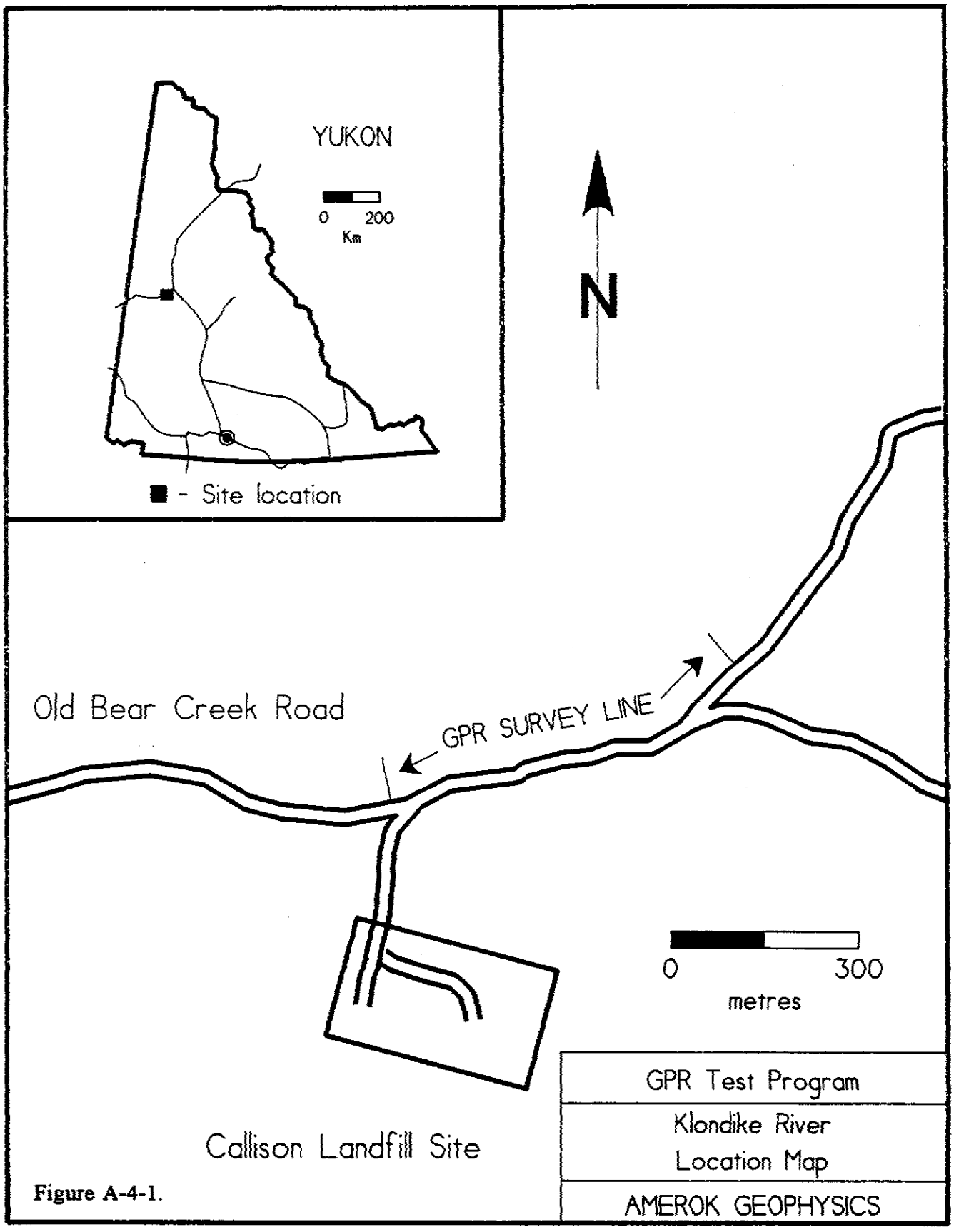
YUKON
0 200
Km
■ - Site location
N
Old Bear Creek Road
GPR SURVEY LINE
0 300
metres
Callison Landfill Site
GPR Test Program
Klondike River
Location Map
AMEROK GEOPHYSICS

**Figure A-4-1.**

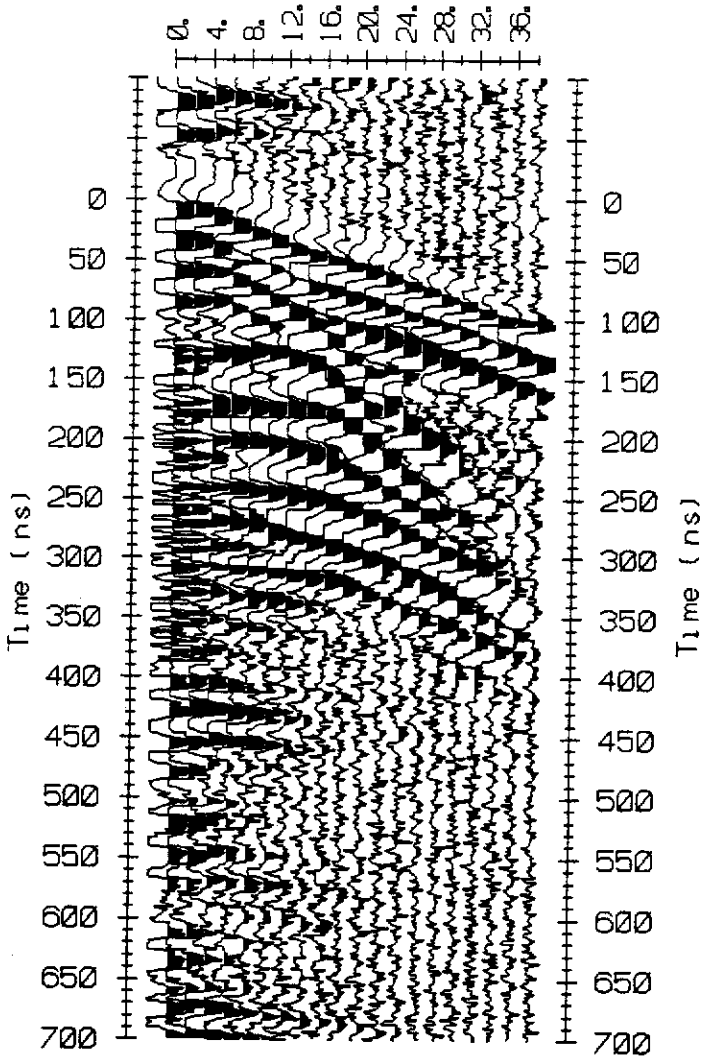


Figure A-4-2. Klondike River 50 MHz CMP radargram. Measurement interval 2 m in separations from 2 to 34 m.

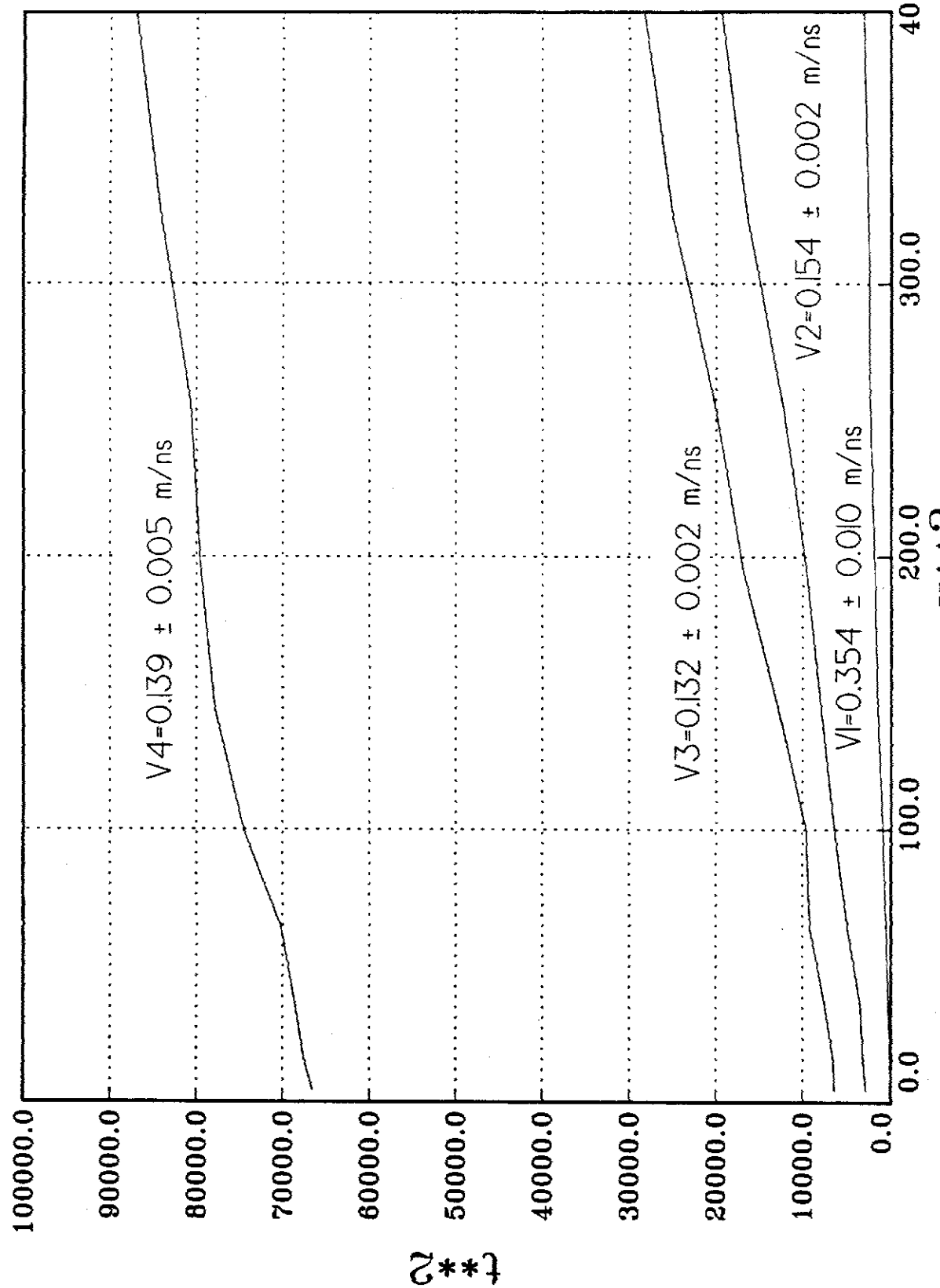


**Figure A-4-3. Klondike River $X^2$-$T^2$ diagram. Velocities derived from linear regression are plotted near curves.**

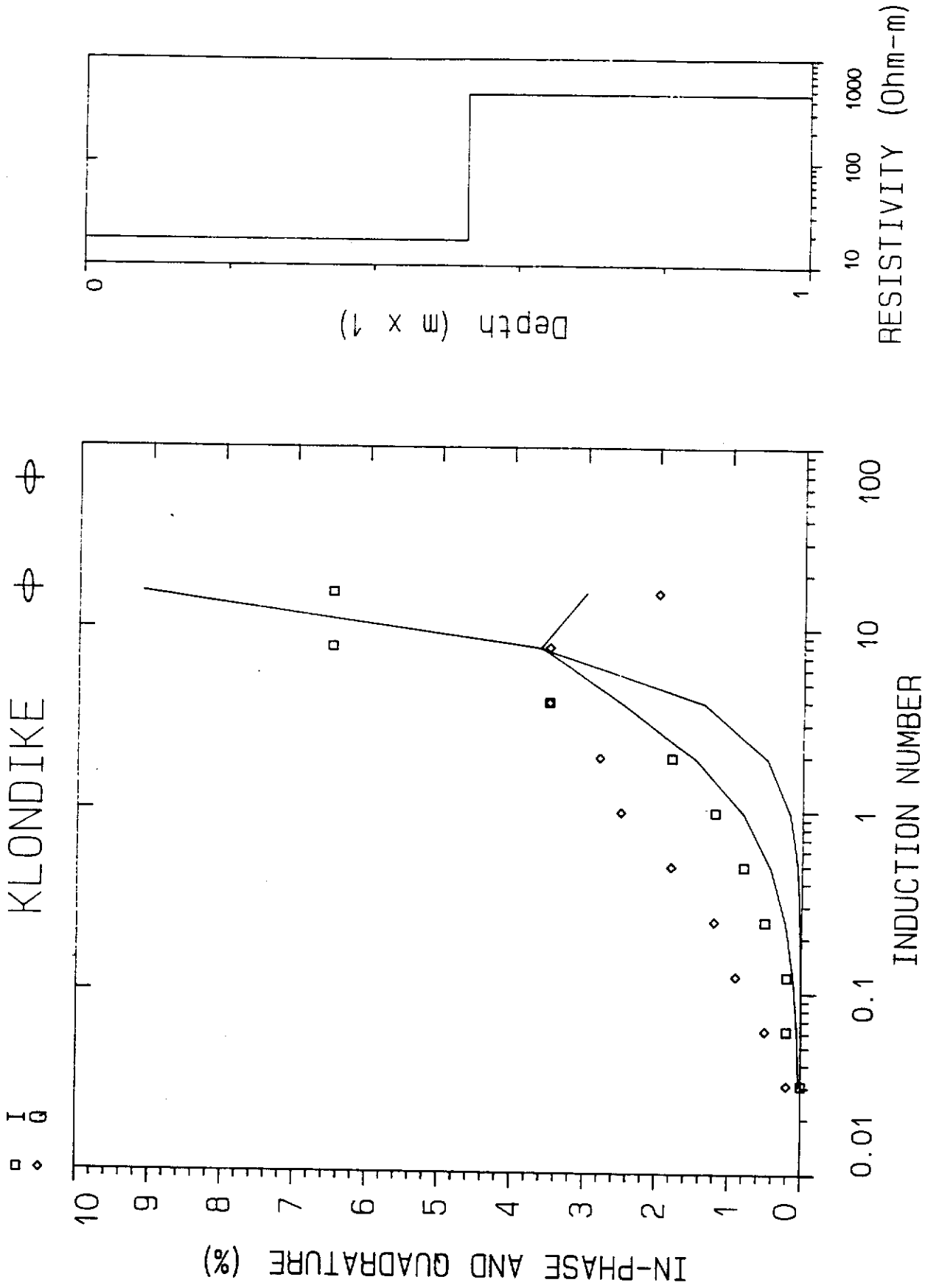


Figure A-4-4. Klondike River HLEM sounding results. Synthetic and measured data is on the left. Square symbols indicate measured in-phase, diamonds indicate measured quadrature; curves display synthetic responses. Model is displayed on the right.

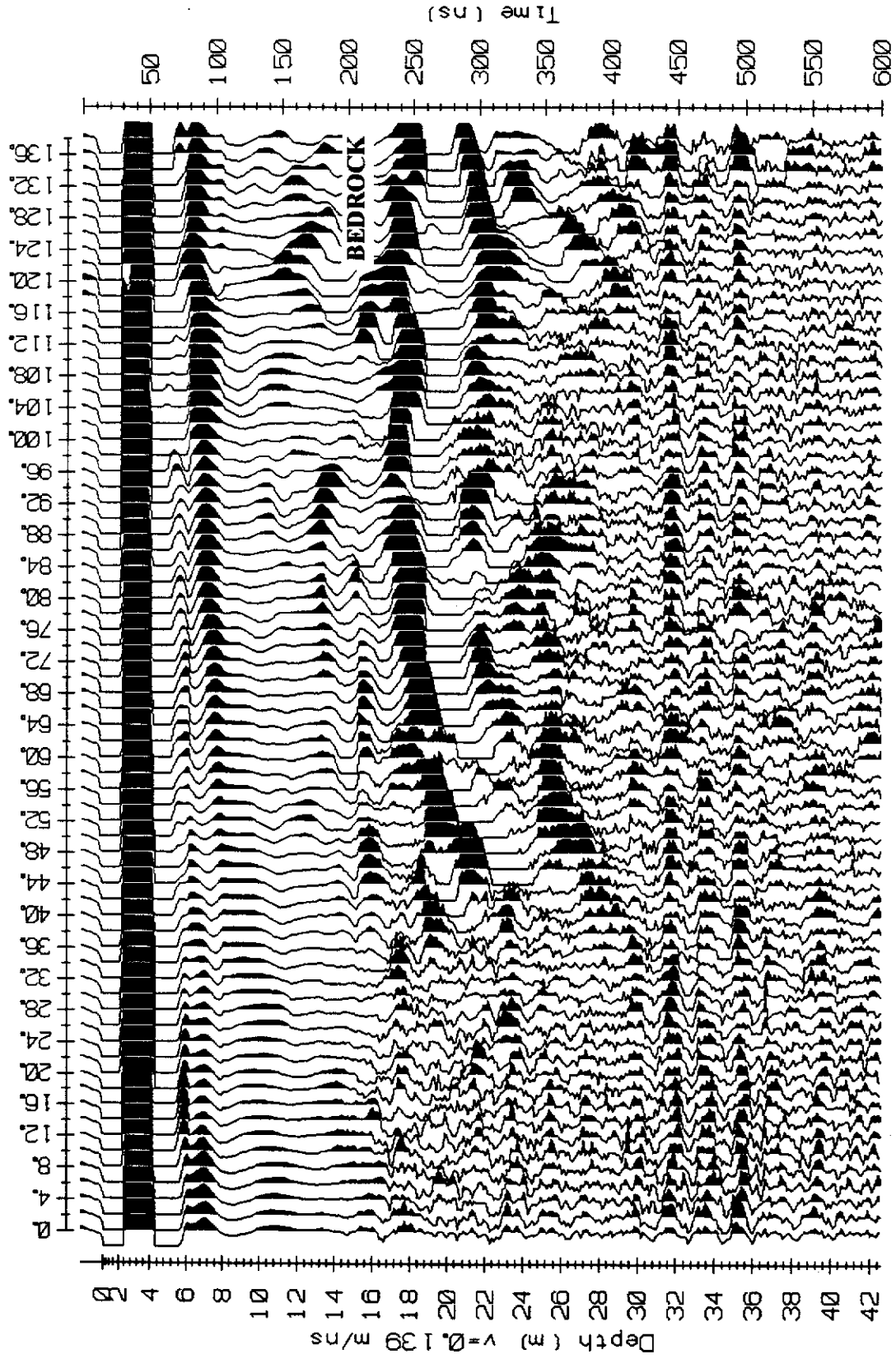


**Figure A-4-5. Excerpt from 25 MHz profile radargram on the Klondike River test line. Near the start of the line, GPR reflections are attenuated beneath a conductive layer of black muck.**

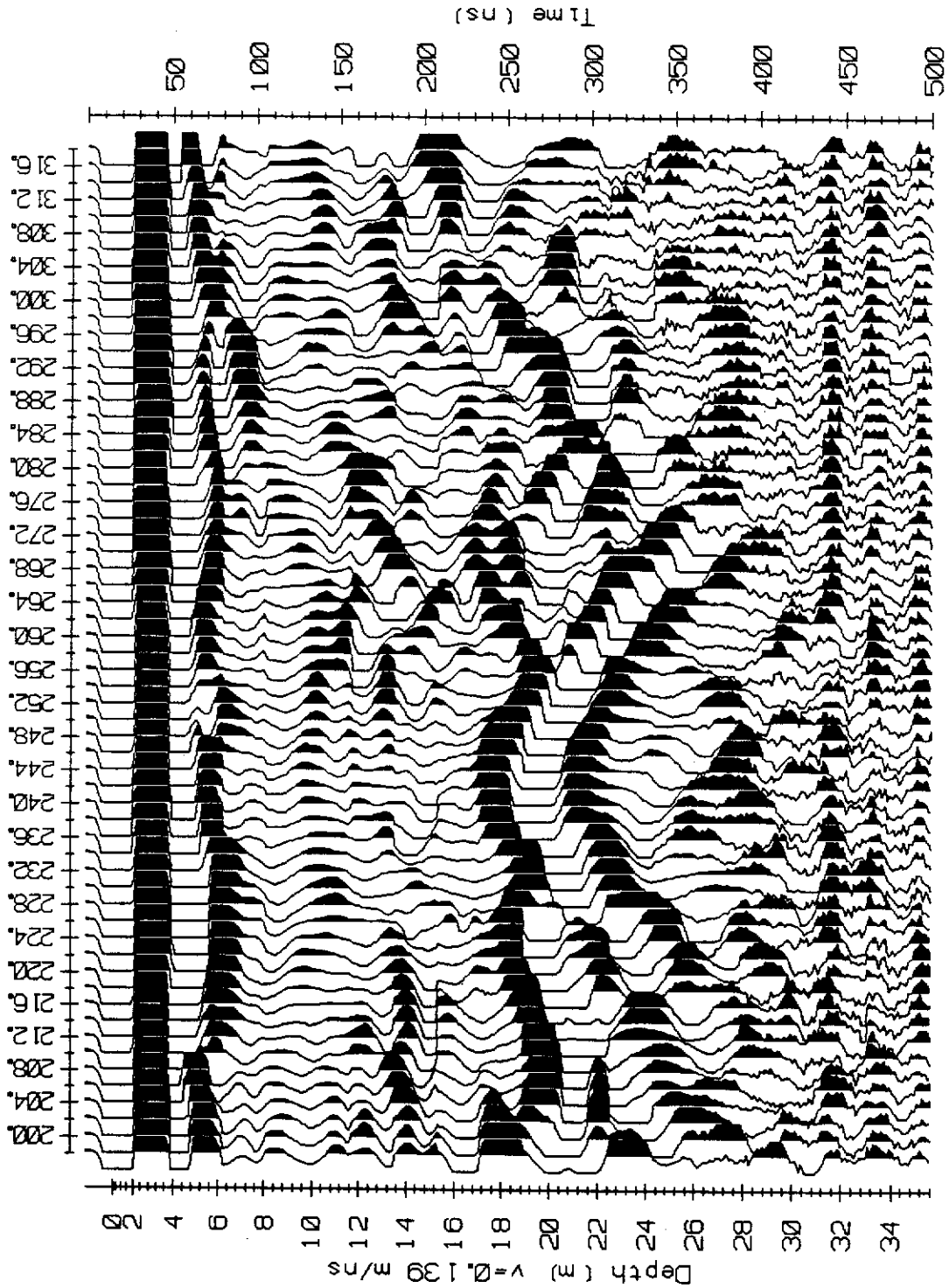


Figure A-4-6. Excerpt from 25 MHz profile radargram on the Klondike River test line. Bedrock contact is irregular, creating diffraction trails in the radargram. The base of seasonal frost and muck are also visible.

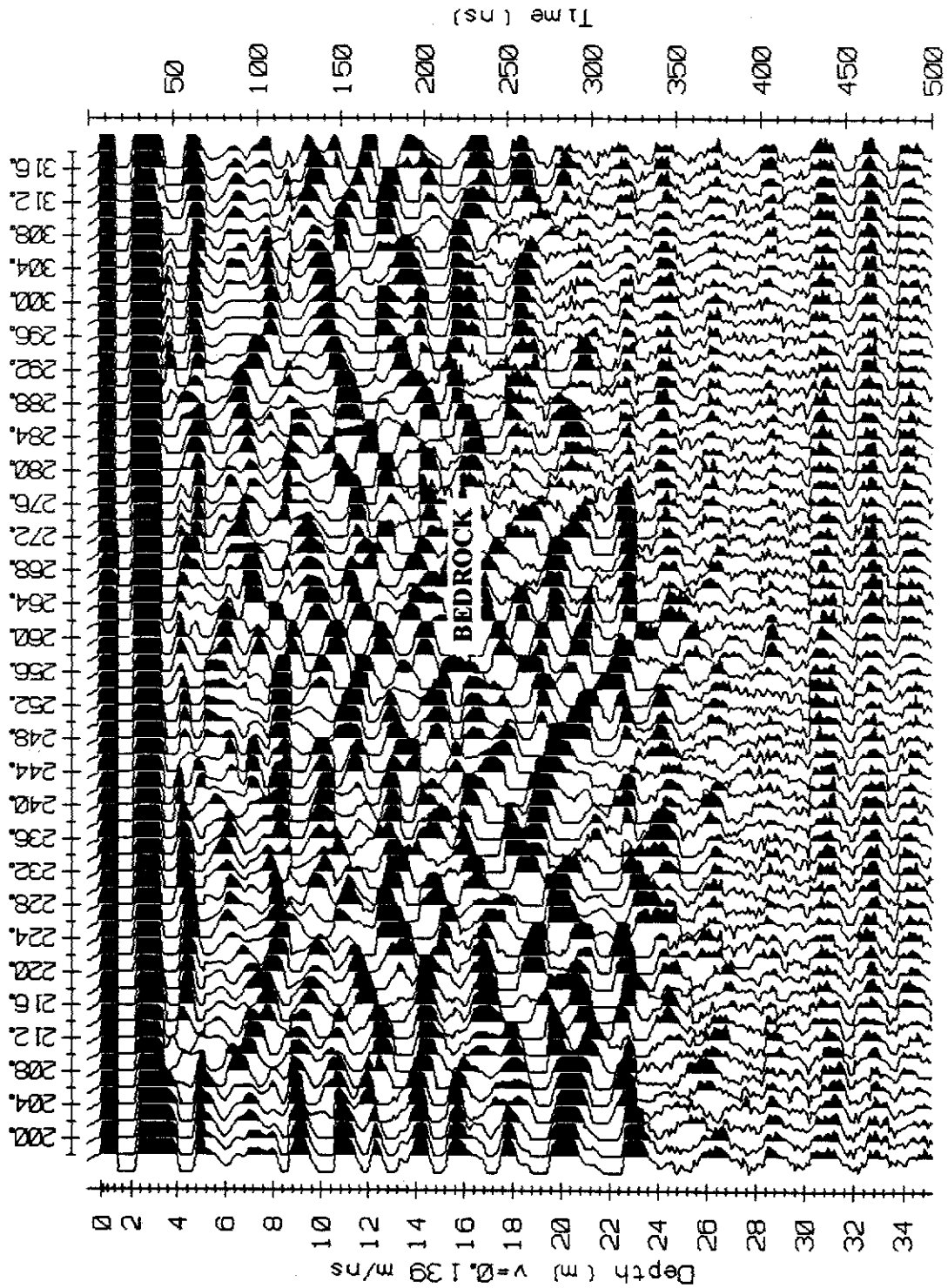


Figure A-4-7. Excerpt from 50 MHz profile radargram on the Klondike River test line showing same area as in Figure A-4-6. Reflection resolution is excellent but additional arrivals tend to clutter the radargram and obscure the bedrock reflection.

## SITE 5 - GOLD RUN CREEK

### A. Site location

The survey site is located on placer claims P36591 - P36600 located on the lower end of Gold Run Creek approximately 1 km above its confluence with Dominion Creek. The property can be reached from Dawson City via the Dominion Creek or Gold Run Creek roads.

### B. Local geology

The survey site is underlain by chlorite-quartz schist and well foliated muscovite-feldspar-quartz schist (Debicki 1984). Bedrock is deeply weathered and overlain by White Channel Gravel and black muck. The entire section is frozen and at the time of the survey, had been stripped of moss and snow.

### C. Survey specifications

The GPR profile survey was conducted along three lines parallelling Yukon Consolidated Gold Corporation (YCGC) drill fences (Figure A-5-1). Hole plugs had been removed during stripping and the drill hole locations shown were relocated during a subsequent topographic survey. A HLEM sounding was conducted near the middle of GPR line 1 and a CMP velocity survey was conducted immediately west of line 1. The CMP velocity survey was conducted with the 25 MHz antennas and an antenna separation varying from 2 to 38 m in 1 m increments. GPR profiles were surveyed with the 25 MHz antennas using a 4 m antenna separation and 2 m station spacing.

### D. Results

The CMP survey radargram is plotted in Figure A-5-2 and the $X^2$-$T^2$ plot is shown in Figure A-5-3; results are tabulated in Table A-5-1. Although several arrivals are present after the air wave, only the arrival at approximately 140 ns was processed as a reflection. A weak arrival at 60 ns and a much stronger one at 80 ns are probably reflections from dipping surfaces or point sources. The points of maximum curvature on these arrivals do not occur at the minimum separation but at separations of 8 and 11 m respectively. The 140 ns arrival has a $V_{NMO}$ within the range expected for a combined layer of muck and gravel and occurs at roughly the same depth as bedrock in this area. The three nearest drill holes bottomed in weathered bedrock at depths of 9.1 to 9.8 m while the apparent depth to the reflector is 8.7 m.

The HLEM resistivity sounding results are displayed in Figure A-5-4 and listed in Table A-5-2; details of the inversion are in Appendix C. The inversion fitting error (RMS error) was 1.11% and the probable measurement error was ± 0.5%. In general, the second layer displays the high resistivity expected of frozen overburden. The very low resistivity of the third layer could be an artifact of the inversion algortithm or be caused by conductive clay alteration in weathered bedrock. It is interesting to note that no reflections were recorded below the apparent bedrock reflector in any of the radargrams.

**Table A-5-1. Gold Run Creek velocity survey results.**

| Layer | $V_{NMO}$ (m/ns) | $V_{DIX}$ (m/ns) | Interval (m) | Remarks |
|---|---|---|---|---|
| 0 | 0.386 ± 0.013 | n/a | 0 | air wave |
| 1 | 0.124 ± 0.005 | 0.124 | 0 - 8.6 | gravel + muck |

**Table A-5-2. Gold Run Creek resistivity sounding results.**

| Layer | Resistivity (Ω-m) | Interval (m) | Remarks |
|---|---|---|---|
| 1 | 9282 | 0 - 2 | air + surface ice |
| 2 | 3431 | 2-13 | muck/gravel |
| 3 | 113 | 13-21 | inversion artifact or weathered bedrock |
| 4 | 2556 | 21+ | bedrock |

The profile radargrams on GPR lines 1 through 3 are shown in figures A-5-5 through A-5-7 together with YCGC drill hole data projected into the sections. Each drill hole contains an upper section of black muck and frozen silt and an underlying dredge section consisting of gravel and a variable thickness of weathered bedrock. It was common practice to drill test holes into fresh bedrock and dredge the weathered bedrock during subsequent mining. Consequently, the total depth of the holes is 1 to 3 greater than the depth to weathered bedrock. If sand was encountered in the drilling, the entire section below the intersection would be counted as dredge section. Holes in which this occurred usually have anomalously thick dredge sections.

Bedrock and the base of muck produce reflections of variable intensity and continuity. On lines 2 and 3, strong and fairly continuous bedrock reflections were recorded. On line 2, the base of muck also appears to have produced a strong reflection (drill hole 4 appears to have intersected sand at a shallow depth). Reflections on line 1 were difficult to pick on account of the steep apparent dip - a problem which could have been rectified with a finer station spacing. Nonetheless, reflections correlating with the base of muck and the top of bedrock were recorded. Because the drill hole locations are not on the GPR lines it is difficult to assess the accuracy of bedrock determinations; in general, it appears that GPR can determine the depth to bedrock to within $\pm$ 1.5 m in this environment. Discrepancies probably result from local undulations in bedrock or changes in $V_{NMO}$ caused by increased thicknesses of muck. Without orientation drilling prior to a survey, it would be difficult to reliably map bedrock in this deposit because of signal cluttering and the variable strength of the bedrock reflection.

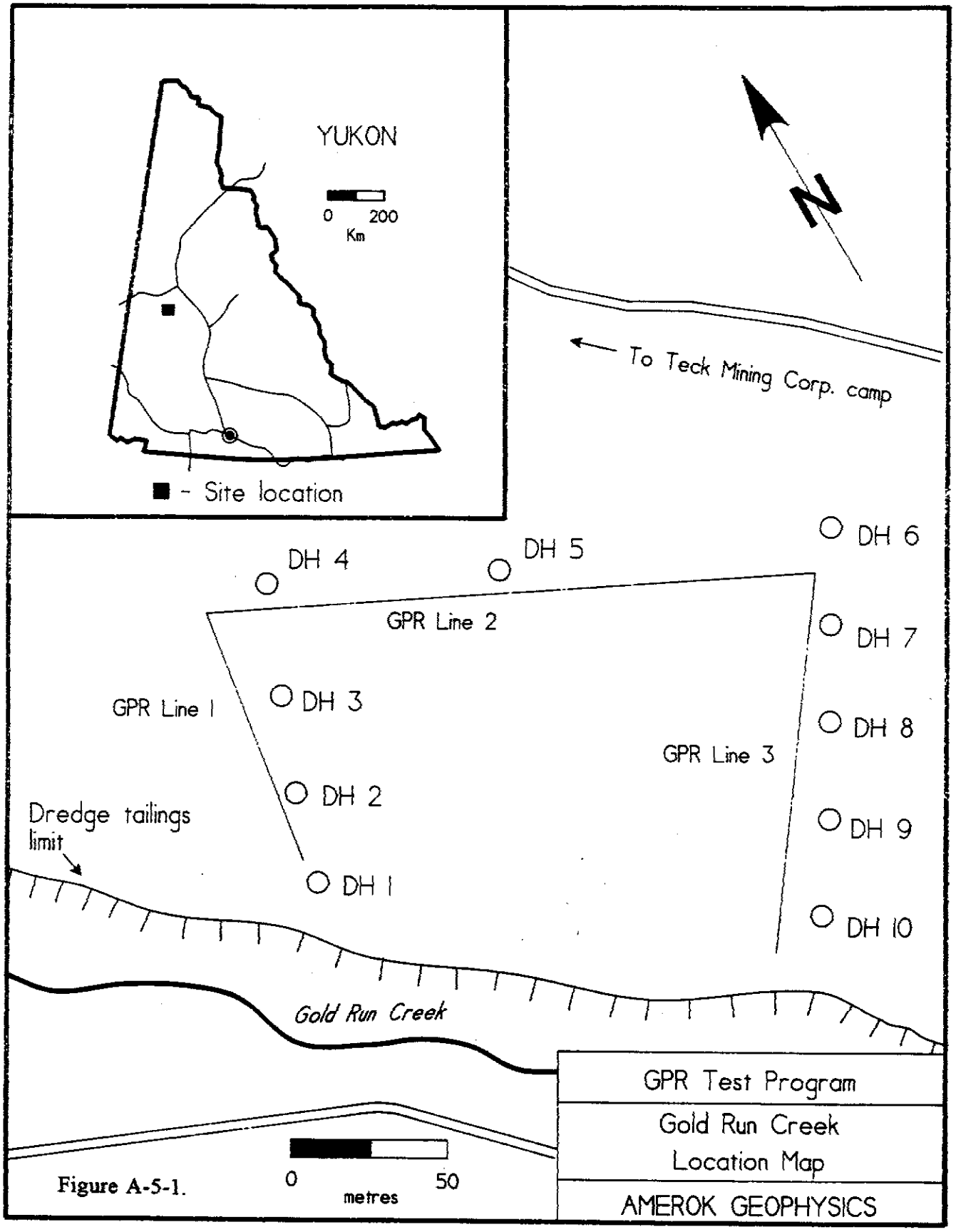
YUKON
0 200
Km
■ - Site location
N
To Teck Mining Corp. camp
DH 4
DH 5
DH 6
DH 7
DH 8
DH 9
DH 10
DH 3
DH 2
DH 1
GPR Line 1
GPR Line 2
GPR Line 3
Dredge tailings limit
Gold Run Creek
0 50
metres
GPR Test Program
Gold Run Creek
Location Map
AMEROK GEOPHYSICS

**Figure A-5-1.**

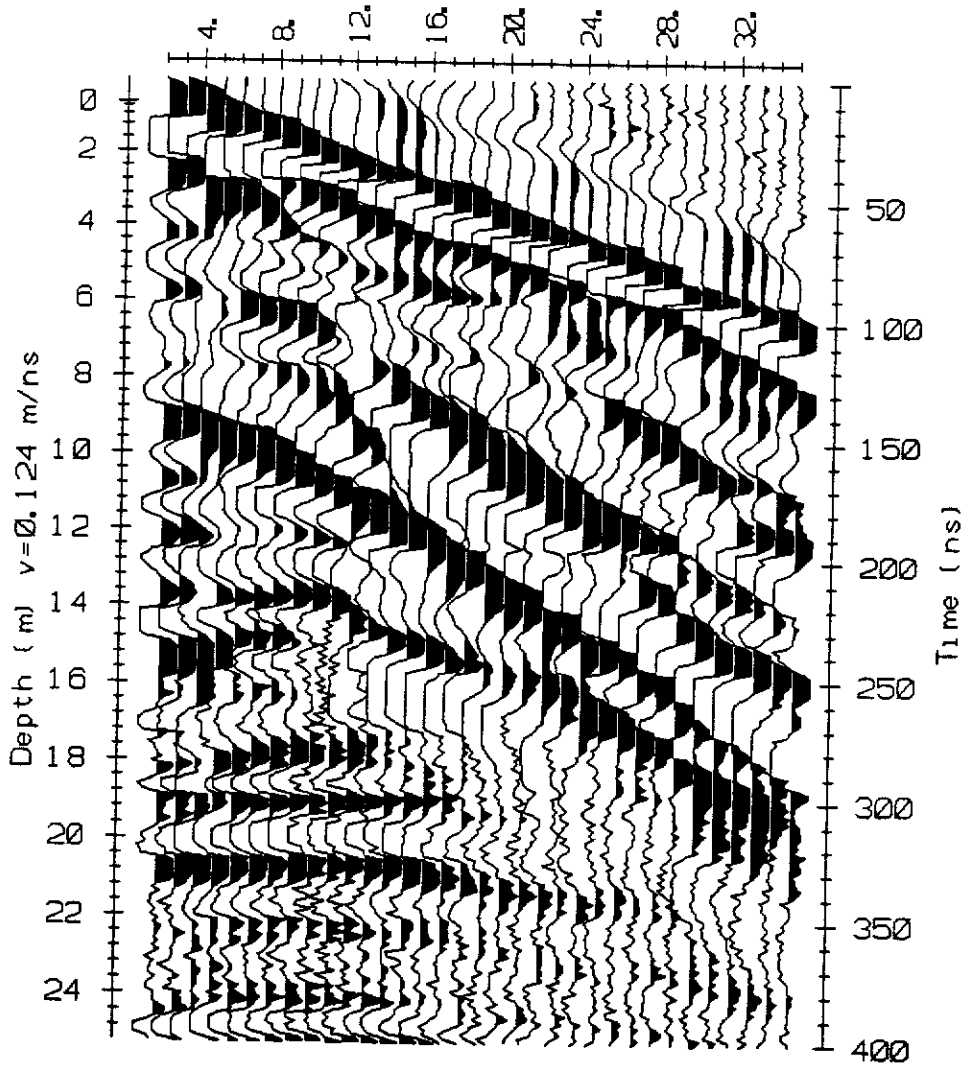


Figure A-5-2. Gold Run Creek 25 MHz CMP radargram. Measurement interval 1m in separations from 2 to 36 m.

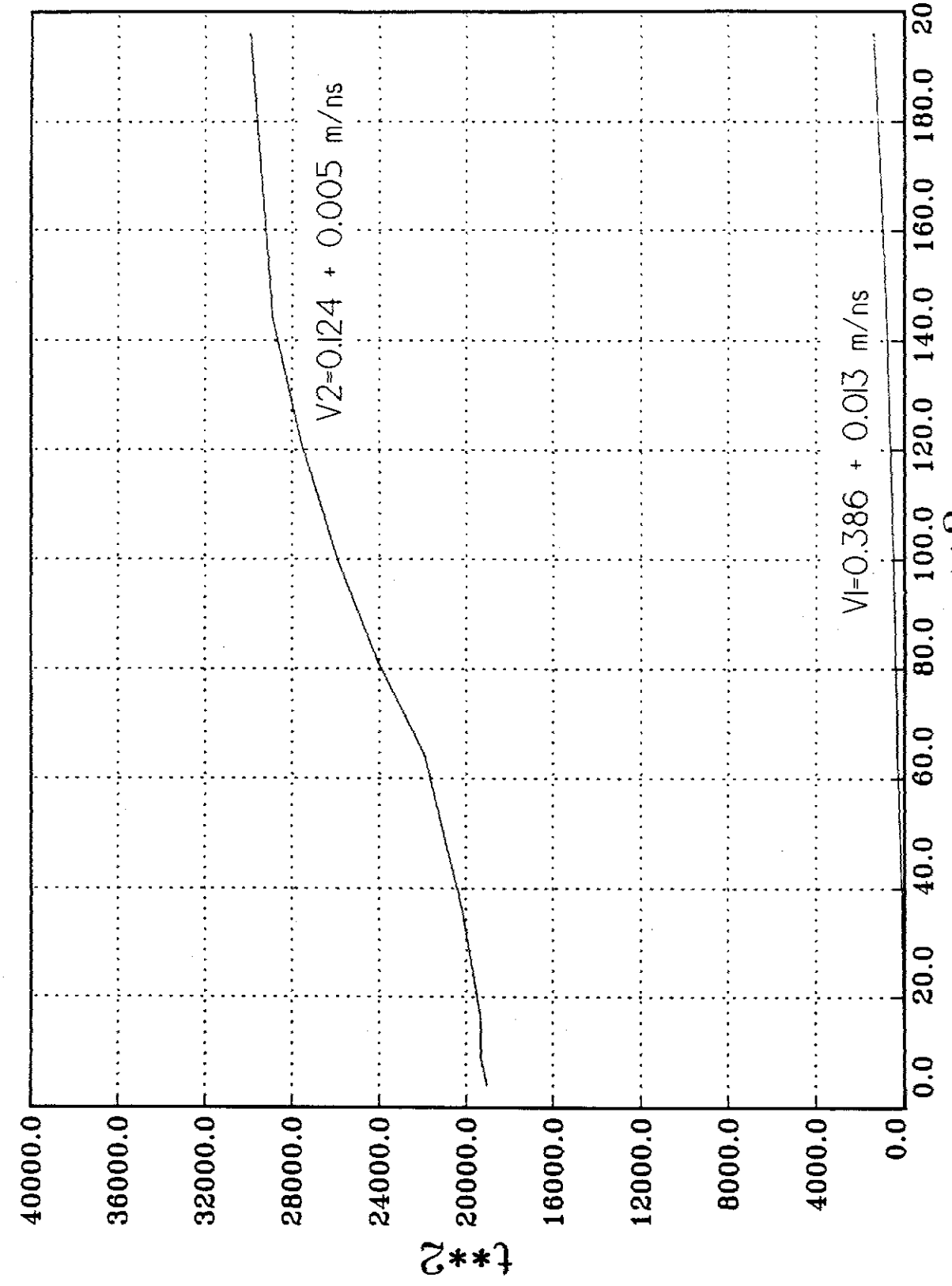


Figure A-5-3. Gold Run Creek $X^2$-$T^2$ diagram. Velocities derived from linear regression are plotted near curves.

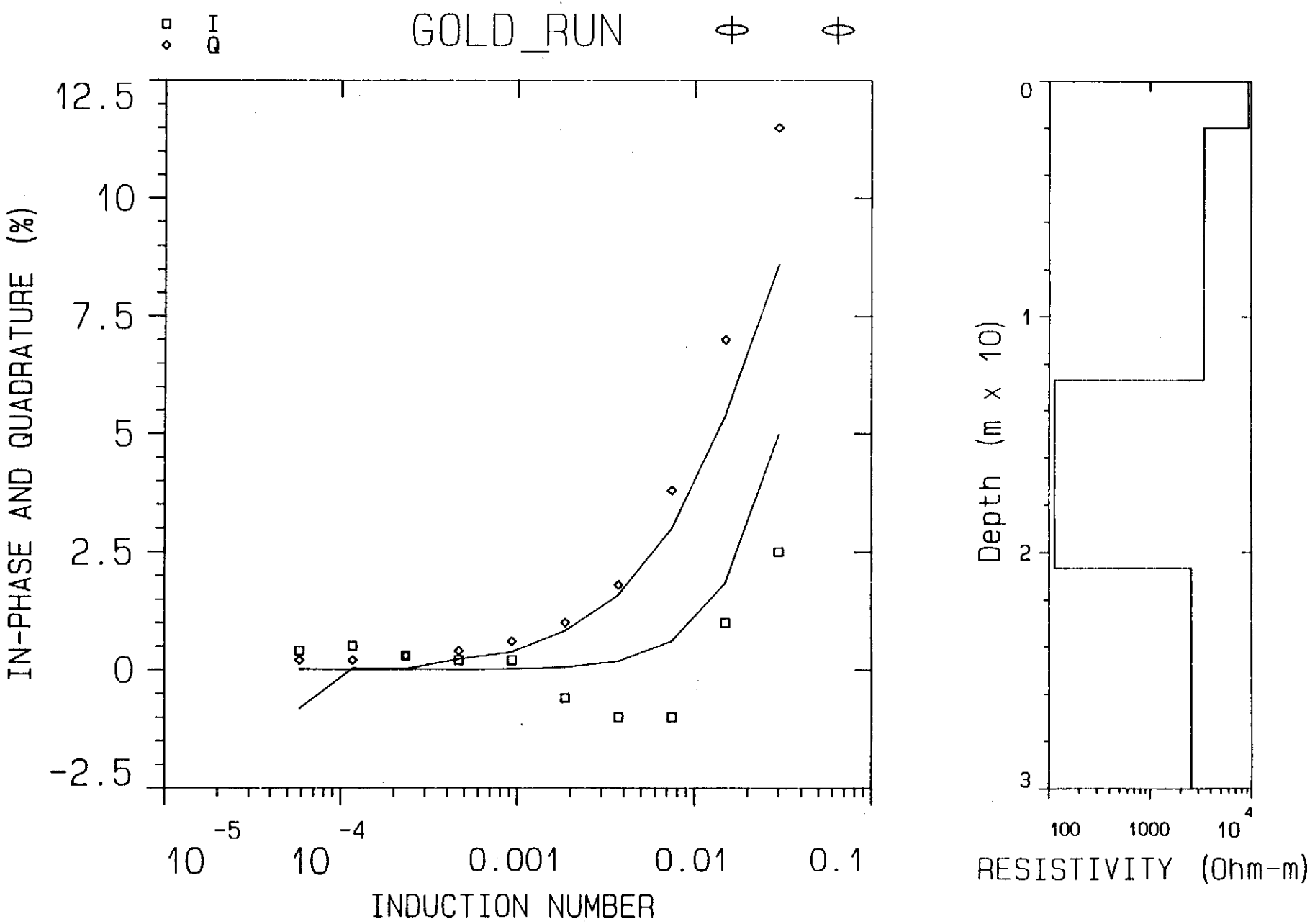


Figure A-5-4. Gold Run Creek HLEM sounding results. Synthetic and measured data is on the left. Square symbols indicate measured in-phase, diamonds indicate measured quadrature; curves display synthetic responses. Model is displayed on the right.

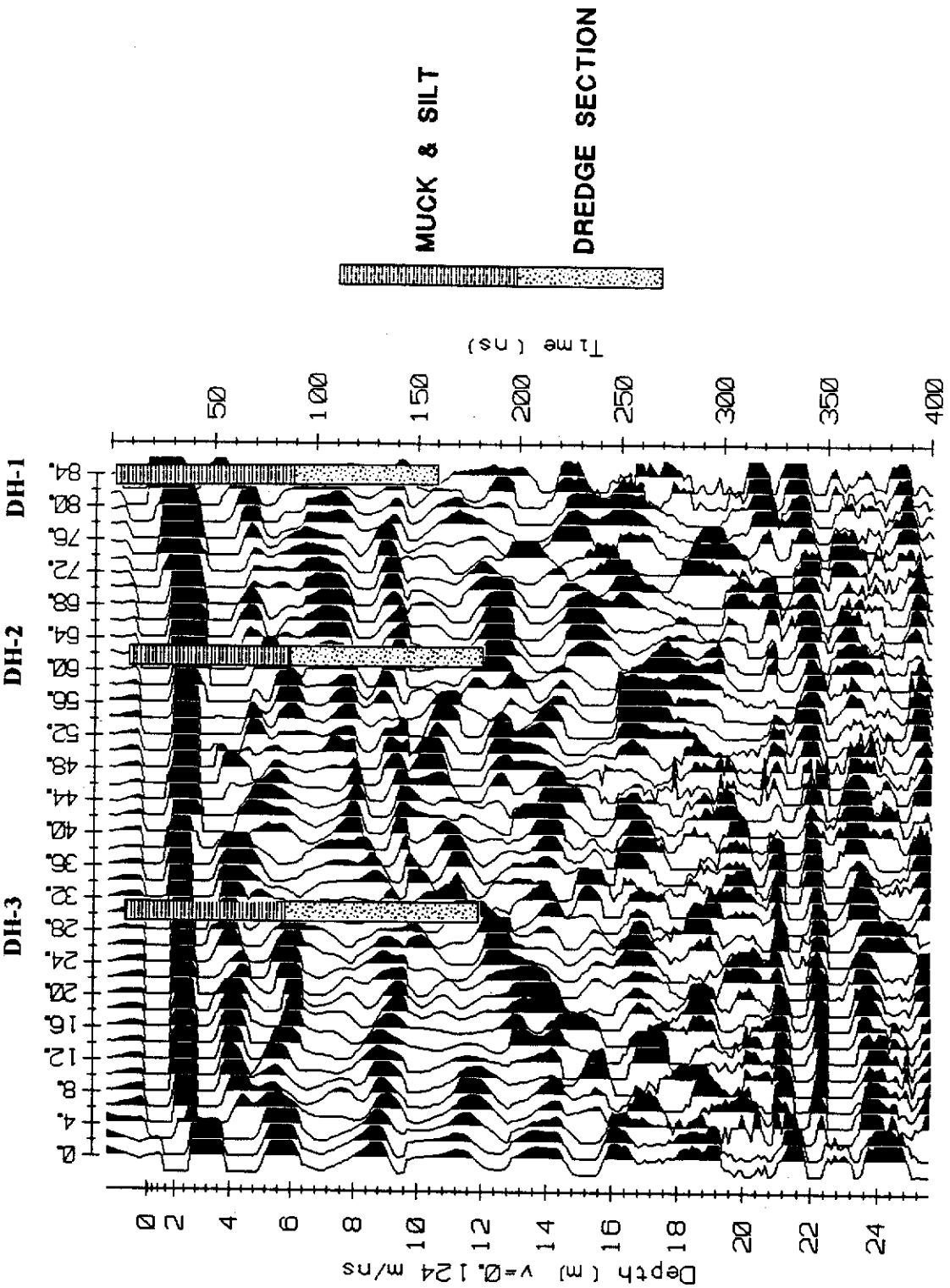


**Figure A-5-5.** Profile radargram along Gold Run Creek, Line 1. Drill holes are projected up to 20 m into the section.

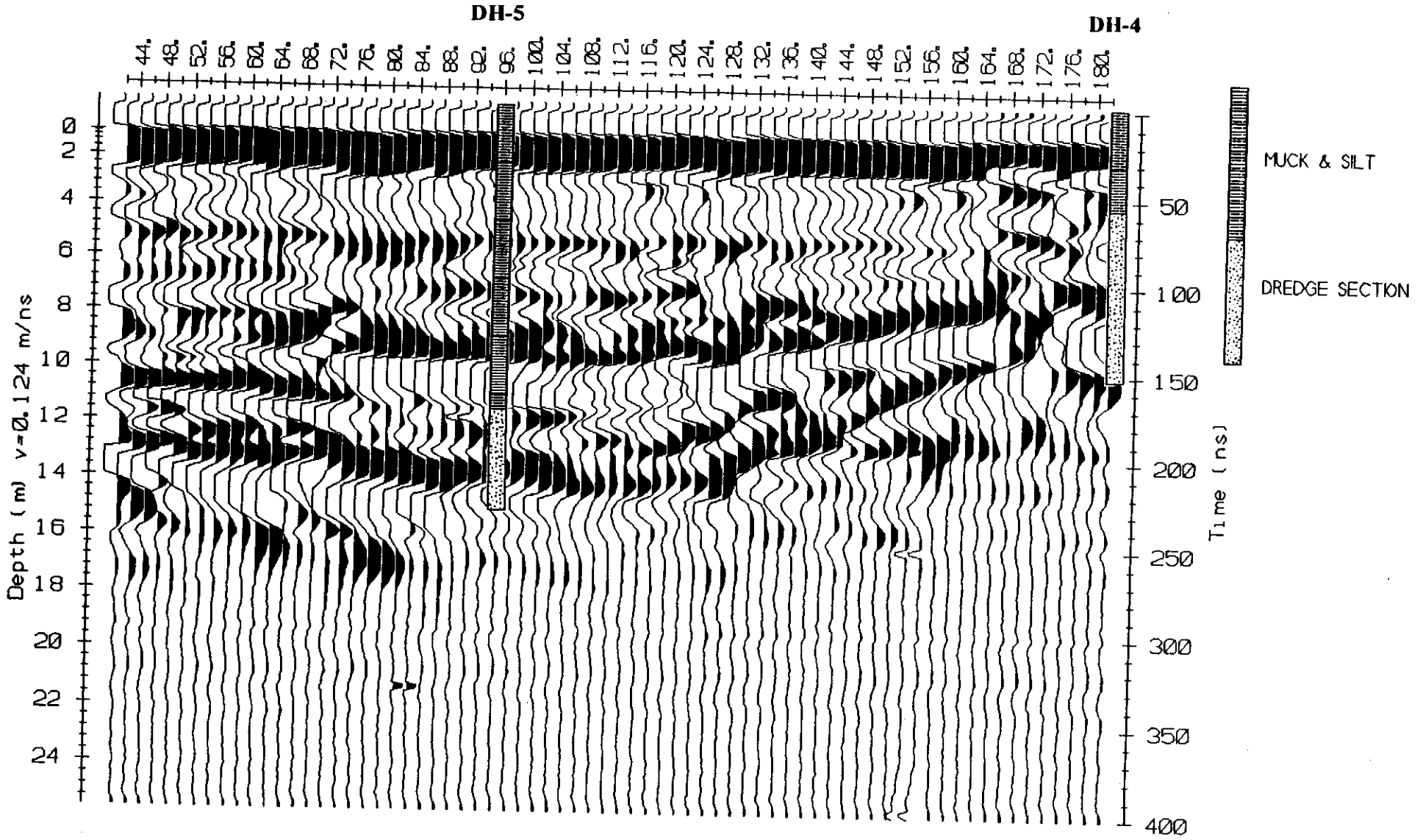


Figure A-5-6. Profile radargram along Gold Run Creek, Line 2. Drill holes are projected up to 20 m into the section.

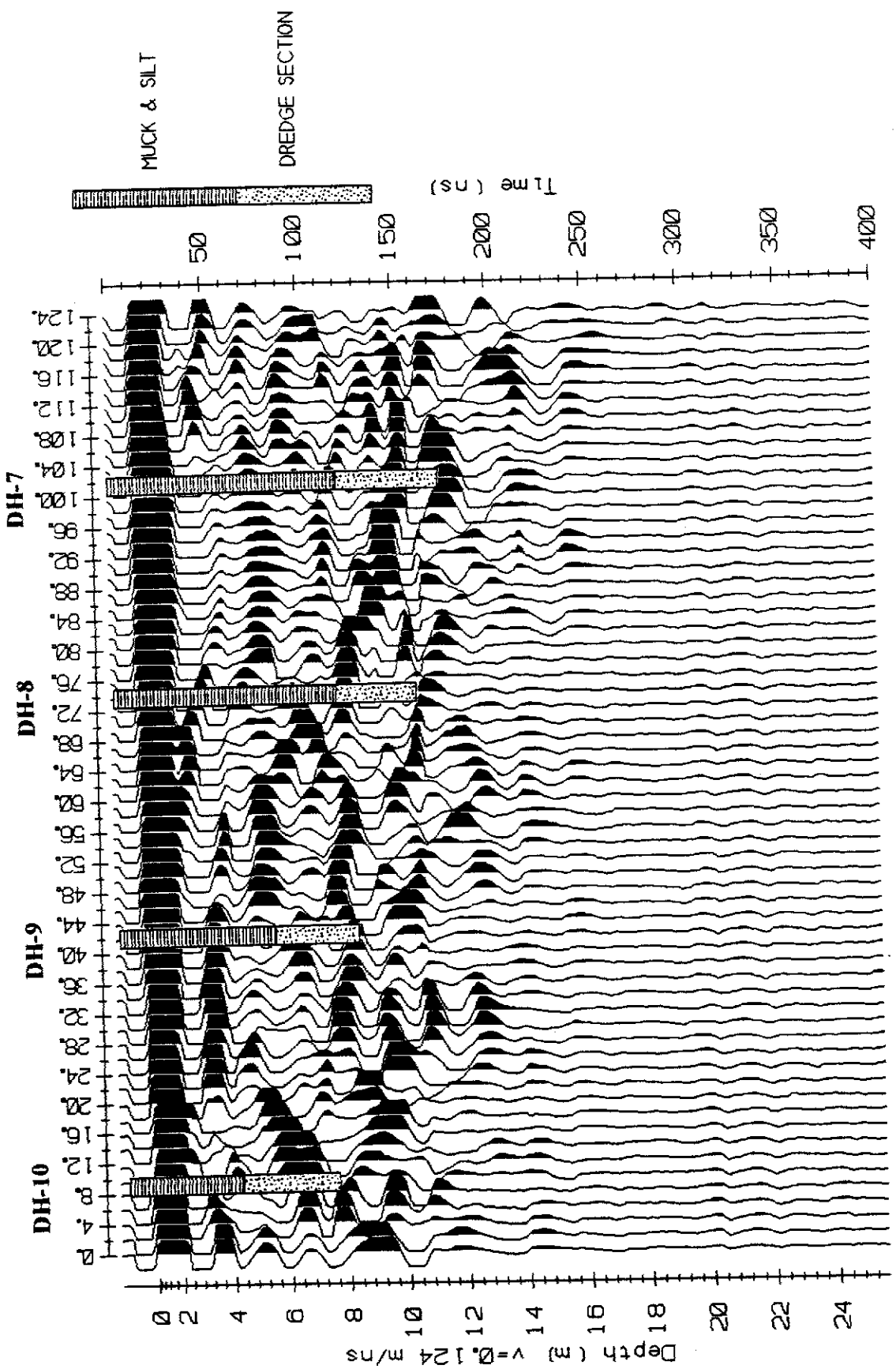


Figure A-5-7. Profile radargram along Gold Run Creek, Line 3. Drill holes are projected up to 20 m into the section.

## SITE 6 - STEWART RIVER

### A. Site location

The survey site is located on placer claims P38717 - P3820 located on the north side (right limit) of the Stewart River. The survey site is approximately 2 km down stream from the McQuesten airstrip. The property can be reached from the Klondike Highway via the McQuesten airstrip road and thence along a 4 wheel drive road parallelling the Stewart River.

### B. Local geology

No bedrock is exposed on the survey site but fresh granite, granodiorite and quartz diorite outcrop on the south side of the Stewart River (Bostock 1963). Bedrock is overlain by gravels, sand and silt derived from a thick blanket of glacial till. Auger drill holes along the GPR line bottomed in a bed of boulder gravel at a depth of 5 to 7 m. In the survey area, the water table is rarely deeper than 3 to 4 m and seasonal frost is usually no deeper than 2 m.

### C. Survey specifications

The GPR profile survey was conducted along the 4x4 access road using the 50 MHz antennas at a 2 m separation. Readings were stacked 128 times and stations read at 2 m intervals. Station 0 is at the north end of the survey line. A HLEM sounding was conducted on the McQuesten airstrip using a 50 m coil spacing. The CMP velocity survey was conducted at the south end of the survey line using the 50 MHz antennas and separations varying from 1 to 30 m in 1 m increments.

### D. Results

The CMP survey radargram is plotted in Figure A-6-2 and the $X^2$-$T^2$ plot is shown in Figure A-6-3; results are listed in Table A-6-1. The survey was conducted on a snow pack of at least 1 m and consequently, high velocity near surface reflections were recorded. The strong arrival at 270 ns also appears as a persistent reflection across most of the profile radargram; it is interpreted to be bedrock at a depth of approximately 18 m. This is consistent with the drill hole information and the presence of nearby outcrop on the south side of the McQuesten River. Weaker early arrivals at 110 and 190 ns may also be reflections but there is no available stratigraphy with which to correlate these reflections.

The results of the HLEM resistivity sounding are shown in Figure A-6-4 and tabulated in Table A-6-2; details of the inversion are in Appendix C. For logistical reasons, the sounding was conducted at the McQuesten Creek airstrip and not on the survey line. The inversion fit was quite good; RMS error was 0.66% and the probable measurement error was $\pm$ 0.5%. As with all the inversions, there was some mismatch between the low frequency in-phase response and the synthetic in-phase response. The highly resistive top layer is a composite of air, snow and frozen ground. The resistivity of the second layer is the best estimate of thawed overburden resistivity. The contact between the second and third layer, which should correspond to the bedrock contact, is at approximately the correct depth. According to Ron Barrett, a resident miner, drilling at the McQuesten airstrip intersected bedrock at a depth of roughly 30 m

**Table A-6-1. Stewart River velocity survey results**

| Layer | $V_{NMO}$ (m/ns) | $V_{DIX}$ (m/ns) | Interval (m) | Remarks |
|---|---|---|---|---|
| 0 | 0.267 $\pm$ 0.005 | n/a | 0 | air + snow |
| 0 | 0.190 $\pm$ 0.005 | n/a | 0 | snow + ice |
| 1 | 0.099 $\pm$ 0.003 | 0.099 | 0 - 5.7 | overbank silt |
| 2 | 0.116 $\pm$ 0.005 | 0.138 | 5.7 - 10.9 | gravel |
| 3 | 0.136 $\pm$ 0.003 | 0.173 | 10.9 - 18.4 | gravel? |

**Table A-6-2. Stewart River resistivity sounding results**

| Layer | Resistivity ($\Omega$-m) | Interval (m) | Remarks |
|---|---|---|---|
| 1 | 8909 | 0 - 9 | air/snow/ice/silt |
| 2 | 255 | 9-25 | gravel/silt/sand |
| 3 | 8075 | 25+ | bedrock |

A portion of the profile radargram is shown in Figure A-6-5 and A-6-6. Figure A-6-5 shows the data processed with conventional automatic gain control (AGC) and relatively low

maximum gain (~1.2% full scale). The radargram is cluttered with near surface multiples and reflections within overburden. To suppress these early arrivals, a predictive gain algorithm based on calculated losses due to spherical spreading and ground conductivity was applied to the data; the result is shown in Figure A-6-6. A prominent reflector at roughly 250 ns together with steeply dipping diffraction trails are enhanced at the expense of earlier arrivals. The irregular nature of the reflector and the presence of diffraction trails probably caused by jointing or other discontinuities suggests that the reflector either bedrock or a lag deposit composed of very large boulders. The depth (14-18 m) would be reasonable for bedrock given that outcrop is present on the opposite side of the Stewart River and that drilling failed to reach bedrock at depths of 5 to 7 m.

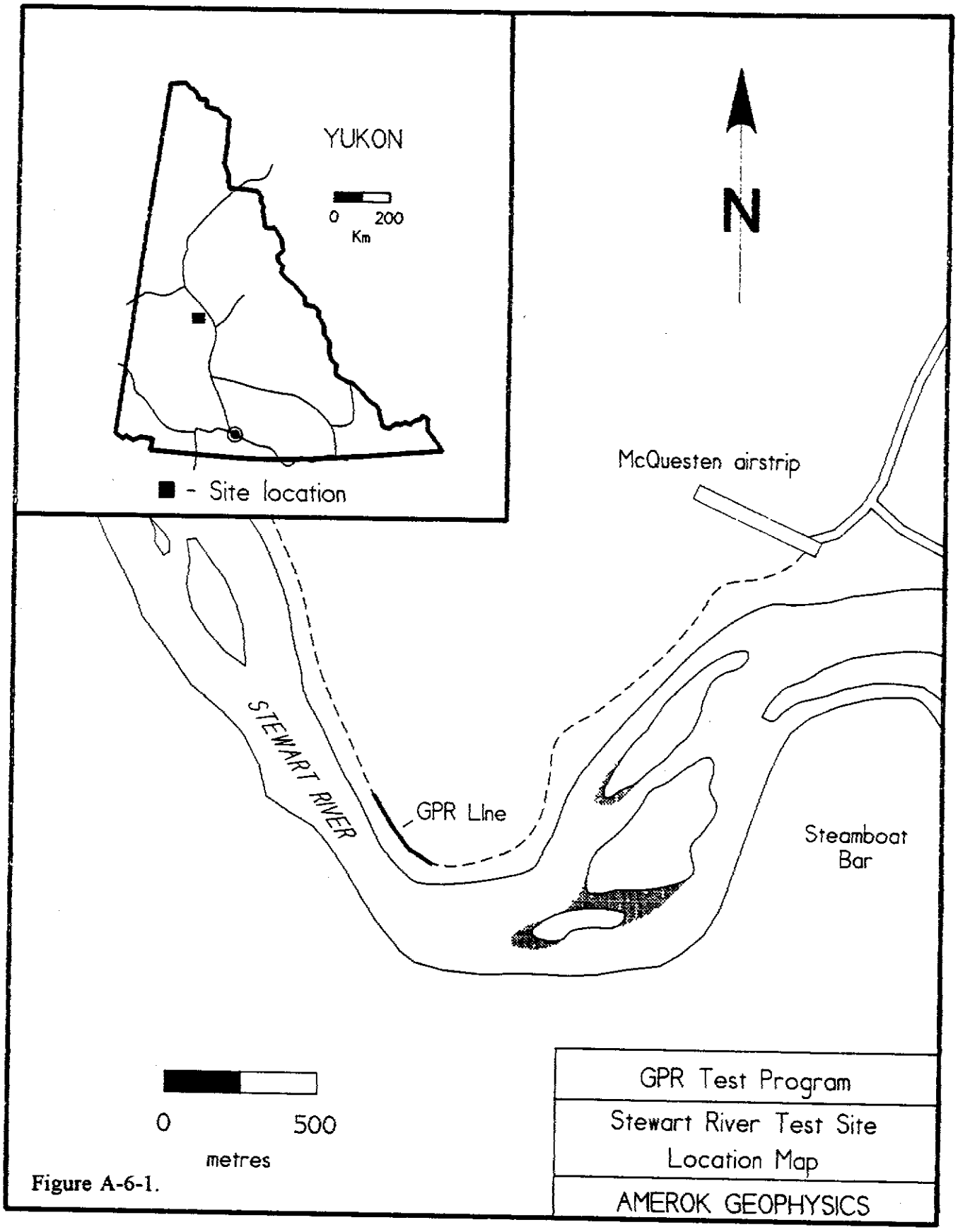
YUKON
0 200
Km
■ - Site location
N
McQuesten airstrip
STEWART RIVER
GPR Line
Steamboat
Bar
0 500
metres
GPR Test Program
Stewart River Test Site
Location Map
AMEROK GEOPHYSICS

Figure A-6-1.

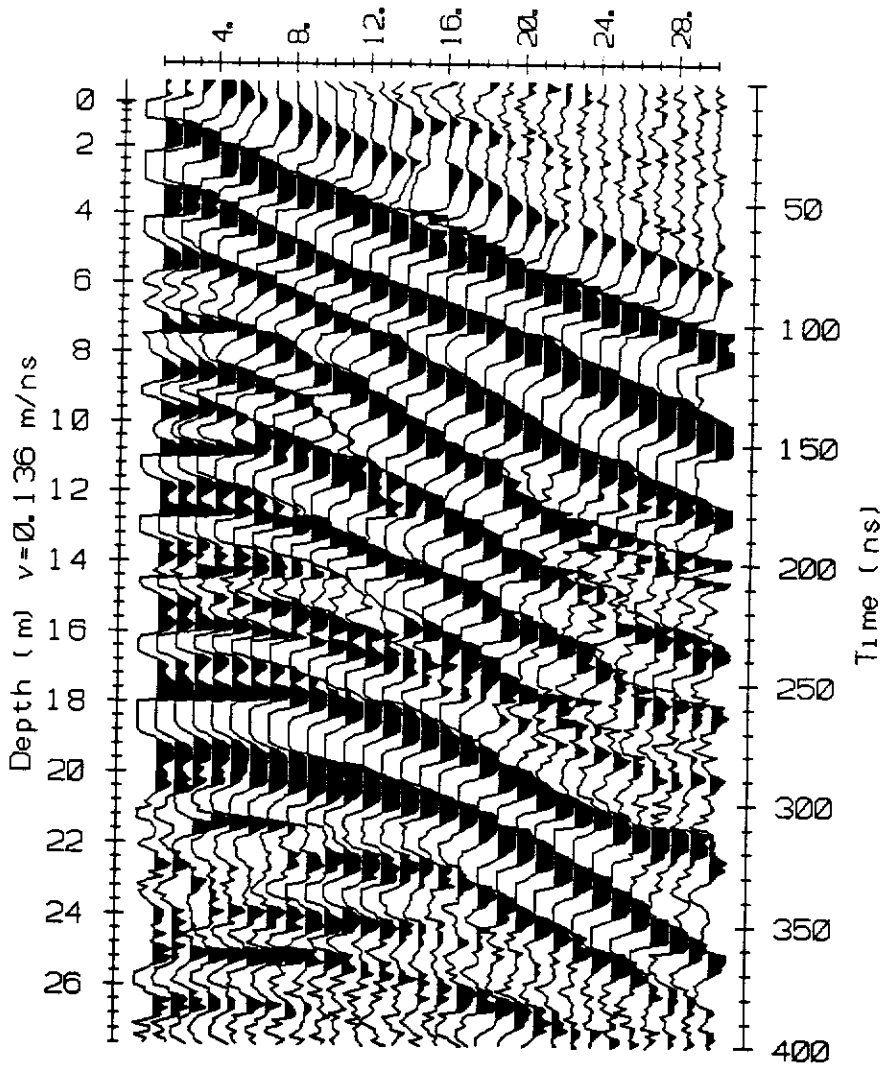


Figure A-6-2. Stewart River 50 MHz CMP radargram. Measurement interval 1m in separations from 2 to 32 m.

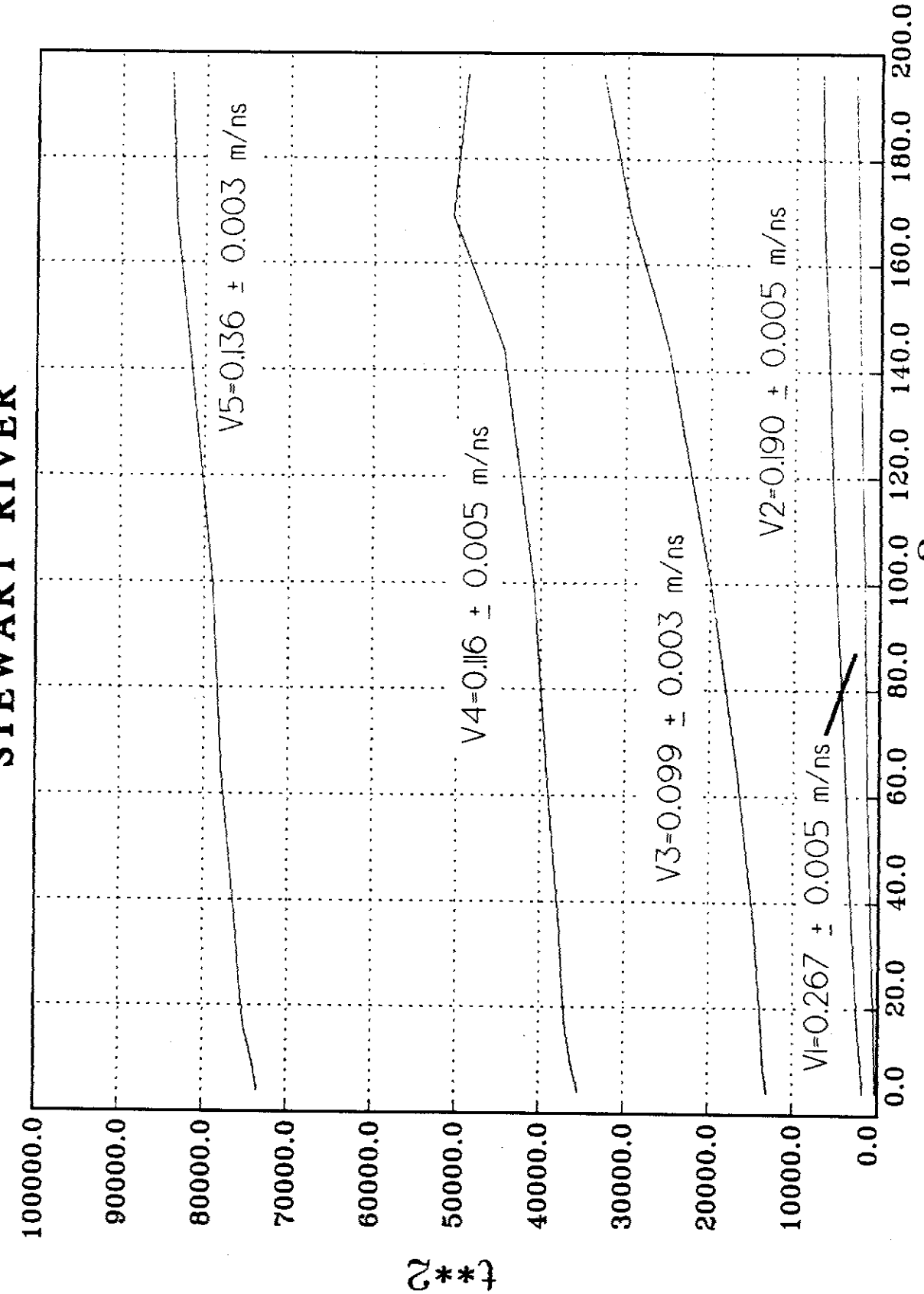


**Figure A-6-3.** Stewart River $X^2$-$T^2$ diagram. Velocities derived from linear regression are plotted near curves.

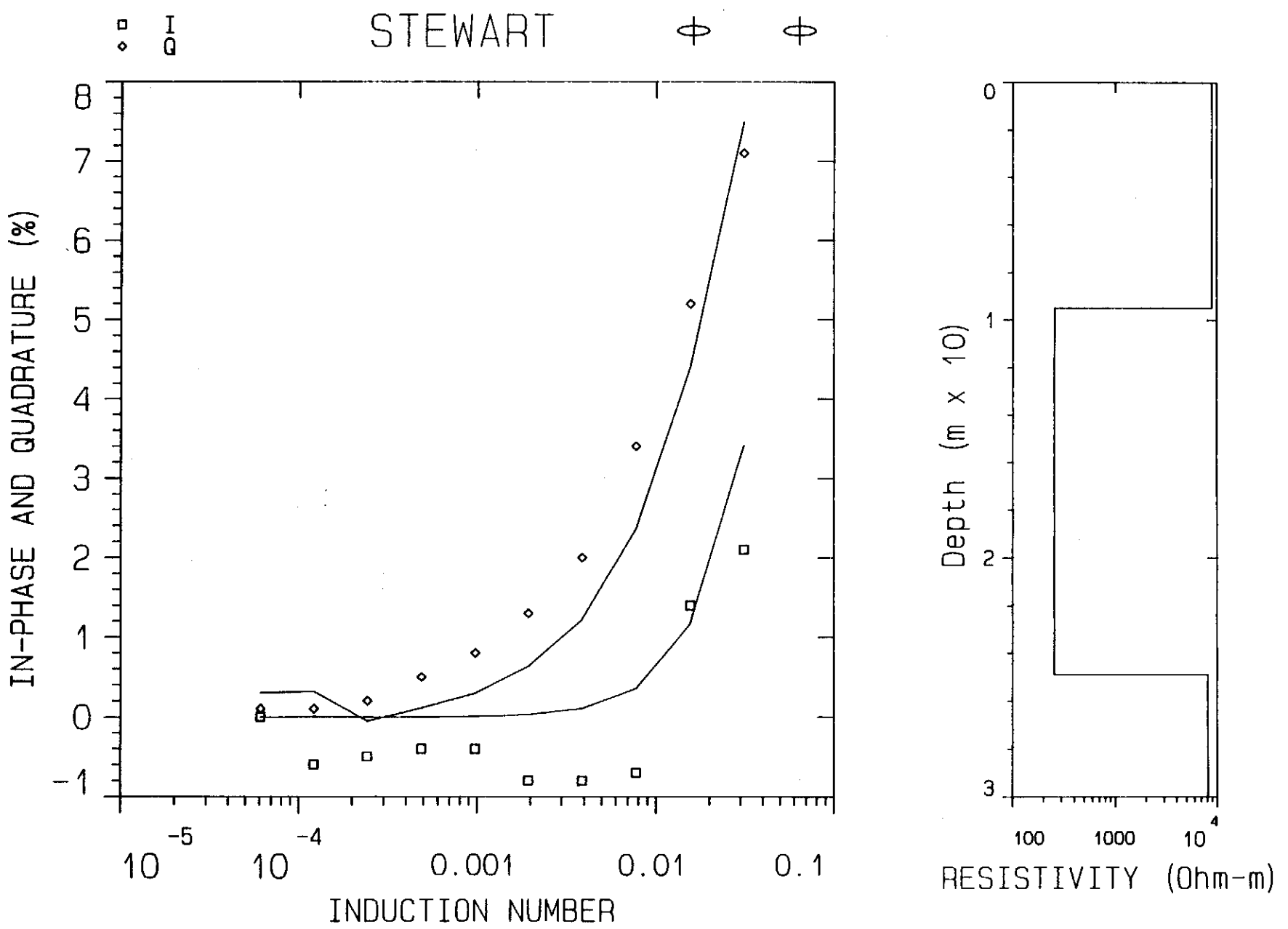


**Figure A-6-4. Stewart River HLEM sounding results. Synthetic and measured data is on the left. Square symbols indicate measured in-phase, diamonds indicate measured quadrature; curves display synthetic responses. Model is displayed on the right.**

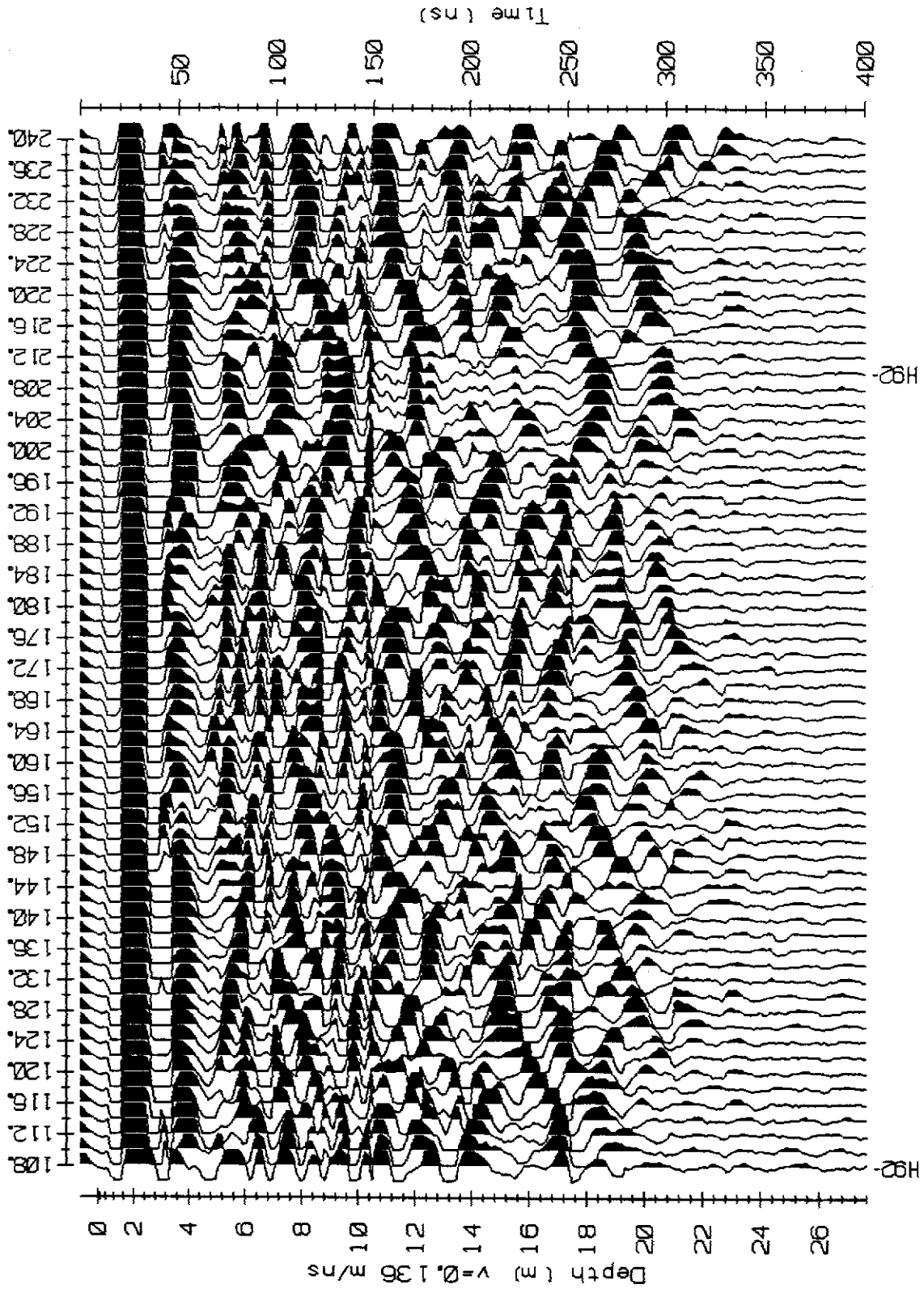


Figure A-6-5. Profile radargram along Stewart River survey line. Drill hole data is not shown; auger drill holes failed to intersect bedrock at depth of 5 to 7 m. Section processed with AGC limited to approximately 1.2% full scale gain.

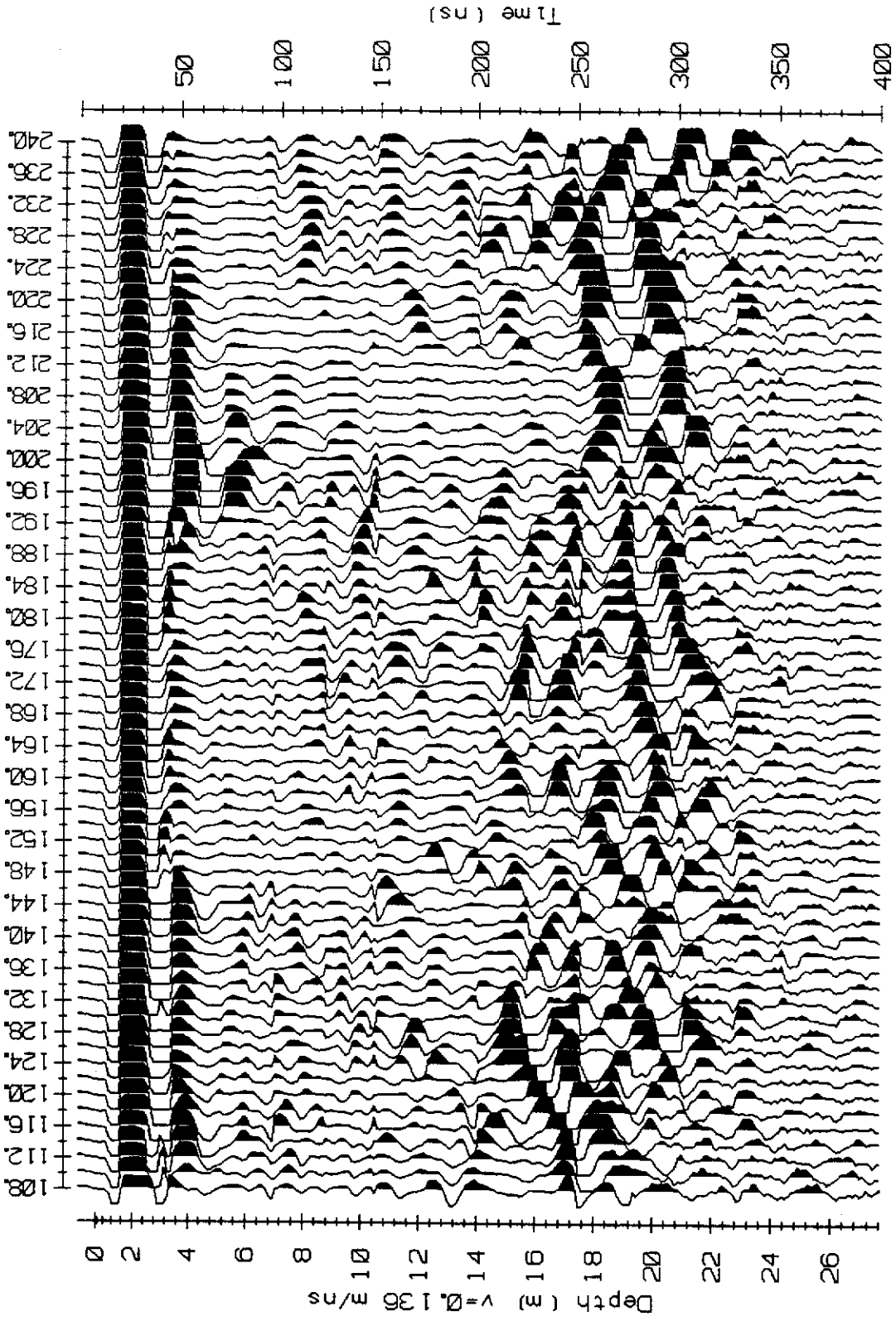


Figure A-6-6. Profile radargram along Stewart River survey line. Drill hole data is not shown; auger drill holes failed to intersect bedrock at depth of 5 to 7 m. Section processed with spherical spreading and exponential loss gain algorithm to enhance later (deeper) arrivals. Gain parameters: v=0.136 m/ns, $\alpha$=1.6 dB/m, gain limit: 1.2%.

# SITE 7 - LIGHTNING CREEK

## A. Site location

The survey site is located on placer claims P2179 to P2193 located on Lightning Creek just above Keno City. Two GPR profile lines were surveyed along the existing road up Lightning Creek. Line 1 starts in the base of a bedrock drain and progresses up a service ramp to the existing road and thence upstream. Line 2 commences just below Thunder Gulch and extends to the junction of Thunder Gulch with Lightning Creek and thence up Thunder Gulch a short distance.

## B. Local geology

The survey site is underlain by fractured quartzite with minor interbedded carbonaceous schist and chloritic phyllite of the Keno Hill Quartzite (Roots and Murphy 1992). The area has been glaciated and bedrock is overlain by coarse gravel and sand covered by boulder till and locally by colluvium. The entire section is thawed below the seasonal frost line. The survey lines were ploughed just prior to the survey.

## C. Survey specifications

The GPR profile survey was conducted with the 25 MHz antennas at a 4 m separation. Readings were stacked 128 times and stations read at 2 m intervals. A HLEM sounding was conducted at the start of GPR Line 1 using a 50 m coil spacing. A CMP velocity survey was conducted at the end of GPR Line 1 with the 25 MHz antennas and an antenna separation varying from 2 to 34 m in 2 m increments.

## D. Results

The CMP radargram is plotted in Figure A-7-2 and the $X^2$-$T^2$ plot is shown in Figure A-7-3; results are tabulated in Table A-7-1. The CMP radargram contains multiples with velocities of 0.100 and 0.089 m/ns. These are attributed to a large velocity contrast between the frozen top of the section and thawed, water saturated strata beneath. The reverberations may be occurring in the top 3 m of the section since the recurrence time averages 63 ns and does not change with depth (ie. these are not bottom multiples).

The results of the HLEM resistivity sounding are displayed in Figure A-7-4 and tabulated in Table A-7-2; a detailed description of the inversion is in Appendix C. The inversion fit was quite good with an RMS error of 0.75% and probable measurement error was $\pm$ 0.5%. Low in-phase and quadrature measurements were recorded at the 50 m coil

spacing indicating that the overburden has a high resistivity. This is surprising given that the deposit is thawed and can only be ascribed to the absence of clay in the overburden. The very low resistivity of the half-space is probably an artifact of the inversion algorithm and should not be taken as a true measure of bedrock resistivity. The depth to the top of the half-space (21 m) is quite close to the depth to bedrock in a nearby drill hole (18 m). The hole is approximately 40 m from the sounding site.

**Table A-7-1. Lightning Creek velocity survey results.**

| Layer | $V_{NMO}$ (m/ns) | $V_{DIX}$ (m/ns) | Interval (m) | Remarks |
|---|---|---|---|---|
| 0 | 0.190 ± 0.002 | n/a | 0 | surface ice, air |
| 1 | 0.100 ± 0.002 | 0.100 | 0 - 5.2 | gravel above water table (?) |
| 1 | 0.103 ± 0.002 | n/a | n/a | multiple |
| 2 | 0.089 ± 0.002 | 0.083 | 5.2 - 9.4 | water saturated gravel |
| 2 | 0.088 ± 0.004 | n/a | n/a | multiple |
| 2 | 0.086 ± 0.002 | n/a | n/a | multiple |

**Table A-7-2. Lightning Creek resistivity sounding results.**

| Layer | Resistivity (Ω-m) | Interval (m) | Remarks |
|---|---|---|---|
| 1 | 12K | 0-3 | air/ice |
| 2 | 67K | 3-7 | |
| 3 | 5460 | 7-21 | overburden |
| 4 | 53 | 21+ | inversion artifact |

Portions of radargrams recorded on GPR lines 1 and 2 are shown in Figures A-7-5 and A-7-6. Both profiles were processed using the spherical and exponential gain algorithm described under Site 6. Parameters used include V=0.089 m/ns, a=1.7 dB/m and a maximum

gain of 1.2% full range. Drill hole and excavation data are plotted on the radargrams and corrections have been made for surface topography.

Figure A-7-5 shows an excerpt along GPR Line 1. The survey line starts at the bottom of a bedrock drain and progresses up past a drill hole to the main road up Lightning Creek. Following the GPR survey, the bedrock drain was completed and bedrock encountered at the depth shown at station 0. A reverse circulation drill hole further along the road bottomed in bedrock or large boulder lag at 19.5 m. A moderately strong discordant reflection at 550 to 600 ns corresponds to the indicated bedrock intersections but is difficult to pick from amongst the earlier arrivals and their multiples. Without drill hole data, it would have been difficult to pick the bedrock reflection with any confidence.

Figures A-7-6 shows an excerpt from GPR Line 2 near the confluence of Lightning Creek and Thunder Gulch. A reverse circulation drill hole is also plotted on the radargram. As in the previous example, signal cluttering is a problem and were it not for the drill hole, an interpreter could easily pick the wrong arrival as the bedrock reflection.

These radargrams illustrate how GPR can be limited by signal cluttering when the bedrock velocity contrast is not significantly greater than velocity contrast between layers in the overburden. The apparent resistivity of the sediments is very high and attenuation of GPR signals is not a problem here. Rather, the large velocity contrast between frozen ground and water-saturated thawed ground generates high amplitude multiples which obscure bedrock reflections. Compounding this, it appears that the velocity contrast between the bedrock and overburden is either small or gradational.

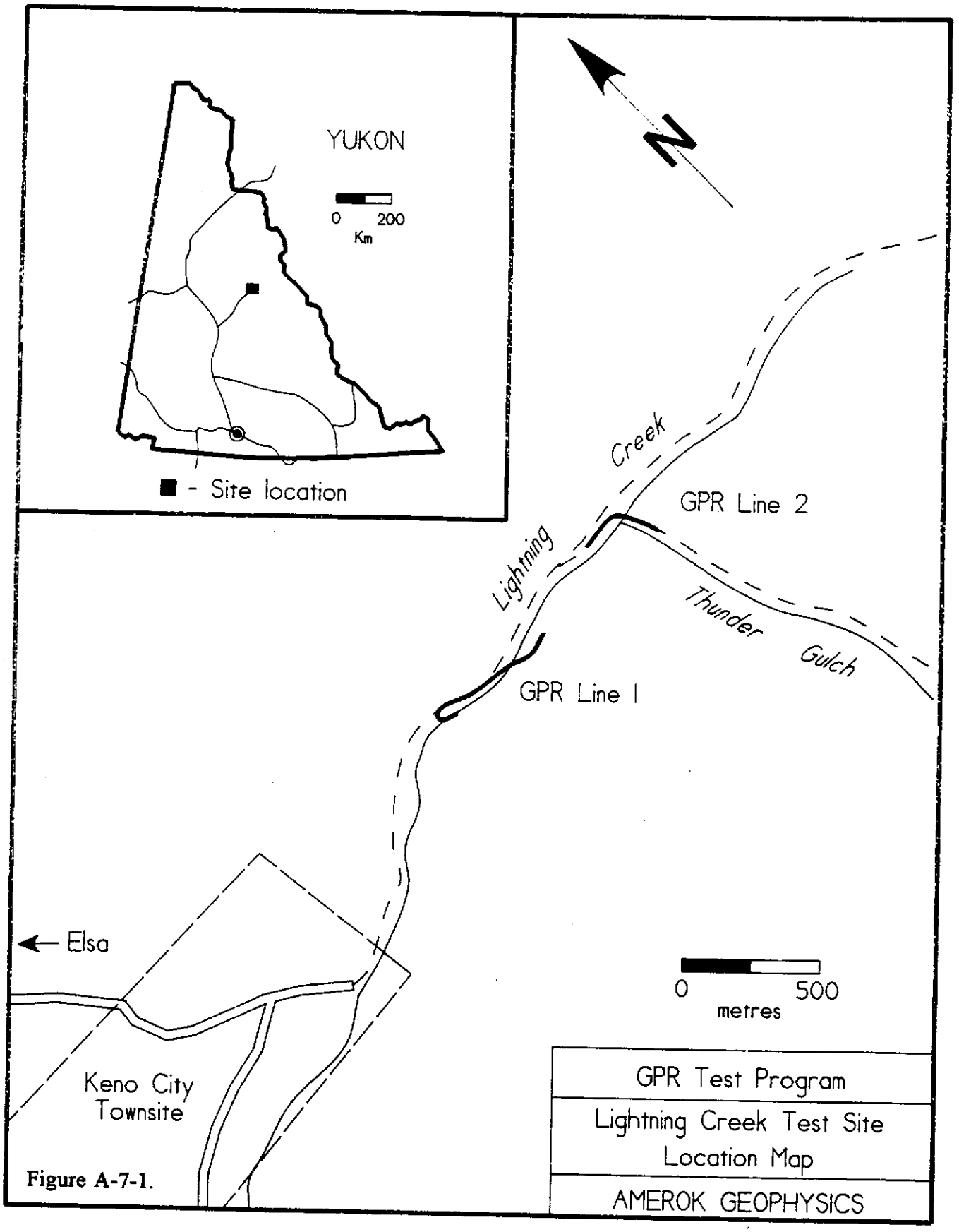
YUKON
0 200
Km
■ - Site location
N
Creek
Lightning
GPR Line 2
Thunder
Gulch
GPR Line 1
← Elsa
Keno City
Townsite
0 500
metres
GPR Test Program
Lightning Creek Test Site
Location Map
AMEROK GEOPHYSICS

**Figure A-7-1.**

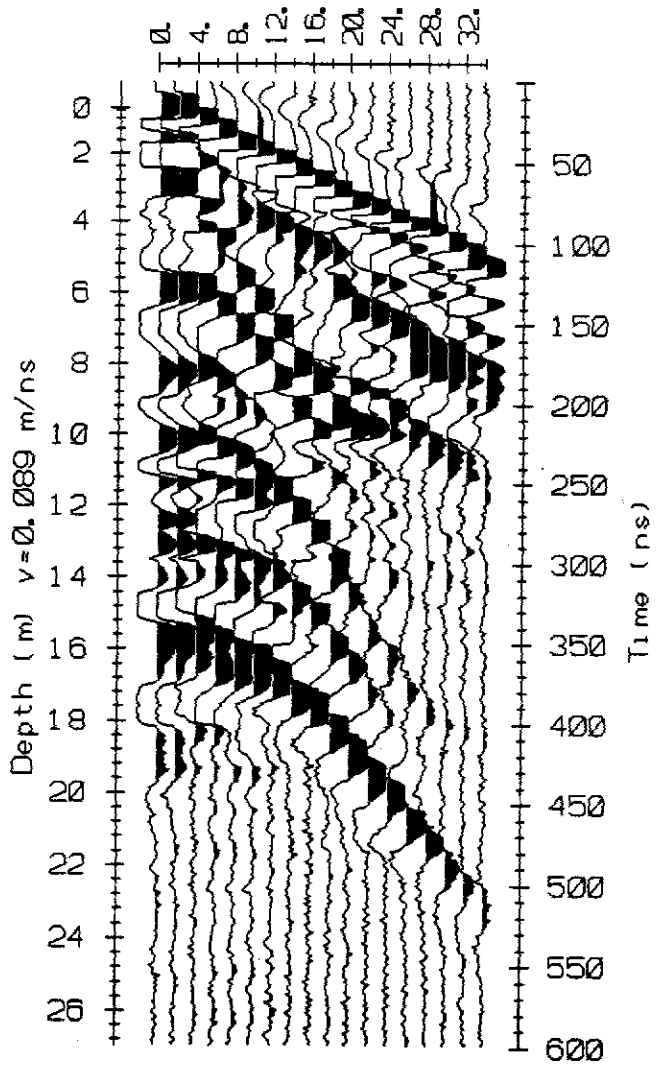


Figure A-7-2. Lightning Creek 25 MHz CMP radargram. Measurement interval 2m in separations from 2 to 34 m.

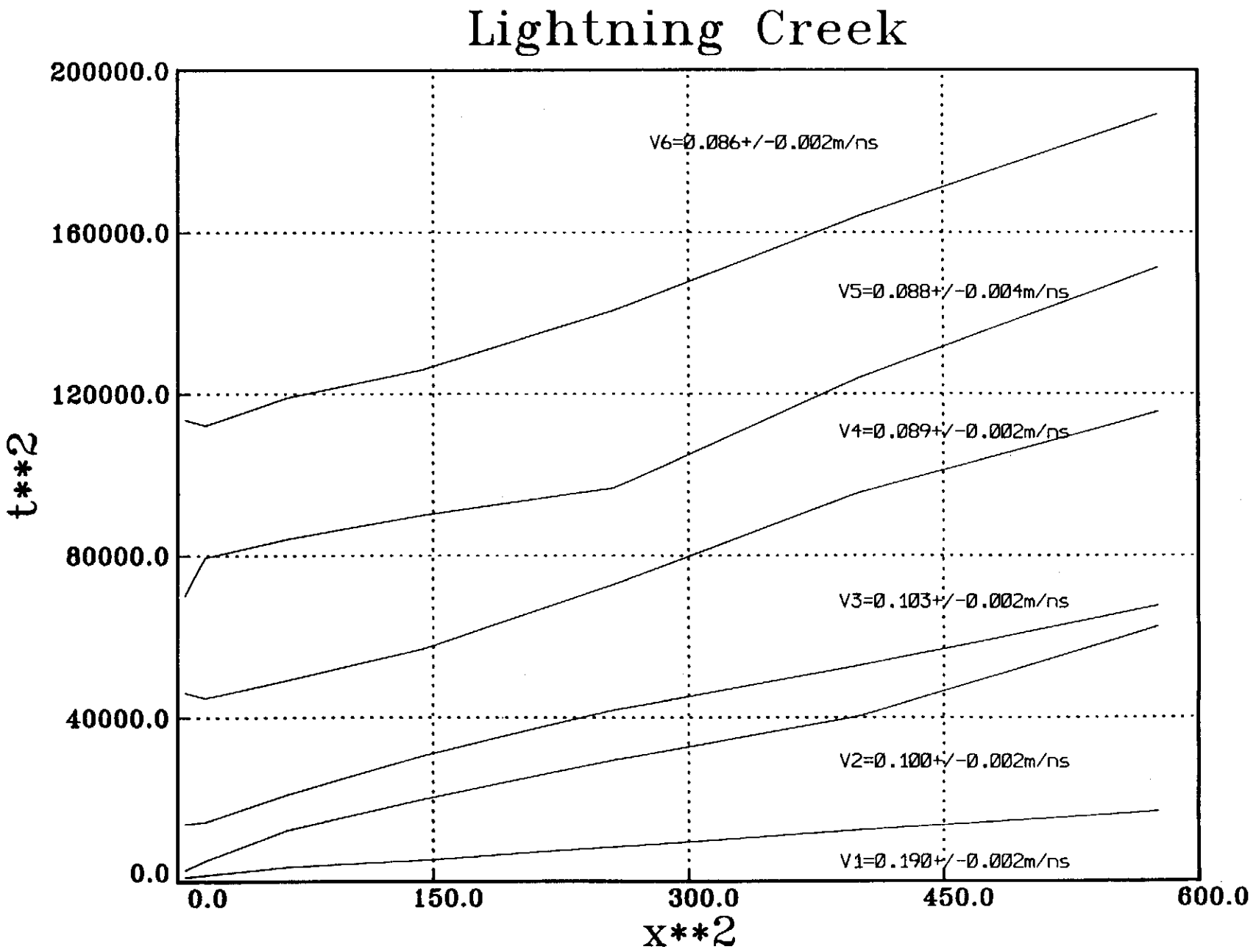


Figure A-7-3. Lightning Creek $X^2$-$T^2$ diagram. Velocities derived from linear regression are plotted near curves.

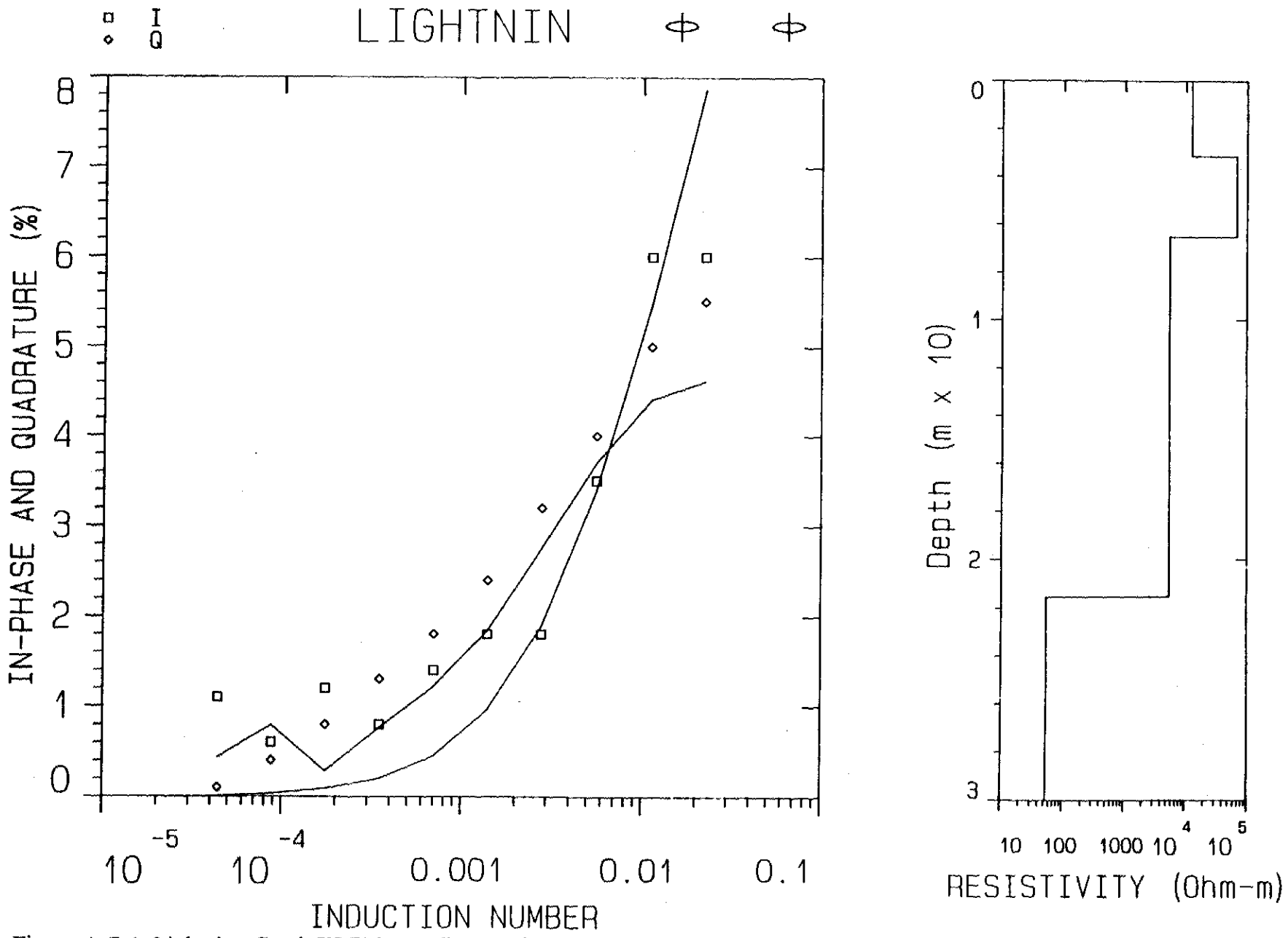


Figure A-7-4. Lightning Creek HLEM sounding results. Synthetic and measured data is on the left. Square symbols indicate measured in-phase, diamonds indicate measured quadrature; curves display synthetic responses. Model is displayed on the right.

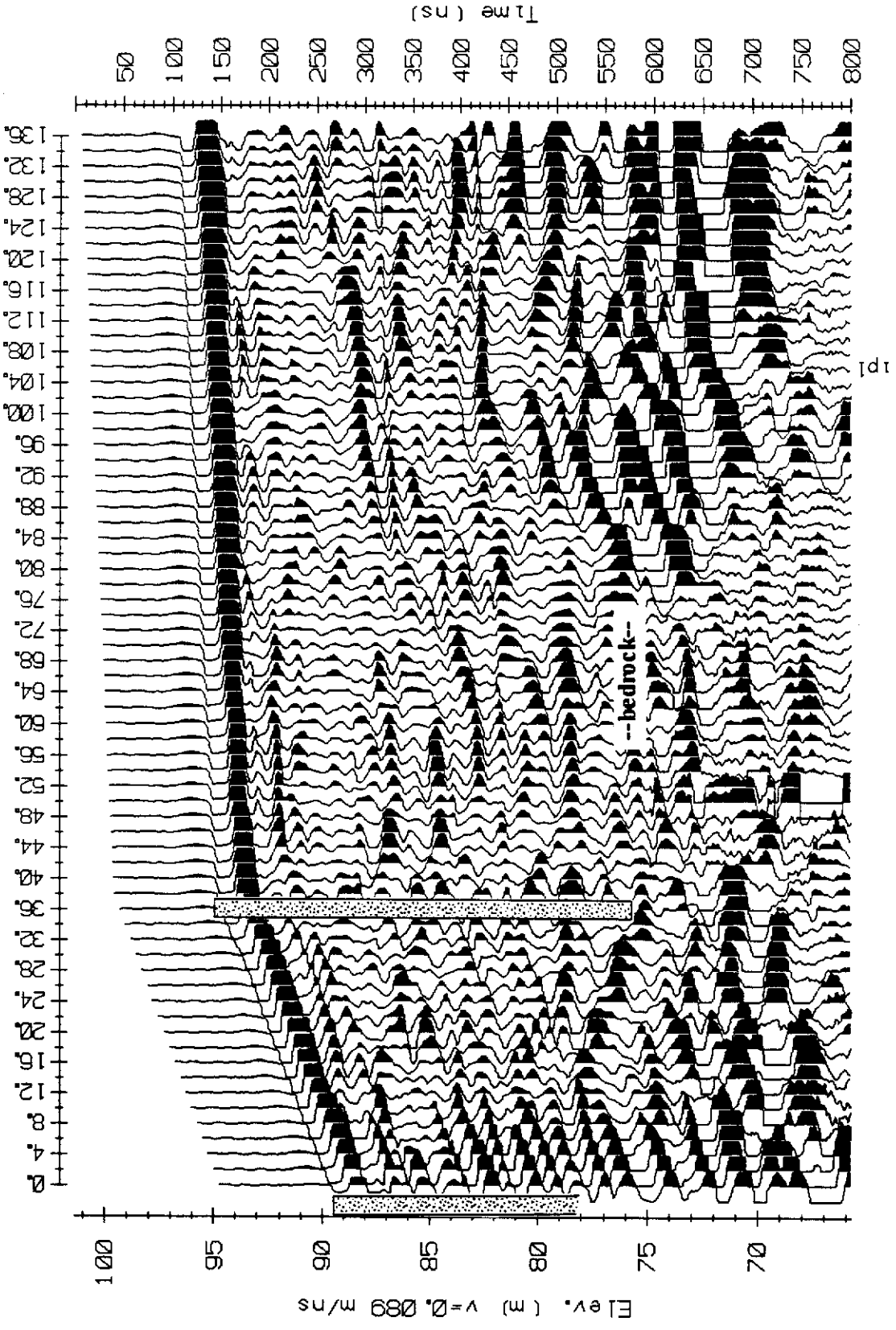


Figure A-7-5. Profile radargram along Lightning Creek survey line 1. Drill hole and excavation data is superimposed on the radargram.

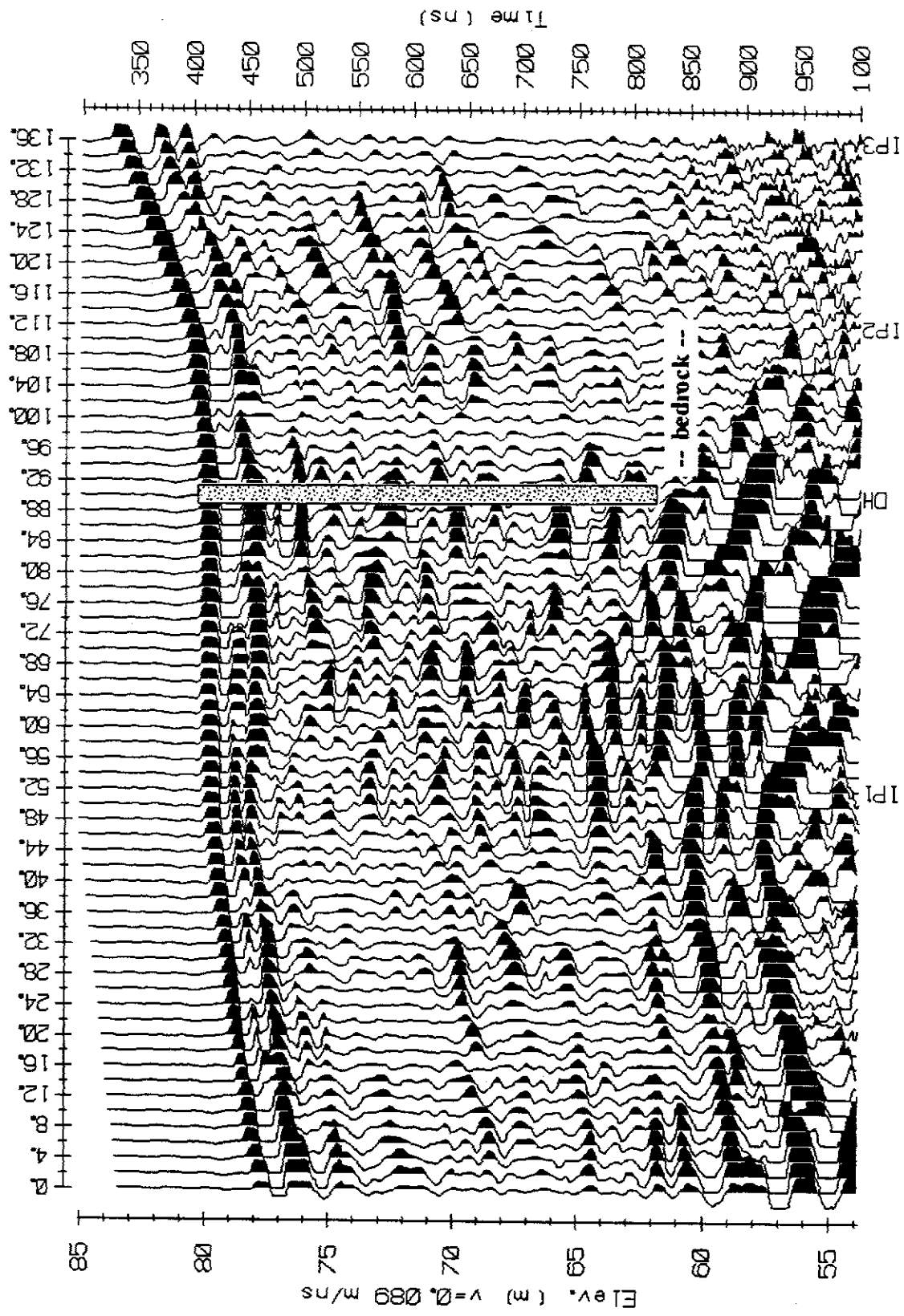


Figure A-7-6. Profile radargram along Lightning Creek survey line 2 near the confluence of Lightning Creek and Thunder Gulch. Drill hole and excavation data is superimposed on the radargram.

## SITE 8 - DUNCAN CREEK

### A. Site location

The survey site is located on placer lease P8722 and placer claims P2166-67 and P3677-80. The GPR survey line starts 130 m west of the Duncan Creek Road, runs east to the road and thence south along it to the Duncan Creek Golddusters mine site entrance.

### B. Local geology

The survey site is underlain by fractured quartzite and phyllite of the Hyland Group (Roots and Murphy 1992). The area has been glaciated and bedrock is overlain by coarse gravel and sand covered by boulder till with interbedded sand and silt. Seismic and drilling programs in the area have determined that bedrock is at depths in excess of 35 m in the area covered by the GPR survey (Power 1992). The entire section is thawed below the seasonal frost line. The GPR survey line was covered by approximately 1.5 m of snow at the time of the survey.

### C. Survey specifications

The GPR profile survey was conducted with the 25 MHz antennas at a 4 m separation. Readings were stacked 128 times and stations read at 2 m intervals. A HLEM sounding was conducted 100 m from the south end of the GPR line using a 50 m coil spacing. A CMP velocity survey was conducted at the end of the GPR Line with the 25 MHz antennas and an antenna separation varying from 2 to 38 m in 2 m increments.

### D. Results

The CMP survey radargram is plotted in Figure A-8-2 and the $X^2$-$T^2$ plot is shown in Figure A-8-3; results are tabulated in Table A-8-1. The CMP survey detected reflections to an apparent depth of only 11 m and failed to detect a bedrock reflector. The $V_{NMO}$ of the deepest reflector (0.128 m/ns) was selected as the most representative velocity for the overburden and used for depth determinations in the profile radargrams.

The results of the HLEM resistivity sounding are shown in Figure A-8-4 and tabulated in Table A-8-2; details of the inversion are listed in Appendix C. The inversion fitting error (RMS error) was 0.74% and the probable measurement error was $\pm$ 0.5%. In addition to being a good fit, the model agrees with the known geology. Low resistivities were expected given the clay content of the overburden and the high in-phase and quadrature responses recorded during the survey. The resistivity of the second layer is in the range expected for

glacial till and associated sediments while the resistivity of the third layer also corresponds to that expected for schistose metamorphic rocks and quartzite (McNeill 1980). The depth to the base of the second layer - the inferred top of bedrock - is also approximately the depth expected in this area.

**Table A-8-1. Duncan Creek velocity survey results.**

| Layer | $V_{NMO}$ (m/ns) | $V_{DIX}$ (m/ns) | Interval (m) | Remarks |
|---|---|---|---|---|
| 0 | 0.334 ± 0.005 | n/a | 0 | air wave |
| 0 | 0.244 ± 0.006 | n/a | 0 | snow/ice/ entrained air |
| 1 | 0.135 ± 0.002 | 0.135 | 0 - 5.6 | frozen gravel or till |
| 2 | 0.128 ± 0.002 | 0.??? 12-1 | 5.6 - 10.2 | gravel or till |

**Table A-8-2. Duncan Creek resistivity sounding results.**

| Layer | Resistivity (Ω-m) | Interval (m) | Remarks |
|---|---|---|---|
| 1 | 13K | 0 - 1 | air/snow |
| 2 | 290 | 1-34 | overburden |
| 3 | 1450 | 34+ | bedrock |

An excerpt from the profile radargram are shown in Figures A-8-5. The survey line passes quite close to a reverse circulation drill hole which bottomed in overburden at 37 m. Reflections from the base of the snow pack and from the base of the uppermost till layer were recorded but no reflections below 16 to 18 m were detected. This suggests a practical depth of penetration in this environment of about 15 m.

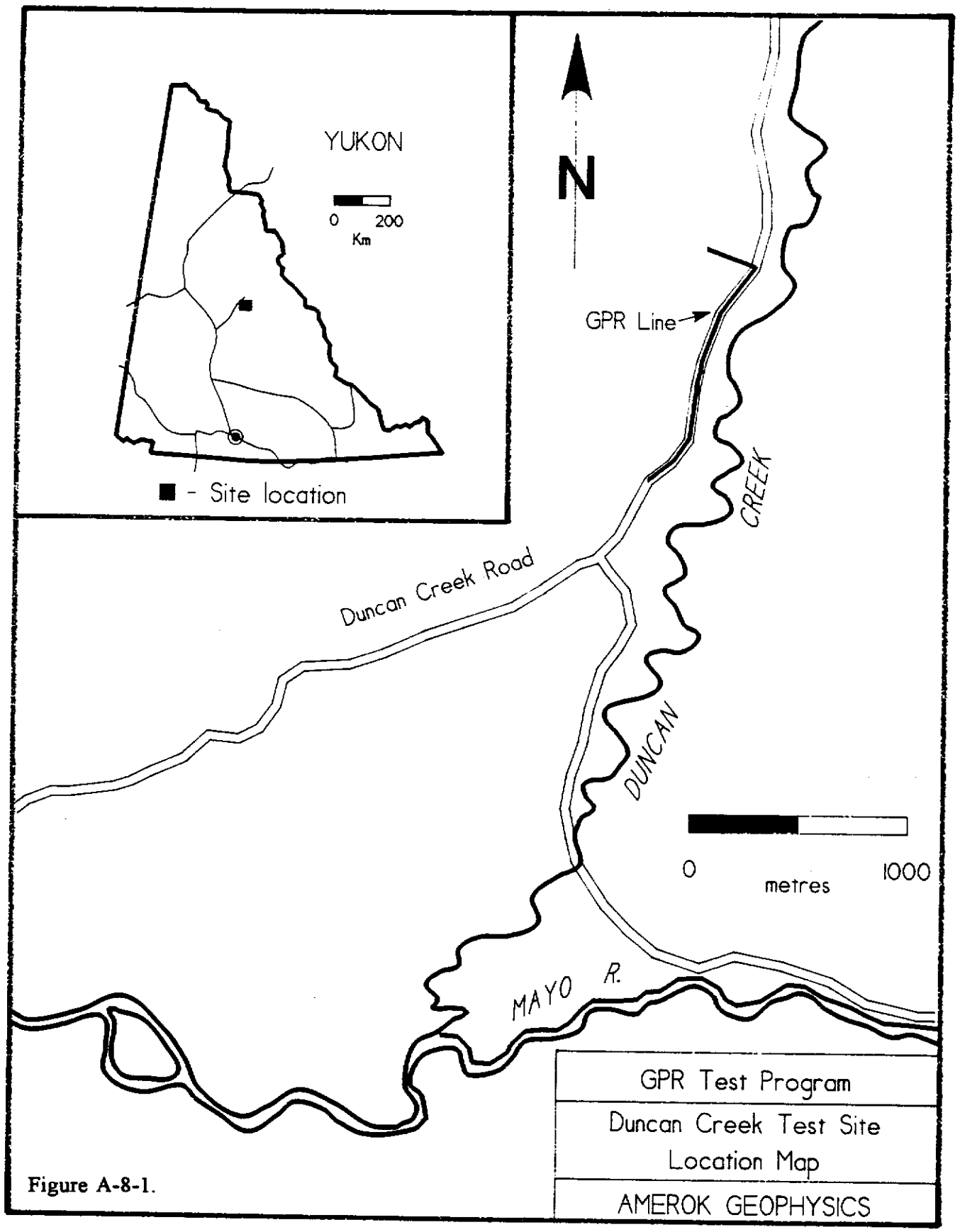
YUKON
0 200
Km
■ - Site location
N
GPR Line
CREEK
Duncan Creek Road
DUNCAN
0 metres 1000
MAYO R.
GPR Test Program
Duncan Creek Test Site
Location Map
AMEROK GEOPHYSICS

**Figure A-8-1.**

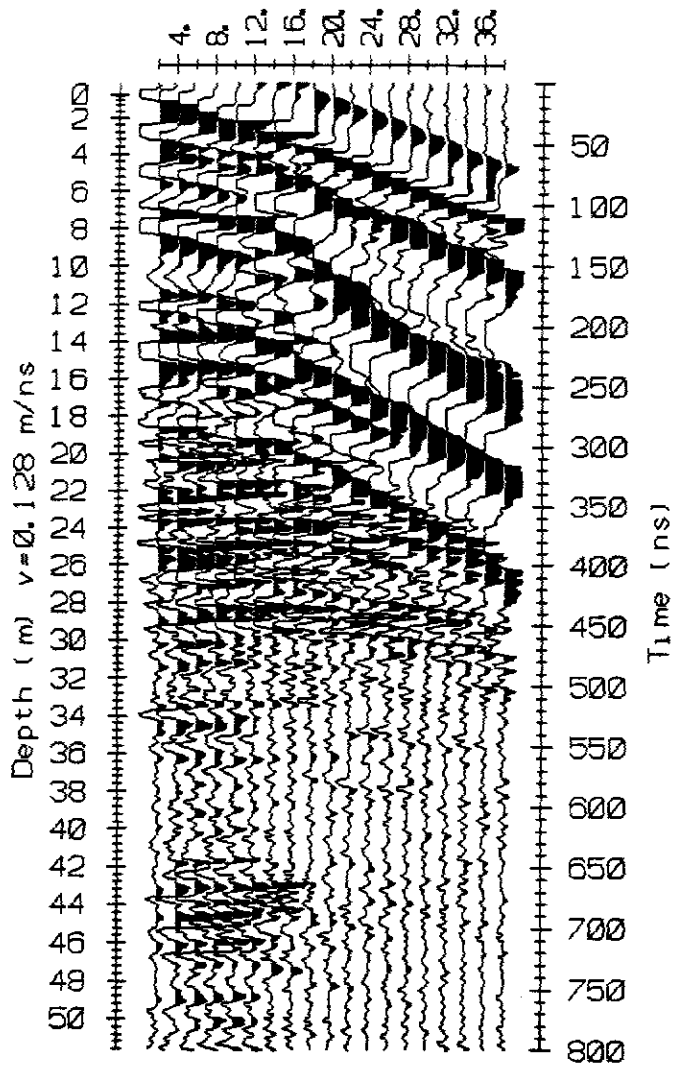


Figure A-8-2. Duncan Creek 25 MHz CMP radargram. Measurement interval 2m in separations from 2 to 38 m.

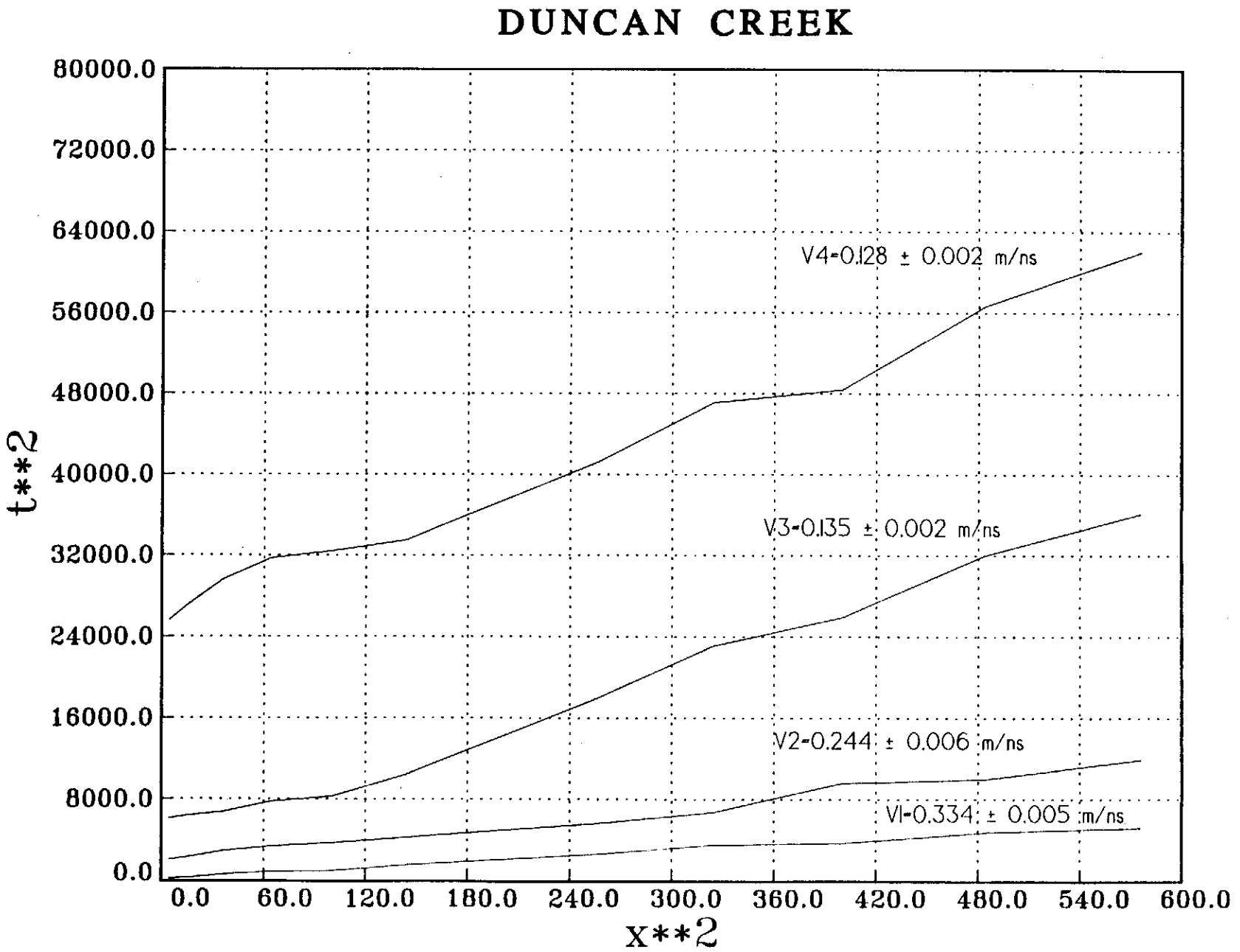


Figure A-8-3. Duncan Creek $X^2$-$T^2$ diagram. Velocities derived from linear regression are plotted near curves.

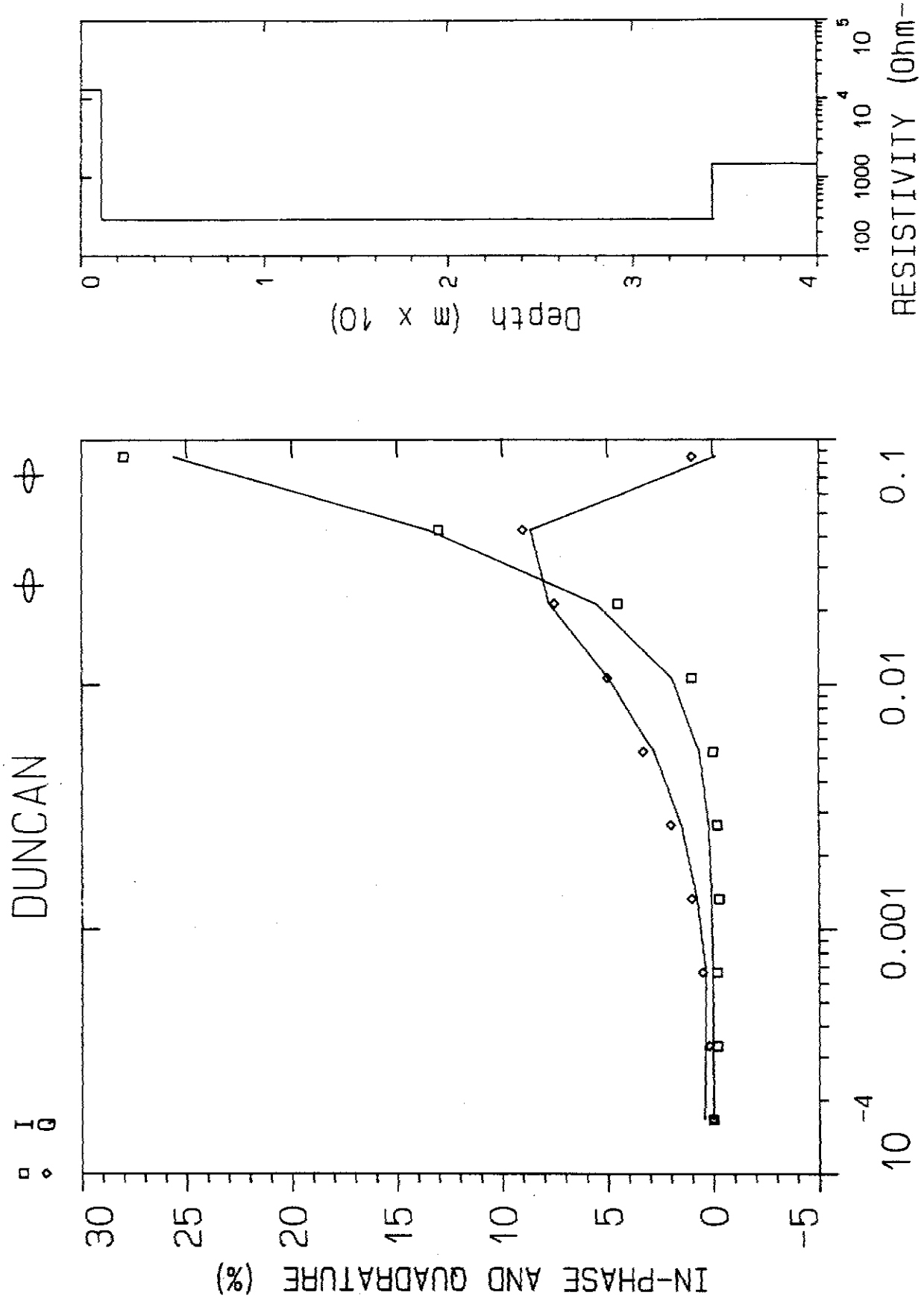


**Figure A-8-4. Duncan Creek HLEM sounding results. Synthetic and measured data is on the left. Square symbols indicate measured in-phase, diamonds indicate measured quadrature; curves display synthetic responses. Model is displayed on the right.**

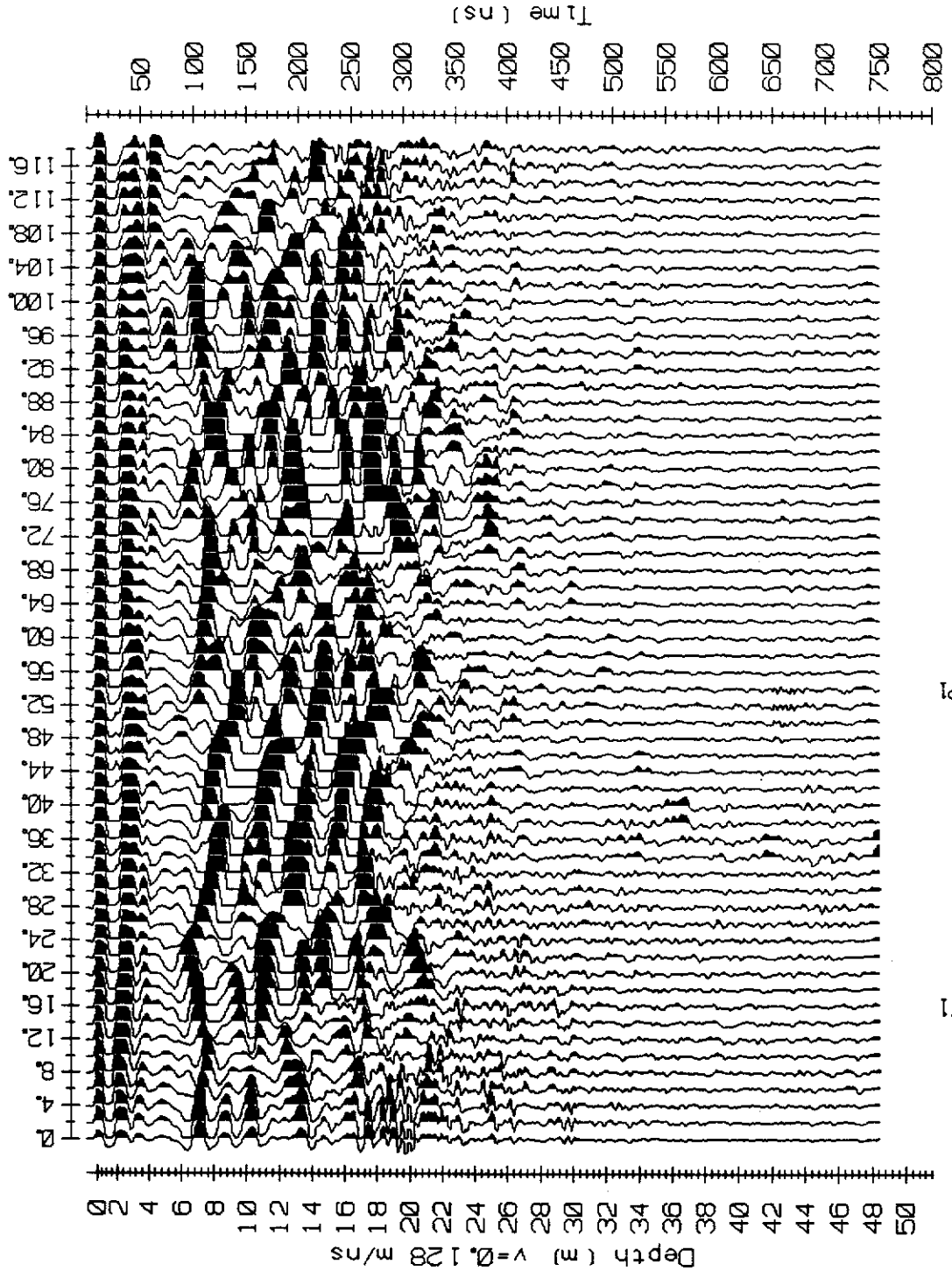


Figure A-8-5. Profile radargram along Duncan Creek survey line. Base of snow pack and upper till layer are visible in radargram.

## SITE 9 - DOMINION CREEK

### A. Site location

The survey site is located on the lower end of Dominion Creek on the Ross Mining Services property (FIgure A-9-1). Two lines were surveyed; GPR Line 1 is between the first and second bridge crossings on the Dominion Creek Road and GPR Line 2 is approximately 1 km south of the Gold Run Creek Road. GPR Line 1 follows an existing drill fence and GPR Line 2 extends from the break in slope west of the Dominion Creek Road to the edge of the 1992 workings on Dominion Creek.

### B. Local geology

The survey site is underlain by chlorite-quartz schist and well foliated muscovite-feldspar-quartz schist (Debicki 1984). Bedrock is overlain by coarse White Channel Gravels and capped by black muck. The entire section is thoroughly frozen. GPR Line 1 was covered by approximately 1.5 m of snow at the time of the survey and Line 2 was ploughed immediately prior to the survey.

### C. Survey specifications

The GPR profile survey was conducted with the 25 MHz antennas at a 4 m separation. Readings were stacked 128 times and stations read at 2 m intervals. A HLEM sounding was conducted 100 m from the east end of the GPR Line 2 using a 50 m coil spacing. A CMP velocity survey was conducted at approximately station 220 on GPR Line 1 with the 25 MHz antennas and an antenna separation varying from 2 to 36 m in 2 m increments.

### D. Results

The CMP survey radargram is plotted in Figure A-9-2, the $X^2$-$T^2$ plot is shown in Figure A-9-3 and the results are tabulated in Table A-9-1. Arrivals at 30, 80, 120, 190 and 300 ns were processed. Aside from the air wave, there appears to be 2 surface waves; one within the snow pack and a second within ground ice. The third reflector correlates well with the base of muck and the velocity is that expected in this material. The last two arrivals may originate from dipping reflectors as the point of maximum curvature on the two reflections is not coincident with the minimum antenna spacing. This would invalidate the Dix and NMO velocities for these two layers. The 190 ns reflection originates at the top of weathered bedrock and a $V_{NMO}$ of 0.140 m/ns was used as the overburden velocity in the profile radargrams.

The results of the HLEM resistivity sounding are displayed in Figure A-9-4 and tabulated in Table A-9-2; details of the inversion are listed in Appendix C. The inversion was poor with an inversion fitting error (RMS error) of 5.5%. The site appears to be resistive but the electrical structure is not well modelled with a stratified earth.

**Table A-9-1. Dominion Creek velocity survey results.**

| Layer | $V_{NMO}$ (m/ns) | $V_{DIX}$ (m/ns) | Interval (m) | Remarks |
|---|---|---|---|---|
| 0 | 0.267 ± 0.009 | n/a | 0 | snow/air |
| 0 | 0.170 ± 0.003 | n/a | 0 | snow/ice |
| 1 | 0.121 ± 0.003 | 0.121 | 0 - 7.3 | frozen muck |
| 2 | 0.146 ± 0.002 | 0.175 | 7.3 - 13.9 | gravel |
| 3 | 0.161 ± 0.006 | 0.179 | 13.9 - 24.3 | weathered bedrock (?) |

**Table A-9-2. Dominion Creek resistivity sounding results.**

| Layer | Resistivity (Ω-m) | Interval (m) | Remarks |
|---|---|---|---|
| 1 | 13K | 0 - 0.4 | air |
| 2 | 34 | 0.4 - 4 | surface muck |
| 3 | 2237 | 4 - 9 | |
| 4 | 9574 | 9+ | |

An excerpt from the profile radargram on GPR Line 1 is shown in Figures A-9-5. The survey line follows an auger drill fence and drill hole logs are plotted on the radargram. The top of weathered bedrock and the base of black muck are prominent, continuous reflections at approximately 75 and 200 ns. There is a very good correlation between drill hole depths to bedrock and GPR indicated depths to bedrock with the mismatch attributable to snow pack or a slight error in velocity. The flat attitude of both reflectors greatly enhances the strength of their reflections.

An excerpt from the profile radargram on GPR Line 2 is shown in Figure A-9-6. Bedrock is at a depth of approximately 22 m in the drill hole but no reflections from horizons below 12 m were recorded. This may be caused by either electrical conductivity losses or by scattering. Below the irregular, discontinuous reflector at 150 ns, steeply dipping diffractions are present suggesting that the radar wave energy is scattered by this reflector. This would occur if the layer consisted of very large boulders. Alternatively, the overburden may contain a layer of low resistivity - as the HLEM sounding inversion suggests - and this could also attenuate any deep reflections. The base of muck is well defined by the 60 ns reflection however and variation in the thickness of this unit does not produce an corresponding change in the strength of later reflections. Taken together, the evidence suggests that scattering rather than attenuation may be be limiting penetration at this site.

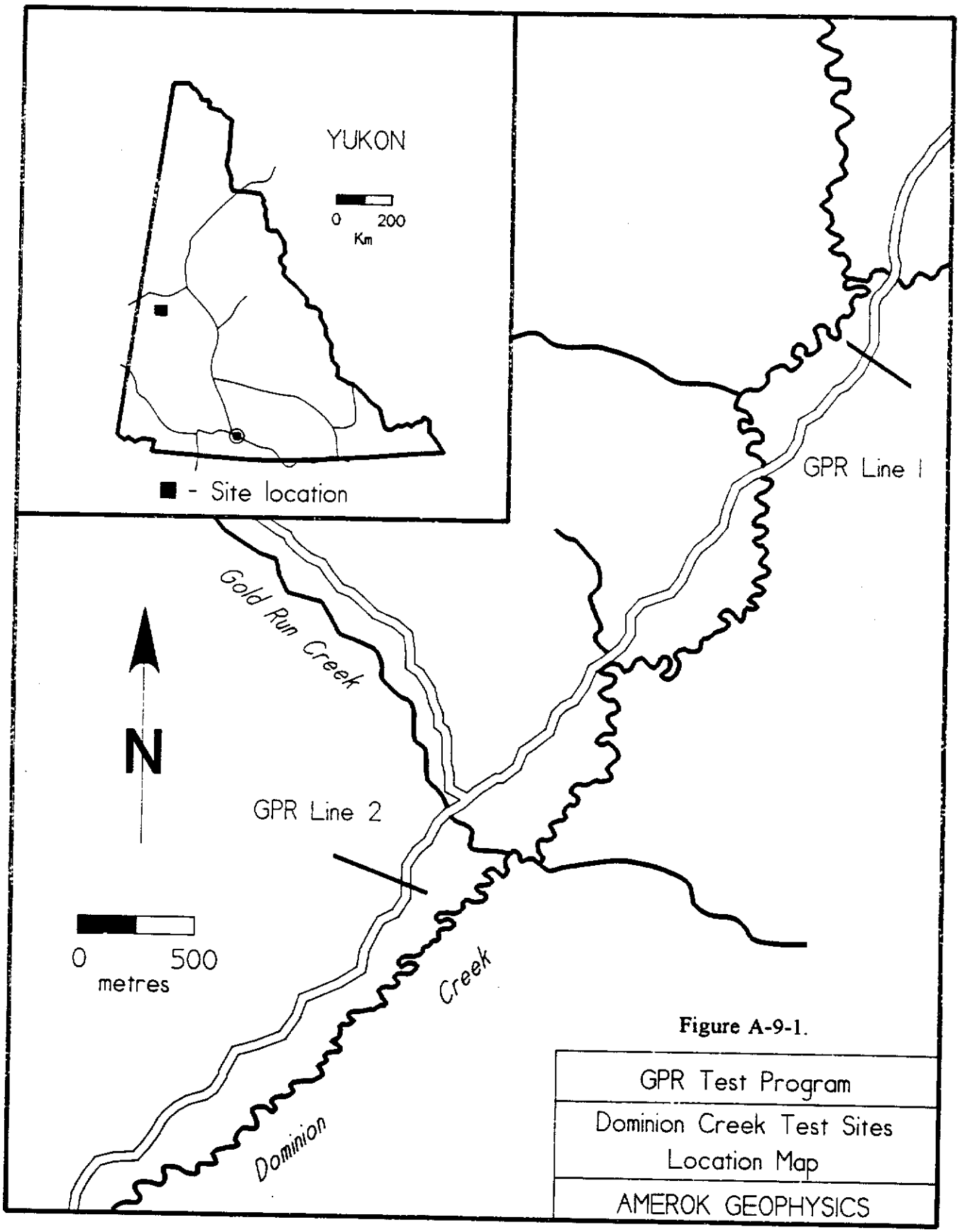
YUKON
0 200
Km
■ - Site location
GPR Line 1
Gold Run Creek
N
GPR Line 2
0 500
metres
Creek
Dominion
GPR Test Program
Dominion Creek Test Sites
Location Map
AMEROK GEOPHYSICS

**Figure A-9-1.**

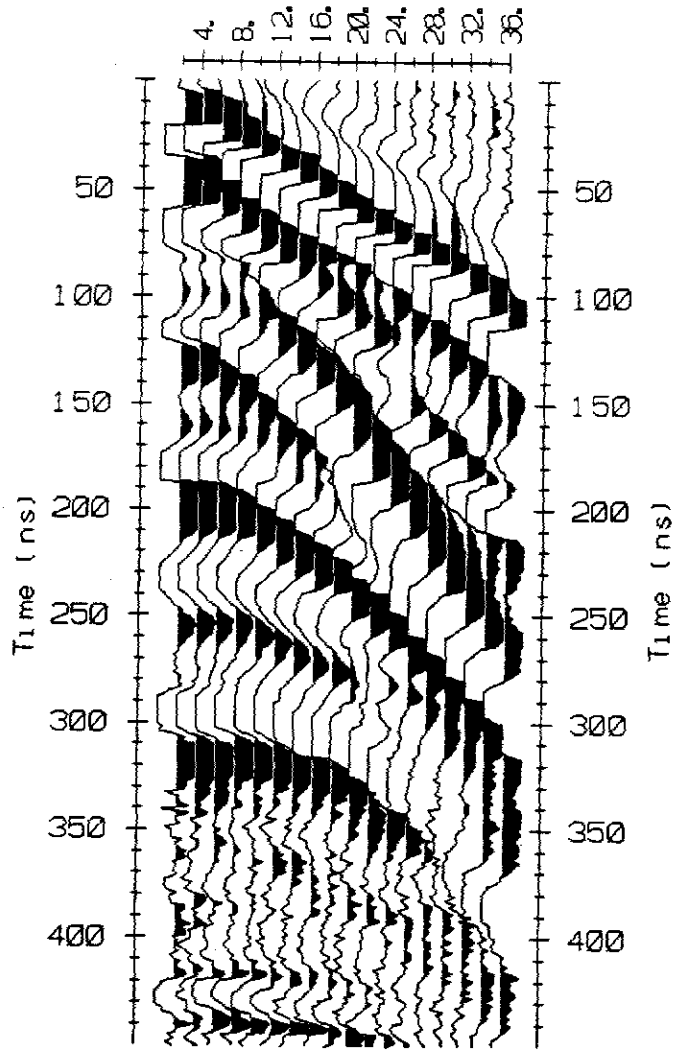


Figure A-9-2. Dominion Creek 25 MHz CMP radargram. Measurement interval 2m in separations from 2 to 36 m.

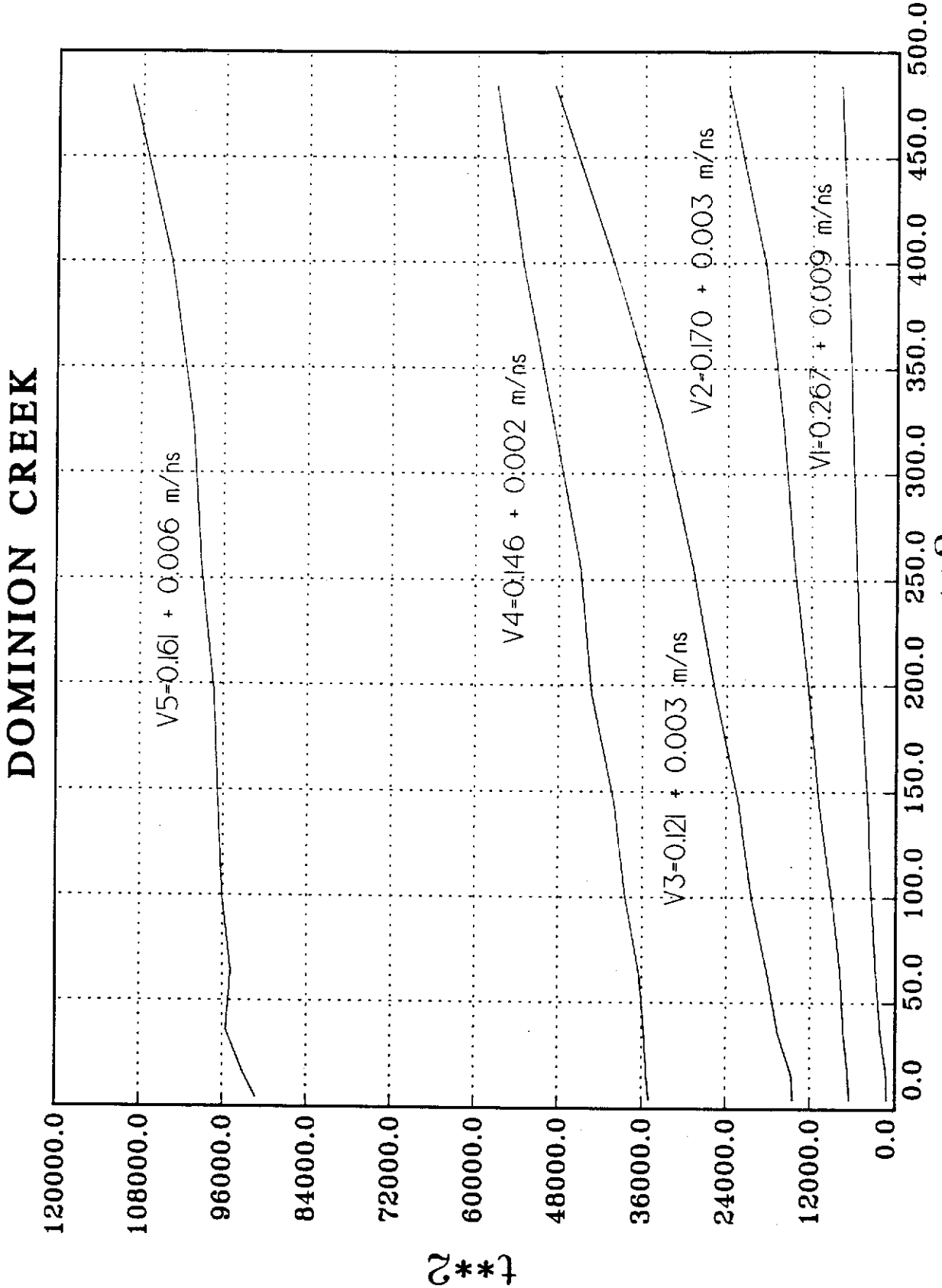


Figure A-9-3. Dominion Creek $X^2$-$T^2$ diagram. Velocities derived from linear regression are plotted near curves.

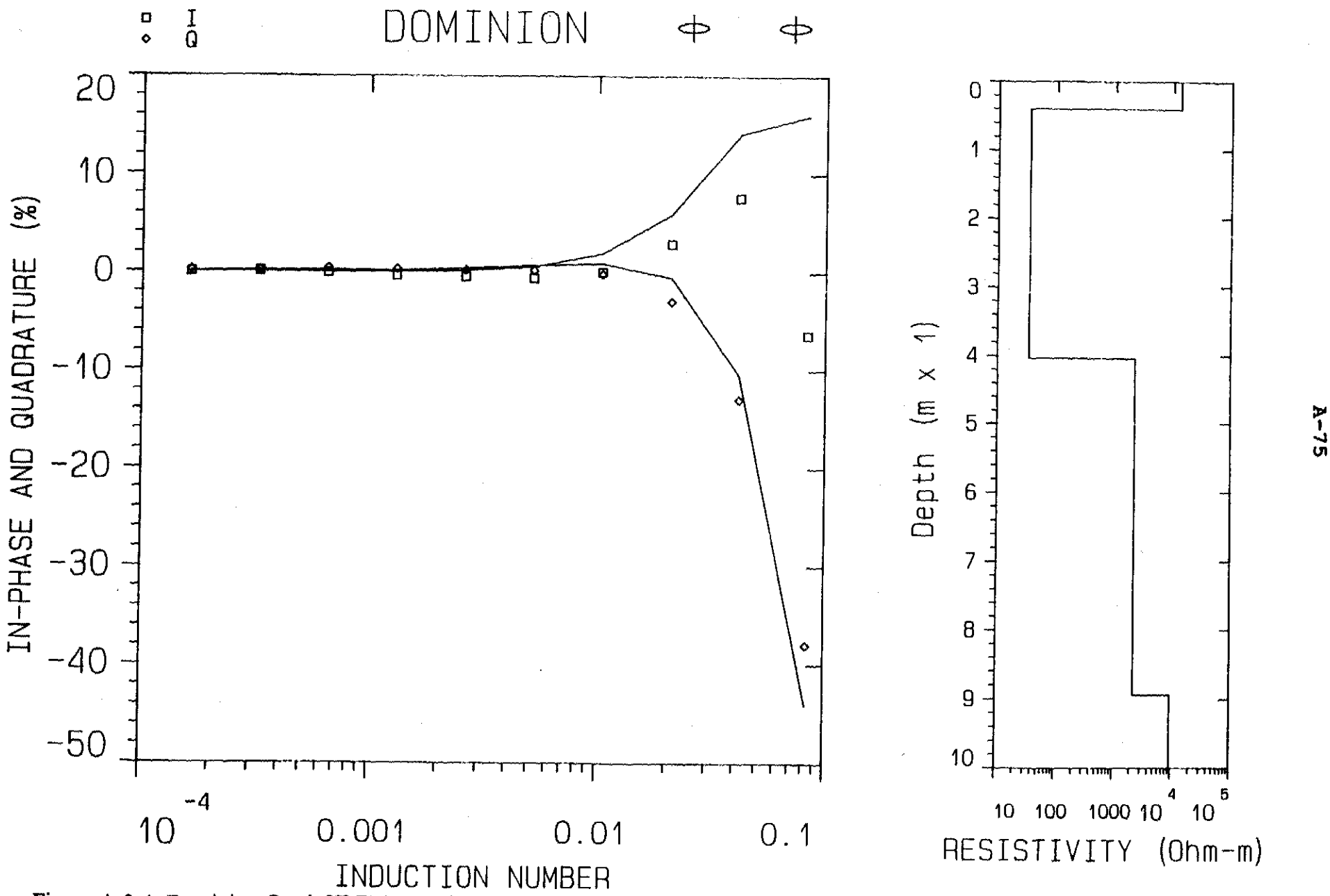


**Figure A-9-4. Dominion Creek HLEM sounding results. Synthetic and measured data is on the left. Square symbols indicate measured in-phase, diamonds indicate measured quadrature; curves display synthetic responses. Model is displayed on the right.**

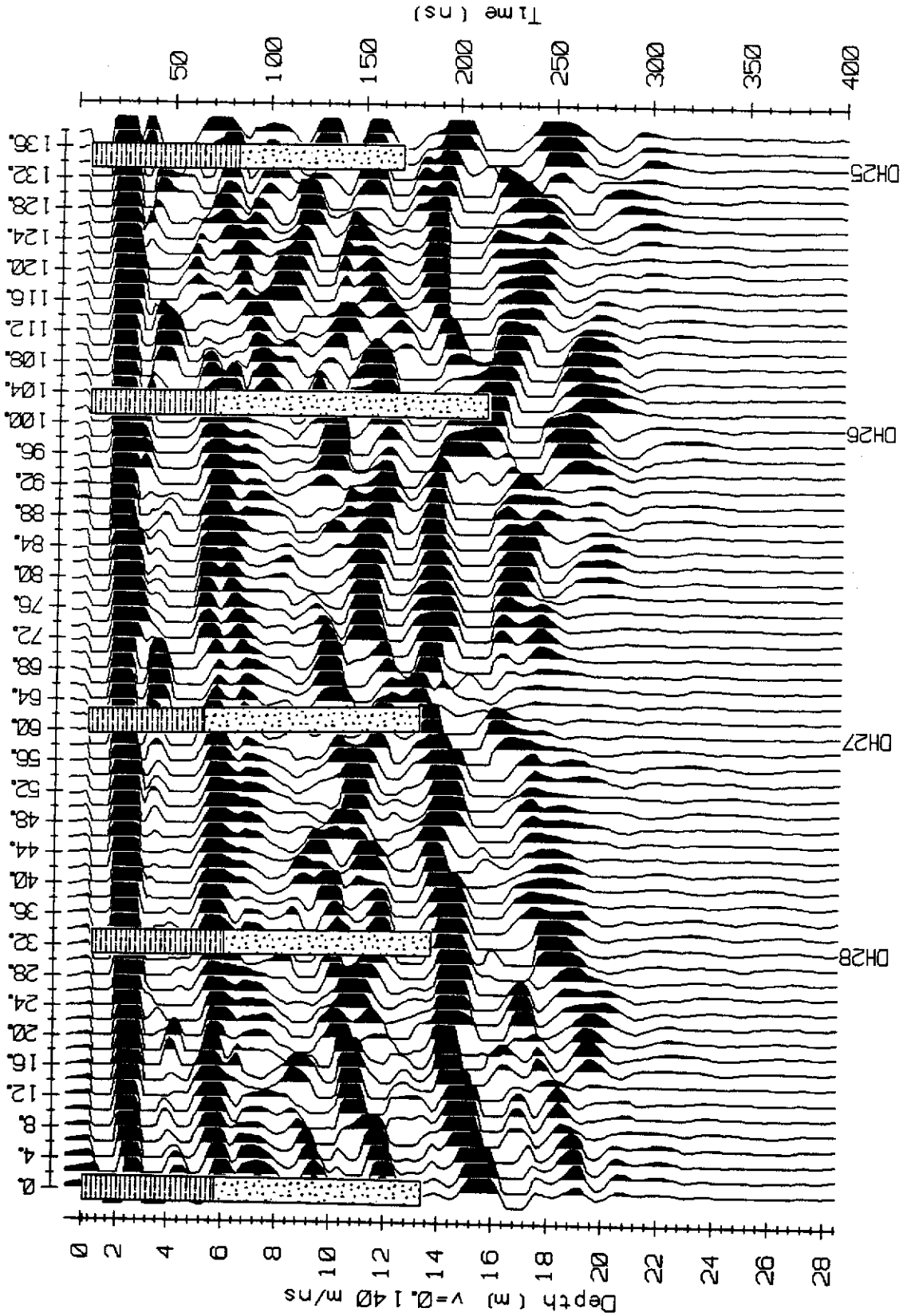


Figure A-9-5. Profile radargram along Dominion Creek survey line 1. Drill hole sections showing muck (dashed lines) and gravel (dots) are plotted on the radargram. Both bedrock and base of muck produce strong reflections.

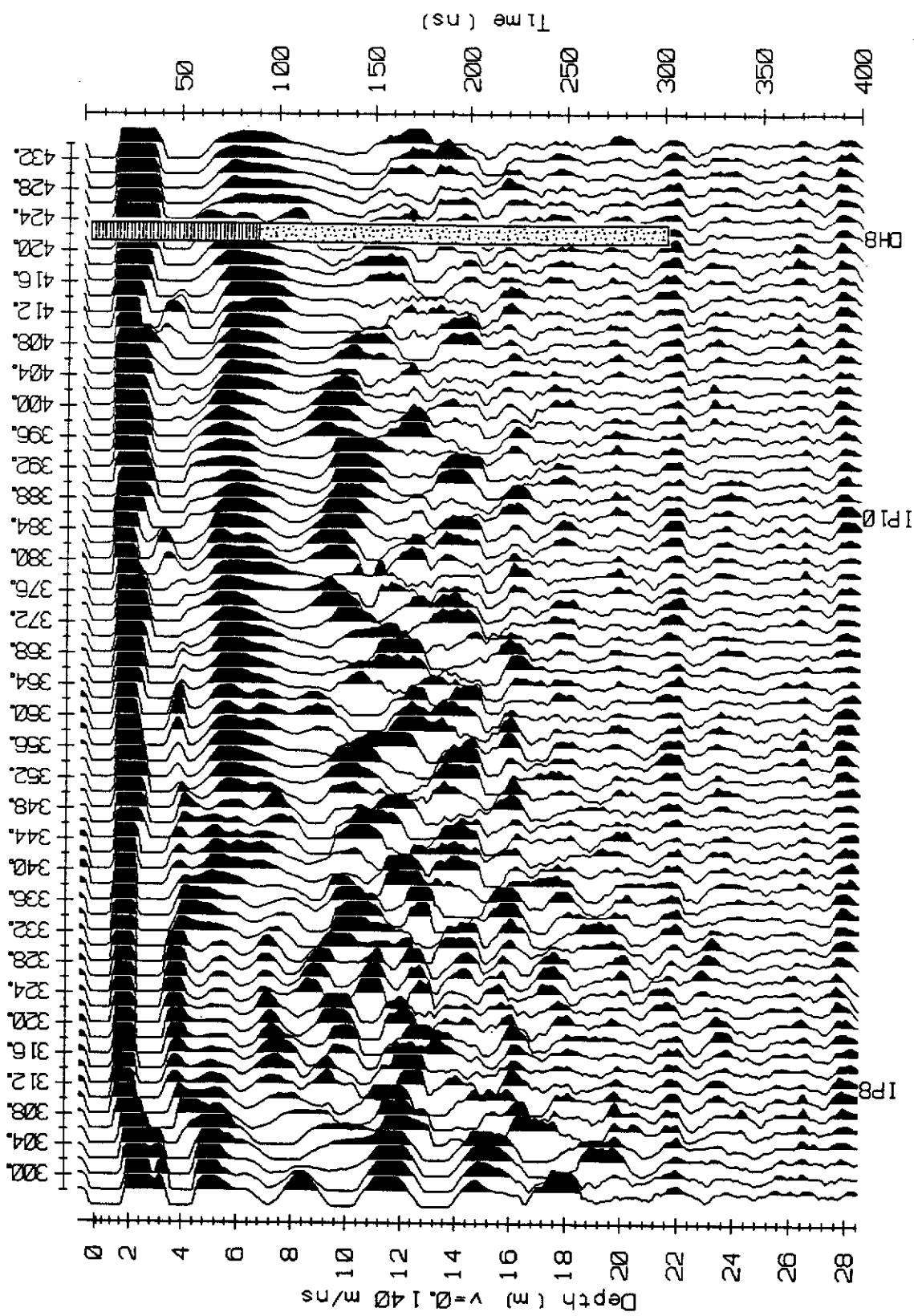


Figure A-9-6. Profile radargram along Dominion Creek survey line 2. Drill hole section showing muck (dashed lines) and gravel (dots) is plotted on the radargram. Base of muck produces a continuous reflection but bedrock does not produce a reflection.

## SITE 10 - DISCOVERY CREEK

### A. Site location

The survey site is located on placer claims P3884 and P3887-97 on Discovery Creek in the Mount Nansen area. The property is approximately 50 miles west of Carmacks and can be reached via the Nansen Road and an extension starting near the Mount Nansen Mine. (Figure A-10-1).

### B. Local geology

The survey site is underlain by granodiorite, andesite and latite (Carlson 1987). Bedrock is deeply weathered and overlain by gravels and colluvium. The gravels are very immature, with a high clay content and predominantly subangular clasts. Placer deposits are spotty and high grade; some deposits are in fact elluvial deposits formed from the weathering of underlying veins. The entire section was frozen at the time of the survey.

### C. Survey specifications

The survey was conducted on a 3 line-km survey grid ploughed with a CAT just prior to the survey. The GPR profile survey was conducted with the 25 MHz antennas at a 4 m separation. Readings were stacked 128 times and stations read at 2 m intervals. A HLEM sounding was conducted west of GPR Line 2 using a 50 m coil spacing. A CMP velocity survey was conducted 200 m southwest of GPR Line 11 with the 25 MHz antennas and an antenna separation varying from 2 to 36 m in 2 m increments.

### D. Results

The CMP survey radargram is plotted in Figure A-10-2, the $X^2$-$T^2$ plot is shown in Figure A-10-3 and results are tabulated in Table A-10-1. In addition to the air wave, surface waves in snow and muck were generated. Nearby drilling and excavation indicate that the 160 ns arrival is a bedrock reflection and the corresponding $V_{NMO}$ was used as the overburden velocity.

Results of the HLEM resistivity sounding are shown in Figure A-10-4 and tabulated in Table A-10-2; details of the HLEM inversion are in Appendix C. The inversion fit is good with an RMS error of 1.0% and measurement error of $\pm$ 0.5%. The high resistivity of the first layer is a composite resistivity of snow and air. The second layer and half-space correspond to overburden and bedrock respectively. The depth to the contact (11m) agrees with the GPR-measured depth to bedrock in this area. The resistivity of the overburden is

low and may reflect the high clay content in the gravel and colluvium.

**Table A-10-1. Discovery Creek velocity survey results.**

| Layer | $V_{NMO}$ (m/ns) | $V_{DIX}$ (m/ns) | Interval (m) | Remarks |
|---|---|---|---|---|
| 0 | 0.175 ± 0.004 | n/a | 0 | ice/snow |
| 0 | 0.123 ± 0.001 | n/a | 0 | colluvium |
| 2 | 0.148 ± 0.004 | 0.148 | 0 - 12.1 | top of bedrock |

**Table A-10-2. Discovery Creek resistivity sounding results.**

| Layer | Resistivity (Ω-m) | Interval (m) | Remarks |
|---|---|---|---|
| 1 | 14K | 0 - 0.2 | air |
| 2 | 181 | 0.2 - 11 | overburden |
| 3 | 652 | 11+ | bedrock |

Discontinuous irregular reflections were recorded on the survey lines, reflecting the deep weathering and rugged relief of bedrock. Figure A-10-5 is an excerpt from the profile survey on Line 11 together with a superimposed reverse circulation drill hole. In this area, strong reflections from bedrock and weaker reflections from the base of colluvium were recorded. There is good agreement between the drill hole and radar indicated depth to bedrock. Figure A-10-6 show the profile radargram on Line 7 and illustrates the more common occurrence with good reflections recorded only in the creek bottom and on small bedrock benches. Reflections are weak or absent where bedrock dips at a moderate to steep angle and signal strength may be further degraded by conductive overburden.

A trial production survey was conducted on upper Discovery Creek over a 3 line-km grid consisting of 14 survey lines (Figure A-10-1). The results of the trial indicate that a GPR survey can cover approximately 1.5 to 2 line-km per day under winter conditions. This includes set-up and disassembly, profile, velocity and topographic surveys. If the survey is conducted on a regular grid, bedrock topography can be defined over a wide area. As an example, Figure A-10-7 displays the interpolated bedrock topography in the region between GPR Line 1 and Line 8 (dashed area in Figure A-10-1). The high flat areas are regions where no depth to bedrock is available. The property owner mined from Line 1 through to

the area just below the ridge (A) and confirmed that the model provided a good general picture of the bedrock topography. The ridge turned out to be a resistant auriferous quartz vein. These maps are useful only as a guide to the overall topography of the bedrock and should not be used in locating targets on the survey lines where the GPR profiles would be more accurate.

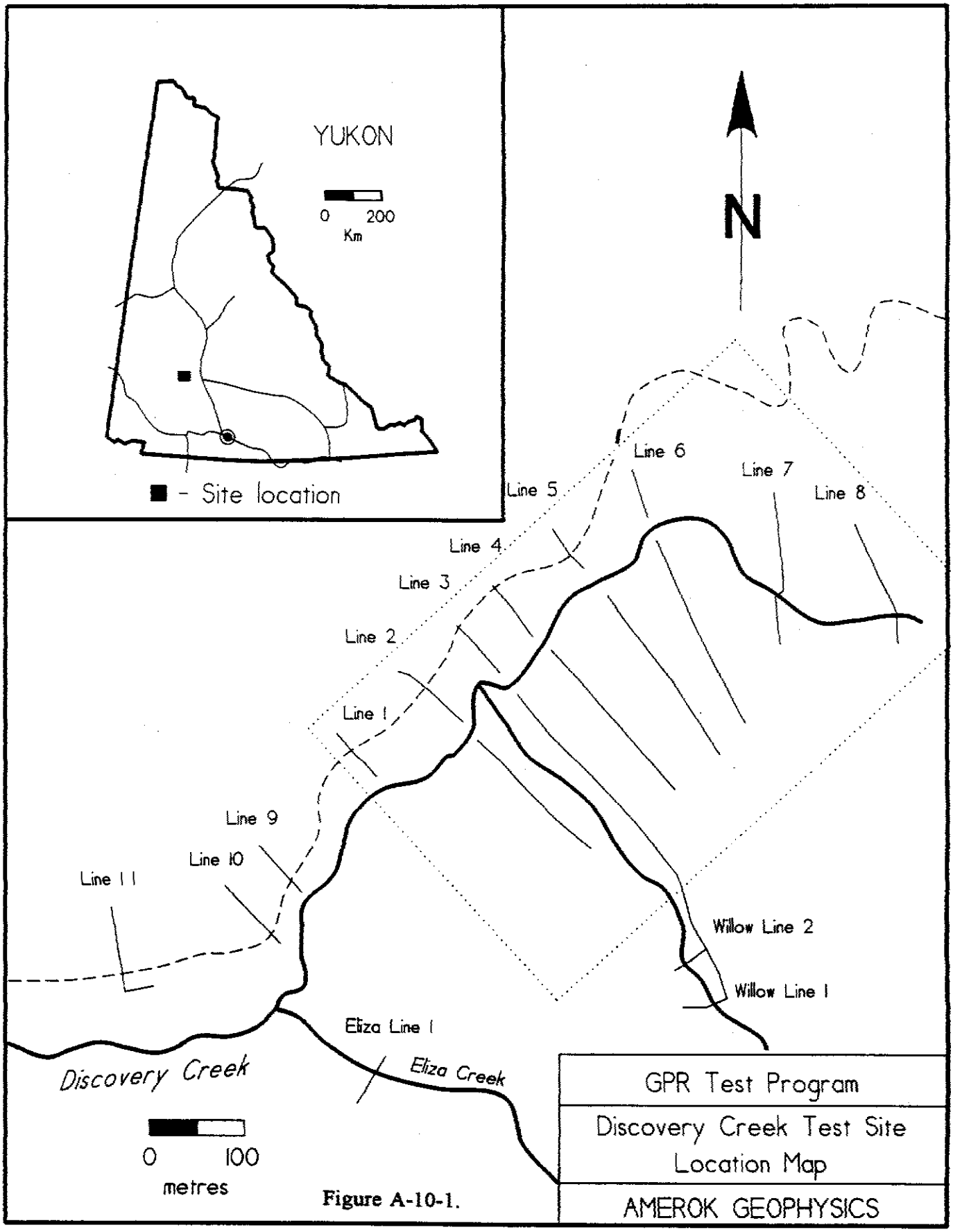
YUKON
0 200
Km
■ - Site location
N
Line 1
Line 2
Line 3
Line 4
Line 5
Line 6
Line 7
Line 8
Line 9
Line 10
Line 11
Willow Line 2
Willow Line 1
Eliza Line 1
Discovery Creek
Eliza Creek
0 100
metres
GPR Test Program
Discovery Creek Test Site
Location Map
AMEROK GEOPHYSICS

**Figure A-10-1.**

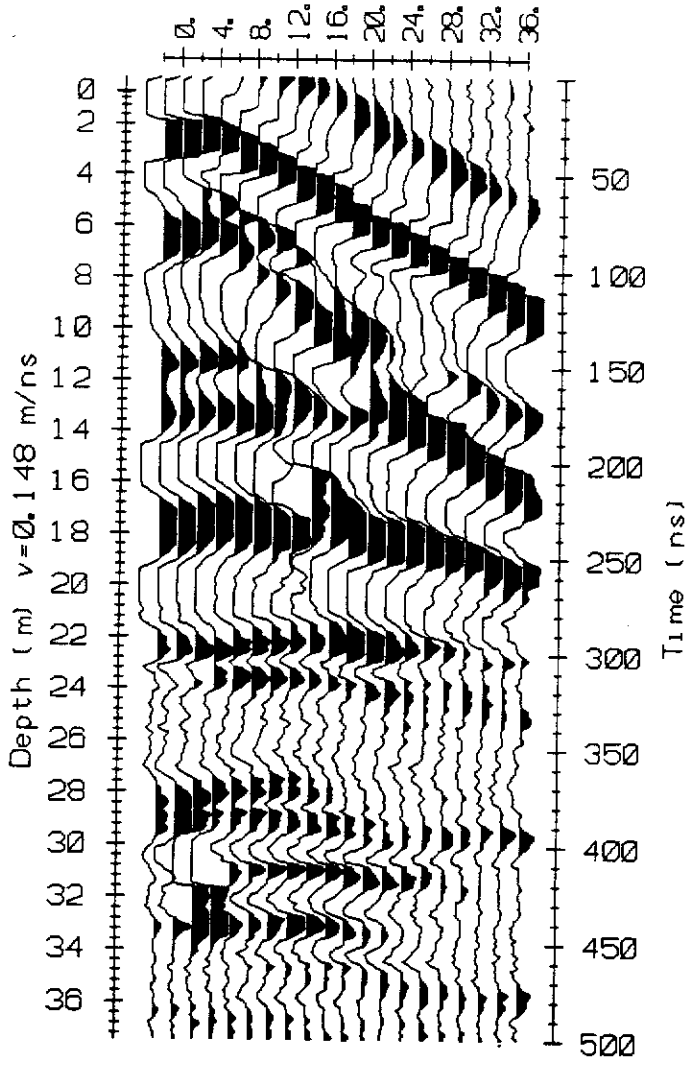


Figure A-10-2. Discovery Creek 25 MHz CMP radargram. Measurement interval 2m in separations from 2 to 36 m.

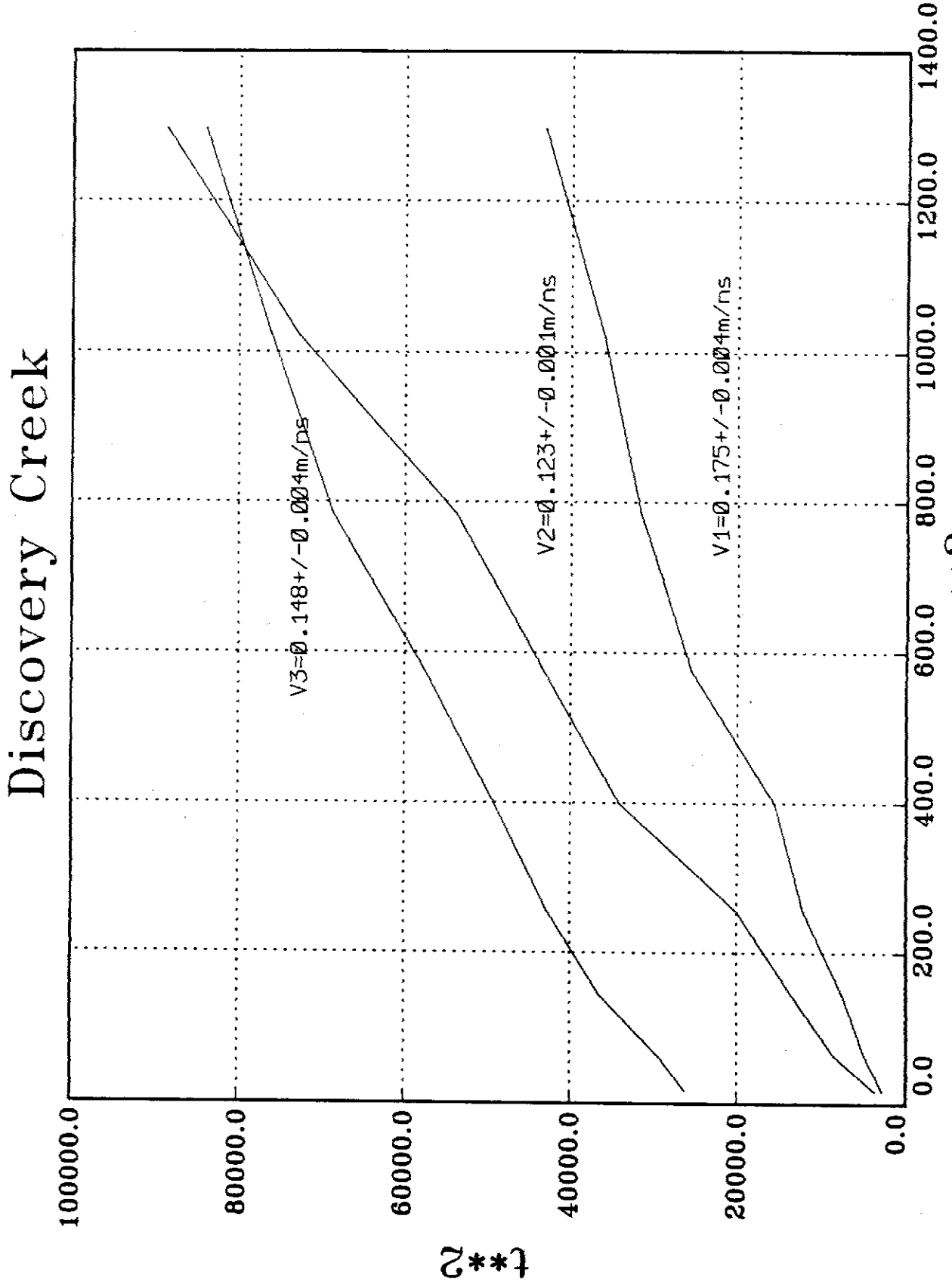


Figure A-10-3. Discovery Creek $X^2$-$T^2$ diagram. Velocities derived from linear regression are plotted near curves.

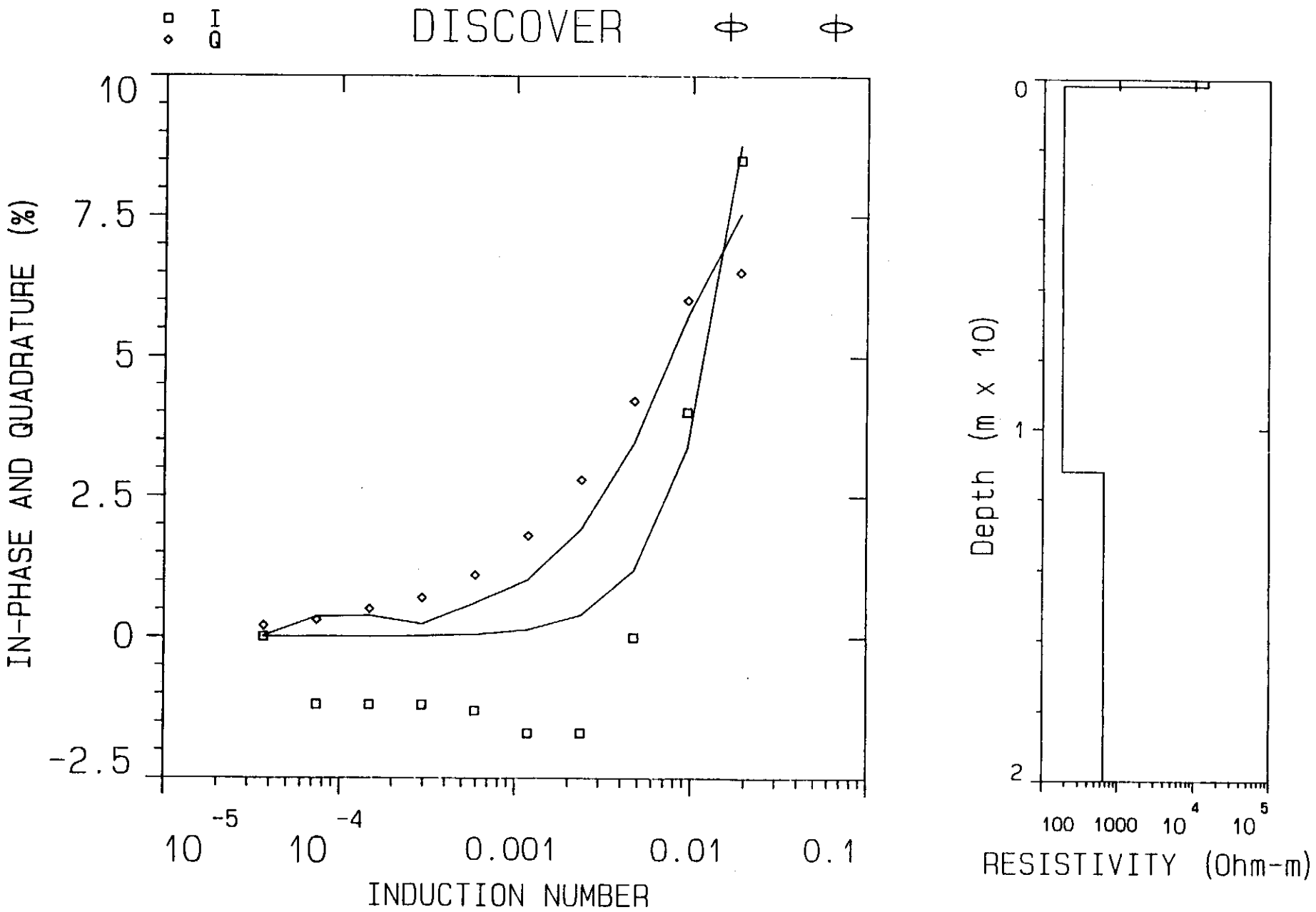


**Figure A-10-4. Discovery Creek HLEM sounding results. Synthetic and measured data is on the left. Square symbols indicate measured in-phase, diamonds indicate measured quadrature; curves display synthetic responses. Model is displayed on the right.**

Sensors & Software Inc.

# SPECIFICATIONS

## RADAR PARAMETERS

| | |
|---|---|
| System Performance | 133 dB |
| Programmable Time Window | 10 - 250 ns |
| Programmable Sampling Interval | 100 - 1000 ps |
| Programmable Stacking Range | 1 - 2048 stacks |

## CONTROL CONSOLE

| | |
|---|---|
| Size | 25 x 16 x 16cm |
| Weight | 2.8 Kg |
| Power | 12V DC (2.5 Amp) |
| Control & Data Port | RS232 Serial (optional Parallel) |

## TRANSMITTER ELECTRONICS

| | |
|---|---|
| Output Voltage | 200V |
| Repetition Rate | 30 kHz |
| Size | 23 x 16 x 5cm |
| Weight | 1.6 Kg |

## RECEIVER ELECTRONICS

| | |
|---|---|
| Size | 23 x 16 x 5cm |
| Weight | 2.0 Kg |
| Data Resolution | 16 bit |

## CONTROL & DISPLAY

| | |
|---|---|
| Computer | MS-DOS* PC**, 640Kbytes RAM, RS232 port |
| Data Storage | Floppy, hard or RAM disk |
| Hard Copy | PC** compatible printers |
| Software : | EKKO_RUN, plus a complete line of processing programs |

## ANTENNAS

| | 225 MHz | 450 MHz | 900 MHz |
|---|---|---|---|
| Size | 40 x 23 x 7cm | 23 x 16 x 6cm | 23 x 16 x 6cm |
| Weight | 1.0 Kg | 0.7 Kg | 0.7 Kg |

* MS-DOS Trademark of Microsoft Corp. ** PC Trademark of International Business Machines Corp.

pulseEKKO 1000

5566 Tomken Road, Mississauga, Ontario, Canada L4W 1P4, Phone: (905) 624-8909 Fax: (905) 624-9365

# Appendix C. HLEM Inversion Results

DATA SET: SOYA

CLIENT: Canada/Yukon MDA
LOCATION: Soya Creek, Yukon
COUNTY: Swamp Creek area
PROJECT: 92-19 GPR Test Survey
ELEVATION: 0.00
SOUNDING COORDINATES: X: 0.0000 Y: 0.0000

DATE: 04-APR-93
SOUNDING: 00001
AZIMUTH: E-W
EQUIPMENT: Maxmin I-10
COIL SEPARATION: 25.000 m

Horizontal Coplanar Loops

FITTING ERROR: 0.914 PERCENT

| L # | RESISTIVITY (ohm-m) | THICKNESS (meters) | ELEVATION (meters) | CONDUCTANCE (Siemens) | RESISTANCE (Ohms) |
|---|---|---|---|---|---|
| | | | 0.0 | | |
| 1 | 2703.6 | 5.46 | -5.46 | 0.00202 | 14779.4 |
| 2 | 769.9 | 11.41 | -16.87 | 0.0148 | 8785.6 |
| 3 | 509649.4 | | | | |

ALL PARAMETERS ARE FREE

| No. | FREQUENCY (Hz) | SPACING (m) | IN-PHASE (%) DATA | IN-PHASE (%) SYNTHETIC | DIFFERENCE (percent) |
|---|---|---|---|---|---|
| 1 | 110.0 | 25.00 | 0.200 | 0.00583 | -0.194 |
| 2 | 220.0 | 25.00 | 1.000E-20 | -0.00183 | -0.00183 |
| 3 | 440.0 | 25.00 | 0.300 | 1.788E-04 | -0.299 |
| 4 | 880.0 | 25.00 | -0.400 | -2.921E-04 | 0.399 |
| 5 | 1760.0 | 25.00 | -0.500 | 9.537E-05 | 0.500 |
| 6 | 3520.0 | 25.00 | -1.00 | 0.00255 | 1.00 |
| 7 | 7040.0 | 25.00 | -1.20 | 0.00933 | 1.20 |
| 8 | 14080.0 | 25.00 | -1.70 | 0.0374 | 1.73 |
| 9 | 28160.0 | 25.00 | -1.60 | 0.142 | 1.74 |
| 10 | 56320.0 | 25.00 | -1.70 | 0.523 | 2.22 |

| No. | FREQUENCY (Hz) | SPACING (m) | QUADRATURE (%) DATA | QUADRATURE (%) SYNTHETIC | DIFFERENCE (percent) |
|---|---|---|---|---|---|
| 11 | 110.0 | 25.00 | 0.0100 | -0.147 | -0.157 |
| 12 | 220.0 | 25.00 | 0.0100 | 0.0925 | 0.0825 |
| 13 | 440.0 | 25.00 | 0.800 | 0.0346 | -0.765 |
| 14 | 880.0 | 25.00 | 0.200 | 0.0284 | -0.171 |
| 15 | 1760.0 | 25.00 | 0.200 | 0.111 | -0.0881 |

| No. | FREQUENCY (Hz) | SPACING (m) | QUADRATURE (%) DATA | QUADRATURE (%) SYNTHETIC | DIFFERENCE (percent) |
|---|---|---|---|---|---|
| 16 | 3520.0 | 25.00 | 0.400 | 0.189 | -0.210 |
| 17 | 7040.0 | 25.00 | 0.700 | 0.390 | -0.309 |
| 18 | 14080.0 | 25.00 | 1.30 | 0.777 | -0.522 |
| 19 | 28160.0 | 25.00 | 2.70 | 1.53 | -1.16 |
| 20 | 56320.0 | 25.00 | 3.50 | 2.98 | -0.519 |

PARAMETER RESOLUTION MATRIX:
"F" INDICATES FIXED PARAMETER

| | | | | | |
|---|---|---|---|---|---|
| P 1 | 0.91 | | | | |
| P 2 | 0.00 | 0.45 | | | |
| P 3 | 0.00 | 0.00 | 0.00 | | |
| T 1 | 0.00 | -0.05 | 0.00 | 0.06 | |
| T 2 | 0.00 | -0.47 | 0.00 | 0.09 | 0.52 |
| | P 1 | P 2 | P 3 | T 1 | T 2 |

DATA SET: FRY_PAN

CLIENT: Canada/Yukon MDA
LOCATION: Frying Pan Creek
COUNTY: Burwash area
PROJECT: 92-19 GPR Test Survey
ELEVATION: 0.00
SOUNDING COORDINATES: X: 0.0000 Y: 0.0000

DATE: 04-APR-93
SOUNDING: 00001
AZIMUTH: N-S
EQUIPMENT: Maxmin I-10
COIL SEPARATION: 25.000 m

Horizontal Coplanar Loops

FITTING ERROR: 0.921 PERCENT

| L # | RESISTIVITY (ohm-m) | THICKNESS (meters) | ELEVATION (meters) | CONDUCTANCE (Siemens) | RESISTANCE (Ohms) |
|---|---|---|---|---|---|
| | | | 0.0 | | |
| 1 | 7262.8 | 1.50 * | -1.50 | 2.065E-04 | 10894.2 |
| 2 | 137.3 | 8.00 * | -9.50 | 0.0582 | 1098.8 |
| 3 | 1002.3 | | | | |

"*" INDICATES FIXED PARAMETER

| No. | FREQUENCY (Hz) | SPACING (m) | IN-PHASE (%) DATA | IN-PHASE (%) SYNTHETIC | DIFFERENCE (percent) |
|---|---|---|---|---|---|
| 1 | 110.0 | 25.00 | 1.10 | -0.00357 | -1.10 |
| 2 | 220.0 | 25.00 | 0.0100 | 3.815E-04 | -0.00962 |
| 3 | 440.0 | 25.00 | -0.100 | -0.00297 | 0.0970 |
| 4 | 880.0 | 25.00 | -0.800 | 0.00994 | 0.809 |
| 5 | 1760.0 | 25.00 | -0.900 | 0.0275 | 0.927 |
| 6 | 3520.0 | 25.00 | -1.00 | 0.0954 | 1.09 |
| 7 | 7040.0 | 25.00 | -1.80 | 0.304 | 2.10 |
| 8 | 14080.0 | 25.00 | -1.20 | 0.954 | 2.15 |
| 9 | 28160.0 | 25.00 | 3.20 | 2.85 | -0.340 |
| 10 | 56320.0 | 25.00 | 7.20 | 7.82 | 0.626 |

| No. | FREQUENCY (Hz) | SPACING (m) | QUADRATURE (%) DATA | QUADRATURE (%) SYNTHETIC | DIFFERENCE (percent) |
|---|---|---|---|---|---|
| 11 | 110.0 | 25.00 | 1.000E-20 | 0.0183 | 0.0183 |
| 12 | 220.0 | 25.00 | 0.100 | 0.0114 | -0.0885 |
| 13 | 440.0 | 25.00 | 0.300 | 0.254 | -0.0457 |
| 14 | 880.0 | 25.00 | 0.200 | 0.309 | 0.109 |
| 15 | 1760.0 | 25.00 | 0.600 | 0.491 | -0.108 |

| No. | FREQUENCY (Hz) | SPACING (m) | QUADRATURE (%) DATA | QUADRATURE (%) SYNTHETIC | DIFFERENCE (percent) |
|---|---|---|---|---|---|
| 16 | 3520.0 | 25.00 | 1.10 | 0.901 | -0.198 |
| 17 | 7040.0 | 25.00 | 2.20 | 1.74 | -0.456 |
| 18 | 14080.0 | 25.00 | 4.20 | 3.24 | -0.959 |
| 19 | 28160.0 | 25.00 | 7.00 | 5.54 | -1.45 |
| 20 | 56320.0 | 25.00 | 8.10 | 7.77 | -0.326 |

PARAMETER RESOLUTION MATRIX:
"F" INDICATES FIXED PARAMETER

| | | | | | |
|---|---|---|---|---|---|
| P 1 | 0.93 | | | | |
| P 2 | 0.00 | 0.91 | | | |
| P 3 | 0.00 | 0.21 | 0.19 | | |
| F 1 | 0.00 | 0.00 | 0.00 | 0.00 | |
| F 2 | 0.00 | 0.00 | 0.00 | 0.00 | 0.00 |
| | P 1 | P 2 | P 3 | F 1 | F 2 |

DATA SET: LIVINGST

CLIENT: Canada/Yukon MDA
LOCATION: Upper Livingstone Creek
COUNTY: Livingstone Creek
PROJECT: 92-19 GPR Test Survey
ELEVATION: 0.00
DATE: 04-APR-93
SOUNDING: 00001
AZIMUTH: E-W
EQUIPMENT: Maxmin I-10
COIL SEPARATION: 50.000 m
SOUNDING COORDINATES: X: 0.0000 Y: 0.0000

Horizontal Coplanar Loops

FITTING ERROR: 1.195 PERCENT

| L # | RESISTIVITY (ohm-m) | THICKNESS (meters) | ELEVATION (meters) | CONDUCTANCE (Siemens) | RESISTANCE (Ohms) |
|---|---|---|---|---|---|
| | | | 0.0 | | |
| 1 | 5088.5 | 1.02 | -1.02 | 2.022E-04 | 5234.4 |
| 2 | 547.8 | 14.24 | -15.27 | 0.0260 | 7804.3 |
| 3 | 114.6 | 18.32 | -33.59 | 0.159 | 2101.0 |
| 4 | 775.9 | | | | |

ALL PARAMETERS ARE FREE

| No. | FREQUENCY (Hz) | SPACING (m) | IN-PHASE (%) DATA | IN-PHASE (%) SYNTHETIC | DIFFERENCE (percent) |
|---|---|---|---|---|---|
| 1 | 110.0 | 50.00 | 1.00 | 0.00176 | -0.998 |
| 2 | 220.0 | 50.00 | 2.50 | 0.0185 | -2.48 |
| 3 | 440.0 | 50.00 | 1.80 | 0.0462 | -1.75 |
| 4 | 880.0 | 50.00 | 2.60 | 0.149 | -2.45 |
| 5 | 1760.0 | 50.00 | 2.40 | 0.461 | -1.93 |
| 6 | 3520.0 | 50.00 | 2.80 | 1.39 | -1.40 |
| 7 | 7040.0 | 50.00 | 4.00 | 3.92 | -0.0730 |
| 8 | 14080.0 | 50.00 | 9.00 | 9.77 | 0.770 |
| 9 | 28160.0 | 50.00 | 21.00 | 19.78 | -1.21 |
| 10 | 56320.0 | 50.00 | 28.00 | 28.98 | 0.981 |

| No. | FREQUENCY (Hz) | SPACING (m) | QUADRATURE (%) DATA | QUADRATURE (%) SYNTHETIC | DIFFERENCE (percent) |
|---|---|---|---|---|---|
| 11 | 110.0 | 50.00 | 0.200 | 0.300 | 0.100 |
| 12 | 220.0 | 50.00 | 0.500 | 0.304 | -0.195 |
| 13 | 440.0 | 50.00 | 0.700 | 0.693 | -0.00654 |
| 14 | 880.0 | 50.00 | 1.30 | 1.31 | 0.0165 |

| No. | FREQUENCY (Hz) | SPACING (m) | QUADRATURE (%) DATA | QUADRATURE (%) SYNTHETIC | DIFFERENCE (percent) |
|---|---|---|---|---|---|
| 15 | 1760.0 | 50.00 | 2.40 | 2.53 | 0.134 |
| 16 | 3520.0 | 50.00 | 4.00 | 4.64 | 0.642 |
| 17 | 7040.0 | 50.00 | 6.80 | 7.79 | 0.990 |
| 18 | 14080.0 | 50.00 | 10.50 | 10.87 | 0.374 |
| 19 | 28160.0 | 50.00 | 11.00 | 9.67 | -1.32 |
| 20 | 56320.0 | 50.00 | -2.50 | -2.08 | 0.412 |

PARAMETER RESOLUTION MATRIX:
"F" INDICATES FIXED PARAMETER

| | | | | | | | |
|---|---|---|---|---|---|---|---|
| P 1 | 0.78 | | | | | | |
| P 2 | 0.01 | 0.87 | | | | | |
| P 3 | 0.00 | -0.10 | 0.75 | | | | |
| P 4 | -0.02 | 0.05 | -0.04 | 0.36 | | | |
| T 1 | 0.00 | 0.18 | -0.02 | 0.00 | 0.04 | | |
| T 2 | 0.00 | 0.13 | 0.23 | -0.04 | 0.05 | 0.74 | |
| T 3 | 0.00 | -0.13 | -0.32 | -0.19 | -0.01 | 0.28 | 0.55 |
| | P 1 | P 2 | P 3 | P 4 | T 1 | T 2 | T 3 |

DATA SET: KLONDIKE

CLIENT: Canada/Yukon MDA
LOCATION: Left Limit
COUNTY: Klondike River
PROJECT: 92-19 GPR Test Survey
ELEVATION: 0.00
SOUNDING COORDINATES: X: 0.0000 Y: 0.0000

DATE: 04-APR-93
SOUNDING: 00001
AZIMUTH: E-W
EQUIPMENT: Maxmin I-10
COIL SEPARATION: 25.000 m

Horizontal Coplanar Loops

FITTING ERROR: 1.291 PERCENT

| L # | RESISTIVITY (ohm-m) | THICKNESS (meters) | ELEVATION (meters) | CONDUCTANCE (Siemens) | RESISTANCE (Ohms) |
|---|---|---|---|---|---|
| | | | 0.0 | | |
| 1 | 320.4 | 0.0469 | -0.0469 | 1.463E-04 | 15.03 |
| 2 | 17.12 | 0.524 | -0.571 | 0.0306 | 8.98 |
| 3 | 466.7 | | | | |

ALL PARAMETERS ARE FREE

| No. | FREQUENCY (Hz) | SPACING (m) | IN-PHASE (%) DATA | IN-PHASE (%) SYNTHETIC | DIFFERENCE (percent) |
|---|---|---|---|---|---|
| 1 | 110.0 | 25.00 | 1.000E-20 | 2.146E-04 | 2.146E-04 |
| 2 | 220.0 | 25.00 | 0.200 | 0.00267 | -0.197 |
| 3 | 440.0 | 25.00 | 0.200 | 0.00719 | -0.192 |
| 4 | 880.0 | 25.00 | 0.500 | 0.0192 | -0.480 |
| 5 | 1760.0 | 25.00 | 0.800 | 0.0574 | -0.742 |
| 6 | 3520.0 | 25.00 | 1.20 | 0.166 | -1.03 |
| 7 | 7040.0 | 25.00 | 1.80 | 0.478 | -1.32 |
| 8 | 14080.0 | 25.00 | 3.50 | 1.34 | -2.15 |
| 9 | 28160.0 | 25.00 | 6.50 | 3.64 | -2.85 |
| 10 | 56320.0 | 25.00 | 6.50 | 9.06 | 2.56 |

| No. | FREQUENCY (Hz) | SPACING (m) | QUADRATURE (%) DATA | QUADRATURE (%) SYNTHETIC | DIFFERENCE (percent) |
|---|---|---|---|---|---|
| 11 | 110.0 | 25.00 | 0.200 | 0.0353 | -0.164 |
| 12 | 220.0 | 25.00 | 0.500 | 0.0690 | -0.430 |
| 13 | 440.0 | 25.00 | 0.900 | 0.111 | -0.788 |
| 14 | 880.0 | 25.00 | 1.20 | 0.219 | -0.980 |
| 15 | 1760.0 | 25.00 | 1.80 | 0.424 | -1.37 |

| No. | FREQUENCY (Hz) | SPACING (m) | QUADRATURE (%) DATA | QUADRATURE (%) SYNTHETIC | DIFFERENCE (percent) |
|---|---|---|---|---|---|
| 16 | 3520.0 | 25.00 | 2.50 | 0.805 | -1.69 |
| 17 | 7040.0 | 25.00 | 2.80 | 1.46 | -1.33 |
| 18 | 14080.0 | 25.00 | 3.50 | 2.48 | -1.01 |
| 19 | 28160.0 | 25.00 | 3.50 | 3.58 | 0.0831 |
| 20 | 56320.0 | 25.00 | 2.00 | 2.94 | 0.942 |

PARAMETER RESOLUTION MATRIX:
"F" INDICATES FIXED PARAMETER

| | | | | | |
|---|---|---|---|---|---|
| P 1 | 0.01 | | | | |
| P 2 | 0.00 | 0.47 | | | |
| P 3 | 0.00 | 0.00 | 0.93 | | |
| T 1 | 0.00 | 0.00 | -0.01 | 0.00 | |
| T 2 | 0.00 | -0.48 | -0.03 | 0.00 | 0.49 |
| | P 1 | P 2 | P 3 | T 1 | T 2 |

DATA SET: GOLD_RUN

CLIENT: Canada/Yukon MDA
LOCATION: Teck Corporation
COUNTY: Gold Run Creek
PROJECT: 92-19 GPR Test Survey
ELEVATION: 0.00
SOUNDING COORDINATES: X: 0.0000 Y: 0.0000

DATE: 04-APR-93
SOUNDING: 00001
AZIMUTH: E-W
EQUIPMENT: Maxmin I-10
COIL SEPARATION: 25.000 m

Horizontal Coplanar Loops

FITTING ERROR: 1.113 PERCENT

| L # | RESISTIVITY (ohm-m) | THICKNESS (meters) | ELEVATION (meters) | CONDUCTANCE (Siemens) | RESISTANCE (Ohms) |
|---|---|---|---|---|---|
| | | | 0.0 | | |
| 1 | 9282.2 | 1.95 | -1.95 | 2.111E-04 | 18191.5 |
| 2 | 3431.3 | 10.73 | -12.69 | 0.00313 | 36844.5 |
| 3 | 113.0 | 7.98 | -20.67 | 0.0705 | 902.6 |
| 4 | 2556.1 | | | | |

ALL PARAMETERS ARE FREE

| No. | FREQUENCY (Hz) | SPACING (m) | IN-PHASE (%) DATA | IN-PHASE (%) SYNTHETIC | DIFFERENCE (percent) |
|---|---|---|---|---|---|
| 1 | 110.0 | 25.00 | 0.400 | 0.0133 | -0.386 |
| 2 | 220.0 | 25.00 | 0.500 | 0.00385 | -0.496 |
| 3 | 440.0 | 25.00 | 0.300 | 0.00840 | -0.291 |
| 4 | 880.0 | 25.00 | 0.200 | 0.00315 | -0.196 |
| 5 | 1760.0 | 25.00 | 0.200 | 0.0177 | -0.182 |
| 6 | 3520.0 | 25.00 | -0.600 | 0.0538 | 0.653 |
| 7 | 7040.0 | 25.00 | -1.00 | 0.185 | 1.18 |
| 8 | 14080.0 | 25.00 | -1.00 | 0.608 | 1.60 |
| 9 | 28160.0 | 25.00 | 1.00 | 1.85 | 0.851 |
| 10 | 56320.0 | 25.00 | 2.50 | 4.98 | 2.48 |

| No. | FREQUENCY (Hz) | SPACING (m) | QUADRATURE (%) DATA | QUADRATURE (%) SYNTHETIC | DIFFERENCE (percent) |
|---|---|---|---|---|---|
| 11 | 110.0 | 25.00 | 0.200 | -0.822 | -1.02 |
| 12 | 220.0 | 25.00 | 0.200 | 0.0308 | -0.169 |
| 13 | 440.0 | 25.00 | 0.300 | 0.0144 | -0.285 |
| 14 | 880.0 | 25.00 | 0.400 | 0.225 | -0.174 |

| No. | FREQUENCY (Hz) | SPACING (m) | QUADRATURE (%) DATA | QUADRATURE (%) SYNTHETIC | DIFFERENCE (percent) |
|---|---|---|---|---|---|
| 15 | 1760.0 | 25.00 | 0.600 | 0.375 | -0.224 |
| 16 | 3520.0 | 25.00 | 1.00 | 0.824 | -0.175 |
| 17 | 7040.0 | 25.00 | 1.80 | 1.59 | -0.206 |
| 18 | 14080.0 | 25.00 | 3.80 | 3.00 | -0.792 |
| 19 | 28160.0 | 25.00 | 7.00 | 5.39 | -1.60 |
| 20 | 56320.0 | 25.00 | 11.50 | 8.59 | -2.90 |

PARAMETER RESOLUTION MATRIX:
"F" INDICATES FIXED PARAMETER

| | | | | | | | |
|---|---|---|---|---|---|---|---|
| P 1 | 0.33 | | | | | | |
| P 2 | 0.00 | 0.00 | | | | | |
| P 3 | 0.00 | 0.01 | 0.15 | | | | |
| P 4 | 0.00 | 0.00 | 0.01 | 0.00 | | | |
| T 1 | 0.00 | 0.00 | 0.02 | 0.00 | 0.00 | | |
| T 2 | 0.00 | 0.01 | 0.12 | 0.01 | 0.02 | 0.11 | |
| T 3 | 0.00 | -0.01 | -0.11 | -0.01 | -0.01 | -0.08 | 0.09 |
| | P 1 | P 2 | P 3 | P 4 | T 1 | T 2 | T 3 |

DATA SET: STEWART

CLIENT: Canada/Yukon MDA
LOCATION: Clear Creek area
COUNTY: Stewart River
PROJECT: 92-19 GPR Test Survey
ELEVATION: 0.00
SOUNDING COORDINATES: X: 0.0000 Y: 0.0000

DATE: 04-APR-93
SOUNDING: 00001
AZIMUTH: E-W
EQUIPMENT: Maxmin I-10
COIL SEPARATION: 25.000 m

Horizontal Coplanar Loops

FITTING ERROR: 0.663 PERCENT

| L # | RESISTIVITY (ohm-m) | THICKNESS (meters) | ELEVATION (meters) | CONDUCTANCE (Siemens) | RESISTANCE (Ohms) |
|---|---|---|---|---|---|
| | | | 0.0 | | |
| 1 | 8908.6 | 9.49 | -9.49 | 0.00107 | 84588.6 |
| 2 | 255.0 | 15.41 | -24.91 | 0.0604 | 3931.6 |
| 3 | 8074.6 | | | | |

ALL PARAMETERS ARE FREE

| No. | FREQUENCY (Hz) | SPACING (m) | IN-PHASE (%) DATA | IN-PHASE (%) SYNTHETIC | DIFFERENCE (percent) |
|---|---|---|---|---|---|
| 1 | 110.0 | 25.00 | 1.000E-20 | -0.00647 | -0.00647 |
| 2 | 220.0 | 25.00 | -0.600 | 0.00174 | 0.601 |
| 3 | 440.0 | 25.00 | -0.500 | -0.00125 | 0.498 |
| 4 | 880.0 | 25.00 | -0.400 | 0.00330 | 0.403 |
| 5 | 1760.0 | 25.00 | -0.400 | 0.00857 | 0.408 |
| 6 | 3520.0 | 25.00 | -0.800 | 0.0279 | 0.827 |
| 7 | 7040.0 | 25.00 | -0.800 | 0.102 | 0.902 |
| 8 | 14080.0 | 25.00 | -0.700 | 0.359 | 1.05 |
| 9 | 28160.0 | 25.00 | 1.40 | 1.16 | -0.231 |
| 10 | 56320.0 | 25.00 | 2.10 | 3.40 | 1.30 |

| No. | FREQUENCY (Hz) | SPACING (m) | QUADRATURE (%) DATA | QUADRATURE (%) SYNTHETIC | DIFFERENCE (percent) |
|---|---|---|---|---|---|
| 11 | 110.0 | 25.00 | 0.100 | 0.295 | 0.195 |
| 12 | 220.0 | 25.00 | 0.100 | 0.315 | 0.215 |
| 13 | 440.0 | 25.00 | 0.200 | -0.0529 | -0.252 |
| 14 | 880.0 | 25.00 | 0.500 | 0.113 | -0.386 |
| 15 | 1760.0 | 25.00 | 0.800 | 0.294 | -0.505 |

| No. | FREQUENCY (Hz) | SPACING (m) | QUADRATURE (%) DATA | QUADRATURE (%) SYNTHETIC | DIFFERENCE (percent) |
|---|---|---|---|---|---|
| 16 | 3520.0 | 25.00 | 1.30 | 0.633 | -0.666 |
| 17 | 7040.0 | 25.00 | 2.00 | 1.21 | -0.782 |
| 18 | 14080.0 | 25.00 | 3.40 | 2.36 | -1.03 |
| 19 | 28160.0 | 25.00 | 5.20 | 4.40 | -0.794 |
| 20 | 56320.0 | 25.00 | 7.10 | 7.49 | 0.396 |

PARAMETER RESOLUTION MATRIX:
"F" INDICATES FIXED PARAMETER

| | | | | | |
|---|---|---|---|---|---|
| P 1 | 0.30 | | | | |
| P 2 | 0.00 | 0.22 | | | |
| P 3 | 0.00 | 0.00 | 0.00 | | |
| T 1 | 0.00 | 0.12 | 0.00 | 0.08 | |
| T 2 | 0.00 | -0.12 | 0.00 | -0.06 | 0.07 |
| | P 1 | P 2 | P 3 | T 1 | T 2 |

DATA SET: LIGHTNIN

CLIENT: Canada/Yukon MDA
LOCATION: Lightning Creek
COUNTY: Mayo District
PROJECT: 92-19 GPR Test Survey
ELEVATION: 0.00
SOUNDING COORDINATES: X: 0.0000 Y: 0.0000

DATE: 04-APR-93
SOUNDING: 00001
AZIMUTH: E-W
EQUIPMENT: Maxmin I-10
COIL SEPARATION: 25.000 m

Horizontal Coplanar Loops

FITTING ERROR: 0.753 PERCENT

| L # | RESISTIVITY (ohm-m) | THICKNESS (meters) | ELEVATION (meters) | CONDUCTANCE (Siemens) | RESISTANCE (Ohms) |
|---|---|---|---|---|---|
| | | | 0.0 | | |
| 1 | 12376.4 | 3.15 | -3.15 | 2.548E-04 | 39022.6 |
| 2 | 67511.9 | 3.37 | -6.52 | 4.993E-05 | 227588.7 |
| 3 | 5459.5 | 15.02 | -21.55 | 0.00275 | 82049.8 |
| 4 | 53.44 | | | | |

ALL PARAMETERS ARE FREE

| No. | FREQUENCY (Hz) | SPACING (m) | IN-PHASE (%) DATA | IN-PHASE (%) SYNTHETIC | DIFFERENCE (percent) |
|---|---|---|---|---|---|
| 1 | 110.0 | 25.00 | 1.10 | 0.00546 | -1.09 |
| 2 | 220.0 | 25.00 | 0.600 | 0.0344 | -0.565 |
| 3 | 440.0 | 25.00 | 1.20 | 0.0887 | -1.11 |
| 4 | 880.0 | 25.00 | 0.800 | 0.200 | -0.599 |
| 5 | 1760.0 | 25.00 | 1.40 | 0.451 | -0.948 |
| 6 | 3520.0 | 25.00 | 1.80 | 0.967 | -0.832 |
| 7 | 7040.0 | 25.00 | 1.80 | 1.89 | 0.0966 |
| 8 | 14080.0 | 25.00 | 3.50 | 3.39 | -0.104 |
| 9 | 28160.0 | 25.00 | 6.00 | 5.46 | -0.532 |
| 10 | 56320.0 | 25.00 | 6.00 | 7.86 | 1.86 |

| No. | FREQUENCY (Hz) | SPACING (m) | QUADRATURE (%) DATA | QUADRATURE (%) SYNTHETIC | DIFFERENCE (percent) |
|---|---|---|---|---|---|
| 11 | 110.0 | 25.00 | 0.100 | 0.430 | 0.330 |
| 12 | 220.0 | 25.00 | 0.400 | 0.792 | 0.392 |
| 13 | 440.0 | 25.00 | 0.800 | 0.280 | -0.519 |
| 14 | 880.0 | 25.00 | 1.30 | 0.768 | -0.531 |

| No. | FREQUENCY (Hz) | SPACING (m) | QUADRATURE (%) DATA | QUADRATURE (%) SYNTHETIC | DIFFERENCE (percent) |
|---|---|---|---|---|---|
| 15 | 1760.0 | 25.00 | 1.80 | 1.22 | -0.577 |
| 16 | 3520.0 | 25.00 | 2.40 | 1.84 | -0.557 |
| 17 | 7040.0 | 25.00 | 3.20 | 2.75 | -0.441 |
| 18 | 14080.0 | 25.00 | 4.00 | 3.69 | -0.301 |
| 19 | 28160.0 | 25.00 | 5.00 | 4.40 | -0.591 |
| 20 | 56320.0 | 25.00 | 5.50 | 4.61 | -0.885 |

PARAMETER RESOLUTION MATRIX:
"F" INDICATES FIXED PARAMETER

| | | | | | | | |
|---|---|---|---|---|---|---|---|
| P 1 | 0.93 | | | | | | |
| P 2 | 0.00 | 0.00 | | | | | |
| P 3 | 0.00 | 0.00 | 0.00 | | | | |
| P 4 | 0.00 | 0.00 | -0.01 | 0.68 | | | |
| T 1 | 0.00 | 0.00 | 0.00 | 0.02 | 0.04 | | |
| T 2 | 0.00 | 0.00 | 0.01 | 0.02 | 0.05 | 0.05 | |
| T 3 | 0.00 | 0.00 | 0.02 | 0.11 | 0.19 | 0.20 | 0.83 |
| | P 1 | P 2 | P 3 | P 4 | T 1 | T 2 | T 3 |

DATA SET: DUNCAN

CLIENT: Canada/Yukon MDA
LOCATION: Duncan Creek
COUNTY: Mayo District
PROJECT: 92-19 GPR Test Survey
ELEVATION: 0.00
SOUNDING COORDINATES: X: 0.0000 Y: 0.0000

DATE: 04-APR-93
SOUNDING: 00001
AZIMUTH: E-W
EQUIPMENT: Maxmin I-10
COIL SEPARATION: 50.000 m

Horizontal Coplanar Loops

FITTING ERROR: 0.736 PERCENT

| L # | RESISTIVITY (ohm-m) | THICKNESS (meters) | ELEVATION (meters) | CONDUCTANCE (Siemens) | RESISTANCE (Ohms) |
|---|---|---|---|---|---|
| | | | 0.0 | | |
| 1 | 13025.7 | 1.13 | -1.13 | 8.676E-05 | 14720.1 |
| 2 | 289.5 | 33.22 | -34.35 | 0.114 | 9619.4 |
| 3 | 1450.0 | | | | |

ALL PARAMETERS ARE FREE

| No. | FREQUENCY (Hz) | SPACING (m) | IN-PHASE (%) DATA | IN-PHASE (%) SYNTHETIC | DIFFERENCE (percent) |
|---|---|---|---|---|---|
| 1 | 110.0 | 50.00 | 1.000E-20 | -0.00477 | -0.00477 |
| 2 | 220.0 | 50.00 | -0.200 | 0.00203 | 0.202 |
| 3 | 440.0 | 50.00 | -0.200 | 0.0179 | 0.217 |
| 4 | 880.0 | 50.00 | -0.300 | 0.0621 | 0.362 |
| 5 | 1760.0 | 50.00 | -0.200 | 0.199 | 0.399 |
| 6 | 3520.0 | 50.00 | 1.000E-20 | 0.638 | 0.638 |
| 7 | 7040.0 | 50.00 | 1.00 | 1.95 | 0.954 |
| 8 | 14080.0 | 50.00 | 4.50 | 5.51 | 1.01 |
| 9 | 28160.0 | 50.00 | 13.00 | 13.49 | 0.492 |
| 10 | 56320.0 | 50.00 | 28.00 | 25.62 | -2.37 |

| No. | FREQUENCY (Hz) | SPACING (m) | QUADRATURE (%) DATA | QUADRATURE (%) SYNTHETIC | DIFFERENCE (percent) |
|---|---|---|---|---|---|
| 11 | 110.0 | 50.00 | 0.0100 | 0.411 | 0.401 |
| 12 | 220.0 | 50.00 | 0.200 | 0.355 | 0.155 |
| 13 | 440.0 | 50.00 | 0.500 | 0.336 | -0.163 |
| 14 | 880.0 | 50.00 | 1.00 | 0.745 | -0.254 |
| 15 | 1760.0 | 50.00 | 2.00 | 1.48 | -0.510 |

| No. | FREQUENCY (Hz) | SPACING (m) | QUADRATURE (%) DATA | QUADRATURE (%) SYNTHETIC | DIFFERENCE (percent) |
|---|---|---|---|---|---|
| 16 | 3520.0 | 50.00 | 3.30 | 2.78 | -0.517 |
| 17 | 7040.0 | 50.00 | 5.00 | 4.95 | -0.0404 |
| 18 | 14080.0 | 50.00 | 7.50 | 7.75 | 0.255 |
| 19 | 28160.0 | 50.00 | 9.00 | 8.63 | -0.366 |
| 20 | 56320.0 | 50.00 | 1.00 | -0.102 | -1.10 |

PARAMETER RESOLUTION MATRIX:
"F" INDICATES FIXED PARAMETER

| | | | | | |
|---|---|---|---|---|---|
| P 1 | 0.59 | | | | |
| P 2 | 0.00 | 0.91 | | | |
| P 3 | 0.00 | 0.03 | 0.03 | | |
| T 1 | 0.00 | 0.09 | 0.00 | 0.06 | |
| T 2 | 0.00 | -0.18 | -0.08 | 0.10 | 0.43 |
| | P 1 | P 2 | P 3 | T 1 | T 2 |

DATA SET: DOMINION

CLIENT: Canada/Yukon MDA
LOCATION: Ross Mining Services
COUNTY: Dominion Creek
PROJECT: 92-19 GPR Test Survey
ELEVATION: 0.00
SOUNDING COORDINATES: X: 0.0000 Y: 0.0000

DATE: 04-APR-93
SOUNDING: 00001
AZIMUTH: E-W
EQUIPMENT: Maxmin I-10
COIL SEPARATION: 50.000 m

Horizontal Coplanar Loops

FITTING ERROR: 5.529 PERCENT

| L # | RESISTIVITY (ohm-m) | THICKNESS (meters) | ELEVATION (meters) | CONDUCTANCE (Siemens) | RESISTANCE (Ohms) |
|---|---|---|---|---|---|
| | | | 0.0 | | |
| 1 | 13281.1 | 0.402 | -0.402 | 3.030E-05 | 5345.2 |
| 2 | 34.32 | 3.63 | -4.03 | 0.105 | 124.8 |
| 3 | 2237.3 | 4.90 | -8.94 | 0.00219 | 10964.7 |
| 4 | 9573.6 | | | | |

ALL PARAMETERS ARE FREE

| No. | FREQUENCY (Hz) | SPACING (m) | IN-PHASE (%) DATA | IN-PHASE (%) SYNTHETIC | DIFFERENCE (percent) |
|---|---|---|---|---|---|
| 1 | 110.0 | 50.00 | 1.000E-20 | -0.00160 | -0.00160 |
| 2 | 220.0 | 50.00 | 0.100 | -0.00169 | -0.101 |
| 3 | 440.0 | 50.00 | -0.1000 | 0.0118 | 0.111 |
| 4 | 880.0 | 50.00 | -0.400 | 0.0399 | 0.439 |
| 5 | 1760.0 | 50.00 | -0.500 | 0.151 | 0.651 |
| 6 | 3520.0 | 50.00 | -0.600 | 0.550 | 1.15 |
| 7 | 7040.0 | 50.00 | 1.000E-20 | 1.91 | 1.91 |
| 8 | 14080.0 | 50.00 | 2.90 | 5.91 | 3.01 |
| 9 | 28160.0 | 50.00 | 7.60 | 14.14 | 6.54 |
| 10 | 56320.0 | 50.00 | -6.40 | 16.02 | 22.42 |

| No. | FREQUENCY (Hz) | SPACING (m) | QUADRATURE (%) DATA | QUADRATURE (%) SYNTHETIC | DIFFERENCE (percent) |
|---|---|---|---|---|---|
| 11 | 110.0 | 50.00 | 0.200 | 0.0333 | -0.166 |
| 12 | 220.0 | 50.00 | 0.200 | 0.180 | -0.0197 |
| 13 | 440.0 | 50.00 | 0.400 | 0.185 | -0.214 |
| 14 | 880.0 | 50.00 | 0.300 | 0.177 | -0.122 |

| No. | FREQUENCY (Hz) | SPACING (m) | QUADRATURE (%) DATA | QUADRATURE (%) SYNTHETIC | DIFFERENCE (percent) |
|---|---|---|---|---|---|
| 15 | 1760.0 | 50.00 | 0.200 | 0.383 | 0.183 |
| 16 | 3520.0 | 50.00 | 0.200 | 0.691 | 0.491 |
| 17 | 7040.0 | 50.00 | -0.200 | 0.903 | 1.10 |
| 18 | 14080.0 | 50.00 | -3.00 | -0.572 | 2.42 |
| 19 | 28160.0 | 50.00 | -13.00 | -10.49 | 2.50 |
| 20 | 56320.0 | 50.00 | -38.00 | -44.11 | -6.11 |

PARAMETER RESOLUTION MATRIX:
"F" INDICATES FIXED PARAMETER

| | | | | | | | |
|---|---|---|---|---|---|---|---|
| P 1 | 0.00 | | | | | | |
| P 2 | 0.00 | 0.27 | | | | | |
| P 3 | 0.00 | 0.00 | 0.00 | | | | |
| P 4 | 0.00 | 0.00 | 0.00 | 0.00 | | | |
| T 1 | 0.00 | 0.01 | 0.00 | 0.00 | 0.00 | | |
| T 2 | 0.00 | -0.25 | 0.00 | 0.00 | -0.01 | 0.23 | |
| T 3 | 0.00 | 0.00 | 0.00 | 0.00 | 0.00 | 0.00 | 0.00 |
| | P 1 | P 2 | P 3 | P 4 | T 1 | T 2 | T 3 |

DATA SET: DISCOVER

CLIENT: Canada/Yukon MDA
LOCATION: Discovery Creek
COUNTY: Nansen District
PROJECT: 92-19 GPR Test Survey
ELEVATION: 0.00
SOUNDING COORDINATES: X: 0.0000 Y: 0.0000

DATE: 04-APR-93
SOUNDING: 00001
AZIMUTH: E-W
EQUIPMENT: Maxmin I-10
COIL SEPARATION: 25.000 m

Horizontal Coplanar Loops

FITTING ERROR: 0.986 PERCENT

| L # | RESISTIVITY (ohm-m) | THICKNESS (meters) | ELEVATION (meters) | CONDUCTANCE (Siemens) | RESISTANCE (Ohms) |
|---|---|---|---|---|---|
| | | | 0.0 | | |
| 1 | 14660.5 | 0.190 | -0.190 | 1.301E-05 | 2795.6 |
| 2 | 180.7 | 11.02 | -11.21 | 0.0609 | 1991.9 |
| 3 | 651.5 | | | | |

ALL PARAMETERS ARE FREE

| No. | FREQUENCY (Hz) | SPACING (m) | IN-PHASE (%) DATA | IN-PHASE (%) SYNTHETIC | DIFFERENCE (percent) |
|---|---|---|---|---|---|
| 1 | 110.0 | 25.00 | 1.000E-20 | -4.828E-04 | -4.828E-04 |
| 2 | 220.0 | 25.00 | -1.20 | 0.00741 | 1.20 |
| 3 | 440.0 | 25.00 | -1.20 | 0.00110 | 1.20 |
| 4 | 880.0 | 25.00 | -1.20 | 0.0193 | 1.21 |
| 5 | 1760.0 | 25.00 | -1.30 | 0.0456 | 1.34 |
| 6 | 3520.0 | 25.00 | -1.70 | 0.134 | 1.83 |
| 7 | 7040.0 | 25.00 | -1.70 | 0.401 | 2.10 |
| 8 | 14080.0 | 25.00 | 1.000E-20 | 1.19 | 1.19 |
| 9 | 28160.0 | 25.00 | 4.00 | 3.37 | -0.624 |
| 10 | 56320.0 | 25.00 | 8.50 | 8.76 | 0.261 |

| No. | FREQUENCY (Hz) | SPACING (m) | QUADRATURE (%) DATA | QUADRATURE (%) SYNTHETIC | DIFFERENCE (percent) |
|---|---|---|---|---|---|
| 11 | 110.0 | 25.00 | 0.200 | 0.0137 | -0.186 |
| 12 | 220.0 | 25.00 | 0.300 | 0.355 | 0.0551 |
| 13 | 440.0 | 25.00 | 0.500 | 0.373 | -0.126 |
| 14 | 880.0 | 25.00 | 0.700 | 0.224 | -0.475 |
| 15 | 1760.0 | 25.00 | 1.10 | 0.610 | -0.489 |

| No. | FREQUENCY (Hz) | SPACING (m) | QUADRATURE (%) DATA | QUADRATURE (%) SYNTHETIC | DIFFERENCE (percent) |
|---|---|---|---|---|---|
| 16 | 3520.0 | 25.00 | 1.80 | 1.02 | -0.777 |
| 17 | 7040.0 | 25.00 | 2.80 | 1.92 | -0.875 |
| 18 | 14080.0 | 25.00 | 4.20 | 3.45 | -0.740 |
| 19 | 28160.0 | 25.00 | 6.00 | 5.71 | -0.285 |
| 20 | 56320.0 | 25.00 | 6.50 | 7.52 | 1.02 |

PARAMETER RESOLUTION MATRIX:
"F" INDICATES FIXED PARAMETER

| | | | | | |
|---|---|---|---|---|---|
| P 1 | 0.92 | | | | |
| P 2 | 0.00 | 0.79 | | | |
| P 3 | 0.00 | 0.16 | 0.11 | | |
| T 1 | 0.00 | 0.03 | 0.00 | 0.01 | |
| T 2 | 0.00 | -0.22 | -0.12 | 0.05 | 0.57 |
| | P 1 | P 2 | P 3 | T 1 | T 2 |